Genetic Control of Schwann Cell Differentiation

Genetische regulatie van Schwann cel differentiatie

Siska Driegen

Layout: Tom de Vries Lentsch
Cover photography: Paul Driegen, Siska Driegen
Cover design: Siska Driegen, Tom de Vries Lentsch
Printed by: Optima Grafische Communicatie, Rotterdam

Genetic Control of Schwann Cell Differentiation

Genetische regulatie van Schwann cel differentiatie

Proefschrift

ter verkrijging van de graad van doctor aan de
Erasmus Universiteit Rotterdam
op gezag van de
rector magnificus

prof.dr. S.W.J. Lamberts

en volgens besluit van het College voor Promoties.

De openbare verdediging zal plaatsvinden op
woensdag 18 oktober 2006 om 13:45 uur

door

Margretha Johanna Franciska Driegen

geboren te Enkhuizen.

Promotor:	Prof.dr. F.G. Grosveld
Overige leden:	Prof.dr. C.P. Verrijzer Dr. J.N.J. Philipsen Dr. J.C. Holstege
Copromotor:	Dr.ir. D.N. Meijer

Contents

	Preface	7
1	Introduction	13
2	A cell-type specific allele of the POU gene *Oct-6* reveals Schwann cell autonomous function in nerve development and regeneration	33
3	The POU proteins Brn-2 and Oct-6 share important functions in Schwann cell development	45
4	A generic tool for biotinylation of tagged proteins in transgenic mice	59
5	Cell autonomy of the mouse *claw paw* mutation	67
6	The *claw paw* mutation reveals a role for *Lgi4* in peripheral nerve development	83
7	Conclusions and summary	95
8	Samenvatting	107
	List of abbreviations	113
	Curriculum vitae	114
	Dankwoord	117

Preface

Preface

The nervous system is arguably the most complex organ system in vertebrates. It allows the organism to sense and integrate environmental information, control body posture and movement, regulate the internal organs and develop complex behaviour. Also, all higher cognitive functions are generated by the nervous system. Despite its complexity, the nervous system consists of only two principal cell types: neurons and glial cells. Although neurons can adopt a bewildering variety of morphologies they elaborate from their soma two main structures: the dendrites and axons (see figure 1A). Axons are the 'output' structure of the neuron and they either contact other neurons or target organs such as muscle or gland. The neuron receives 'input' from multiple, up to thousands, of other neurons that form contacts, synapses, on the dendritic tree and soma. Glial cells were originally considered the connective or supporting tissue of the nervous system. The name for these cells, neuroglia, coined by Rudolph Virchow, the eminent 19th century cell biologist and pathologist, literally means 'nerve glue', a reflection of the modest role these cells were supposed to have. However, over the last decade it has become clear that glial cells are not mere structural cells but are in fact involved in every functional and structural aspect of neuronal shape and function[1]. This is particularly evident in the role myelin-forming glial cells have in shape and function, and thus the evolution, of complex nervous systems.

Communication between neurons and their targets relies on electrical impulses, called action potentials, which travel the length of the axon as a series of membrane depolarisations/repolarizations, very much like a wave moves along the surface of the ocean. The speed, with which the action potential is propagated, inversely correlates with the internal resistance of the axon, a property that largely depends on the diameter of the axon[2]. Thus, large calibre axons have higher conduction velocities than smaller calibre axons. The action potential of the axon depend on the properties of the voltage-gated Na^+/K^+ channels and the Na^+/K^+ gradient over the axonal membrane that is maintained, at the expense of ATP, by the Na^+-K^+ pump[3]. The ATP expense associated with maintaining this gradient increases with the square of the radius of the axon. Therefore, the evolution of faster neuronal circuits in larger animals cannot be solely based on increasing the diameter of axons, as an upper limit is quickly reached because of the exponential growth in energy costs associated with maintaining the Na^+/K^+ gradient over the axonal membrane. The evolution of compact nervous systems in larger animals has become possible through a novel structure produced and maintained by glial cells[4]. This structure is referred to as myelin. Myelin consists of specialized layers of cell membrane of dedicated glia cells that ensheath the axon. Two types of myelin forming glia cells exist: oligodendrocytes in the central division of the nervous system and Schwann cells in the peripheral division. An early drawing of a myelinated fibre is presented in figure 1B.

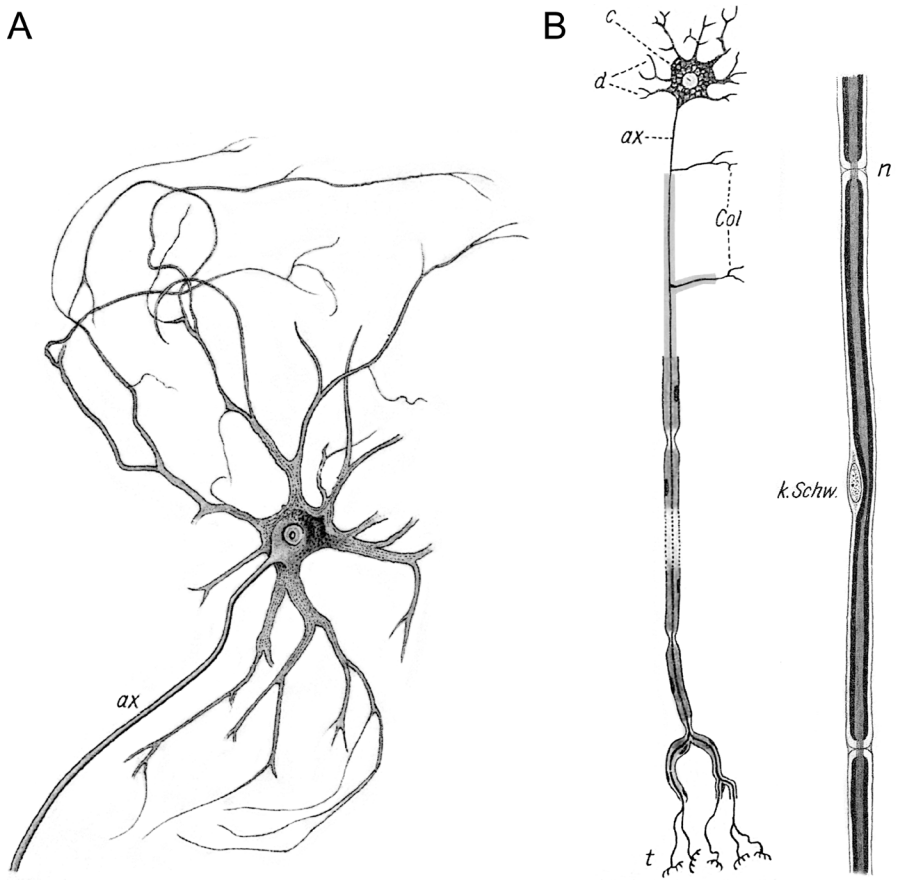

Figure 1. (A) is a nerve cell (taken from *ref 5*). The (ax) in the drawing indicates the axon. The other fibers are the dendrites. (B) shows two myelinated axons. In the left axon (taken from *ref 6*) is (c) the cell body, (d) the dendrites, (ax) the axon, (col) the collaterals and (t) the terminals. In the right drawing is (n) the node of Ranvier and (k.Sch.) is the nucleus of the Schwann cell (taken from *ref 7*).

One functionally important consequence of myelin is that axonal depolarisation is restricted to the nodes of Ranvier, the space in between adjacent myelin sheaths, and that the capacitance of the axonal membrane under the myelin sheath is strongly reduced. Consequently action potentials jump from node to node, a process referred to as saltatory conduction, with a speed that is ten to a hundred times faster than conduction velocities of non-myelinated axons of similar diameter.

With this evolutionary innovation also came new vulnerabilities, as evidenced by the many neurological diseases that are caused by instability or breakdown of the myelin sheath. Prime examples of such diseases are multiple sclerosis, Guillain-Barré syndrome and the

hereditary motor and sensory neuropathies (HMSN) also referred to as Charcot-Marie-Tooth (CMT) disease. In fact, CMT is the most common hereditary disease of the nervous system affecting 1 in 4000 individuals in North America[8]. No cure is available for these diseases and the therapeutic possibilities are very limited. The development of future treatments for these diseases will be based on a detailed understanding of the basic biology of the myelin-forming cell and the pathogenic mechanisms involved in the etiology of the disease.

The work described in this thesis addresses a number of questions related to the process of myelin formation by Schwann cells in the peripheral nervous system. In particular, we have focused on the role the POU domain transcription factor Oct-6 (POU3f1, Tst-1, Scip) plays in the transcriptional program of myelination and on the natural mouse mutant claw paw (clp), which is characterized by congenital hypomyelination of its peripheral nervous system. In the first chapter we will briefly discuss the structure and function of myelin, the pathology of demyelinating diseases and the development of the Schwann cell lineage.
The Oct-6 transcription factor is transiently expressed in the Schwann cell lineage and plays a critical role in the initiation of myelination. In the absence of Oct-6, Schwann cells stall for a prolonged time at the promyelin stage of differentiation resulting in a delayed onset of myelination. Oct-6 is strongly upregulated in response to unknown axonal signals. We have identified the cis-acting element within the *Oct-6* locus through which these signals activate the gene. This element is called the Schwann cell enhancer or SCE and we demonstrate that it is sufficient and required to confer temporally and spatially correct expression of the gene (chapter 2). We further demonstrate that a second POU domain transcription factor, closely related to Oct-6 is expressed in Schwann cells. This factor, Brn-2, seems to be a redundant factor as in the absence of both Oct-6 and Brn-2 the myelination program is even further delayed than in Oct-6 mutant Schwann cells alone (chapter 3). As it is anticipated that Oct-6 and Brn-2 interact with other nuclear factors to execute their function, we adopted a specific labelling approach to purify and identify such cooperating nuclear factors. As a first step we generated a generic mouse model that allows the specific labelling of transgenic protein in any tissue of the mouse. The results of these studies are described in chapter 4. The congenital hypomyelination observed in clp mice shares a number of characteristic features with the hypomyelination phenotype of Oct-6 mutant animals. These similarities suggested that the two genes might act in the same or in a non-redundant parallel pathway. In chapter 5 we describe our studies into the cell-autonomy of the clp mutation. Through a collaborative effort with the laboratory of Dr. John Bermingham Jr at the McLaughlin Research Institute in Great Falls, Montana, we have identified the genetic lesion underlying the clp phenotype. We found that the *clp* mutation results in intracellular retention of a novel gene called *Lgi4*. This secreted protein is expressed in Schwann cells and is probably involved in direct Schwann cell-axon communication. These studies are described in chapter 6. In the final chapter we summarize and discuss our findings and suggest future research directions.

Chapter 1

Introduction

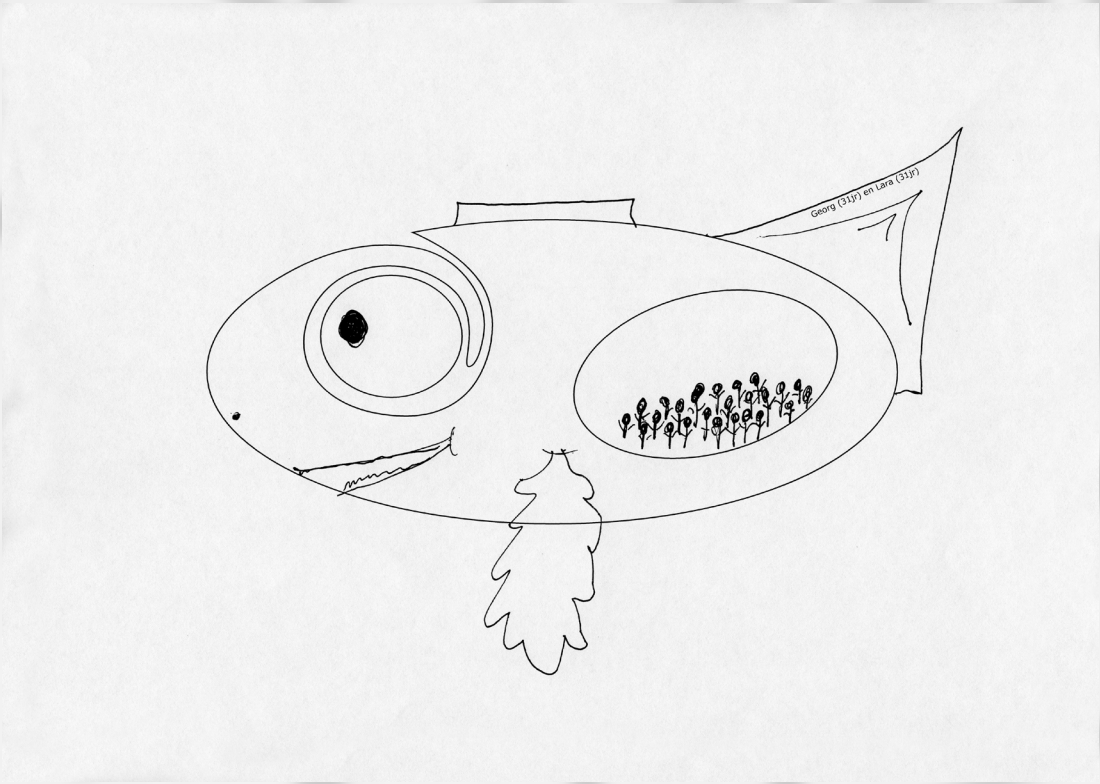

Structure and function of myelin

Schwann cells in the peripheral nervous system (PNS) and the oligodendrocytes and astrocytes in the central nervous system (CNS) are the myelin forming glia cells. The structure of myelin produced by these different cells is in essence identical, although important differences exist and different sets of proteins are used to build myelin[9,10]. In addition, while Schwann cells produce one myelin sheath around an axon, an oligodendrocyte can serve several axons producing multiple myelin sheaths (figure 1). In the following paragraphs we will be focusing on myelin of the PNS.

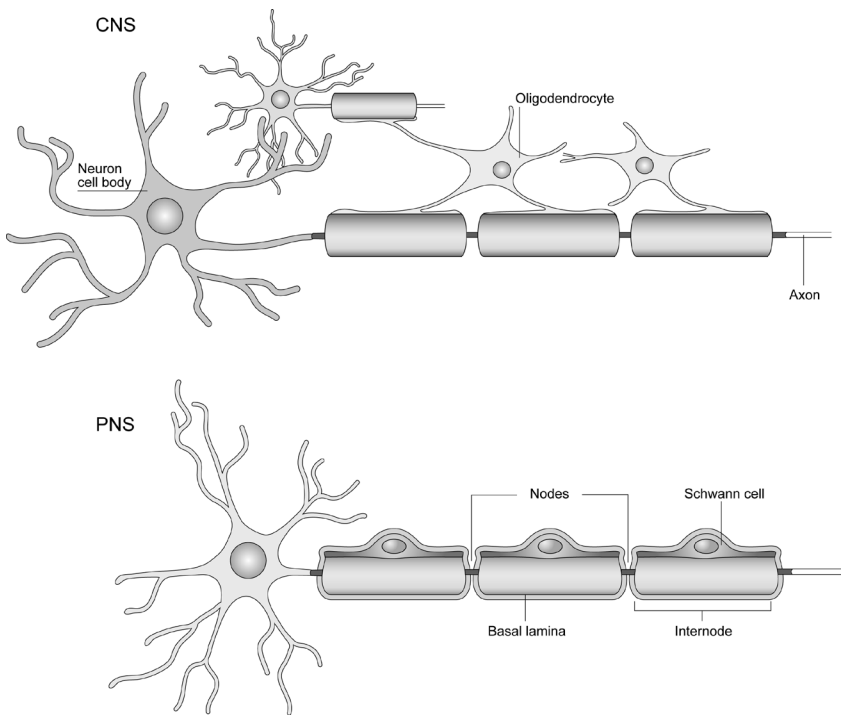

Figure 1. In the CNS the oligodendrocytes can myelinate more than one axon at the same time, while in the PNS the Schwann cell can only myelinate one axon. Also the nodes of Ranvier are indicated in the PNS figure (taken from *ref 11*).

The myelin sheath was originally described as the oily substance that covers the inner axial fibre or axis cylinder and was thought to be the product of the axial fibre itself[12]. It was not until the introduction of the electron microscope in the middle of the 20th century and the development of suitable fixation and contrasting techniques that it was unequivocally demonstrated that the myelin sheath is in fact a product of the Schwann cell. It was demonstrated that the myelin sheath is a specialization of the cell membrane that wraps around the

axon like a scroll around a rod. During development, Schwann cells will initially loosely wrap an axon but as progressively more wraps are added, cytoplasm is removed resulting in the apposition of the cytoplasmic faces of the membrane and compaction of the sheath. The larger the diameter of the axon the more myelin wraps will form[13,14]. In cross sections through the myelin sheath the apposition of the cytoplasmic side of the membrane will appear as thick electron dense lines referred to as the major dense line while the apposition of the outer surface of the membrane forms a thinner intraperiod line (see figure 2).

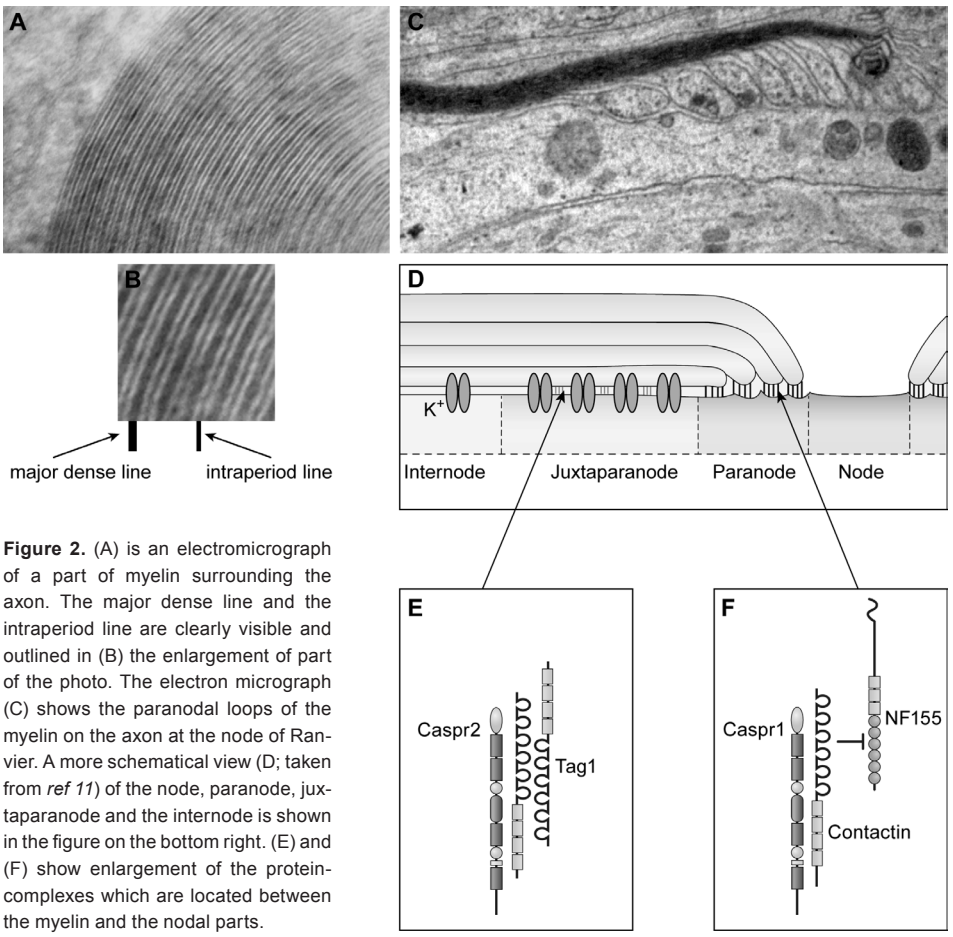

Figure 2. (A) is an electromicrograph of a part of myelin surrounding the axon. The major dense line and the intraperiod line are clearly visible and outlined in (B) the enlargement of part of the photo. The electron micrograph (C) shows the paranodal loops of the myelin on the axon at the node of Ranvier. A more schematical view (D; taken from *ref 11*) of the node, paranode, juxtaparanode and the internode is shown in the figure on the bottom right. (E) and (F) show enlargement of the protein-complexes which are located between the myelin and the nodal parts.

The myelin membrane differs from the cell membrane in that it is enriched in specific lipids and incorporates a specific set of proteins. The surface area of myelin membrane of a myelinating Schwann cell wrapping 40 rounds of myelin along a length of 500 µm axon (10 µm diameter) is around 700,000 μm^2, 7000 times more then the surface area of

for example a red blood cell, which is estimated at 100 μm^2. The most abundant lipid in the myelin membrane is cholesterol (~25% of total lipid weigth) in addition to galactocerebroside and its sulfatide, which account for 14-25% and 2-7% of lipids respectively[9]. The stability of these huge slabs of wrapped myelin membrane is a function of the myelin proteins. The bulk of myelin proteins fall into two classes: glycoproteins and basic proteins. The most abundant protein (50-70% of myelin proteins) is myelin protein zero (mpz or P_0) which is a single transmembrane glycoprotein with an extracellular domain that is structurally similar to an immunoglobulin-related cell adhesion domain. This extracellular domain is involved in homophilic interactions between two opposing myelin membranes and contributes to the intraperiod line[4,15]. In $P_0^{-/-}$ mice the intraperiod line is not formed properly leading to instability of the myelin sheath, which results in a demyelinating neuropathy in these mice[16]. Overexpression of P_0 results in dysmyelination of the peripheral nerves[17,18]. Thus, the amount of P_0 needs to be regulated carefully. Mutations in *mpz* are a major cause of peripheral neuropathies in humans underlying the clinical symptoms of CMT1B and Dejerine Sottas syndrome (see table 1). Many of these mutations interfere with the proper processing of the protein resulting in reduced expression. Another important myelin glycoprotein is the tetraspanning protein peripheral myelin protein 22 (PMP22)[19]. The carbohydrate moiety on the first extracellular loop of the protein may contribute to adhesive interaction similar to those of P_0[4]. Also mutations in *PMP22* are a major cause of demyelinating neuropathies in humans. In fact, duplication of the chromosomal region spanning this gene is the underlying cause of the most common hereditary peripheral neuropathy usually referred to as HMSN1 or CMT1A[20-23].

At the margins of the myelin sheath, cytoplasm is not extruded and these loops fold down onto the axolemma where they form tight junctions with the axonal membrane (figure 2). The space between two adjacent myelin segments is referred to as the node of Ranvier. These so-called paranodal myelin loops are of functional importance as they regionalize the axonal membrane into a nodal, paranodal and juxtaparanodal segment. The nodal membrane is highly enriched in voltage gated sodium channels (1200 of Na^+ channels/μm^2)[24] while the internodal axonal membrane (underlying the compact myelin sheath) is almost completely devoid of Na^+ channels[11]. K^+ channels are localized in the juxtaparanodal membrane and are separated from the Na^+ channels by the septate-like junctions of the paranodal domain. This separation is functionally important, as loss of these junctions results in a shift of the K^+ channels towards the node and altered electrophysiological properties of the nerve fibre[25]. The formation and stabilization of the septate-like junctions is governed by the adhesive properties of the cell adhesion molecules Caspr-1 and Neurofascin. Caspr-1 interacts with contactin in *cis*[26]. This interaction is already established at the endoplasmatic reticulum and is necessary for Caspr-1 to be transported to the plasma membrane[27]. The complex is expressed at the membrane and the extracellular part of the complex interacts with NF-155, which is expressed on the membrane of the paranodal loop[28]. It is thought that this interaction of the Caspr-1/contactin complex with the NF-155 is important for the tight attachment of the paranodal loop to the paranode. The paranode

is also thought to act as a barrier for the K^+ channels that are located in the juxtaparanode and the Na^+ channels located at the node[11]. Caspr-2, a molecule closely related to Caspr-1, is found at the juxtaparanode and interacts there with the K^+ channels[29]. Caspr-2 also interacts with the Tag1 glycoprotein which seems to be important in tethering the K^+ channels at the juxtaparanode[30,31]. The function of the K^+ channels at the juxtaparanode is thought to be the maintenance of the resting potential of the axonal membrane[11].
The paranodal loops are not the only regions of non-compact myelin. Spiral interruptions of non-compact myelin occur in the internodal myelin membrane and are referred to as Schmidt-Lanterman incisures. The Schmidt-Lanterman incisures are thought to function in the transport of nutritional and signalling molecules from the outermesaxon to the innermesaxon and vice versa[4]. The transport of the molecules through the Schmidt-Lanterman incisures is faster and more energy efficient to transport molecules, because the cell is not forced to uncompact complete myelin membranes at the moment molecules need to pass. Connexin32 (Cx32), a gap junction molecule, has been shown to be localized at the Schmidt-Lanterman incisures in the Schwann cell[32]. Normally Cx32 forms gap junctions between cells, but in the Schwann cell it appears to form gap junctions between the myelin layers in the Schmidt-Lanterman incisures[33]. These Cx32 forming gap junctions could be important for the Schwann cell because it could make a radial pathway for molecules with a size up to 1000 Da[32]. Using the radial pathway instead of the circumferential pathway would be a 1000 fold shorter in a myelin sheath that is unrolled about 4 mm long, but compacted just 4 μm[32,34].

The nerve is protected by a nerve sheath

The peripheral nerves are protected by a layer of connective tissue called the nerve sheath. Axons lie in small groups together, surrounded by the endoneurium. Several of these small groups form a small bundle and are surrounded by the perineurium. Blood vessels lie between these small bundles and are separated by the perineurium from direct contact with the axons. Several of these small bundles form the nerve and the nerve is surrounded by the epineurium (figure 3).

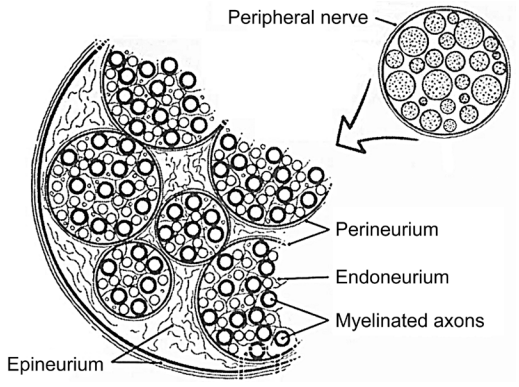

Figure 3. The peripheral nerve has three layers that protect the nerve: an epineurium, a perineurium and an endoneurium (taken from *ref 35*).

The perineurium is formed from mesenchymal cells in the surrounding of the nerve bundle. Initially they form an irregular layer and then go through a mesenchymal-epithelial transition in 2-3 weeks. After this transition a compact multilayer around the nerve is established. The epineurium and the endoneurium are then formed by large deposits of collagen, which also reinforces the nerve bundle[36-40].

Experiments done by Parmantier and colleagues showed that Desert hedgehog (Dhh) protein is very important for the development of a normal epi-, peri- and endoneurium. Dhh mutant mice showed thinner layers of cells forming the perineurium. Also the cells did not form tight junctions with the other cells in the layer[39]. Normally the epi-, peri, and endoneurium protect the nerves from harmful effects like unwanted molecules and intruding cells. It was also shown with the same experiments that Dhh was derived from the Schwann cells. The natural mouse mutant clp does also have a thinner epineurium and was tested for Dhh levels. *Clp* mice showed significantly lower amounts of Dhh in developing nerves then wild type mice[41].

Mutation affecting myelin function and/or stability

Mutations in a number of genes, most notably those encoding structural myelin proteins, cause hereditary motor and sensory neuropathies (HMSN) also called Charcot Marie-Tooth (CMT) neuropathies in humans. CMT has several variants of which CMT1A with a prevalence of 1:2500 is the most common[8]. The CMT1A variant is caused by a duplication of a 1.5 Mb fragment on chromosome 17, which contains the PMP22 gene. This duplication causes PMP22 to be expressed at a higher level[20-23]. Dejerine-Sottas syndrome (DSS) is an even more severe form of CMT and is caused by four copies of the PMP22 gene[42]. In patients with hereditary neuropathy with pressure palsies (HNPP) there is a deletion of one of the alleles of PMP22[43]. In all three of the above mentioned neuropathies the nerve conduction velocity is slowed because there is a partial or complete loss of the myelin sheet. Nerve biopsies of patients with CMT1A also show 'onion bulbs', which are formed by layers of collagen and Schwann cell processes[44].

The severity of the disease in humans depends on the type of the mutation. Mouse models have been developed to study these mutations. Five mouse mutants are mainly studied: the Trembler (Tr) mouse, the Trembler J (TrJ) mouse, the *PMP22*$^{+/-}$and the *PMP22*$^{-/-}$ mouse and also a mouse that over expresses PMP22 . The Tr and the TrJ mutation are both point mutations in the PMP22 gene, G150D and L16P respectively[23,45]. Both mutations were originally discovered in mice and later shown to exists in patients[46,47]. Trembler mice are more severely affected by their point mutations than the PMP22 heterozygous mouse, because they have less myelin than PMP heterozygous mouse[48]. The PMP22 in the Tr and in the TrJ mice cannot reach the myelin membrane. The PMP22 protein seems to remain localized in the endoplasmatic reticulum (ER)[46,49]. In both heterozygous Tr and TrJ mice, wild type(wt)-PMP22 does not reach the plasma membrane. In TrJ mice it is shown that

this is because the wt-PMP22 forms heterodimers with the TrJ-PMP22. These heterodimers are not able to go to the plasma membrane because of the TrJ-PMP22 which is not able to leave the ER[46].

The PMP22$^{+/-}$ mouse develops a demyelinating peripheral neuropathy which is reminiscent of patients with HNPP, while the PMP22$^{-/-}$ is even more severe[50,51].

Mutation in P_0 cause CMT1B which is a relatively mild variant, but can also cause DSS or congenital hypomyelination (CH)[15] more severe forms of CMT. The $P_0^{-/-}$ mouse is used as a model for studying DSS, while the heterozygous P_0 mouse is used for the study of CMT1B. The variants that are caused by mutations in the myelin genes are not the only forms of CMT[4].

CMT2 are neuropathies that show an axonal or neuronal defect. Demyelination occurs in these forms, but is a secondary effect caused by degeneration of Schwann cells that lose contact with its axon[4,52].

CMT also has variants that are caused by genes that are important for the Schwann cells and the myelination process but are not a part of the myelin layer itself. These genes are Cx32, Krox-20 and myotubularin-related protein-2 (MTMR-2)[4].

The variant CMT1X is caused by mutations in Cx32. Patients have an abnormal myelin compaction and a reduced nerve conduction velocity. The mutations found until now are evenly spread over the gene. Most mutations are missense mutations that cause single amino acid changes. Partial deletion and insertion causing frame shifts and premature stop codons are also found[33,53-55]. In most mutant forms the protein is still produced but is not able to leave the Golgi[56].This could have a negative or even toxic effect on the cell and in this way disturbing normal myelination processes.

Another variant of CMT1 is caused by mutation in the Krox-20 gene[4]. Krox-20 is a very important gene for the onset of myelination, which will be discussed in the next section.

The forms of CMT that are categorized in CMT4 are the recessive forms of the disease. MTMR-2 is the cause of CMT4B. It is not exactly known what the function of MTMR-2 is in the peripheral nerve, but it has been found that MTMR-2 is enriched in peripheral nerves and Schwann cells which starts already during embryonic development[57,58]. Nerve biopsies from patients with CMT4B show irregular folding of myelin and also redundant loops of myelin[59].

CMT4F is caused by mutations in the periaxin gene. Periaxin is an important myelin protein which is mostly found on the outside of the myelin sheath and on the border with the node, so in the non-compact parts of the myelin. It is not quite clear yet how periaxin mutations influence the onset of the neuropathy. Periaxin null mice show hypermyelination and demyelination at later stages of life[62].

The Schwann cell lineage does develop from the neural crest. Before a Schwann cell adopts a myelinating or a non-myelinating phenotype the cell has to go through several transitions in which many genes are activated. This developmental process will be discussed in the next section.

Gene	Mouse models	Human genetic defect	Neuropathy
PMP22	PMP22$^{+/-}$ PMP22$^{-/-}$ Trembler TremblerJ	Trisomy Quatrosomy Deletion	CMT1A DSS HNPP
P_0	$P_0^{+/-}$ $P_0^{-/-}$	Mutations Deletion	CMT1B DSS
Cx-32	Cx-32$^{-/-}$ [60]	Mutations	CMT-X
Krox-20	Krox-20$^{-/-}$ [61]	Mutations	CMT1
MTMR-2		Mutations	CMT4B
Periaxin	PRX $^{-/-}$ [62]	Mutations	CMT4F

Table 1: Overview of the various genes and available mouse models as well as the genetic human defects of the neuropathy they cause (for additional references see text).

Development of the Schwann cell lineage

The neural crest is a transient embryonic population of cells that originate from the dorsal margin of the neural tube. These cells give rise to a wide variety of cell types[63]. The cells that are derived from the neural crest are all the neurons and glia of the sympathetic nervous system, which include the satellite cells in the dorsal root ganglia and all the Schwann cells in the PNS[64-66]. The focus will be on the development of the Schwann cells from the neural crest.

Before a Schwann cell becomes a myelinating or a non-myelinating Schwann cell it has to go through several developmental stages. There are three major transitions during this process. The first one is the transition of the neural crest cell to the Schwann cell precursor. The second transition is from the Schwann cell precursor to the immature Schwann cell and the final transition takes place when the immature Schwann cell proceeds to the non-myelinating or the myelinating Schwann cell phenotype[67-69]. Schwann cell precursors can be found in developing embryonic nerves from embryonic day 12 to 13 (E12-13) of gestation. Immature Schwann cells are found from E15 to birth[70,71]. The myelinating Schwann cells will initially make their transition during the first postnatal week and the non-myelinating Schwann cells will follow in the second postnatal week[72]. During these transitions many processes take place in the cells, which involve many transcription factors and growth factors for the timing and regulations of these transitions. Until now several transcription factors have been found to play a role in this process. The most important transcription factors, involved in the transition of the immature Schwann cell to the myelinating Schwann cell, are Oct-6[73,74], Brn-2[75] and Krox-20[61,76]. Krox-24 is restricted to non-myelinating Schwann cells[77]. Other transcription factors, which are involved in the development of the neural crest cell to myelinating or non-myelinating Schwann cell are

Sox10, Sox2, Pax-3 and AP-2. Next to the transcription factors there are also growth factors involved such as neuregulin (NRG) and Notch. The *clp* gene which has recently been identified as the *Lgi-4* (leucine-rich, glioma inactivated) gene is also involved in nerve development[78]. *Clp* mutant mice have delayed myelination, but it is not known yet how Lgi4 is involved in the myelination program.

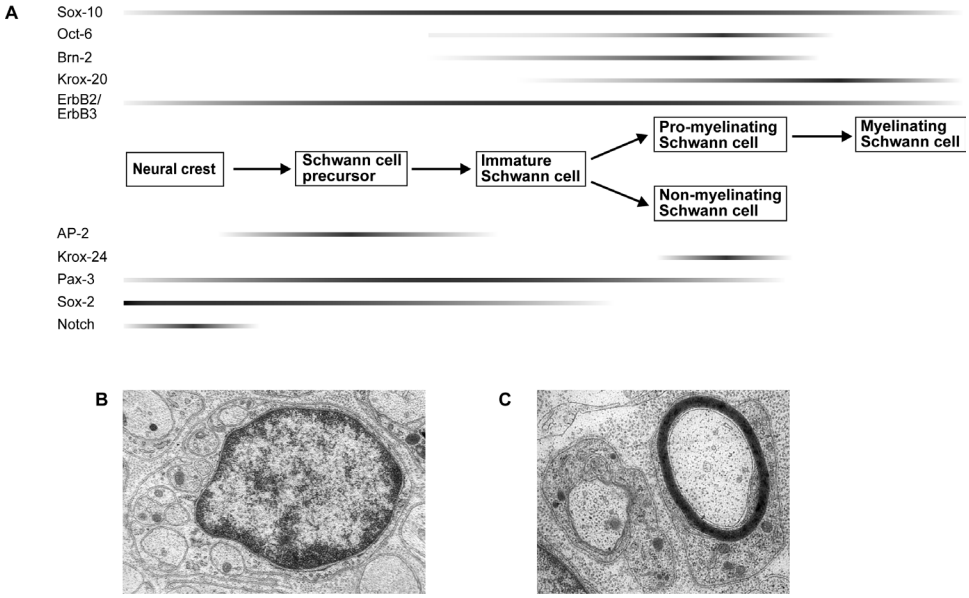

Figure 4. (A) Expression patterns of several transcription factors and growth factors during the development of the Schwann cell lineage. (B) shows a non-myelinating Schwann cell, while in (C) the left cell is a pre-myelinating Schwann cell and the right cell a myelinated Schwann cell.

Oct-6 and Brn-2 are both POU domain transcription factors, which have two regulatory domains: the POU-specific domain and the POU homeodomain. The POU homeodomain is highly conserved in these transcription factors. Both POU domains are involved in binding DNA[79]. Oct-6 and Brn-2 also have almost the same expression pattern. Both are upregulated in the pro-myelinating stage of the myelinating Schwann cell and are down-regulated when myelination proceeds. Brn-2 expression diminishes just before Oct-6 expression does[75].

The expression of Oct-6 is regulated by a downstream regulatory sequence that is named the Schwann cell enhancer (SCE)[80]. In mice carrying a null allele for the SCE myelination is transiently blocked. But with a delay the nerves eventually become myelinated[81]. Experiments have shown that Brn-2 is a possible candidate to take over the function of Oct-6 in these Oct-6 mutants, because in the absence of Oct-6 Brn-2 expression stays upregulated longer than in a wildtype mouse. Myelination will occur in almost the same rate as in wild type mice[75].

Krox-20 expression follows Oct-6 expression. The regulatory element of *Krox-20* has POU binding sites, which indicates that Oct-6 could bind to these regulatory sequences and activate the expression of Krox-20[82]. The *Krox-20* homozygous mutant has a complete block in myelination demonstrating that when Krox-20 is absent there is no other factor able to activate myelination. This makes Krox-20 very important for the myelination process[61]. Recently, it has been shown that Krox-20 regulates other genes and does so in a complex with Nab-1 and/or Nab-2. When a double *Nab1*$^{-/-}$*Nab2*$^{-/-}$ mutant was analysed it showed the same block in myelination as the *Krox-20* mutant. Even when Krox-20 was overexpressed in these *Nab* mutant animals, myelination was still blocked. This indicated that Nab1 and Nab2 are required to mediate the effects of Krox-20 in myelinating cells[83]. Nab proteins control the transcriptional activity of the complex by repression or activation[84,85].
Other positive control transcription factors are Sox10 and Pax-3. Sox10 is expressed in the neural crest cell and expression continues throughout the Schwann cell lineage[86]. In Sox10 mutant mice Schwann cell precursors and immature Schwann cells are completely absent. This indicates that Sox10 plays a crucial role in the development of the Schwann cell lineage from the neural crest. Experiments have shown that Sox10 regulates the expression of the ErbB3 receptor, which is essential for NRG-1 signalling[87] (discussed below). Thus when there is no Sox10 expression, ErbB3 expression is not upregulated and NRG-1 is not able to signal through this receptor. Sox10 has also been found to regulate the expression of P_0[88].
Pax-3 is another positive regulator of Schwann cell development. *Pax-3* mutant mice, splotch[89] and splotch delayed[90], show no Schwann cell lineage at all and a strongly reduced number of Schwann cells respectively[91]. Expression of Pax-3 starts at E12 in mice. Expression is high around birth when the Schwann cells make the decision to myelinate or to remain in a non-myelinating state[92,93]. It is thought that Pax-3 is involved in this decision. In an experiment where Pax-3 was injected into cultured Schwann cells, these Schwann cells showed a decline in myelin basic protein, which is a characteristic molecule of myelin, and an upregulation of markers for non-myelinating Schwann cells[93]. The function of Notch is not completely clear. Notch expression in neural crest cultures showed that there is a strong tendency of the cells to make the transition toward the Schwann cell precursor state, indicating that Notch is a strong positive regulator of Schwann cell development involved in the decision of a cell in becoming a Schwann cell precursor[94].
Recently, two transcription factors have been shown to have a negative regulatory effect on the development of the Schwann cell lineage: Sox2 and AP-2. Sox2 is involved in the suppression of several myelination-related genes. It was shown that overexpression of Sox2 in Schwann cell/neuron co-cultures inhibited myelination[95].
The transcription factor *AP-2* gene family consists of three members: *AP-2*α, *AP-2*β[96-98] and *AP-2*γ[99-101]. Both AP-2α and AP-2γ are expressed in early embryonic nerves and expression peaks at E12/E13, when Schwann cell precursors are found in the developing nerve. When the transition of Schwann cell precursor to immature Schwann cell takes place, AP-2 is downregulated. Forced expression of AP-2α in Schwann cell precursor cultures showed

a delay in the transition of Schwann cell precursors to immature Schwann cells[102]. Thus AP-2α seems to be a negative regulator of Schwann cell development.

Growth factors and the initiation of myelination

Several growth factors have been implicated in the differentiation of Schwann cells, in particular in myelin formation.

For example, it has been demonstrated that the brain derived-neurotrophic factor (BDNF) stimulates myelination in Schwann cell/neuron co-cultures. In addition, sequestering BDNF with a soluble TrkB-Fc (BDNF binds to the TrkB and $p75^{NTR}$ receptors) fusion results in reduced myelination. Addition of the neurotrophin NT3 had the opposite effect in these cultures: Increased levels of NT3 inhibit myelination and sequestration of NT3 with a soluble TrkC-Fc fusion protein promotes myelination. Indeed, NT3 levels drop precipitously in actively myelinating cultures and developing nerves. These results were confirmed *in vivo* through injection of BDNF or NT3 in the vicinity of the sciatic nerve of newborn mice. Analysis of the myelination status of the sciatic nerve 48 hours after neurotrophin injection showed increased myelination in BDNF injected animals while myelination was reduced in NT3 injected animals[103,104].

The positive effect of BDNF on myelination is most likely mediated through the $p75^{NTR}$ receptor and not through the TrkB receptor. In fact, Schwann cells express only the truncated versions of the TrkB receptors that lack tyrosine kinase activity. It is suggested that these truncated TrkB isoforms negatively modulate myelination through sequestration of BDNF[104].

In a similar series of experiments, Chan and colleagues provided evidence for a positive role of the classical neurotrophic factor nerve growth factor (NGF) in myelination by Schwann cells. Surprisingly, NGF has the opposite effect on myelination by oligodendrocytes. These data suggest that NGF affects the receptivity of axons to myelination and that different axonal signals control myelination in the peripheral and central nervous system[105].

The injection of GDNF in peripheral nerves of mice showed an increase in the number of myelinated axons. This was probably caused by the proliferation of Schwann cells along the unmyelinated axons which then assume a 1:1 relationship with those axons and myelinate these normally unmyelinated units[106]. Thus, a delicate balance of neurotrophic factors and their receptors modulate myelination in the developing nerve.

Neuregulin-1 (NRG-1) is found to be crucial for the process of myelination. NRG-1 signals through the heterodimeric complex of the ErbB2/ErbB3 receptor[107,108]. The NRG-1, the ErbB2 and the ErbB3 mutants all show the same phenotype. The NRG-1 and ErbB3 mutants have no Schwann cell precursors while in the ErbB2 mutant the Schwann cell precursors have lost the ability to migrate[109-111]. The axonally-derived NRG-1 is thought to be important for the selection of Schwann cells. Schwann cells that are not in contact with an

axon have no access to NRG. Schwann cells need NRG for their survival, so only Schwann cells that are in contact with the axon and have access to NRG are able to survive[108]. Next to the survival of the Schwann cell lineage, NRG-1 also seems to be important for the migration of Schwann cells along the axon, as was shown in zebrafish[112]. Taveggia and colleagues provided evidence that the membrane bound type III NRG-1 plays an important role in Schwann cell adhesion and initiation of myelination[113]. Another important function of NRG is the involvement of the protein in the regulation of myelin sheath thickness during myelination[114].

Regulation of myelination is a very complex process that is still not understood in detail. In the following chapters we provide experimental evidence that corroborates the notion that the POU domain transcription factors Oct-6 and Brn-2 play key roles in orchestrating the transcriptional program of myelination. In addition, we provide evidence that Lgi4, a novel Schwann cell-derived protein, plays a role in axonal sorting and myelin formation.

References

1. Miller G. Neuroscience. The dark side of glia. Science 2005;308(5723):778-81.
2. Waxman SG, Bennett MV. Relative conduction velocities of small myelinated and non-myelinated fibres in the central nervous system. Nat New Biol 1972;238(85):217-9.
3. Kandel ER, Schwartz JH, Jessell TM. Principles of Neural Science. New York: McGraw-hill; 2000.
4. Lazzarini RA, editor. Myelin biology *and* disorders. 1st ed. San Diego: Elsevier Academic Press; 2003.
5. Deiters O. Untersuchungen uber Gehirn und Ruckenmark de Menschen und der Saugetiere (nach dem Tode de Verfassers herausgegeben von M. Schultze Braunschweig, 1865); 1865.
6. Bloom W, Sandstrom RH. Anat. Rec 1935;64.
7. Boeke J, Groodt Ad, Heringa GC. Leerboek der algemeene en bijzondere weefselleer. Utrecht: Oosthoek's uitgeverij mij.; 1948.
8. Skre H. Genetic and clinical aspects of Charcot-Marie-Tooth's disease. Clin Genet 1974;6(2):98-118.
9. Garbay B, Heape AM, Sargueil F, Cassagne C. Myelin synthesis in the peripheral nervous system. Prog Neurobiol 2000;61(3):267-304.
10. Peters A, Palay SL, Webster Hd. The fine structure of the nervous system. Oxford: Oxford University Press, Inc; 1991.
11. Poliak S, Peles E. The local differentiation of myelinated axons at nodes of Ranvier. Nat Rev Neurosci 2003;4(12):968-80.
12. Jacobson M. Foundations of neuroscience. New York: Plenum Press; 1995.
13. Friede RL. Relation between myelin sheath thickness, internode geometry, and sheath resistance. Exp Neurol 1986;92(1):234-47.

14. Friede RL, Samorajski T. Relation between the number of myelin lamellae and axon circumference in fibers of vagus and sciatic nerves of mice. J Comp Neurol 1967;130(3):223-31.
15. Eichberg J. Myelin P0: new knowledge and new roles. Neurochem Res 2002;27(11):1331-40.
16. Giese KP, Martini R, Lemke G, Soriano P, Schachner M. Mouse P0 gene disruption leads to hypomyelination, abnormal expression of recognition molecules, and degeneration of myelin and axons. Cell 1992;71(4):565-76.
17. Wrabetz L, Feltri ML, Quattrini A, Imperiale D, Previtali S, D'Antonio M, Martini R, Yin X, Trapp BD, Zhou L and others. P(0) glycoprotein overexpression causes congenital hypomyelination of peripheral nerves. J Cell Biol 2000;148(5):1021-34.
18. Yin X, Kidd GJ, Wrabetz L, Feltri ML, Messing A, Trapp BD. Schwann cell myelination requires timely and precise targeting of P(0) protein. J Cell Biol 2000;148(5):1009-20.
19. Snipes GJ, Suter U, Welcher AA, Shooter EM. Characterization of a novel peripheral nervous system myelin protein (PMP-22/SR13). J Cell Biol 1992;117(1):225-38.
20. Matsunami N, Smith B, Ballard L, Lensch MW, Robertson M, Albertsen H, Hanemann CO, Muller HW, Bird TD, White R and others. Peripheral myelin protein-22 gene maps in the duplication in chromosome 17p11.2 associated with Charcot-Marie-Tooth 1A. Nat Genet 1992;1(3):176-9.
21. Patel PI, Roa BB, Welcher AA, Schoener-Scott R, Trask BJ, Pentao L, Snipes GJ, Garcia CA, Francke U, Shooter EM and others. The gene for the peripheral myelin protein PMP-22 is a candidate for Charcot-Marie-Tooth disease type 1A. Nat Genet 1992;1(3):159-65.
22. Timmerman V, Nelis E, Van Hul W, Nieuwenhuijsen BW, Chen KL, Wang S, Ben Othman K, Cullen B, Leach RJ, Hanemann CO and others. The peripheral myelin protein gene PMP-22 is contained within the Charcot-Marie-Tooth disease type 1A duplication. Nat Genet 1992;1(3):171-5.
23. Valentijn LJ, Bolhuis PA, Zorn I, Hoogendijk JE, van den Bosch N, Hensels GW, Stanton VP, Jr., Housman DE, Fischbeck KH, Ross DA and others. The peripheral myelin gene PMP-22/GAS-3 is duplicated in Charcot-Marie-Tooth disease type 1A. Nat Genet 1992;1(3):166-70.
24. Rosenbluth J. Intramembranous particle distribution at the node of Ranvier and adjacent axolemma in myelinated axons of the frog brain. J Neurocytol 1976;5(6):731-45.
25. Rasband MN, Trimmer JS. Developmental clustering of ion channels at and near the node of Ranvier. Dev Biol 2001;236(1):5-16.
26. Peles E, Nativ M, Lustig M, Grumet M, Schilling J, Martinez R, Plowman GD, Schlessinger J. Identification of a novel contactin-associated transmembrane receptor with multiple domains implicated in protein-protein interactions. Embo J 1997;16(5):978-88.
27. Faivre-Sarrailh C, Gauthier F, Denisenko-Nehrbass N, Le Bivic A, Rougon G, Girault JA. The glycosylphosphatidyl inositol-anchored adhesion molecule F3/contactin is required for surface transport of paranodin/contactin-associated protein (caspr). J Cell Biol 2000;149(2):491-502.
28. Tait S, Gunn-Moore F, Collinson JM, Huang J, Lubetzki C, Pedraza L, Sherman DL, Colman DR, Brophy PJ. An oligodendrocyte cell adhesion molecule at the site of assembly of the paranodal axo-glial junction. J Cell Biol 2000;150(3):657-66.
29. Poliak S, Gollan L, Martinez R, Custer A, Einheber S, Salzer JL, Trimmer JS, Shrager P, Peles E. Caspr2, a new member of the neurexin superfamily, is localized at the juxtaparanodes of myelinated axons and associates with K+ channels. Neuron 1999;24(4):1037-47.

30. Poliak S, Salomon D, Elhanany H, Sabanay H, Kiernan B, Pevny L, Stewart CL, Xu X, Chiu SY, Shrager P and others. Juxtaparanodal clustering of Shaker-like K+ channels in myelinated axons depends on Caspr2 and TAG-1. J Cell Biol 2003;162(6):1149-60.
31. Traka M, Goutebroze L, Denisenko N, Bessa M, Nifli A, Havaki S, Iwakura Y, Fukamauchi F, Watanabe K, Soliven B and others. Association of TAG-1 with Caspr2 is essential for the molecular organization of juxtaparanodal regions of myelinated fibers. J Cell Biol 2003;162(6):1161-72.
32. Scherer SS, Deschenes SM, Xu YT, Grinspan JB, Fischbeck KH, Paul DL. Connexin32 is a myelin-related protein in the PNS and CNS. J Neurosci 1995;15(12):8281-94.
33. Bergoffen J, Scherer SS, Wang S, Scott MO, Bone LJ, Paul DL, Chen K, Lensch MW, Chance PF, Fischbeck KH. Connexin mutations in X-linked Charcot-Marie-Tooth disease. Science 1993;262(5142):2039-42.
34. Friede RL, Bischhausen R. The precise geometry of large internodes. J Neurol Sci 1980;48(3):367-81.
35. Haines DH, editor. Fundamental Neuroscience. 2nd ed. Philadelphia: Churchill Livingstone; 2002.
36. Bunge MB, Wood PM, Tynan LB, Bates ML, Sanes JR. Perineurium originates from fibroblasts: demonstration in vitro with a retroviral marker. Science 1989;243(4888):229-31.
37. Kristensson K, Olsson Y. The perineurium as a diffusion barrier to protein tracers. Differences between mature and immature animals. Acta Neuropathol (Berl) 1971;17(2):127-38.
38. Olsson Y. Microenvironment of the peripheral nervous system under normal and pathological conditions. Crit Rev Neurobiol 1990;5(3):265-311.
39. Parmantier E, Lynn B, Lawson D, Turmaine M, Namini SS, Chakrabarti L, McMahon AP, Jessen KR, Mirsky R. Schwann cell-derived Desert hedgehog controls the development of peripheral nerve sheaths. Neuron 1999;23(4):713-24.
40. Schiavinato A, Morandin AR, Guidolin D, Lini E, Nunzi MG, Fiori MG. Perineurium of sciatic nerve in normal and diabetic rodents: freeze-fracture study of intercellular junctional complexes. J Neurocytol 1991;20(6):459-70.
41. Darbas A, Jaegle M, Walbeehm E, van den Burg H, Driegen S, Broos L, Uyl M, Visser P, Grosveld F, Meijer D. Cell autonomy of the mouse claw paw mutation. Dev Biol 2004;272(2):470-82.
42. Hanemann CO, Muller HW. Pathogenesis of Charcot-Marie-Tooth 1A (CMT1A) neuropathy. Trends Neurosci 1998;21(7):282-6.
43. Chance PF, Alderson MK, Leppig KA, Lensch MW, Matsunami N, Smith B, Swanson PD, Odelberg SJ, Disteche CM, Bird TD. DNA deletion associated with hereditary neuropathy with liability to pressure palsies. Cell 1993;72(1):143-51.
44. Suter U, Scherer SS. Disease mechanisms in inherited neuropathies. Nat Rev Neurosci 2003;4(9):714-26.
45. Suter U, Welcher AA, Ozcelik T, Snipes GJ, Kosaras B, Francke U, Billings-Gagliardi S, Sidman RL, Shooter EM. Trembler mouse carries a point mutation in a myelin gene. Nature 1992;356(6366):241-4.
46. Tobler AR, Liu N, Mueller L, Shooter EM. Differential aggregation of the Trembler and Trembler J mutants of peripheral myelin protein 22. Proc Natl Acad Sci U S A 2002;99(1):483-8.
47. Devaux JJ, Scherer SS. Altered ion channels in an animal model of Charcot-Marie-Tooth disease type IA. J Neurosci 2005;25(6):1470-80.

48. Garbay B, Domec C, Fournier M, Bonnet J. Developmental expression of the P0 glycoprotein and basic protein mRNAs in normal and trembler mutant mice. J Neurochem 1989;53(3):907-11.
49. Naef R, Adlkofer K, Lescher B, Suter U. Aberrant protein trafficking in Trembler suggests a disease mechanism for hereditary human peripheral neuropathies. Mol Cell Neurosci 1997;9(1):13-25.
50. Adlkofer K, Frei R, Neuberg DH, Zielasek J, Toyka KV, Suter U. Heterozygous peripheral myelin protein 22-deficient mice are affected by a progressive demyelinating tomaculous neuropathy. J Neurosci 1997;17(12):4662-71.
51. Adlkofer K, Martini R, Aguzzi A, Zielasek J, Toyka KV, Suter U. Hypermyelination and demyelinating peripheral neuropathy in Pmp22-deficient mice. Nat Genet 1995;11(3):274-80.
52. Scherer SS, Salzer JL. Glial cell development. Jessen KR, Richardson WD, editors. Oxford: Oxford University Press; 2001.
53. Fairweather N, Bell C, Cochrane S, Chelly J, Wang S, Mostacciuolo ML, Monaco AP, Haites NE. Mutations in the connexin 32 gene in X-linked dominant Charcot-Marie-Tooth disease (CMTX1). Hum Mol Genet 1994;3(1):29-34.
54. Janssen EA, Kemp S, Hensels GW, Sie OG, de Die-Smulders CE, Hoogendijk JE, de Visser M, Bolhuis PA. Connexin32 gene mutations in X-linked dominant Charcot-Marie-Tooth disease (CMTX1). Hum Genet 1997;99(4):501-5.
55. Rouger H, LeGuern E, Birouk N, Gouider R, Tardieu S, Plassart E, Gugenheim M, Vallat JM, Louboutin JP, Bouche P and others. Charcot-Marie-Tooth disease with intermediate motor nerve conduction velocities: characterization of 14 Cx32 mutations in 35 families. Hum Mutat 1997;10(6):443-52.
56. Deschenes SM, Walcott JL, Wexler TL, Scherer SS, Fischbeck KH. Altered trafficking of mutant connexin32. J Neurosci 1997;17(23):9077-84.
57. Berger P, Young P, Suter U. Molecular cell biology of Charcot-Marie-Tooth disease. Neurogenetics 2002;4(1):1-15.
58. Bolino A, Marigo V, Ferrera F, Loader J, Romio L, Leoni A, Di Duca M, Cinti R, Cecchi C, Feltri ML and others. Molecular characterization and expression analysis of Mtmr2, mouse homologue of MTMR2, the Myotubularin-related 2 gene, mutated in CMT4B. Gene 2002;283(1-2):17-26.
59. Bolino A, Muglia M, Conforti FL, LeGuern E, Salih MA, Georgiou DM, Christodoulou K, Hausmanowa-Petrusewicz I, Mandich P, Schenone A and others. Charcot-Marie-Tooth type 4B is caused by mutations in the gene encoding myotubularin-related protein-2. Nat Genet 2000;25(1):17-9.
60. Nelles E, Butzler C, Jung D, Temme A, Gabriel HD, Dahl U, Traub O, Stumpel F, Jungermann K, Zielasek J and others. Defective propagation of signals generated by sympathetic nerve stimulation in the liver of connexin32-deficient mice. Proc Natl Acad Sci U S A 1996;93(18):9565-70.
61. Topilko P, Schneider-Maunoury S, Levi G, Baron-Van Evercooren A, Chennoufi AB, Seitanidou T, Babinet C, Charnay P. Krox-20 controls myelination in the peripheral nervous system. Nature 1994;371(6500):796-9.
62. Williams AC, Brophy PJ. The function of the Periaxin gene during nerve repair in a model of CMT4F. J Anat 2002;200(4):323-30.

63. Douarin NML, Kalcheim C. The neural crest. Bard JBL, Barlow PW, Kirk DL, editors. Cambridge: Cambridge University Press; 1999.
64. Anderson DJ. Cell and molecular biology of neural crest cell lineage diversification. Curr Opin Neurobiol 1993;3(1):8-13.
65. Jessen KR, Mirsky R. Schwann cells: early lineage, regulation of proliferation and control of myelin formation. Curr Opin Neurobiol 1992;2(5):575-81.
66. Pannese E. The satellite cells of the sensory ganglia. Adv Anat Embryol Cell Biol 1981;65:1-111.
67. Mirsky R, Jessen KR. Schwann cell development, differentiation and myelination. Curr Opin Neurobiol 1996;6(1):89-96.
68. Jessen KR, Mirsky R. Embryonic Schwann cell development: the biology of Schwann cell precursors and early Schwann cells. J Anat 1997;191 (Pt 4):501-5.
69. Jessen KR, Mirsky R. Origin and early development of Schwann cells. Microsc Res Tech 1998;41(5):393-402.
70. Jessen KR, Brennan A, Morgan L, Mirsky R, Kent A, Hashimoto Y, Gavrilovic J. The Schwann cell precursor and its fate: a study of cell death and differentiation during gliogenesis in rat embryonic nerves. Neuron 1994;12(3):509-27.
71. Dong Z, Brennan A, Liu N, Yarden Y, Lefkowitz G, Mirsky R, Jessen KR. Neu differentiation factor is a neuron-glia signal and regulates survival, proliferation, and maturation of rat Schwann cell precursors. Neuron 1995;15(3):585-96.
72. Zorick TS, Lemke G. Schwann cell differentiation. Curr Opin Cell Biol 1996;8(6):870-6.
73. Arroyo EJ, Bermingham JR, Jr., Rosenfeld MG, Scherer SS. Promyelinating Schwann cells express Tst-1/SCIP/Oct-6. J Neurosci 1998;18(19):7891-902.
74. Jaegle M, Mandemakers W, Broos L, Zwart R, Karis A, Visser P, Grosveld F, Meijer D. The POU factor Oct-6 and Schwann cell differentiation. Science 1996;273(5274):507-10.
75. Jaegle M, Ghazvini M, Mandemakers W, Piirsoo M, Driegen S, Levavasseur F, Raghoenath S, Grosveld F, Meijer D. The POU proteins Brn-2 and Oct-6 share important functions in Schwann cell development. Genes Dev 2003;17(11):1380-91.
76. Zorick TS, Syroid DE, Arroyo E, Scherer SS, Lemke G. The transcription factors SCIP and Krox-20 mark distinct stages and cell fates in Schwann cell differentiation. Mol Cell Neurosci 1996;8(2-3):129-45.
77. Topilko P, Levi G, Merlo G, Mantero S, Desmarquet C, Mancardi G, Charnay P. Differential regulation of the zinc finger genes Krox-20 and Krox-24 (Egr-1) suggests antagonistic roles in Schwann cells. J Neurosci Res 1997;50(5):702-12.
78. Bermingham JR, Jr., Shearin H, Pennington J, O'Moore J, Jaegle M, Driegen S, van Zon A, Darbas A, Ozkaynak E, Ryu EJ and others. The claw paw mutation reveals a role for Lgi4 in peripheral nerve development. Nat Neurosci 2006;9(1):76-84.
79. Wegner M, Drolet DW, Rosenfeld MG. POU-domain proteins: structure and function of developmental regulators. Curr Opin Cell Biol 1993;5(3):488-98.
80. Mandemakers W, Zwart R, Jaegle M, Walbeehm E, Visser P, Grosveld F, Meijer D. A distal Schwann cell-specific enhancer mediates axonal regulation of the Oct-6 transcription factor during peripheral nerve development and regeneration. Embo J 2000;19(12):2992-3003.
81. Ghazvini M, Mandemakers W, Jaegle M, Piirsoo M, Driegen S, Koutsourakis M, Smit X, Grosveld F, Meijer D. A cell type-specific allele of the POU gene Oct-6 reveals Schwann cell autonomous function in nerve development and regeneration. Embo J 2002;21(17):4612-20.

82. Ghislain J, Desmarquet-Trin-Dinh C, Jaegle M, Meijer D, Charnay P, Frain M. Characterisation of cis-acting sequences reveals a biphasic, axon-dependent regulation of Krox-20 during Schwann cell development. Development 2002;129(1):155-66.
83. Le N, Nagarajan R, Wang JY, Svaren J, LaPash C, Araki T, Schmidt RE, Milbrandt J. Nab proteins are essential for peripheral nervous system myelination. Nat Neurosci 2005;8(7):932-40.
84. Sevetson BR, Svaren J, Milbrandt J. A novel activation function for NAB proteins in EGR-dependent transcription of the luteinizing hormone beta gene. J Biol Chem 2000;275(13):9749-57.
85. Svaren J, Sevetson BR, Golda T, Stanton JJ, Swirnoff AH, Milbrandt J. Novel mutants of NAB corepressors enhance activation by Egr transactivators. Embo J 1998;17(20):6010-9.
86. Kuhlbrodt K, Herbarth B, Sock E, Hermans-Borgmeyer I, Wegner M. Sox10, a novel transcriptional modulator in glial cells. J Neurosci 1998;18(1):237-50.
87. Britsch S, Goerich DE, Riethmacher D, Peirano RI, Rossner M, Nave KA, Birchmeier C, Wegner M. The transcription factor Sox10 is a key regulator of peripheral glial development. Genes Dev 2001;15(1):66-78.
88. Peirano RI, Goerich DE, Riethmacher D, Wegner M. Protein zero gene expression is regulated by the glial transcription factor Sox10. Mol Cell Biol 2000;20(9):3198-209.
89. Epstein DJ, Vekemans M, Gros P. Splotch (Sp2H), a mutation affecting development of the mouse neural tube, shows a deletion within the paired homeodomain of Pax-3. Cell 1991;67(4):767-74.
90. Franz T. Defective ensheathment of motoric nerves in the Splotch mutant mouse. Acta Anat (Basel) 1990;138(3):246-53.
91. Moase CE, Trasler DG. Delayed neural crest cell emigration from Sp and Spd mouse neural tube explants. Teratology 1990;42(2):171-82.
92. Blanchard AD, Sinanan A, Parmantier E, Zwart R, Broos L, Meijer D, Meier C, Jessen KR, Mirsky R. Oct-6 (SCIP/Tst-1) is expressed in Schwann cell precursors, embryonic Schwann cells, and postnatal myelinating Schwann cells: comparison with Oct-1, Krox-20, and Pax-3. J Neurosci Res 1996;46(5):630-40.
93. Kioussi C, Gross MK, Gruss P. Pax3: a paired domain gene as a regulator in PNS myelination. Neuron 1995;15(3):553-62.
94. Morrison SJ, Perez SE, Qiao Z, Verdi JM, Hicks C, Weinmaster G, Anderson DJ. Transient Notch activation initiates an irreversible switch from neurogenesis to gliogenesis by neural crest stem cells. Cell 2000;101(5):499-510.
95. Le N, Nagarajan R, Wang JY, Araki T, Schmidt RE, Milbrandt J. Analysis of congenital hypomyelinating Egr2Lo/Lo nerves identifies Sox2 as an inhibitor of Schwann cell differentiation and myelination. Proc Natl Acad Sci U S A 2005;102(7):2596-601.
96. Williams T, Admon A, Luscher B, Tjian R. Cloning and expression of AP-2, a cell-type-specific transcription factor that activates inducible enhancer elements. Genes Dev 1988;2(12A):1557-69.
97. Moser M, Imhof A, Pscherer A, Bauer R, Amselgruber W, Sinowatz F, Hofstadter F, Schule R, Buettner R. Cloning and characterization of a second AP-2 transcription factor: AP-2 beta. Development 1995;121(9):2779-88.

98. Ohtaka-Maruyama C, Hanaoka F, Chepelinsky AB. A novel alternative spliced variant of the transcription factor AP2alpha is expressed in the murine ocular lens. Dev Biol 1998;202(1):125-35.
99. Bosher JM, Totty NF, Hsuan JJ, Williams T, Hurst HC. A family of AP-2 proteins regulates c-erbB-2 expression in mammary carcinoma. Oncogene 1996;13(8):1701-7.
100. Chazaud C, Oulad-Abdelghani M, Bouillet P, Decimo D, Chambon P, Dolle P. AP-2.2, a novel gene related to AP-2, is expressed in the forebrain, limbs and face during mouse embryogenesis. Mech Dev 1996;54(1):83-94.
101. Oulad-Abdelghani M, Bouillet P, Chazaud C, Dolle P, Chambon P. AP-2.2: a novel AP-2-related transcription factor induced by retinoic acid during differentiation of P19 embryonal carcinoma cells. Exp Cell Res 1996;225(2):338-47.
102. Stewart HJ, Brennan A, Rahman M, Zoidl G, Mitchell PJ, Jessen KR, Mirsky R. Developmental regulation and overexpression of the transcription factor AP-2, a potential regulator of the timing of Schwann cell generation. Eur J Neurosci 2001;14(2):363-72.
103. Chan JR, Cosgaya JM, Wu YJ, Shooter EM. Neurotrophins are key mediators of the myelination program in the peripheral nervous system. Proc Natl Acad Sci U S A 2001;98(25):14661-8.
104. Cosgaya JM, Chan JR, Shooter EM. The neurotrophin receptor p75NTR as a positive modulator of myelination. Science 2002;298(5596):1245-8.
105. Chan JR, Watkins TA, Cosgaya JM, Zhang C, Chen L, Reichardt LF, Shooter EM, Barres BA. NGF controls axonal receptivity to myelination by Schwann cells or oligodendrocytes. Neuron 2004;43(2):183-91.
106. Hoke A, Ho T, Crawford TO, LeBel C, Hilt D, Griffin JW. Glial cell line-derived neurotrophic factor alters axon schwann cell units and promotes myelination in unmyelinated nerve fibers. J Neurosci 2003;23(2):561-7.
107. Davies AM. Neuronal survival: early dependence on Schwann cells. Curr Biol 1998;8(1):R15-8.
108. Garratt AN, Britsch S, Birchmeier C. Neuregulin, a factor with many functions in the life of a schwann cell. Bioessays 2000;22(11):987-96.
109. Meyer D, Birchmeier C. Multiple essential functions of neuregulin in development. Nature 1995;378(6555):386-90.
110. Morris JK, Lin W, Hauser C, Marchuk Y, Getman D, Lee KF. Rescue of the cardiac defect in ErbB2 mutant mice reveals essential roles of ErbB2 in peripheral nervous system development. Neuron 1999;23(2):273-83.
111. Riethmacher D, Sonnenberg-Riethmacher E, Brinkmann V, Yamaai T, Lewin GR, Birchmeier C. Severe neuropathies in mice with targeted mutations in the ErbB3 receptor. Nature 1997;389(6652):725-30.
112. Lyons DA, Pogoda HM, Voas MG, Woods IG, Diamond B, Nix R, Arana N, Jacobs J, Talbot WS. erbb3 and erbb2 are essential for schwann cell migration and myelination in zebrafish. Curr Biol 2005;15(6):513-24.
113. Taveggia C, Zanazzi G, Petrylak A, Yano H, Rosenbluth J, Einheber S, Xu X, Esper RM, Loeb JA, Shrager P and others. Neuregulin-1 type III determines the ensheathment fate of axons. Neuron 2005;47(5):681-94.
114. Michailov GV, Sereda MW, Brinkmann BG, Fischer TM, Haug B, Birchmeier C, Role L, Lai C, Schwab MH, Nave KA. Axonal neuregulin-1 regulates myelin sheath thickness. Science 2004;304(5671):700-3.

Chapter 2

A cell-type specific allele of the POU gene *Oct-6* reveals Schwann cell autonomous function in nerve development and regeneration

Merhnaz Ghazvini, Wim Mandemakers, Martine Jaegle, Marko Piirso, Siska Driegen, Manousos Koutsourakis, Xsander Smit, Frank Grosveld and Dies Meijer

EMBO, 2002

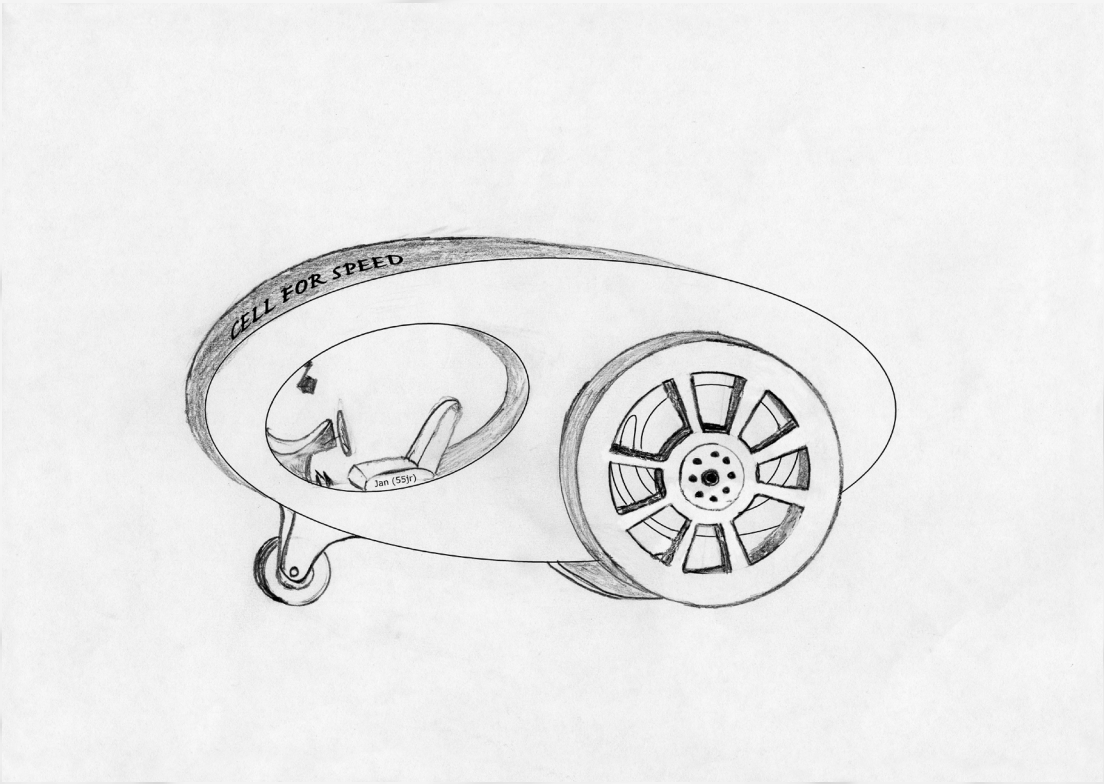

The EMBO Journal Vol. 21 No. 17 pp. 4612–4620, 2002

A cell type-specific allele of the POU gene *Oct-6* reveals Schwann cell autonomous function in nerve development and regeneration

Merhnaz Ghazvini[1], Wim Mandemakers[1,2], Martine Jaegle[1], Marko Piirsoo[1,3], Siska Driegen[1,4], Manousos Koutsourakis[1,5], Xsander Smit[6], Frank Grosveld[1] and Dies Meijer[1,7]

Departments of [1]Cell Biology and Genetics, [4]Neuroscience and [6]Reconstructive Surgery, Erasmus University Rotterdam, PO Box 1738, 3000DR Rotterdam, The Netherlands

[2]Present address: Department of Neurobiology, Stanford University, School of Medicine, Stanford, CA, USA
[3]Present address: National Institute of Chemical Physics and Biophysics, Tallinn, Estonia
[5]Present address: Institut de Genetique et de Biologie Moleculaire et Cellulaire, Illkirch, France

[7]Corresponding author
e-mail: meijer@gen.fgg.eur.nl

M.Ghazvini and W.Mandemakers contributed equally to this work

While an important role for the POU domain transcription factor Oct-6 in the developing peripheral nerve has been well established, studies into its exact role in nerve development and regeneration have been hampered by the high mortality rate of newborn *Oct-6* mutant animals. In this study we have generated a Schwann cell-specific *Oct-6* allele through deletion of the Schwann cell-specific enhancer element (SCE) in the *Oct-6* locus. Analysis of mice homozygous for this allele (Δ*SCE* allele) reveals that rate-limiting levels of Oct-6 in Schwann cells are dependent on the SCE and that this element does not contribute to Oct-6 regulation in other cell types. We demonstrate a Schwann cell autonomous function for Oct-6 during nerve development as well as in regenerating nerve. Additionally, we show that Krox-20, an important regulatory target of Oct-6 in Schwann cells, is activated, with delayed kinetics, through an Oct-6-independent mechanism in these mice.

Keywords: enhancer/glia/myelin/Oct-6/POU domain

Introduction

Over the years, a considerable research effort has focused on how the myelination programme in Schwann cells is regulated. This cellular differentiation programme is characterized by dramatic metabolic and morphological changes, including polarization of the cell by deposition of a basal lamina, the production of massive amounts of cell membrane, incorporating myelin-specific lipids and proteins, and the spiralling of these lamellae around the axon (reviewed in Mezei, 1993; Garbay *et al*., 2000). The myelin organelle further matures into structurally and functionally distinct domains of compact and non-compact myelin such as the Schmidt–Lantermann incisures and paranodal loops (Arroyo and Scherer, 2000; Peles and Salzer, 2000; Pedraza *et al*., 2001). The synthesis and maintenance of myelin is an exquisitely sensitive process, as demonstrated by the many, inherited or acquired, demyelinating and dysmyelinating diseases such as Guillain-Barré Syndrome and the hereditary motor and sensory neuropathies. If we are to understand the interactions between glial cells and neurones that shape and maintain the functionally mature histo-architecture of the nerve or lead to pathogenesis, it is important to elucidate the molecular basis of the myelination programme.

Myelination involves the coordinate and sequential activation of sets of genes whose expression is controlled by transcription factors that are modulated during Schwann cell differentiation. While many transcription factors are known to be present in premyelinating and myelinating Schwann cells, two transcription factors have gained prominence in recent years for their important role in regulation of the myelination programme (Wegner, 2000; Topilko and Meijer, 2001). These transcription factors are the zinc finger protein Krox20 (Egr-2) and the POU-homeodomain protein Oct-6/SCIP/Tst-1 (referred to as Oct-6 in this paper) (Monuki *et al*., 1989; Meijer *et al*., 1990; Suzuki *et al*., 1990; Topilko *et al*., 1994). Both genes are dynamically expressed within the Schwann cell lineage, during development as well as during nerve regeneration, and their regulated expression depends on continued axonal contact (Scherer *et al*., 1994; Zorick *et al*., 1996). Genetic and cell biological studies have revealed that these transcription factors act in a genetic cascade (Topilko and Meijer, 2001). In promyelin Schwann cells, *Oct-6* expression is strongly increased in response to an unknown axonal contact-related signal and subsequently activates a set of genes that includes *Krox-20*. Induction of high-level Krox-20 expression leads to the activation of an additional set of genes including the major myelin genes and those involved in lipid metabolism (Nagarajan *et al*., 2001). Oct-6 is strongly down-regulated after the peak of myelination. A third transcription factor, Sox-10, is expressed throughout the development of the Schwann cell lineage and possibly interacts with both Oct-6 and Krox-20 in regulating their target genes (Kuhlbrodt *et al*., 1998).

Further study into the role of Oct-6 in nerve development and regeneration is hampered by the fact that *Oct-6* knock-out mice die shortly after birth because of breathing insufficiency, most likely caused by a defect in migration and differentiation of neurones in the brainstem (Bermingham *et al*., 1996). To circumvent this problem of early postnatal lethality, one would have to generate a viable Schwann cell-specific allele for *Oct-6*. Such a mouse would be of great value, allowing studies into the role of Oct-6 in nerve regeneration and allowing study of

Oct-6 protein domains, target genes and potential Oct-6 redundant proteins.

Recently, we have identified putative regulatory elements within the *Oct-6* locus using DNase I hypersensitivity mapping. Eight hypersensitive sites were mapped within a region of 35 kb. Using a deletion mapping approach in transgenic mice, we characterized a major *cis*-acting element within the *Oct-6* locus on which intracellular signalling pathways converge to activate *Oct-6* gene expression (Mandemakers *et al*., 2000). This element, the *Oct-6* Schwann cell enhancer or SCE, is characterized by two DNase I hypersensitive sites. The SCE was shown to be sufficient to drive regulated expression within the Schwann cell lineage of transgenic mice. However, endogenous *Oct-6* gene expression is not restricted to the Schwann cell lineage but is also expressed in the developing nervous system and skin. Expression is particularly high in the hippocampus, cortex, superior colliculus and brainstem nuclei, such as those of the hypoglossus and facial nerves (He *et al*., 1989; Alvarez-Bolado *et al*., 1995). No consistent transgene expression was observed in any of these brain regions in mice carrying a β-*galactosidase* reporter gene under the control of the SCE.

Based on these results, we hypothesized that deletion of the SCE from its normal chromosomal context would result in a Schwann cell-specific *Oct-6* null allele. To test this hypothesis, we have generated mice homozygous for this deletion allele, the Δ*SCE* allele, and found that *Oct-6* gene expression is affected in the Schwann cell lineage but not in any other cell type examined. These results demonstrate that the SCE is the decisive *cis*-regulating element governing Schwann cell-specific expression of the gene and that the SCE does not contribute to other aspects of the *Oct-6* expression pattern. Consequently, these mice, which are viable, have allowed us to study, for the first time, the role of Oct-6 in regeneration. Our results demonstrate that activation of *Oct-6* gene expression in reactive Schwann cells in regenerating nerves depends on the SCE and that the temporally correct activation of the myelination programme requires Oct-6. Also, our results demonstrate that the peripheral nerve phenotype observed in *Oct-6* mutant animals results from a loss of function of Oct-6 in Schwann cells and not in neurones. Additionally, we provide evidence that Oct-6 protein levels are rate limiting in the differentiation of promyelin Schwann cells into myelinating cells, demonstrating the importance of precise quantitative expression during development and regenerative processes. Furthermore, we show that *Krox-20* gene expression is activated in these mice with delayed kinetics, involving an Oct-6-independent mechanism.

Results

Deletion of the Oct-6 SCE through gene targeting

To delete the 4.3 kb SCE, a gene targeting vector was constructed in which the SCE was replaced with a *puromycin* selection cassette (Figure 1A). A negative selection cassette was introduced (*Py-TK*) flanking the 5′ homologous region, allowing counterselection of randomly integrated targeting constructs. The *puromycin* selection cassette was flanked by LoxP sites, which allowed deletion of the *puromycin* gene and its regulatory sequences from the targeted allele using Cre recombinase (Le and Sauer, 2001). Of the 141 embryonic stem (ES) cell clones that were puromycin resistant and ganciclovir insensitive, four were found to contain a homologous recombination event, as judged by Southern blot analysis (Figure 1B). Of those four, three had additional random integrations of the targeting cassette and were discarded. The one correctly targeted ES cell clone had a correct number of chromosomes and was used to generate chimeric mice. Chimeric animals were mated to *Zp3-Cre* transgenic female animals (D.Drabek). *Zp3-Cre* transgenic animals express high levels of the Cre recombinase in the oocyte, resulting in the removal of the puromycin cassette on the paternal chromosome in the zygote. Offspring in which the puromycin cassette was removed and the *Zp3-Cre* transgene was absent were identified using Southern blot analysis. These mice were used for further analysis.

Deletion of the SCE results in loss of Oct-6 expression in the Schwann cell lineage but not in other lineages

Adult mice heterozygous for the targeted allele, *Oct-6*$^{\Delta SCE/+}$, were intercrossed and offspring were genotyped. All three genotypes were represented in the offspring of these intercrosses at the expected Mendelian frequencies (out of 122 pups, 38 were *Oct-6*$^{\Delta SCE/\Delta SCE}$, 54 were *Oct-6*$^{\Delta SCE/+}$ and 30 were wild type). To examine whether Oct-6 expression in Schwann cells of the developing nerve was affected by the homozygous deletion of the SCE, we collected sciatic nerves from *Oct-6*$^{\Delta SCE/+}$ and *Oct-6*$^{\Delta SCE/\Delta SCE}$ pups at day 8 after birth and processed them for immunohistochemistry. While large numbers of Oct-6-positive Schwann cell nuclei were observed in nerves of *Oct-6*$^{\Delta SCE/+}$ animals, no Oct-6-positive nuclei were observed in the nerve of *Oct-6*$^{\Delta SCE/\Delta SCE}$ animals (Figure 2A and B). Thus, homozygous deletion of the SCE results in a strong reduction of Oct-6 expression to levels beyond detection in our immunohistochemistry experiment.

As mentioned above, *Oct-6*$^{\Delta SCE/\Delta SCE}$ and *Oct-6*$^{\Delta SCE/+}$ genotypes were found among the offspring of heterozygote crosses at the expected Mendelian ratios. In contrast, heterozygous crosses between mice carrying an insertional null allele for *Oct-6* (the *βgeo* allele) produced only a few offspring alive at 10 days post-partum, and homozygous for the null allele (Bermingham *et al*., 1996; Jaegle *et al*., 1996). It was found that most *Oct-6*$^{\beta geo/\beta geo}$ animals die of respiratory distress shortly after birth (Bermingham *et al*., 1996). This high incidence of lethality in newborn *Oct-6* null mice was attributed to a disorganization or reduction in cell number of cervical motor neurone groups of the phrenic nucleus and possibly medullar nuclei involved in breathing regulation, such as the nucleus tractus solitarius. Thus, the apparent lack of respiratory distress in neonatal *Oct-6*$^{\Delta SCE/\Delta SCE}$ mice suggests that the function of these nuclei is not affected by the deletion of the SCE. We therefore examined whether Oct-6 expression in a number of brain regions was affected by deletion of the SCE. We first examined Oct-6 expression in the medulla of the same animals as presented in Figure 2A and B. As can be seen in Figure 2C and D, Oct-6 is highly expressed in a subset of neurones in the nuclei of the hypoglossal nerve (XII) and the

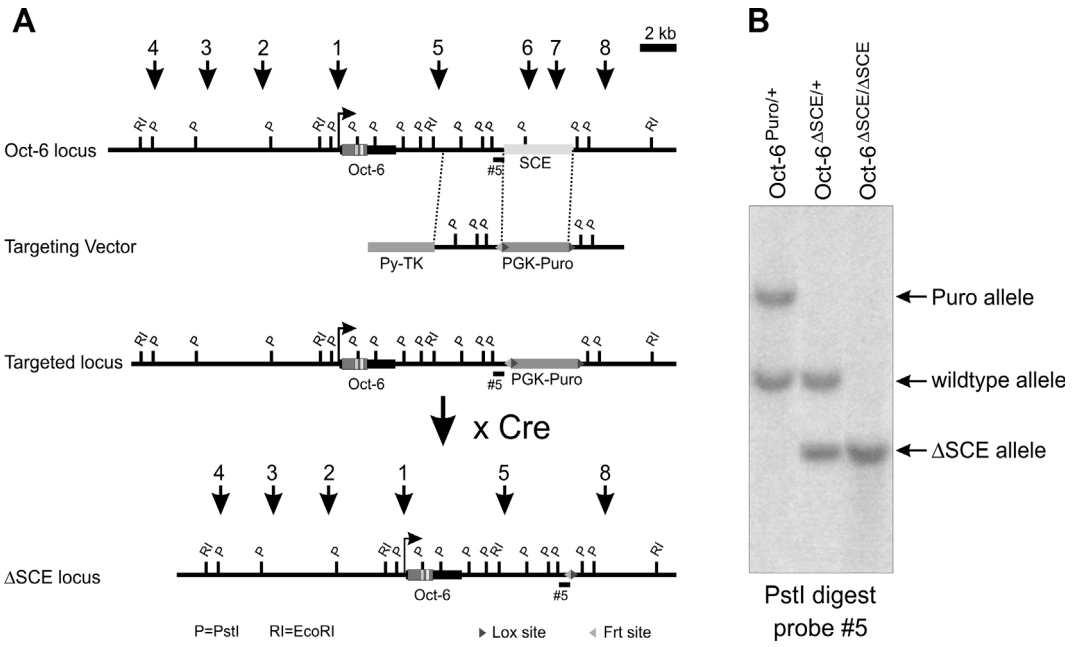

Fig. 1. Deletion of the 4.3 kb SCE from the *Oct-6* locus. (**A**) Gene targeting scheme for the *Oct-6* SCE. The SCE is indicated with a light green bar and is located ~12 kb downstream of the *Oct-6* gene CAP site. The intronless *Oct-6* transcription unit is indicated with a thick black line and the open reading frame is dark green with the POU-specific domain and POU homeodomain highlighted in blue and yellow, respectively. The relative positions of the mapped DNase I HSSs are indicated by numbered arrows. The SCE contains HSS6 and HSS7. In the targeting vector, a *puromycin* selection gene driven by the *pgk-1* promoter replaces the 4.3 kb *Hpa*I–*Msc*I fragment containing the SCE. LoxP sites (red triangles) flank the selection cassette, while an FRT site (green triangle) is present directly 5′ of the 5′ LoxP site. The orange box represents the counterselection cassette containing the HSV *TK* gene plus promoter linked to a polyoma virus enhancer. The probe used to identify the correctly targeted allele at the 5′ end is indicated (5). The locus after the predicted homologous recombination event and removal of the *puromycin* cassette by Cre recombinase is shown. (**B**) Southern analysis of mice carrying the targeted allele before and after removing the selection cassette. Using probe 5, the targeted allele is identified by a 3.5 kb *Pst*I fragment, while a 1.8 kb band identifies the wild-type allele. Removal of the selection cassette is demonstrated by the appearance of a 1.1 kb *Pst*I fragment with probe 5.

solitary tract. The identity of these Oct-6-positive neurones was confirmed by, in addition to anatomical criteria, immunostaining with antibodies directed against choline acetyltransferase, a general marker for cholinergic neurones (data not shown). Oct-6 expression in these neurones was not affected by the deletion of the SCE. In addition, we found that Oct-6 is normally expressed in neurones of the CA1 field of the hippocampus, putative amacrine neurones in the inner nuclear layer of the retina, superior colliculus and the skin (Figure 2E–H; data not shown). In fact we have not observed a tissue or cell type other than Schwann cells in which deletion of the SCE affects Oct-6 expression. These results demonstrate that deletion of the SCE from its normal genomic context leads to a severe reduction of *Oct-6* gene expression in Schwann cells, while expression in other tissues is not affected, thus providing a plausible explanation for the viability of Δ*SCE* homozygous animals. Thus, the SCE is required for Schwann cell-specific expression of the *Oct-6* gene, but does not contribute to regulation of the gene in other cell types.

Developmental delay in peripheral nerve development

Mice homozygous for complete loss-of-function alleles show delayed peripheral nerve development with Schwann cells transiently arrested at the promyelin stage of differentiation. It has been assumed that this developmental delay results from loss of Oct-6 function in the Schwann cell lineage. However, as Oct-6 is widely expressed during embryonic development throughout the neurectoderm, it is possible that part of the phenotype results from loss of Oct-6 function in neurones or their precursors (Alvarez-Bolado *et al.*, 1995; Zwart *et al.*, 1996). Analysis of peripheral nerve development in Δ*SCE* homozygous animals should resolve this issue, as in these animals Oct-6 expression is selectively lost in the Schwann cell lineage only. Therefore, we examined electron microscopically the developmental maturation of the sciatic nerve in *Oct-6*$^{\Delta SCE/+}$ and *Oct-6*$^{\Delta SCE/\Delta SCE}$ animals at different postnatal stages (Figure 3). In the sciatic nerve of heterozygous animals at postnatal day 4 (P4), many Schwann cells are actively myelinating, with significant numbers of cells still at the promyelin stage (Figure 3A). Four days later, at P8, most, if not all, prospective myelinating cells have progressed beyond the promyelin stage and are actively engaged in elaborating myelin around their associated axon (Figure 3C). In contrast, in nerves of animals homozygous for the SCE deletion, a majority of Schwann cells are found in a promyelin configuration during the first week of postnatal

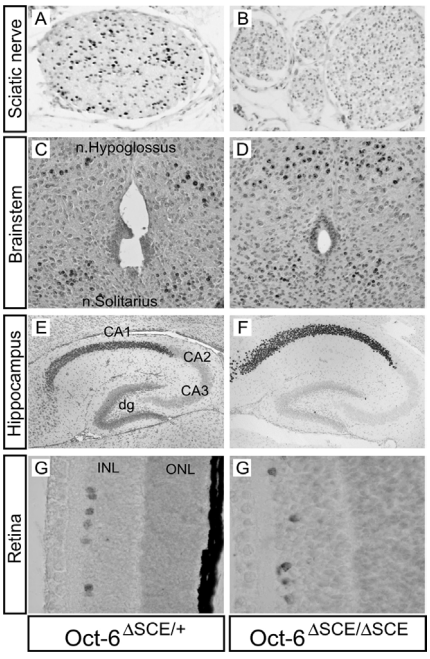

Fig. 2. The Δ*SCE* allele affects Oct-6 expression in the Schwann cell lineage only. (**A**) A brown precipitate identifies Oct-6 protein-expressing Schwann cell nuclei in transverse sections of sciatic nerve of *Oct-6*$^{\Delta SCE/+}$ mice at P8. (**B**) None of the Schwann cells in the sciatic nerve of *Oct-6*$^{\Delta SCE/\Delta SCE}$ mice expresses high levels of Oct-6 at this stage. In contrast, Oct-6 expression is not affected in the brainstem of *Oct-6*$^{\Delta SCE/\Delta SCE}$ mice, in particular the nucleus hypoglossus or nucleus solitarius [compare (**C**) and (**D**); P8]. Also, neurones in the hippocampal CA1 field express high levels of Oct-6 and this expression is not affected by the deletion of the SCE [compare (**E**) and (**F**); P8]. Oct-6 is expressed in a subset of neurones in the inner (INL) but not the outer (ONL) nuclear layer of the developing retina (P8). Although we made no further attempt to identify these neurones, their position within the nuclear layer corresponds to amacrine neurones. Again, expression of Oct-6 in these neurones is not affected by deletion of the SCE [compare (**G**) and (**H**)]. All paraffin sections are counterstained with haematoxylin.

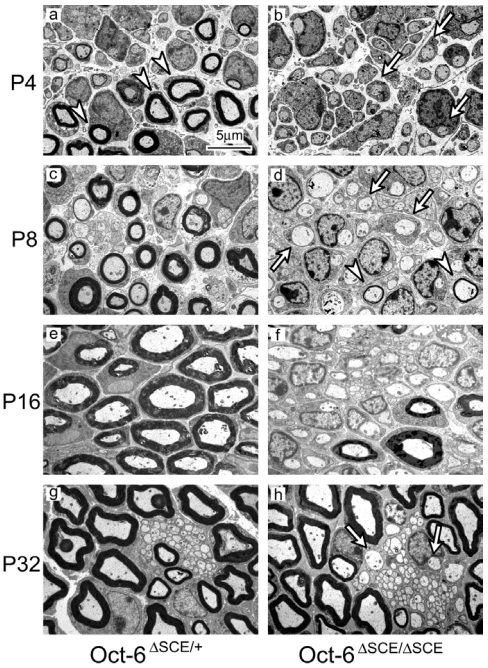

Fig. 3. Schwann cell differentiation is delayed at the promyelin stage in developing nerves of *Oct-6*$^{\Delta SCE/\Delta SCE}$ mice relative to heterozygous mice. (**A**–**H**) Representative electron micrographs of transverse sections through the sciatic nerve of homozygous and heterozygous animals at different postnatal stages of development. While condensed myelin figures are abundantly present at P4 in heterozygous animals [arrowheads in (A)], such myelin figures are only appearing at P8 in homozygous animals [arrowheads in (D)]. Most Schwann cells at P4 and P8 in homozygous animals are morphologically (and molecularly; see Figure 2) at the promyelin stage [arrows in (B) and (D)]. Promyelin figures are still found at P32 in mutant animals [arrows in (H)], while in heterozygous animals all myelin-competent Schwann cells are at later stages of myelination.

life (Figure 3B and D). Only in the second week are increasing numbers of myelinating cells observed (Figure 3F). By 4.5 weeks of postnatal development, most myelinating Schwann cells have elaborated myelin, although few promyelin figures are still observed at this time, especially around groups of non-myelinated low-calibre fibres (arrows in Figure 3H). Thus, while most prospective myelinating Schwann cells in heterozygous nerves have initiated myelination by P8, the vast majority of such cells in homozygous animals only do so between P16 and P32. These results suggest that the delay in nerve development, as observed in *Oct-6*$^{\beta geo/\beta geo}$ and *Oct-6*$^{\Delta SCE/\Delta SCE}$ mice, results primarily from loss of Oct-6 function in Schwann cells and not in neurones.

The SCE deletion is a Schwann cell-specific Oct-6 hypomorphic mutation

The developmental delay in peripheral nerves of mice homozygous for the Δ*SCE* allele appears slightly milder than that observed in mice homozygous for the *βgeo* allele (full knock out). This is particularly evident at P8 (Figure 4A). At this stage, no myelin figures are observed in the nerves of *Oct-6*$^{\beta geo/\beta geo}$ mice, while few myelin figures are present in the nerves of *Oct-6*$^{\Delta SCE/\Delta SCE}$ mice. This difference in severity of peripheral nerve phenotype could be due to non-Schwann cell autonomous or systemic effects of the *Oct-6 βgeo* allele that add to the Schwann cell autonomous effect. Alternatively, it is possible that the Δ*SCE* allele is a hypomorphic *Oct-6* allele characterized by low-level residual expression of Oct-6 protein not detected in our immunohistochemistry experiments (Figure 2A). We therefore examined Oct-6 expression at P8 in nerves of animals heterozygous or homozygous for the Δ*SCE* allele using the more sensitive western blotting technique (Figure 4B; see also Figure 6). Low amounts of Oct-6 protein are observed in P8 nerve extracts of *Oct-6*$^{\Delta SCE/\Delta SCE}$ mice, while *Oct-6*$^{\beta geo/\beta geo}$ mice do not express Oct-6 (data not shown). It is, therefore, likely that the Δ*SCE* allele is a strong hypomorphic allele.

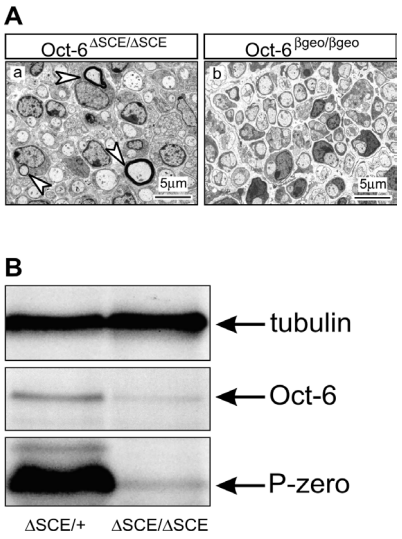

Fig. 4. The Δ*SCE* allele is a hypomorphic allele of *Oct-6*. (**A**) Comparison of sciatic nerve morphology in *Oct-6*$^{\Delta SCE/\Delta SCE}$ (a) and *Oct-6*$^{\beta geo/\beta geo}$ (b) mice at P8 reveals that a minority of Schwann cells in *Oct-6*$^{\Delta SCE/\Delta SCE}$ mice have progressed to form compact myelin (arrowheads). In contrast, all Schwann cells are still at the promyelin stage of differentiation in sciatic nerve of *Oct-6*$^{\beta geo/\beta geo}$ mice. (**B**) Mice homozygous for the Δ*SCE* allele express strongly reduced levels of Oct-6 in Schwann cells of the developing nerve at P8. Western blot experiments showing low levels of Oct-6 protein in nerve extracts from *Oct-6*$^{\Delta SCE/\Delta SCE}$ animals. The amounts of protein loaded per lane were similar, as demonstrated by the similar intensities of the α-tubulin immunoreactive band. In accordance with the delayed myelination status of sciatic nerve in *Oct-6*$^{\Delta SCE/\Delta SCE}$ animals, low levels of P-zero protein are detected at this stage. Nerve development in heterozygous mice is normal and myelinating Schwann cells express high levels of P-zero.

Krox-20 activation is delayed in Schwann cells of Oct-6$^{\Delta SCE/\Delta SCE}$ *mice*

Schwann cell differentiation is arrested at the promyelin stage in *Oct-6* and *Krox-20* null mice. However, this differentiation arrest is transient in *Oct-6* mutant mice, while the arrest is permanent in *Krox-20* null mice, although these mice die before 3 weeks of age. Previously, we have shown that one important target of Oct-6 regulation in myelinating Schwann cells is the zinc-finger transcription factor Krox-20 (Ghislain *et al*., 2002). In particular, we have shown that Krox-20 is not expressed in Schwann cells during the first week of postnatal development in *Oct-6* null mice. One could speculate that the failure to initiate myelination on schedule in *Oct-6* mutant animals results from a failure to activate *Krox-20* gene expression. The transient nature of the differentiation block in *Oct-6* mutant animals then suggests that *Krox-20* is activated at a later stage in an Oct-6-independent manner.

To address this question, we collected sciatic nerves of *Oct-6*$^{\Delta SCE/+}$ and *Oct-6*$^{\Delta SCE/\Delta SCE}$ mice at different postnatal stages, and examined the temporal expression of Oct-6 and Krox-20 and myelin protein P-zero by immunohistochemistry (Figure 5). P-zero is the major myelin protein in peripheral myelin and its accumulation in the compacting myelin sheath provides a convenient measure for the progression of myelin formation in the developing nerve (Greenfield *et al*., 1973). We first confirmed that Schwann cells in P8 *Oct-6*$^{\Delta SCE/+}$ nerves express high levels of Oct-6, while no Oct-6 expression was observed in Schwann cells of *Oct-6*$^{\Delta SCE/\Delta SCE}$ nerves (Figure 5A). Also, in agreement with our previous observations, Krox-20 expression is undetectable in P8 *Oct-6*$^{\Delta SCE/\Delta SCE}$ nerves, while Schwann cells in *Oct-6*$^{\Delta SCE/+}$ nerves do express Krox-20 at this stage (Ghislain *et al*., 2002). In addition, P-zero protein expression is severely reduced in Schwann cells of P8 nerves of *Oct-6*$^{\Delta SCE/\Delta SCE}$ animals. However, at P32, Krox-20 is expressed in Schwann cells in nerves of *Oct-6*$^{\Delta SCE/\Delta SCE}$ animals and extensive myelination is evident by the high level of P-zero immunoreactivity, showing characteristic ring structures in transverse sections (arrows in Figure 5I). Thus, in the absence of Oct-6 function, Krox-20 expression is eventually activated at the time extensive myelination is observed.

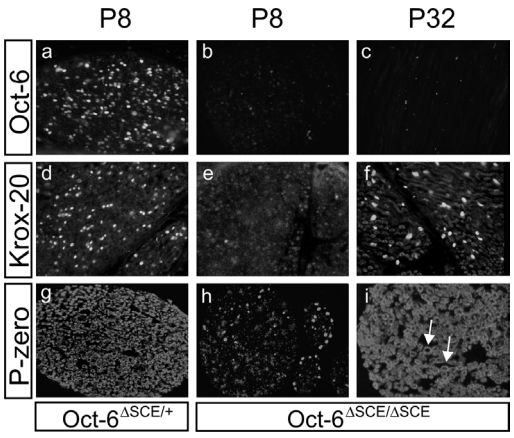

Fig. 5. Oct-6 expression is lost in Schwann cells of mice homozygous for the Δ*SCE* allele. (**A**) Homozygous deletion of the SCE results in loss of Oct-6 expression in Schwann cells of the developing nerve and delayed appearance of Krox-20 and the major myelin protein P-zero. Transverse sections of paraffin-embedded sciatic nerves at P8 or P32 from *Oct-6*$^{\Delta SCE/+}$ and *Oct-6*$^{\Delta SCE/\Delta SCE}$ mice were incubated with antibodies against Oct-6, Krox-20 or P-zero. P-zero immunoreactivity reveals the typical ring-like myelin structures indicated by arrows in (**I**).

Nerve regeneration

Oct-6 gene expression is strongly increased in reactive Schwann cells during nerve regeneration (Scherer *et al*., 1994; Zorick *et al*., 1996). Previous work has suggested that the SCE is sufficient to mediate this reactivation of *Oct-6* gene expression during regeneration (Mandemakers *et al*., 2000). However, in these experiments, the SCE was coupled to the *Oct-6* promoter and upstream region. It is, therefore, possible that activation of *Oct-6* gene expression in reactive Schwann cells is mediated through elements outside the SCE, such as the promoter. To assess whether the SCE is also necessary for reactivation of *Oct-6* gene expression and, if so, whether Oct-6 function is required in reactive Schwann cells in regenerating nerves, we first comparatively examined Oct-6 expression in regenerating nerves of *Oct-6*$^{\Delta SCE/+}$ and *Oct-6*$^{\Delta SCE/\Delta SCE}$ animals. Oct-6 is highly expressed in Schwann cells of the regenerating

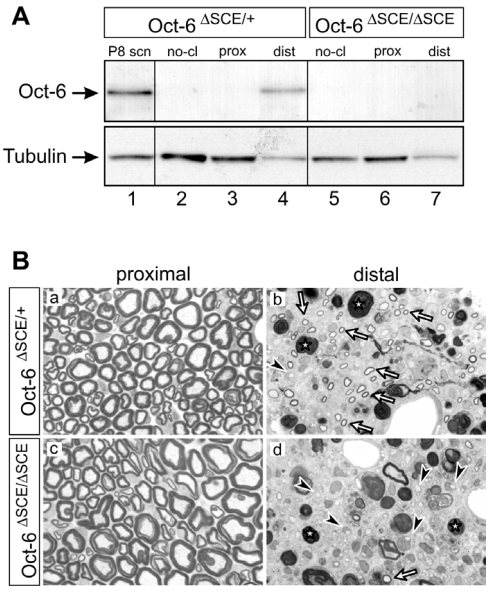

Fig. 6. Oct-6 regulation and function in the regenerating nerve. (**A**) Reactivation of Oct-6 expression is mediated through the SCE. Western blot analysis of sciatic nerves 12 days after crush lesion from adult *Oct-6*$^{\Delta SCE/+}$ (lanes 2–4) and *Oct-6*$^{\Delta SCE/\Delta SCE}$ mice (lanes 5–7). Nerves were divided in a proximal part (prox, lanes 3 and 6) and a distal part (dist, lanes 4 and 7) of equal length. Controls included are the undamaged nerves, contralateral to those operated on (no-cl, lanes 2 and 5), and developing sciatic nerve at P8 (P8 scn). Oct-6 is not expressed in Schwann cells of the adult nerve, while at P8, Schwann cells express high levels of Oct-6. Tubulin served as loading control. However, tubulin expression is reduced in the distal part of the regenerating nerve because of incomplete regeneration. (**B**) Schwann cell myelination is delayed in regenerating nerves of *Oct-6*$^{\Delta SCE/\Delta SCE}$ mice. Regenerating nerves, 12 days post-operation, were examined by light microscopy. Nerves were embedded in plastic and semi-thin sections were cut at 5 mm proximal (a and c) and 3 mm distal (b and d) to the lesion site. Sections were stained with ppd. In both genotypes, much myelin debris is still present (asterisk in b and d). Many regenerating fibres in the *Oct-6*$^{\Delta SCE/\Delta SCE}$ mouse are ensheathed by Schwann cells that have not elaborated compact myelin yet (arrowheads in b and d). In contrast, many compact myelin figures are found surrounding the regenerating fibres in *Oct-6*$^{\Delta SCE/+}$ mice (arrows in b and d).

distal nerve stump 8 days after axotomy (Scherer *et al*., 1994; Zorick *et al*., 1996; Mandemakers *et al*., 2000; Figure 6A). In contrast, Oct-6 expression is not detectable at this stage in the regenerating nerve of *Oct-6*$^{\Delta SCE/\Delta SCE}$ mice (Figure 6A). Thus, the SCE is also required for reactivation of *Oct-6* gene expression during regeneration.

We next examined how nerve regeneration at the morphological level was affected in the absence of *Oct-6* reactivation. The sciatic nerves of *Oct-6*$^{\Delta SCE/+}$ or *Oct-6*$^{\Delta SCE/\Delta SCE}$ animals were crush lesioned at mid-femoral level. The extent of regeneration was assessed by serial sectioning and microscopic analysis of the regenerating nerves. At 12 days post-transection, many regenerating axon fibres were seen at 3 mm distal of the lesion. In addition, we observed many myelin ovoids that had not been cleared yet by macrophages or had not been autophagocytosed (arrowheads in Figure 6B, b and d). The degree of degeneration and axonal ingrowth of the distal nerve stumps was similar in *Oct-6*$^{\Delta SCE/+}$ and *Oct-6*$^{\Delta SCE/\Delta SCE}$ nerves. Many regenerating nerve fibres are being actively myelinated in the *Oct-6*$^{\Delta SCE/+}$ nerves, as demonstrated by the many thin compact myelin figures (arrow in Figure 6B, b). In contrast, myelination of regenerating fibres in *Oct-6*$^{\Delta SCE/\Delta SCE}$ nerves was much less advanced at this stage. Many fibres that had not yet progressed beyond the promyelin stage of ensheathment and those that were myelinated had thinner myelin sheaths. These observations indicate that, as in development, myelination is delayed in the absence of *Oct-6* gene function.

Discussion

In the work described here, we have generated a viable and Schwann cell-specific *Oct-6* knock-out mouse through deletion of the SCE. Analysis of this mouse allowed us to address questions related to the regulation and function of Oct-6 during peripheral nerve development and regeneration.

Deletion of the SCE results in a Schwann cell-specific hypomorphic Oct-6 allele

An *Oct-6* allele in which the SCE is deleted was created through homologous recombination in ES cells and removal of the LoxP-flanked *puromycin* cassette by Cre recombinase. The selection cassette was removed as such cassettes have frequently been found to interfere with expression from the targeted locus (see for example McDevitt *et al*., 1997). Oct-6 expression was found to be severely reduced in the Schwann cell lineage of mice homozygous for the Δ*SCE* allele. These low residual levels of Oct-6 expression could be visualized only by western blotting (Figure 4) and electrophoretic mobility shift assays (not shown), and not by immunohistochemistry (Figures 2 and 3). We estimated that the residual level of Oct-6 expressed in the sciatic nerve at P8 is 5–10% of wild-type Oct-6 levels. These low levels of Oct-6 are not sufficient to sustain normal differentiation of Schwann cells, as *Oct-6*$^{\Delta SCE/\Delta SCE}$ mice exhibit a peripheral nerve phenotype that is only slightly less severe than that observed in *Oct-6*$^{\beta geo/\beta geo}$ mice.

Expression of Oct-6 in neurones in the hippocampus, brainstem and retina was not affected by the deletion of the SCE. These neurones express high levels of Oct-6 at the correct developmental time point. In fact, we have not found any cell lineage that normally expresses Oct-6 (apart from the Schwann cell lineage) in which Oct-6 expression was affected by deletion of the SCE. Thus, *Oct-6* expression in these cell types is under the control of additional elements within the *Oct-6* locus not requiring interaction with hypersensitive site (HSS) 6 and/or HSS7 within the SCE. Other regulatory elements may include some of the HSSs that we have mapped previously (see Figure 1; Mandemakers *et al*., 2000).

The fact that Oct-6 expression is selectively lost in Schwann cells while expression is not affected in neurones of homozygous Δ*SCE* mice helps to resolve the long-standing question of cell autonomy of the peripheral nerve phenotype in *Oct-6* mutant animals. Our results now unequivocally demonstrate that this phenotype results

from a loss of *Oct-6* function in Schwann cells and not in neurones.

Furthermore, it has been suggested previously that the high incidence of neonatal death of mice carrying a null allele (*βgeo* allele) of the *Oct-6* gene is caused primarily by migration or differentiation defects in neurones involved in breathing regulation, and not by defects in peripheral nerves as a consequence of delayed Schwann cell differentiation. The fact that the Δ*SCE* allele does not affect Oct-6 expression in these neurones and that *Oct-6*$^{\Delta SCE/\Delta SCE}$ animals are viable with no evidence of breathing problems, but with the same Schwann cell differentiation defect as in *Oct-6*$^{\beta geo/\beta geo}$ mice, strongly supports the notion that neonatal death in *Oct-6*$^{\beta geo/\beta geo}$ mice does indeed result from a neuronal defect, as originally suggested by Bermingham *et al*. (1996).

Function of the Oct-6 Schwann cell enhancer

Why is expression of *Oct-6* from the Δ*SCE* allele not completely lost in Schwann cells? Traditionally, enhancers have been thought to function by increasing the rate of transcription initiation from a linked promoter. In recent years, it has been shown that in some cases enhancers not so much influence the rate of transcription initiation, but instead increase the chance that a linked promoter is activated. In this probabilistic model, enhancers are thought to function through a mechanism that involves modifications to the local chromatin configuration or relocation to an active centre within the nucleus (Fiering *et al*., 2000; Hume, 2000). This model predicts that an enhancer increases the percentage of cells in a population expressing the gene. In transgenic mice experiments, such a mechanism might explain the often observed variegated expression of the transgene (Elliott *et al*., 1995; Milot *et al*., 1996). The low level of Oct-6 expression we observed in the developing nerve of *Oct-6*$^{\Delta SCE/\Delta SCE}$ animals could thus result from either a small number of Schwann cells expressing the gene at normal levels, or a very low expression in most Schwann cells. We did not observe individual Schwann cells expressing normal levels of Oct-6 in P8 *Oct-6*$^{\Delta SCE/\Delta SCE}$ nerves (see Figure 2B: a field containing >100 nuclei). Therefore, it appears that the SCE functions as a classical enhancer in Schwann cells by modulating the rate or the frequency of transcription of the linked gene.

The reduced levels of Oct-6 expressed in Schwann cells of *Oct-6*$^{\Delta SCE/\Delta SCE}$ mice result in a slightly less severe peripheral nerve phenotype than that observed in *Oct-6*$^{\beta geo/\beta geo}$ mice, which do not express Oct-6 at all. In particular, we found that the number of Schwann cells that have entered the myelinating phase of differentiation at P8 is lower in *Oct-6*$^{\beta geo/\beta geo}$ mice than in *Oct-6*$^{\Delta SCE/\Delta SCE}$ mice. These observations suggest that the level of Oct-6 determines the rate at which a Schwann cell progresses through the promyelin stage of differentiation. This suggests that increased levels of Oct-6 might result in an increased rate of differentiation of Schwann cells, potentially resulting in early onset of myelination and hypermyelination. Weinstein *et al*. (1995) have previously shown that expression of a mutant form of the Oct-6 protein (ΔSCIP) under the control of the P-zero promoter in Schwann cells of transgenic animals results in early onset of myelination and hypermyelination. Although these results were initially interpreted differently, involving a dominant-negative action of the ΔSCIP protein, more recent interpretation suggests that the protein acts as a dominant positive (Wu *et al*., 2001). This reinterpretation strongly suggests that the levels of Oct-6 are rate limiting in Schwann cell differentiation. Such transcription factor dose-dependent differentiation has also been demonstrated for a number of other systems, including the haematopoietic system (McDevitt *et al*., 1997; Vivian *et al*., 1999). For example, it has been demonstrated that 80% reduction in Gata-1 expression levels results in a decreased rate or efficiency of red blood cell maturation.

How would the rate of Schwann cell differentiation depend on the level of Oct-6 protein? It is possible that high levels of Oct-6 are needed to saturate all potential binding sites in the *cis*-acting elements of target genes. Lower levels of Oct-6 would then result in lower transcription rates of these targets and a longer time for the differentiation programme to complete. One potential target of Oct-6 is the *Krox-20* gene. The relevant *Krox-20* myelination-associated enhancer (MSE; myelinating Schwann cell element) contains at least one high-affinity Oct-6 binding site, and several lower-affinity binding sites (Ghislain *et al*., 2002). Although the relevance of these binding sites for *Krox-20* enhancer function has not been assessed genetically, it is possible that full *Krox-20* enhancer activation depends on maximum occupancy of the Oct-6 binding sites. In addition, high levels of Oct-6 protein might be required for efficient interaction with other proteins, such as Sox-10 (Kuhlbrodt *et al*., 1998). As these types of interaction are often of low affinity, high protein concentrations are needed. Following activation, Krox-20 expression is maintained through a mechanism that does not involve Oct-6.

We found that Krox-20 expression is activated through an Oct-6-independent mechanism in Schwann cells of Δ*SCE* homozygous animals, albeit with a delay of 10–14 days (Figure 5). Although it is not known whether this delayed activation is mediated through the *Krox-20* MSE, it is possible that an 'Oct-6-like' function, activated after the first week of postnatal development, is involved in Krox-20 activation. Recently, a potential candidate for this function has been postulated (Wu *et al*., 2001). *Brn-5*, a class VI POU domain gene, is expressed at higher levels in advanced stages of nerve development and expression is not dependent on Oct-6. Although the optimal DNA binding sequence for Brn-5 differs from that of Oct-6, both factors can bind to the octamer and octamer-related sequences present in the MSE (Rhee *et al*., 1998). If Brn-5 does indeed serve an Oct-6-redundant function in Schwann cell differentiation, it is expected that expression of Brn-5, from a transgenic construct controlled by the *Oct-6* SCE, will result in a substantial alleviation of the delayed myelination phenotype in an *Oct-6* mutant background. These experiments are currently under way.

Myelination is delayed in regenerating nerves in the absence of Oct-6

Using a nerve lesion paradigm that allows regeneration, we have shown that reactivation of *Oct-6* gene expression in reactive Schwann cells requires the SCE and that Oct-6 is important, as it is in development, for the progression of

Schwann cell differentiation. Both in developing and regenerating nerves, myelination is delayed in the absence of Oct-6. It is, therefore, most likely that the transcriptional programme regulated by Oct-6 is the same in Schwann cells during development as well as during regeneration. Furthermore, we did not observe differences between the two genotypes in the extent and numbers at which regenerating axons enter the distal nerve stump. Also, the extent of clearance of myelin debris did not differ between the two genotypes. Therefore, the Δ*SCE* allele has no obvious effect on Wallerian degeneration. Whether the delayed myelination in *Oct-6* mutant nerves results in reduced functional recovery of the regenerated nerve is not known.

Results presented here and elsewhere could be helpful in the development of strategies to improve peripheral nerve regeneration in several ways (Gondre *et al*., 1998; Mandemakers *et al*., 2000). First, the SCE would be an excellent choice for inclusion in gene therapy vehicles to express neurotrophic factors such as BDNF and GDNF in Schwann cells during a tight window of nerve regeneration. These factors have proven beneficial for regeneration and functional recovery (Xu *et al*., 1995; Menei *et al*., 1998; Terenghi, 1999; Ramer *et al*., 2000). The inclusion of the SCE in such vectors will alleviate complications that arise from continued administration of these factors to the lesioned nerve. Secondly, regenerated axons generally have a lower calibre, thinner myelin sheath and shorter internodes (Beuche and Friede, 1985). Based on the observation that Oct-6 protein levels are limiting in Schwann cell differentiation, we hypothesize that increased Oct-6 levels will increase the rate and extent of myelination of Schwann cells, resulting in restoration of myelin thickness and axonal diameter to near normal. We are currently testing this hypothesis.

In conclusion, we have generated a novel Schwann cell-specific allele of *Oct-6* through deletion of the major Schwann cell-specific regulatory element, the SCE. Analysis of these mice reveals a Schwann cell autonomous function for Oct-6 in nerve development and regeneration. We have further shown that Krox-20 is activated in Schwann cells of these mice through a mechanism that does not involve Oct-6. This new mouse mutant, together with the possibility to generate transgenic mice expressing genes selectively in the Schwannn cell lineage, provides a unique and excellent genetic system to address future questions related to the transcriptional targets of Oct-6, potential Oct-6 redundant functions in Schwann cell development, the study of functional domains of the Oct-6 protein and the role of Oct-6 in nerve regeneration.

Materials and methods

Targeting of the Oct-6 SCE

A genomic clone encompassing the 4.3 kb *Hpa*I–*Msc*I Schwann cell enhancer fragment was subcloned from cosmid clone pTBE 6Cos. From this clone, a 3.2 kb *Msc*I–*Hpa*I fragment, containing homologous genomic sequences 5′ of the SCE, was cloned behind the negative selection cassette py-TK. This selection cassette consists of the herpes simplex virus (HSV) *thymidine kinase* gene including its own promoter and a variant polyoma virus enhancer. A second clone was generated containing the *puromycin* resistance gene driven by the *phosphoglycerate kinase-1* (PGK) promoter. This clone was flanked on both sites by LoxP sites that have the same orientation. An FRT site was introduced immediately 5′ of the 5′ LoxP site. This also introduces a unique *Swa*I site at the 5′ end of this clone. Downstream of the 3′ LoxP site, a unique *Sna*BI site was used to introduce a 2.8 kb *Msc*I fragment containing the 3′ genomic homologous region. The entire fragment, encompassing the FRT–LoxP–PGK–puromycin–LoxP–3′ 2.8 kb *Msc*I, was excised as a *Swa*I–*Not*I fragment and cloned in the *Hpa*I–*Not*I-linearized Py-TK plasmid. This resulted in the targeting vector, as depicted in Figure 1A. The targeting vector was first linearized using *Not*I before electroporation into E14 ES cells. Electroporation and selection of cells in which homologous recombination had occurred were carried out as described. G418-resistant and ganciclovir-insensitive ES cell clones were screened for homologous recombination by Southern blotting of genomic DNA digested with *Pst*I using a ^{32}P-labelled DNA probe derived from the 5′ homologous region (see Figure 1A). Chimeric mice were generated by injection of ES cells from the correctly targeted clone into C57BL/6 blastocyst embryos. Chimeric males were crossed with FVB females and offspring were genotyped by Southern blotting of tail DNA digested with *Pst*I using the probe described above. Offspring carrying the chromosome with the targeted SCE allele were identified (see Figure 1B) and subsequently crossed to mice carrying the *Zp3-Cre* transgene to obtain offspring in which the *puromycin* cassette was removed. These mice were then inter-crossed to obtain mice homozygous for the deleted SCE allele (see Figure 1B).

Immunohistochemistry and western blotting

For western analysis, nerves were isolated and directly lysed in loading buffer, followed by sonication and heating in a boiling water bath. Equal amounts of nerve extracts were resolved on a 12.5% SDS–PAGE gel and transferred to a PVDF membrane (Millipore) by electroblotting. Membranes were blocked with 3% bovine serum albumin (BSA), 0.05% Tween-20 in phosphate-buffered saline (PBS) for 1 h at room temperature. Primary antibodies were diluted in blocking buffer and incubated overnight at room temperature. Primary antibodies used were an Oct-6 rabbit polyclonal antiserum used at 1:300 dilution (Jaegle *et al*., 1996), a P-zero mouse monoclonal (clone P07; Archelos *et al*., 1993) used at 1:1000 dilution, a tubulin antibody (Sigma T-6793) and a rabbit Krox-20 antibody. Filters were subsequently washed five times in 0.5% Tween-20 in PBS and incubated with secondary antibodies conjugated with horseradish peroxidase or alkaline phosphatase (Dako) for 1 h in blocking buffer. Following five washes in 0.5% Tween-20 in PBS, the antigens were visualized by luminol (in the case of horseradish peroxidase) or NBT/BCIP (in the case of alkaline phosphatase) detection methods.

For immunohistochemistry, paraffin sections were dewaxed in xylene and rehydrated in a descending series of alcohol. Sections were blocked in 1% BSA, 0.05% Tween-20/PBS for 2 h at room temperature. Primary antibodies were diluted in blocking buffer and incubated overnight at room temperature. Secondary antibodies used were Oregon Green-conjugated goat anti-rabbit IgGs (Molecular Probes) and Texas Red-conjugated goat anti-mouse IgGs (Molecular Probes). Cell nuclei were visualized by DAPI staining.

Electron microscope analysis

Wild-type and mutant littermates (P4–P32) were anaesthetized with pentobarbital and perfused transcardially, first with PBS followed by 3% paraformaldehyde/1% glutaraldehyde in 100 mM cacodylate buffer pH 7.3. Sciatic nerves were dissected out and immersion fixed overnight in the same fixative or formalin at 4°C. Nerves were then rinsed in 100 mM cacodylate and postfixed in 1% osmium tetroxide/ferricyanide in 100 mM cacodylate overnight at 4°C. Following dehydration through an ascending alcohol series, nerves were embedded in Epon resin as described. One-micrometre sections were cut, mounted on a microscope slide and stained with paraphenylenediamine (ppd; Estable-Puig *et al*., 1965). Sections were examined under an Olympus BX40 light microscope and photographed using an Olympus DP50 digital camera. For electron microscopy, sections were cut at 50–60 nm and mounted on grids. Sections were contrasted with lead acetate and uranyl citrate, and examined using a Philips CM100 transmission electron microscope. Photographs were taken using a Megaview II digital camera.

Animal surgery

Young adult mice were anaesthetized by inhalation of halothane and placed on a heating pad. The sciatic nerve in the left leg was exposed and crushed for two times 15 s at the midfemoral level using No. 5 biology forceps. Animals were killed 12 days after the operation and the lesioned and contralateral nerves were isolated for western analysis. For light and

electron microscope analysis, animals were perfused as described in the previous section.

Acknowledgements

The authors wish to thank Sjaak Philipsen, David Whyat, Elaine Dzierzak and Ben Barres for their critical comments on the manuscript. Juan José Archelos (University of Graz) is thanked for the monoclonal antibody against P-zero protein (clone P07). Hans van den Berg's assistance in animal surgery procedures is greatly acknowledged. Dubi Drabek generated the *Zp3-Cre* transgenic mouse. This work was funded by grants from the Dutch research council (ALW 805-17.281 and MW 903-42-195) and the European Community (Biomed 2 PLp62069).

References

Alvarez-Bolado,G., Rosenfeld,M.G. and Swanson,L.W. (1995) Model of forebrain regionalization based on spatiotemporal patterns of POU-III homeobox gene expression, birthdates and morphological features. *J. Comp. Neurol.*, **355**, 237–295.

Archelos,J.J., Roggenbuck,K., Schneider-Schaulies,J., Linington,C., Toyka,K.V. and Hartung,H.P. (1993) Production and characterization of monoclonal antibodies to the extracellular domain of P0. *J. Neurosci. Res.*, **35**, 46–53.

Arroyo,E.J. and Scherer,S.S. (2000) On the molecular architecture of myelinated fibers. *Histochem. Cell Biol.*, **113**, 1–18.

Bermingham,J.R., Scherer,S.S., O'Connell,S., Arroyo,E., Kalla,K.A., Powell,F.L. and Rosenfeld,M.G. (1996) Tst-1/Oct-6/SCIP regulates a unique step in peripheral myelination and is required for normal respiration. *Genes Dev.*, **10**, 1751–1762.

Beuche,W. and Friede,R.L. (1985) A new approach toward analyzing peripheral nerve fiber populations. II. Foreshortening of regenerated internodes corresponds to reduced sheath thickness. *J. Neuropathol. Exp. Neurol.*, **44**, 73–84.

Elliott,J.I., Festenstein,R., Tolaini,M. and Kioussis,D. (1995) Random activation of a transgene under the control of a hybrid hCD2 locus control region/Ig enhancer regulatory element. *EMBO J.*, **14**, 575–584.

Estable-Puig,J.F., Bauer,W.C. and Blumberg,J.M. (1965) Technical note: paraphenylenediamine staining of osmium-fixed plastic embedded tissue for light and phase microscopy. *J. Neuropathol. Exp. Neurol.*, **24**, 531–536.

Fiering,S., Whitelaw,E. and Martin,D.I. (2000) To be or not to be active: the stochastic nature of enhancer action. *BioEssays*, **22**, 381–387.

Garbay,B., Heape,A.M., Sargueil,F. and Cassagne,C. (2000) Myelin synthesis in the peripheral nervous system. *Prog. Neurobiol.*, **61**, 267–304.

Ghislain,J., Desmarquet-Trin-Dinh,C., Jaegle,M., Meijer,D., Charnay,P. and Frain,M. (2002) Characterisation of *cis*-acting sequences reveals a biphasic, axon-dependent regulation of Krox20 during Schwann cell development. *Development*, **129**, 155–166.

Gondre,M., Burrola,P. and Weinstein,D.E. (1998) Accelerated nerve regeneration mediated by Schwann cells expressing a mutant form of the POU protein SCIP. *J. Cell Biol.*, **141**, 493–501.

Greenfield,S., Brostoff,S., Eylar,E.H. and Morell,P. (1973) Protein composition of myelin of the peripheral nervous system. *J. Neurochem.*, **20**, 1207–1216.

He,X., Treacy,M.N., Simmons,D.M., Ingraham,H.A., Swanson,L.W. and Rosenfeld,M.G. (1989) Expression of a large family of POU-domain regulatory genes in mammalian brain development. *Nature*, **340**, 35–41.

Hume,D.A. (2000) Probability in transcriptional regulation and its implications for leukocyte differentiation and inducible gene expression. *Blood*, **96**, 2323–2328.

Jaegle,M., Mandemakers,W., Broos,L., Zwart,R., Karis,A., Visser,P., Grosveld,F. and Meijer,D. (1996) The POU factor Oct-6 and Schwann cell differentiation. *Science*, **273**, 507–510.

Kuhlbrodt,K., Herbarth,B., Sock,E., Enderich,J., Hermans-Borgmeyer,I. and Wegner,M. (1998) Cooperative function of POU proteins and SOX proteins in glial cells. *J. Biol. Chem.*, **273**, 16050–16057.

Le,Y. and Sauer,B. (2001) Conditional gene knockout using Cre recombinase. *Mol. Biotechnol.*, **17**, 269–275.

Mandemakers,W., Zwart,R., Jaegle,M., Walbeehm,E., Visser,P., Grosveld,F. and Meijer,D. (2000) A distal Schwann cell-specific enhancer mediates axonal regulation of the Oct-6 transcription factor during peripheral nerve development and regeneration. *EMBO J.*, **19**, 2992–3003.

McDevitt,M.A., Shivdasani,R.A., Fujiwara,Y., Yang,H. and Orkin,S.H. (1997) A 'knockdown' mutation created by *cis*-element gene targeting reveals the dependence of erythroid cell maturation on the level of transcription factor GATA-1. *Proc. Natl Acad. Sci. USA*, **94**, 6781–6785.

Meijer,D., Graus,A., Kraay,R., Langeveld,A., Mulder,M.P. and Grosveld,G. (1990) The octamer binding factor Oct6: cDNA cloning and expression in early embryonic cells. *Nucleic Acids Res.*, **18**, 7357–7365.

Menei,P., Montero-Menei,C., Whittemore,S.R., Bunge,R.P. and Bunge,M.B. (1998) Schwann cells genetically modified to secrete human BDNF promote enhanced axonal regrowth across transected adult rat spinal cord. *Eur. J. Neurosci.*, **10**, 607–621.

Mezei,C. (1993) Myelination in the peripheral nerve during development. In Griffin,J.W., Low,P.A. and Poduslo,J.F. (eds), *Peripheral Neuropathy*. W.B.Saunders Co., Philadelphia, PA, pp. 267–281.

Milot,E. *et al*. (1996) Heterochromatin effects on the frequency and duration of LCR-mediated gene transcription. *Cell*, **87**, 105–114.

Monuki,E.S., Weinmaster,G., Kuhn,R. and Lemke,G. (1989) SCIP: a glial POU domain gene regulated by cyclic AMP. *Neuron*, **3**, 783–793.

Nagarajan,R., Svaren,J., Le,N., Araki,T., Watson,M. and Milbrandt,J. (2001) EGR2 mutations in inherited neuropathies dominant-negatively inhibit myelin gene expression. *Neuron*, **30**, 355–368.

Pedraza,L., Huang,J.K. and Colman,D.R. (2001) Organizing principles of the axoglial apparatus. *Neuron*, **30**, 335–344.

Peles,E. and Salzer,J.L. (2000) Molecular domains of myelinated axons. *Curr. Opin. Neurobiol.*, **10**, 558–565.

Ramer,M.S., Priestley,J.V. and McMahon,S.B. (2000) Functional regeneration of sensory axons into the adult spinal cord. *Nature*, **403**, 312–316.

Rhee,J.M., Gruber,C.A., Brodie,T.B., Trieu,M. and Turner,E.E. (1998) Highly cooperative homodimerization is a conserved property of neural POU proteins. *J. Biol. Chem.*, **273**, 34196–34205.

Scherer,S.S., Wang,D.Y., Kuhn,R., Lemke,G., Wrabetz,L. and Kamholz,J. (1994) Axons regulate Schwann cell expression of the POU transcription factor SCIP. *J. Neurosci.*, **14**, 1930–1942.

Suzuki,N., Rohdewohld,H., Neuman,T., Gruss,P. and Scholer,H.R. (1990) Oct-6: a POU transcription factor expressed in embryonal stem cells and in the developing brain. *EMBO J.*, **9**, 3723–3732.

Terenghi,G. (1999) Peripheral nerve regeneration and neurotrophic factors. *J. Anat.*, **194**, 1–14.

Topilko,P. and Meijer,D. (2001) Transcription factors that control Schwann cell development and myelination. In Jessen,K.R. and Richardson,W.D. (eds), *Glial Cell Development: Basic Principles and Clinical Relevance*. Oxford University Press, Oxford, UK, pp. 223–244.

Topilko,P., Schneider-Maunoury,S., Levi,G., Baron-Van Evercooren,A., Chennoufi,A.B., Seitanidou,T., Babinet,C. and Charnay,P. (1994) Krox-20 controls myelination in the peripheral nervous system. *Nature*, **371**, 796–799.

Vivian,J.L., Gan,L., Olson,E.N. and Klein,W.H. (1999) A hypomorphic myogenin allele reveals distinct myogenin expression levels required for viability, skeletal muscle development and sternum formation. *Dev. Biol.*, **208**, 44–55.

Wegner,M. (2000) Transcriptional control in myelinating glia: flavors and spices. *Glia*, **31**, 1–14.

Weinstein,D.E., Burrola,P.G. and Lemke,G. (1995) Premature Schwann cell differentiation and hypermyelination in mice expressing a targeted antagonist of the POU transcription factor SCIP. *Mol. Cell. Neurosci.*, **6**, 212–229.

Wu,R., Jurek,M., Sundarababu,S. and Weinstein,D.E. (2001) The POU gene *Brn-5* is induced by neuregulin and is restricted to myelinating Schwann cells. *Mol. Cell. Neurosci.*, **17**, 683–695.

Xu,X.M., Guenard,V., Kleitman,N., Aebischer,P. and Bunge,M.B. (1995) A combination of BDNF and NT-3 promotes supraspinal axonal regeneration into Schwann cell grafts in adult rat thoracic spinal cord. *Exp. Neurol.*, **134**, 261–272.

Zorick,T.S., Syroid,D.E., Arroyo,E., Scherer,S.S. and Lemke,G. (1996) The transcription factors SCIP and Krox-20 mark distinct stages and cell fates in Schwann cell differentiation. *Mol. Cell. Neurosci.*, **8**, 129–145.

Zwart,R., Broos,L., Grosveld,G. and Meijer,D. (1996) The restricted expression pattern of the POU factor Oct-6 during early development of the mouse nervous system. *Mech. Dev.*, **54**, 185–194.

Received May 22, 2002; revised July 15, 2002; accepted July 17, 2002

Chapter 3

The POU proteins Brn-2 and Oct-6 share important functions in Schwann cell development

Martine Jaegle, Mehrnaz Ghazvini, Wim Mandemakers, Marko Piirsoo, Siska Driegen, Françoise Levavasseur, Smiriti Raghoenath, Frank Grosveld, and Dies Meijer

Genes and Development, 2003

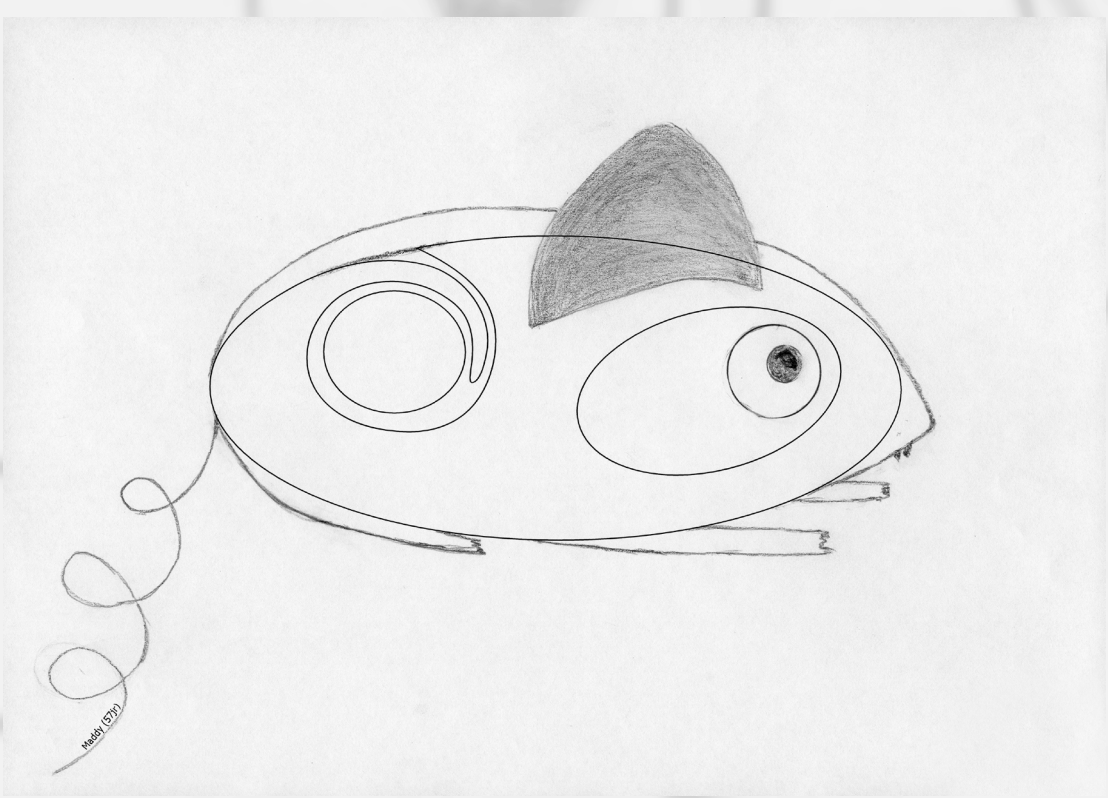

The POU proteins Brn-2 and Oct-6 share important functions in Schwann cell development

Martine Jaegle,[1] Mehrnaz Ghazvini,[1] Wim Mandemakers,[1,3] Marko Piirsoo,[1,4] Siska Driegen,[1,2] Françoise Levavasseur,[1] Smiriti Raghoenath,[1] Frank Grosveld,[1] and Dies Meijer[1,5]

Departments of [1]Cell Biology and Genetics and [2]Neurosciences, Erasmus University Medical Center, 3000DR Rotterdam, Netherlands

The genetic hierarchy that controls myelination of peripheral nerves by Schwann cells includes the POU domain Oct-6/Scip/Tst-1 and the zinc-finger Krox-20/Egr2 transcription factors. These pivotal transcription factors act to control the onset of myelination during development and tissue regeneration in adults following damage. In this report we demonstrate the involvement of a third transcription factor, the POU domain factor Brn-2. We show that Schwann cells express Brn-2 in a developmental profile similar to that of Oct-6 and that *Brn-2* gene activation does not depend on Oct-6. Overexpression of Brn-2 in Oct-6-deficient Schwann cells, under control of the *Oct-6* Schwann cell enhancer (SCE), results in partial rescue of the developmental delay phenotype, whereas compound disruption of both *Brn-2* and *Oct-6* results in a much more severe phenotype. Together these data strongly indicate that Brn-2 function largely overlaps with that of Oct-6 in driving the transition from promyelinating to myelinating Schwann cells.

[*Keywords*: POU domain; myelin; Schwann cell; nerve development]

Received December 20, 2002; revised version accepted April 10, 2003.

The high conduction velocity of nerve fibers is a hallmark of the nervous system of higher vertebrates and depends on structural and molecular specializations that are elaborated during development. These specializations occur through intimate and continued interactions between the neuron and its associated glial cells and result in the elaboration by glial cells of myelin, the important membranous structure that ensheaths and insulates axons (Arroyo and Scherer 2000; Fields and Stevens-Graham 2002; Mirsky et al. 2002). Two glial cell types produce myelin: the oligodendrocyte in the central nervous system (CNS) and the Schwann cell in the peripheral nervous system (PNS). Although very similarly organized, the molecular composition of CNS and PNS myelin differs significantly, and oligodendrocytes and Schwann cells have adopted different, but overlapping, sets of transcriptional regulators to coordinate myelogenesis (Hudson 2001; Topilko and Meijer 2001). These differences reflect their distinct embryonic origins. Whereas oligodendrocytes originate from the neuroepithelial precursors that line the lumen of the spinal cord and ventricles of the brain, Schwann cells derive mainly from the neural crest, a transient embryonic stem (ES) cell population that generates a wide variety of cell types including sensory and autonomic neurons and melanocytes (Le Douarin and Kalcheim 1999; Richardson 2001). Schwann cell precursors populate the early outgrowing nerve bundles, where they proliferate and segregate individual and groups of fibers until the number of Schwann cells and fibers is eventually matched. During the first few days of postnatal development, many Schwann cells establish a 1:1 relationship with axons, cease to proliferate, and initiate myelin formation such that by the end of the first postnatal week of development, all myelin-competent axons are actively being myelinated. Schwann cells that remain associated with groups of lower-caliber fibers will segregate these fibers in cytoplasmic cuffs without myelinating them (Webster 1993). Although virtually nothing is known about the molecular identity of the axon-associated signal(s) that divert Schwann cells along either a myelinating or a nonmyelinating differentiation pathway, significant information has accumulated in recent years about the transcription factors involved in Schwann cell differentiation and myelination.

To date, several transcription factors have been found to be involved in the differentiation of Schwann cells and include the zinc-finger protein Krox20 (Egr-2), the Sry box protein Sox10, and the POU domain protein Pou3f1/

Present addresses: [3]Department of Neurobiology, Stanford University, School of Medicine, Stanford, CA 94305, USA; [4]National Institute of Chemical Physics and Biophysics, Tallinn EE0026, Estonia.
[5]Corresponding author.
E-MAIL d.meijer@erasmusmc.nl; FAX 31-10-408-9468.
Article and publication are at http://www.genesdev.org/cgi/doi/10.1101/gad.258203.

Oct-6/Scip/Tst-1 (referred to here as Oct-6; Topilko and Meijer 2001). Gene targeting experiments in mice have revealed insight into the functional roles of each of these factors and their possible order within a genetic hierarchy. Sox10 is required early in development for the establishment and/or maintenance of Schwann cell precursors from the neural crest (Britsch et al. 2001). At later stages of development, Oct-6 and Krox20 are both required for the differentiation of myelinating Schwann cells at two respective progressive steps in the genetic hierarchy (Topilko et al. 1994; Bermingham et al. 1996; Jaegle et al. 1996; Ghislain et al. 2002). During fetal development, Oct-6 gene expression is induced in immature Schwann cells and peaks in promyelinating and early myelinating cells during the first week of postnatal life (Scherer et al. 1994; Blanchard et al. 1996; Arroyo et al. 1998). Consequently, Oct-6 regulates a set of downstream genes that includes Krox-20 (Blanchard et al. 1996; Ghislain et al. 2002). Krox-20 regulates an additional set of target genes including the major myelin genes and those involved in lipid metabolism (Nagarajan et al. 2001). In addition, Sox10 may continue to participate in these transcription programs, as it interacts with both Oct-6 and Krox20 when bound to adjacent DNA-binding sites (Kuhlbrodt et al. 1998b).

Schwann cell differentiation in nerves of *Krox20* or *Oct-6*-deficient mice is arrested at the promyelin stage (Topilko et al. 1994; Bermingham et al. 1996; Jaegle et al. 1996). However, this differentiation block in *Krox20*$^{-/-}$ mice is permanent, and is transient in *Oct-6* mutant animals (*Oct-6*$^{\beta geo/\beta geo}$). Thus, *Oct-6*$^{\beta geo/\beta geo}$ Schwann cells do eventually activate Krox20 expression and commence myelination, albeit with a delay of 7–10 d, thus suggesting some functional redundancy in the genetic program (Ghazvini et al. 2002). We previously proposed that the transient nature of the differentiation block is the result of an unknown Oct-6-like activity in Schwann cells, with this putative factor acting at a later developmental time than Oct-6 in the Schwann cell lineage (Jaegle and Meijer 1998). Alternatively, the transient block could be the result of a factor that regulates part or all of the transcriptional targets of Oct-6, but does so less efficiently. The most likely candidates for this Oct-6-like activity are the other members of the POU domain transcription factor family, of which there are 15 members in mammals (Ryan and Rosenfeld 1997). Interestingly, two POU domain transcription factors, Brn-1 and Brn-2, have virtually identical DNA-binding characteristics compared to Oct-6. Hence, to provide insight into the genetic program acting alongside Oct-6 in promyelinating Schwann cells, we examined the expression and function of the candidate POU domain transcription factors during development and in Oct-6-deficient mice.

In this report, we show that Schwann cells express Brn-2 in a developmental profile similar to that of Oct-6. We demonstrate that *Brn-2* gene activation is independent of Oct-6, but that Oct-6 negatively regulates Brn-2 expression levels. Higher expression levels of Brn-2 in *Oct-6* mutant Schwann cells result in a partial rescue of the developmental delay phenotype, whereas homozygous deletion of *Brn-2* in *Oct-6* mutant Schwann cells results in a more severe phenotype. Together these data strongly indicate that Brn-2 function largely overlaps with that of Oct-6 in driving the transition from promyelinating to myelinating Schwann cells.

Results

Brn-2 is expressed and regulated in Schwann cells in a manner similar to Oct-6

The transient nature of the Schwann cell defect in Oct-6-deficient mice suggested some redundancy in transcription factor function. Interestingly, previous work on the expression of octamer binding factors Oct-6 and Oct-1 in the developing chick sciatic nerve suggested the presence of a novel octamer-binding activity and possibly a homologous candidate factor involved in developing mouse sciatic nerves (Levavasseur et al. 1998). Hence, to examine the developmental expression profile of this novel binding activity, we performed electrophoretic mobility shift assays (EMSAs) using whole sciatic nerve extracts derived from chick embryos and young chicks. Three complexes can be distinguished (Fig. 1A). The largest complex contains Oct-1, a ubiquitous POU factor, the levels of which are relatively constant at all stages of nerve development (Blanchard et al. 1996). In contrast, the smallest and fastest migrating Oct-6-containing complex is strongly regulated during development. Like in rodents, Oct-6 expression peaks in promyelinating and early myelinating cells (embryonic day 17 and 20; E17 and E20 in Fig. 1A) and is sharply downregulated at later stages of myelination (postnatal day 3; P3). The third, intermediate complex (X) is regulated similarly to Oct-6, but its expression is maintained at reduced levels at later stages (P20 in Fig. 1A). Using different octamer-related DNA-binding sites, such as the HSV1 TAATGARAT motif, and a mutated octamer motif, we found that this novel activity demonstrated binding site preferences very similar to those of Oct-6 (data not shown).

To identify the protein in this complex, we performed EMSA experiments in the presence of antisera against several POU proteins closely related to Oct-6. Although the mobility or intensity of the intermediate complex X was not affected by antibodies against the chicken Oct-6 protein (Fig. 1B, middle lane), a Brn-2-specific goat antiserum strongly reduced the intensity of this complex, thus identifying the protein in the intermediate complex as Brn-2 (Fig. 1B, right lane).

Until recently, expression of Brn-2 in mammalian peripheral nerves had not been described and, paradoxically, only one octamer complex, in addition to Oct-1, had been observed in cultured rat Schwann cells (Kuhn et al. 1991; Sim et al. 2002). Therefore, we next examined the presence of Brn-2-binding activity in the developing sciatic nerve of the mouse at P4 by EMSA. In accordance with previous data, only one prominent protein/DNA complex, in addition to the Oct-1/DNA complex, was observed (Fig. 1C, lane 1). However, in supershift assays

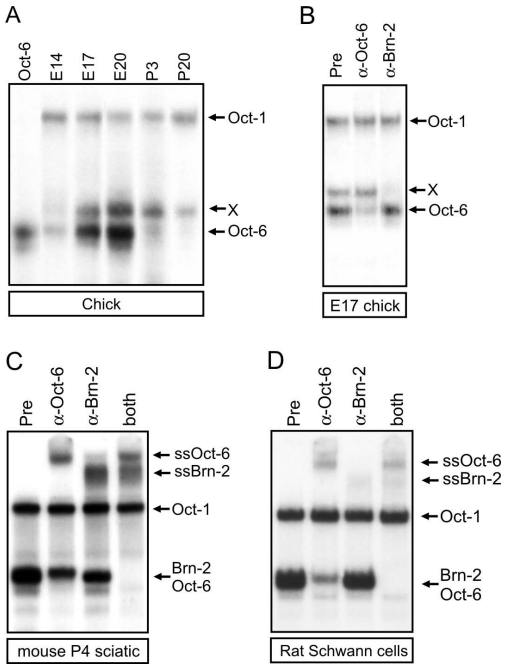

Figure 1. Brn-2 is expressed in chick and mouse sciatic nerves. (*A*) Developmental expression of a novel octamer-binding complex was examined by EMSA using freeze-thaw extracts from chicken nerves at different stages of development [embryonal stages E14, E17, and E20 and postnatal days 3 (P3) and 20 (P20)]. Whole-cell extracts of COS cells expressing chicken Oct-6 (Oct-6) served as a control (Meijer et al. 1990). Free probe is not shown, but all experiments were performed in probe excess. (*B*) Using E17 chick embryonic nerve, extracts identify Brn-2 in complex X, as antibodies directed against the C-terminal part of mouse Brn-2 specifically affect complex X, whereas chicken Oct-6 antibodies (α-Oct-6) affect the Oct-6 complex but not complex X. Preimmune serum (Pre) does not affect either complex. (*C*) Brn-2 is expressed in mouse nerves. Incubation of Oct-6-specific antibodies with P4 mouse whole-nerve extracts and an octamer probe results in the formation of a ternary complex (supershift Oct-6 complex; ssOct-6) and unmasks another complex that is specifically supershifted (ssBrn-2) with mouse Brn-2 antibodies (α-Brn-2). When both antibodies are added all complexes are shifted, demonstrating that no other complexes comigrate with the Oct-6/DNA and Brn-2/DNA complexes. (*D*) Brn-2 is expressed in the Schwann cell lineage. Whole-cell extracts from cultured rat Schwann cells grown in the presence of 20 μM forskolin for 36 h were incubated with the octamer probe in presence of the indicated sera. As in *C*, Oct-6- and Brn-2-specific antibodies identify two comigrating Oct-6 and Brn-2 protein DNA complexes.

using antibodies specific for Oct-6 and Brn-2, this band was found to be composed of two complexes, a Brn-2/DNA complex and an Oct-6/DNA complex (Fig. 1D, lanes 2–4). Thus, Brn-2 protein is expressed in both the developing chick and murine nerve.

Because sciatic nerve extracts are heterogeneous, it is possible that Brn-2 is expressed exclusively in cell types other than Schwann cells, such as endothelial or perineural cells. We therefore examined expression of Brn-2 in pure differentiating primary rat Schwann cell cultures using EMSA (Fig. 1D). These cells express high levels of Oct-6 and moderate levels of Brn-2 (Fig. 1D, cf. lanes 2 and 3). Thus, Brn-2 is expressed in the Schwann cell lineage and is therefore an attractive candidate for the putative Oct-6 like function.

Brn-2 is expressed in Oct-6-deficient Schwann cells

We next examined whether Brn-2 expression is affected by loss of Oct-6 function in Schwann cells. As the vast majority of full *Oct-6* knockout animals (*Oct-6*$^{\beta geo/\beta geo}$) are not viable and die shortly after birth, thus precluding studies at postnatal stages of development, we used in this study animals that carry on one chromosome a full knockout allele (βgeo) and on the other chromosome a Schwann cell-specific Oct-6 strong hypomorphic allele (ΔSCE; Ghazvini et al. 2002). The *Oct-6*$^{\Delta SCE}$ allele was generated through deletion of the Oct-6 Schwann cell enhancer (SCE; Mandemakers et al. 2000). Both *Oct-6*$^{\Delta SCE/\Delta SCE}$ and *Oct-6*$^{\beta geo/\Delta SCE}$ mice are viable and exhibit a peripheral nerve phenotype that is indistinguishable from that observed in nerves of *Oct-6*$^{\beta geo/\beta geo}$ animals (Ghazvini et al. 2002).

Using EMSA and Western blotting, we analyzed Brn-2 expression in the developing nerve of *Oct-6*$^{\beta geo/\Delta SCE}$ mice (Fig. 2). In addition to the expected Oct-1 complex, one abundant octamer complex is observed. Supershift experiments using Oct-6- and Brn-2-specific antibodies identify Brn-2 as the major protein component in this complex (Fig. 2A, cf. lanes 2 and 3), with only very low levels of Oct-6 protein detected, in agreement with previous data (Ghazvini et al. 2002). Both EMSA and Western blot analyses demonstrate that Brn-2 protein levels are increased in *Oct-6*$^{\beta geo/\Delta SCE}$ nerves at P4 compared to heterozygous or wild-type nerves (Fig. 2A,B). The higher Brn-2 protein levels in Oct-6-deficient nerves result from increased transcription of the *Brn-2* gene (or increased *Brn-2* mRNA stability), as reverse transcriptase PCR (RT–PCR) data for Brn-2 expression in P1 mice show that steady-state levels of *Brn-2* mRNA are increased in *Oct-6*$^{\beta geo/\Delta SCE}$ nerves compared to *Oct-6*$^{\Delta SCE/+}$ nerves (Fig. 2C). Immunostaining of single nerve fibers shows that within the nerve, Brn-2 is highly expressed in Schwann cell nuclei (Fig. 2D).

Next we examined developmental regulation of Brn-2 protein expression in nerves of *Oct-6*$^{\Delta SCE/+}$ and *Oct-6*$^{\beta geo/\Delta SCE}$ mice, using Western blotting (Fig. 2E). In heterozygous animals, Brn-2 expression is up-regulated in the late embryonic nerve and peaks during the first postnatal week of development. At later stages (P32), Brn-2 expression is extinguished. Thus, in both chick and mouse, Oct-6 and Brn-2 are similarly regulated, although Brn-2 down-regulation appears to be faster in mice. In Oct-6 mutant nerves, Brn-2 expression appears to be affected in two ways. First, overall Brn-2 expression levels

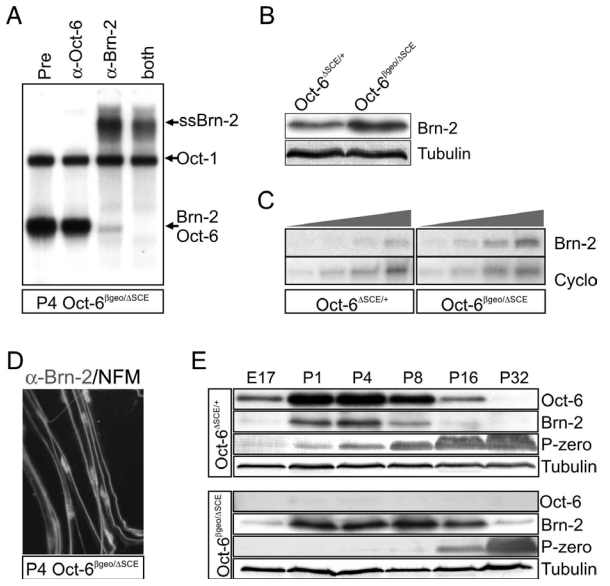

Figure 2. Elevated and protracted expression of Brn-2 in nerves of *Oct-6*$^{\beta geo/\Delta SCE}$ mice. (*A*) EMSA with whole-cell extracts from sciatic nerves of P4 *Oct-6*$^{\beta geo/\Delta SCE}$ mice and a radiolabeled octamer probe reveal a strong complex that migrates at the same position as Brn-2 and Oct-6 DNA complexes. This complex is supershifted with antibodies against Brn-2, unmasking the low residual expression of Oct-6 from the ΔSCE allele. Preimmune serum affects none of these complexes. (*B*) Western blot analysis confirms that Brn-2 protein levels are elevated in the nerves of *Oct-6*$^{\beta geo/\Delta SCE}$ vs. *Oct-6*$^{\Delta SCE/+}$ nerves at P4. Tubulin served as a loading control. (*C*) Semiquantitative RT–PCR using RNA extracted from newborn sciatic nerves shows the higher Brn-2 mRNA steady-state levels in *Oct-6*$^{\beta geo/\Delta SCE}$ mice than in *Oct-6*$^{\Delta SCE/+}$ mice. Cyclophilin mRNA served as a control. (*D*) Brn-2 is expressed in the nucleus of Schwann cells in the nerves of P4 *Oct-6*$^{\beta geo/\Delta SCE}$ mice. Nerves were dissected and teased into single fibers and incubated with antibodies against mouse Brn-2 (α-Brn-2) in green and Neurofilament medium chain (NFM) in red. (*E*) Expression of Brn-2 and Oct-6 was examined in developing nerves of *Oct-6*$^{\Delta SCE/+}$ and *Oct-6*$^{\beta geo/\Delta SCE}$ animals at E17 and P1–P32. Amounts of nerve extract loaded were normalized for acetylated α-tubulin. The build-up of P-zero immunoreactivity over time illustrates the progression of myelination in both genotypes.

are increased (see also Fig. 2A,B). Second, whereas up-regulation of Brn-2 expression follows its normal course, down-regulation of Brn-2 expression is protracted, with significant levels of Brn-2 still present at P32. In both *Oct-6*$^{\Delta SCE/+}$ and *Oct-6*$^{\beta geo/\Delta SCE}$ genetic backgrounds, down-regulation of Brn-2 correlates with the build up of P-zero immunoreactivity, indicating that a myelination-associated signal, which is independent of Oct-6, extinguishes Brn-2 expression.

Together, these data demonstrate that the developmental profile of Brn-2 expression in the nerve is regulated through mechanisms independent of Oct-6, but that Brn-2 expression levels are negatively attenuated by Oct-6.

Role of Brn-2 in Schwann cell development and myelination

Considering the findings that Brn-2 is expressed at relatively high levels in Oct-6-deficient Schwann cells that are transiently blocked in their differentiation, and that Brn-2 DNA-binding characteristics are virtually identical to those of Oct-6, one can suggest several possible roles for Brn-2 in Schwann cells. First, it is possible that Brn-2 regulates the same repertoire of genes as Oct-6 but does so less efficiently, possibly because of different affinities for Oct-6 interacting factors important in target gene regulation. Second, it is possible that Brn-2 function only partially overlaps with Oct-6 and/or that yet another factor, which might be activated at a later developmental time, is responsible for the delayed activation of the myelination program in the absence of Oct-6. It was recently proposed that the POU homeodomain protein Brn-5, a class VI POU protein, might fulfill such a role (Wu et al. 2001). This factor is activated at a later developmental time than Oct-6 and Brn-2, and its activation does not depend on Oct-6. Third, it is possible that Brn-2 negatively regulates Oct-6 targets, possibly through its interaction with the homopolymeric glutamine tract binding protein PQBP-1 (Waragai et al. 1999), and that the balance between Oct-6 and Brn-2 governs the progression of cells into the myelinating phase of differentiation. In the absence of Oct-6 this balance shifts to Brn-2, and cells are inhibited in their differentiation. Thus, to begin to explore the possible roles of Brn-2 and Brn-5 in Schwann cell differentiation, we performed transgenic mouse experiments in which Brn-2 or Brn-5 is overexpressed in the Schwann cell lineage.

To direct expression of Brn-2 or Brn-5 in Schwann cells, we made use of the *Oct-6 SCE* (Fig. 3A). This genetic element drives transgene expression from a generic promoter in Schwann cells with a profile that is identical to that of Oct-6 and very similar to that of Brn-2 but not Brn-5 (Mandemakers et al. 2000). We previously showed that a transgenic construct carrying the *SCE* and an HA-tagged version of Oct-6 rescues the delay in development of the peripheral nerve in Oct-6-deficient mice (Mandemakers et al. 2000). To test whether Brn-2 or Brn-5 overexpression can replace Oct-6 in this rescue, we generated transgenic lines for the three constructs depicted in Figure 3A. These transgenes were subsequently crossed into an *Oct-6*$^{\beta geo/\Delta SCE}$ background, and nerve maturation at P4 was studied by Western blotting and light microscopy (Fig. 3B,C). Additionally, we counted the number of promyelin and myelinating configurations in these nerves and expressed the fraction of myelinating figures divided

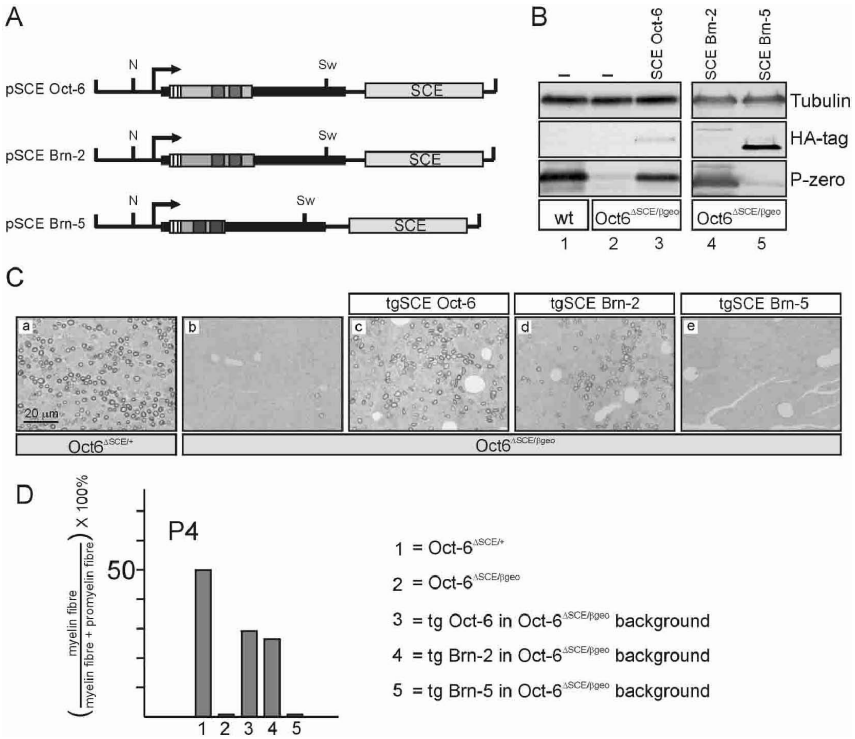

Figure 3. HA-Oct-6 and HA-Brn-2, but not HA-Brn-5, can rescue the developmental delay phenotype of *Oct-6*$^{\beta geo/\Delta SCE}$ mutant mice. (*A*) Schematic representation of the constructs used to generate mice transgenic for HA-Oct-6 (SCE Oct-6), HA-Brn-2 (SCE Brn-2), and HA-Brn-5 (SCE Brn-5). Two restriction sites used in the generation of these constructs are indicated [NotI (N) and SwaI (Sw)]. The SCE is indicated as a gray box and the triple HA-tag as a yellow box. The intron-less Oct-6 gene is shown as a thick black line. The ORF of Oct-6 is in light green, that of Brn-2 is in pink, and that of Brn-5 is in orange, with their POU-specific domain in dark blue and their POU-homeodomain in light blue. (*B*) *Oct-6*$^{\beta geo/\Delta SCE}$ mutant mice that express HA-Oct-6 or HA-Brn-2 show high levels of P-zero protein expression in sciatic nerve. Western blot analysis of P4 sciatic nerve extracts from wild-type (wt; lane *1*), *Oct-6*$^{\beta geo/\Delta SCE}$ (lane *2*), *Oct-6*$^{\beta geo/\Delta SCE}$*/SCE Oct-6* (lane *3*), *Oct-6*$^{\beta geo/\Delta SCE}$*/SCE Brn-2* (lane *4*), and *Oct-6*$^{\beta geo/\Delta SCE}$*/SCE Brn-5* (lane *5*) animals. Levels of HA-tagged proteins are assessed with α-HA antibodies. The amount of protein loaded per lane is estimated by the intensities of the α-tubulin immunoreactive band. (*C*) Comparison of the morphology of cross sections through P4 sciatic nerves of *Oct-6*$^{\Delta SCE/+}$ (panel *a*), *Oct-6*$^{\beta geo/\Delta SCE}$ (panel *b*), *Oct-6*$^{\beta geo/\Delta SCE}$*/SCE Oct-6* (panel *c*), *Oct-6*$^{\beta geo/\Delta SCE}$*/SCE Brn-2* (panel *d*), and *Oct-6*$^{\beta geo/\Delta SCE}$*/SCE Brn-5* (panel *e*) animals. Plastic-embedded osmicated nerves were sectioned at 1 μm and stained with ppd. Myelin is strongly stained by this compound and appears as dark rings in cross sections. Bar, 20 μm. (*D*) Quantification of the promyelin–myelinating transition in nerves of animals in *C*.

by the total number of myelinating and promyelin configurations to obtain a quantitative measure of nerve maturation (Fig. 3D). In the absence of Oct-6, all but a few myelinating Schwann cells are stalled at the promyelin stage of differentiation [Fig. 3C (cf. panels a and b), 3D (50% and 0.5%)], and P-zero protein levels are very low (Fig. 3B, cf. lanes 1 and 2) compared to heterozygous or wild-type animals. Expression of the HA-Oct-6 transgene results in a significant restoration of P-zero protein levels in nerves of *Oct-6*$^{\beta geo/\Delta SCE}$ mice (Fig. 3B, lane 3). At the morphological level, this finding correlates with increased numbers of myelinating Schwann cells, up to 60% of wild-type (Fig. 3C, panel c, 3D). Expression of the HA-Brn-2 transgene also results in significant restoration of P-zero protein levels (Fig. 3B, lane 4) and a strong increase in the numbers of actively myelinating Schwann cells (Fig. 3C, panel d, 3D). In contrast, the HA-Brn-5 transgene is not capable of restoring P-zero protein levels (Fig. 3B, lane 5) and accordingly, no increase in the number of myelinating cells is observed (Fig. 3C, panel e) despite relatively high levels of HA-Brn-5 expression (Fig. 3B, lane 5). Thus, increased Brn-2 expression in early postnatal development results in a significant increase in the number of actively myelinating Schwann cells in transgenic *SCE Brn-2*/*Oct-6*$^{\beta geo/\Delta SCE}$ nerves. This number approaches that observed in nerves of transgenic *SCE Oct-6*/*Oct-6*$^{\beta geo/\Delta SCE}$ animals (Fig. 3D). These results demonstrate that Brn-2 does not an-

tagonize Oct-6 function, but instead functionally substitutes for Oct-6 in promoting the transition from promyelinating to myelinating Schwann cells. Furthermore, our results suggest that Brn-2 levels are rate-limiting in Schwann cells of *Oct-6*$^{\beta geo/\Delta SCE}$ mice.

Schwann cell-specific deletion of Brn-2 does not affect peripheral nerve development

The experimental results described above suggest that Brn-2 and Oct-6 share many transcriptional targets, but do not reveal whether Brn-2 has distinct (non-Oct-6) regulatory targets. In addition, the above experiments do not exclude that other, as yet unidentified transcription factors, contribute to the delayed entry of *Oct-6*$^{\beta geo/\Delta SCE}$ Schwann cells into the myelinating phase of differentiation. To address these questions we examined the effect of loss of Brn-2 function in the Schwann cell lineage. A full null allele of *Brn-2* had been generated previously and revealed a vital function for Brn-2 in the development and survival of endocrine neurons in the hypothalamus (Nakai et al. 1995; Schonemann et al. 1995). As a consequence, the hypothalamic–pituitary axis is disturbed and homozygous animals die before postnatal day 10. Therefore, we generated mice carrying a conditional null allele of *Brn-2* in which deletion of the LoxP-flanked Brn-2 open reading frame (ORF; Fig. 4A) depends on activity of the Cre recombinase in Schwann cells. The introduction of LoxP sites at the *Brn-2* locus, together with a neomycin selection cassette and an eGFP reporter, did not compromise *Brn-2* gene function, as *Brn-2*$^{flox/flox}$ animals are healthy and breed normally.

To achieve Schwann cell-specific deletion of the *Brn-2* gene, we generated transgenic mouse lines in which the Cre recombinase is expressed from *Desert hedgehog* (*Dhh*) regulatory sequences (Fig. 4B). The *Dhh* gene is prominently expressed in Schwann cell precursors of the developing nerves and in Sertoli cells of the testis (Bitgood and McMahon 1995). The cell-type specificity of the recombination event was monitored in offspring of crosses between the *DhhCre* transgenic mice and ROSA26 LacZ reporter (Soriano 1999). Embryos were isolated from these crosses at different developmental stages and stained with Bluo-Gal for β-galactosidase activity. DhhCre activity was observed in the Schwann cell lineage from E12, as evidenced by blue staining of the peripheral nerves (Fig. 4B, panels a,b). DhhCre activity is also observed in the testis, another well documented site of *Dhh* gene expression. Outside the Schwann cell lineage and testis, expression of Cre is ob-

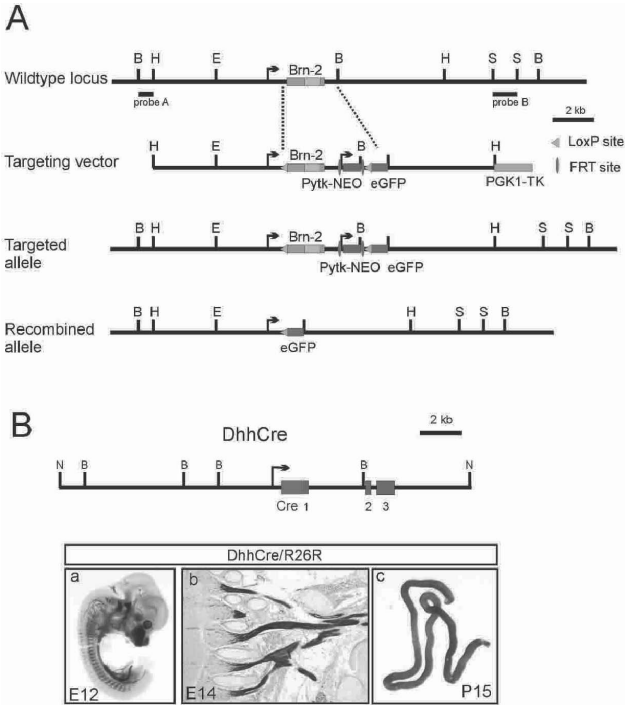

Figure 4. (*A*) The targeting strategy to generate an inducible deletion allele of *Brn-2*. The structure of the wild-type *Brn-2* locus is shown at the *top*. The *Brn-2* single exon gene is represented in olive green with the POU domain in light green. The Southern blot probes A and B are indicated as horizontal black bars. The positions of restriction enzyme cutting sites are shown for BamHI (B), HindIII (H), EcoRI (E) and ScaI (S). In the targeting construct (targeting vector), the neomycin (NEO) expression cassette (purple box) is flanked by FRT sites (vertical red bars) followed by a 3′ LoxP site (blue triangle) and an eGFP reporter gene (dark green box). The orange box represents the counter-selection cassette, containing the thymidine kinase gene (TK). The targeted allele (the floxed allele) obtained after homologous recombination is shown below the targeting construct. Cre-mediated recombination removes *Brn-2* sequences and generates the recombined allele (*bottom*). (*B*) Schwann cell-specific recombination is achieved through expression of the Cre recombinase under control of Dhh gene regulatory sequences. The 19-kb construct containing the entire *Dhh* gene with its three exons (in green) is shown. The Cre recombinase ORF (indicated in red) is preceded by a nuclear localization peptide sequence and cloned in-frame with the *Dhh* ORF. Restrictions sites for NotI (N) and BamHI (B) are indicated. Expression of the Cre recombinase was examined in crossing with the ROSA26lacz (R26R) reporter mouse. (Panel *a*) Whole-mount staining of E12.5 embryo reveals expression in the PNS, the snout, and part of the vasculature. (Panel *b*) Paraffin sections of a stained E14.5 embryo demonstrate the strong expression in immature Schwann cells that populate the peripheral nerves. (Panel *c*) Strong expression is also observed in the seminiferous tubules of the testis, where Dhh is expressed in the Sertoli cells.

served in the skin of the snout, but not in the brain and more specifically the hypothalamic region.

To explore the effect of loss of Brn-2 expression in the Schwann cell lineage, we crossed the *DhhCre* transgene into the *Brn-2*$^{flox/flox}$ background. Offspring from these crosses were healthy and bred normally. Southern blot analysis of DNA derived from sciatic nerves of adult *DhhCre/Brn-2*$^{flox/flox}$ animals revealed that the majority of cells had undergone recombination [cf. the ratio of the 14-kb band (recombined) and the 8.3-kb (not recombined) band in Fig. 5A, lane 4]. The nonrecombined band derives from non-Schwann cells in the nerve that do not express the DhhCre transgene. Recombination within the Schwann cell compartment of the nerve was complete, as judged by the complete loss of Brn-2 expression in nerves of transgenic *DhhCre/Brn-2*$^{flox/flox}$ pups using EMSA (Fig. 5B, cf. lanes 1 and 2). Additionally, loss of Brn-2 did not affect Oct-6 expression levels in these nerves compared with age-matched *Oct-6*$^{\Delta SCE/+}$ nerves (Fig. 5B, cf. lanes 3 and 4). We next examined the effect of complete loss of Brn-2 expression in Schwann cells on nerve development. Light microscopic examination of sciatic nerves of P8 transgenic *DhhCre/Brn-2*$^{flox/flox}$ animals did not reveal clear morphological abnormalities (Fig. 5C). In both *Brn-2*$^{flox/flox}$ and *DhhCre/Brn-2*$^{flox/flox}$ nerves, the majority of Schwann cells associated with larger axons are actively myelinating. Thus, loss of Brn-2 expression in the Schwann cell lineage does not affect the timing or progression of postnatal peripheral nerve development.

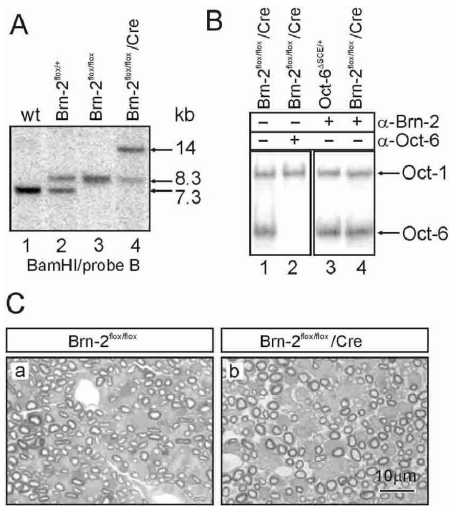

Figure 5. (*A*) The floxed *Brn-2* locus is effectively recombined by the Cre recombinase in peripheral nerve. DNA was extracted from adult sciatic nerve of wild-type (wt), *Brn-2*$^{wt/flox}$, *Brn-2*$^{flox/flox}$, and *Brn-2*$^{flox/flox}$*Cre* (*Brn-2*$^{flox/flox}$ mice transgenic for the *DhhCre* transgene) animals, digested with BamHI, and subjected to Southern blot analysis with probe B. Probe B detects fragments of 7.3 kb (wild-type allele), 8.3 kb (targeted allele), and 14 kb (recombined allele). The nonrecombined band present in lane *4* results from DNA derived from cells that do not express the DhhCre transgene, such as nerve sheath cells. (*B*) The recombination of the *Brn-2* allele in Schwann cells is complete, as *Brn-2*$^{flox/flox}$*Cre* nerves do not express Brn-2 atP4 (lanes *1*,*2*). Complete deletion of *Brn-2* does not affect Oct-6 expression, as Oct-6 expression levels are the same in nerves of *Oct-6*$^{\Delta SCE/+}$ and *Brn-2*$^{flox/flox}$*Cre* animals (cf. lanes *3* and *4*). (*C*) Deletion of *Brn-2* in Schwann cells does not affect the morphological maturation of the nerve. The overall morphology appears very similar in cross sections of nerves from both genotypes. Resin sections (1 µm) of P4 sciatic nerves of *Brn-2*$^{flox/flox}$ (panel *a*) and *Brn-2*$^{flox/flox}$/*Cre* (panel *b*) animals were stained with ppd. Bar, 10 µm (applies to both micrographs).

Schwann cell-specific deletion of Brn-2 and Oct-6 results in a severe hypomyelinating phenotype

To study the role of Brn-2 in Schwann cells deficient for Oct-6, we generated double homozygous mutants by intercrossing transgenic *DhhCre/Brn-2*$^{flox/flox}$/*Oct-6*$^{\Delta SCE/\Delta SCE}$ and transgenic *DhhCre/Brn-2*$^{flox/flox}$/*Oct-6*$^{\beta geo/+}$ mice. The development of peripheral nerves was examined by electron microscopy and quantified as described above. In the absence of Oct-6 function, Schwann cell development is transiently blocked at the promyelin stage (Bermingham et al. 1996; Jaegle et al. 1996; Ghazvini et al. 2002). Whereas >90% of large-caliber axons in nerves of wild-type (data not shown) and heterozygous *Oct-6*$^{\Delta CSE/+}$ animals are myelinated by the third postnatal week (at P16), nerves of *Oct-6*$^{\beta geo/\Delta SCE}$ mice still contain many promyelin configurations (Fig. 6A, panels a,b, 6B, ~60%). A dramatic increase in the severity of this phenotype is observed with the Schwann cell-specific deletion of Brn-2 on the *Oct-6*$^{\beta geo/\Delta SCE}$ genetic background. As shown in Figure 6A, panel c, none of the ensheathing Schwann cells has progressed beyond the promyelin stage of differentiation. To determine whether these cells are permanently blocked in their differentiation, nerve morphology in young adult animals was examined at P56 and P120. At these stages most, if not all, *Oct-6*$^{\beta geo/\Delta SCE}$ Schwann cells have gone on to myelinate their associated axon [Fig. 6A (cf. panels d and e), 6B]. In contrast, nerves of double homozygous animals are abnormal, with many promyelin configurations (~55% at P56 to ~25% at P120) and thinly myelinated axons (Fig. 6A, panels f,i). This morphology resembles that of wild-type nerves during the first week of postnatal development. Therefore, deletion of both *Oct-6* and *Brn-2* results in further delay in the promyelinating–myelinating transition relative to that observed in single *Oct-6* mutants, indicating that, in addition to Oct-6, Brn-2 plays a role in the transition of promyelinating to myelinating Schwann cells.

Discussion

In the present study we have shown that the class III POU domain protein Brn-2 is regulated in parallel with Oct-6 during Schwann cell differentiation. As the previ-

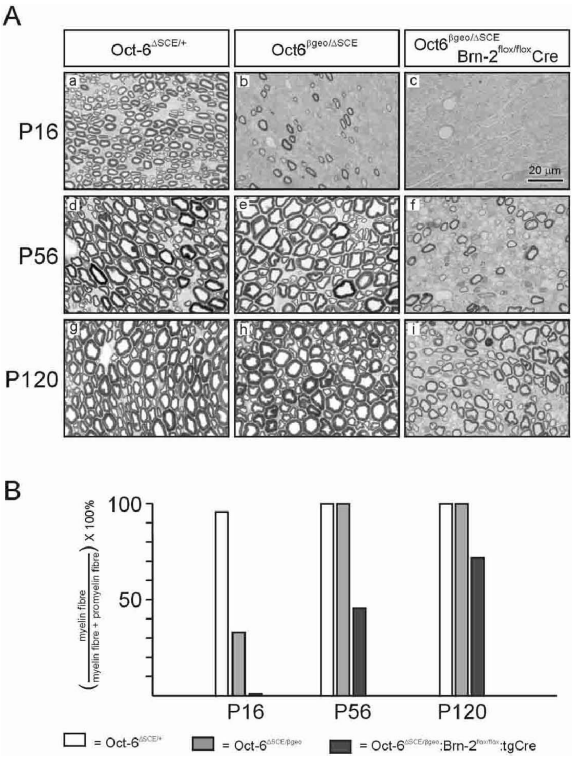

Figure 6. Schwann cell-specific deletion of *Brn-2* in an *Oct-6*$^{\beta geo/\Delta SCE}$ background results in a severe hypomyelination phenotype. (*A*) Representative sections (1 µm; ppd-stained) are shown from sciatic nerves at three developmental time points (P16, P56, and P120). In *Oct-6*$^{\Delta SCE/+}$ mice, most myelin-competent axons are actively being myelinated by P16 (panel *a*). At P56 and P120, these nerves are fully matured (panel *d*). This pattern contrasts with that observed in *Oct-6*$^{\beta geo/\Delta SCE}$ animals, which exhibit a strong delay in the differentiation of Schwann cells (Bermingham et al. 1996; Jaegle et al. 1996; Ghazvini et al. 2002). At P16, a majority of Schwann cells is arrested at the promyelin stage, with only the largest axons myelinating (panel *b*). By P56, most if not all myelinating Schwann cells have elaborated a myelin sheath (panels *e*,*h*; P120). Deletion of *Brn-2* in this genetic background results in a dramatic increase in the severity of the phenotype. At P16, essentially all myelinating Schwann cells are arrested at the promyelin stage of differentiation (panel *c*). Even at P56 and P120, myelination is largely abnormal, with large numbers of cells at the promyelin stage (panel *f*). Those axons that are myelinated have very thin myelin sheaths. Bar: panels *a–f*, 20 µm. (*B*) Quantification of delayed myelination in genotypes presented in *A*.

ous data on the delayed myelination phenotype of Oct-6-deficient mice suggested a redundant activity, we show here that Brn-2 acts as that novel factor. Our genetic evidence, arising from the overexpression of Brn-2 in Oct-6-deficient mice and moreover, the double deficiency of Brn-2 and Oct-6, demonstrates that these POU domain transcription factors share roles as positive regulators of the promyelinating–myelinating transition in Schwann cell development. Considering the importance of peripheral nerve myelination, the activity of both these transcription factors most likely assures the progression of this process.

Regulation of Brn-2 expression in the Schwann cell lineage

Our studies on chick and mouse sciatic nerve at different embryonic and post-hatching or postnatal stages showing that Oct-6 and Brn-2 are regulated similarly during nerve development provided a strong suggestion that Brn-2 plays a role in the onset of myelination. Both genes are activated around the time that most Schwann cells have adopted an immature promyelinating phenotype (E14 in the chick and E17 in the mouse). Expression of both genes peaks in promyelinating Schwann cells and is down-regulated in actively myelinating cells. Using cultured rat Schwann cells as a convenient in vitro system, we found that both Brn-2 and Oct-6 expression is increased upon addition of forskolin (an agent that elevates intracellular cAMP concentration through the reversible activation of adenylyl cyclase; Fig. 1D). Similarly, during nerve regeneration, Sim and colleagues (2002) showed the parallel expression of Brn-2 and Oct-6. Our present studies of Oct-6- and Brn-2-deficient mice demonstrate that the activation of these genes is not interdependent, thus providing a safeguard for myelination in the developing organism.

Intracellular signaling pathways that regulate Oct-6 expression in Schwann cells converge on the SCE, an enhancer element that has been identified in both the mouse and human Oct-6 locus. A first attempt to identify such an enhancer within the Brn-2 locus on the basis of sequence homology has failed thus far. DNaseI hypersensitivity mapping of the Brn-2 locus in Schwann cells should suggest the position of relevant enhancer sequences and facilitate the identification of relevant binding sites within the enhancers of Oct-6 and Brn-2, so as to determine whether the activation of these genes is by means of a similar signaling pathway. One signaling

pathway that is of particular interest in this respect is the NFκB pathway, as Nickols and colleagues (2003) recently provided evidence of its involvement in peripheral nerve myelination and Oct-6 regulation in Schwann cells.

Although Oct-6 and Brn-2 are activated independently, Brn-2 expression levels are attenuated by Oct-6. Brn-2 expression levels are increased (two- to threefold) in Oct-6-deficient Schwann cells compared to wild-type (Figs. 1C, 2A,B). It is at present not known by what mechanism Brn-2 levels are regulated by Oct-6, although our semiquantitative RT–PCR data suggest involvement of transcriptional or posttranscriptional mechanisms rather than translational or posttranslational mechanisms. Brn-2 expression is extinguished through an Oct-6-independent pathway, as Brn-2 expression is down-regulated at later stages of postnatal development, even in the absence of Oct-6 (Fig. 2E).

Role of Brn-2 in Schwann cell development

The coordinated expression of Brn-2 and Oct-6 prompted our in vivo studies of Brn-2 as the additional overlapping activating factor in the Schwann cell developmental program. We found that overexpression of Brn-2 under control of the Oct-6 SCE in Oct-6-deficient Schwann cells results in an increase in the number of Schwann cells that enter the myelinating phase on schedule. Schwann cell-specific deletion of Brn-2 in an Oct-6-deficient background results in a phenotype that is much more severe than that observed in Oct-6 single mutant animals, with Schwann cells arrested at the promyelin stage up to 120 d after birth. These results strongly suggest that Brn-2 shares a role with Oct-6 in Schwann cell development as a positive regulator of the promyelinating–myelinating transition, and identify Brn-2 as the proposed Oct-6 like function in Oct-6 mutant animals (Jaegle and Meijer 1998).

Functional overlap, as demonstrated here for Brn-2 and Oct-6, is a common phenomenon among members of the same transcription factor family and has been described for, among others, members of the Gata and Sp1 family. Within the POU family of transcription factors, overlapping roles have been described for the closely related *Brn-1* and *Brn-2* genes in cortical neuron development (McEvilly et al. 2002; Sugitani et al. 2002). Functional overlap has also been described between *Oct-6* and the more distantly related *Skn-1a/i* POU gene, which are both required for proper differentiation of epidermal keratinocytes (Andersen et al. 1997). In our system, we tested whether the more divergent POU domain gene *Brn-5* could functionally complement *Oct-6*. The choice of *Brn-5* was motivated by the work of Wu and colleagues (2001), who demonstrated that Brn-5 is expressed in myelinating Schwann cells and is regulated independently of Oct-6. High levels of Brn-5 expression did not ameliorate the developmental delay phenotype of nerves in Oct-6-deficient animals. This is not due to a possible inhibitory function of Brn-5, as *SCE-Brn-5/Oct-6*$^{\Delta SCE/+}$ nerves were normally myelinated (data not shown).

Analysis of Brn-2 expression in Oct-6 mutant animals and Brn-2 overexpression studies led us to the conclusion that quantitatively higher levels of Brn-2 protein are required to initiate myelination on schedule. These data, together with the fact that Brn-2 and Oct-6 have very similar DNA-binding preferences, suggest that the differences in biological function between Brn-2 and Oct-6 result mainly from differences in the affinities for interacting factors and/or the repertoire of interacting partners.

POU domain proteins are known to interact with members of the Sry box (Sox) transcription factor family. For example, the activation of the Fgf4 enhancer in ES cells depends on the synergistic interaction between Sox2 and Oct4 proteins (Ambrosetti et al. 1997). In glial cells it has been shown that Sox10 interacts synergistically with Oct-6, but not Brn-1 or Brn-2, to activate transcription when both proteins are bound to adjacent binding sites in an artificial enhancer (Kuhlbrodt et al. 1998a). Synergistic activation required the N-terminal region of Oct-6 and Sox10 (Kuhlbrodt et al. 1998b). Similarly, the oligodendrocyte-enriched Sox11 protein synergizes with Brn2 and Brn-1, but not with Oct-6. Taken together, these data suggest that a specific POU/Sox code exists and postulates that specific POU proteins require specific Sox proteins to exhibit cooperative effects (Kuhlbrodt et al. 1998a,b). If indeed important target genes of Oct-6 in glial cells are regulated through interaction with Sox10, and the pair Brn-2/Sox11 is equivalent to Oct-6/Sox10, the developmental defect in Oct-6-deficient Schwann cells but not in oligodendrocytes (Bermingham et al. 1996) could be explained as follows: Oligodendrocytes express Brn-2/Sox11 in addition to Oct-6/Sox10, whereas Schwann cells express Oct-6/Sox10 and Brn-2 but not Sox11. Further experiments are required to test this hypothesis.

Our data demonstrate that the promyelin-to-myelinating transition is regulated by Oct-6/Brn-2 function, but even in the absence of these POU factors, Schwann cells eventually do enter the myelinating phase of cell differentiation. This is not due to accumulation of Oct-6 protein expressed from the hypomorphic ΔSCE allele (Fig. 2E). Also, as Brn-2 deletion in the Schwann cell lineage is complete, mosaicism of Brn-2 expression cannot explain this delayed myelination (Fig. 5). Two observations are particularly important in understanding the roles of Oct-6 and Brn-2 in Schwann cell differentiation and why even in their absence myelination occurs. First, in the absence of Oct-6, entry into the myelinating phase is delayed *and* the kinetics of this transition are changed (Fig. 6B). Whereas >80% of wild-type Schwann cells have entered the myelinating phase by P8, in the absence of Oct-6 it takes several weeks for the same number of Schwann cells to make this transition into the myelinating phase. In the absence of both Oct-6 and Brn-2, this transition is even further protracted. Second, kinetics of this transition are Oct-6/Brn-2 dosage-dependent. In terms of transcriptional regulation, this suggests that Oct-6 greatly increases the chance that its target genes become activated. The finding that in the absence of

Oct-6 and Brn-2 this chance is not zero indicates that these target genes are activated, albeit less effectively, through other transcription factors, possibly including the ubiquitous POU factor Oct-1.

Notwithstanding, the identification and characterization of Brn-2 and its in vivo role in Schwann cells have provided insight into the transcriptional network of myelination. These results will ultimately lead to a biochemical explanation of the different, yet overlapping roles of Oct-6 and Brn-2 in Schwann cell development and possible intervention strategies to promote myelination in clinical therapeutic settings.

Materials and methods

Gene targeting

A 10.5-kb HindIII fragment of *Brn-2* genomic sequences was isolated from a 129ola ES cell-genomic phage library. Two restrictions sites (HindIII and AgeI) were generated by PCR at the ATG and used to insert a 5′ loxP site. A second clone was generated containing the neomycin gene driven by a thymidine kinase (Pytk) promoter flanked by FRT sites. Next to the 3′FRT site we inserted a 3′ loxP sequence and an eGFP reporter gene. A 1.9-kb fragment containing FRT-Pytk-neomycin-FRT-loxP-eGFP was isolated as a BglII fragment and cloned in a unique BamHI site in the *Brn-2* 3′ untranslated region. We positioned a negative-selection marker gene, a thymidine kinase gene driven by the phosphoglycerate kinase-1 promoter (PGK-tk), downstream from the 3′ homology region.

SpeI-linearized DNA (15 µg) was electroporated into E14 ES cells followed by selection with G418 (200 µg/mL) and 2 µM gancyclovir. Individual clones were screened for homologous recombination by Southern-blot analysis of BamHI and HindIII-digested genomic DNA with 5′ and 3′ external probes (probes A and B). One correctly targeted ES cell clone with a correct karyotype was isolated and injected into C57Bl/6 blastocysts. Male chimeric mice were mated with FVB/N females to transmit the modified *Brn-2* allele to the germ cells (*Brn-2*$^{wt/flox}$). Heterozygous offspring were back-crossed to generate homozygous mutant *Brn-2*$^{flox/flox}$ mice. The different *Brn-2* alleles were genotyped either by Southern blotting or by PCR with the following primers: 5′-GCGCGGCTCCTTTAACCAGAGCGCC-3′ and 5′-CTGGTGAGCGTGGCTGAGCGGGTGC-3′. The wild-type allele will yield a 210-bp PCR product, and *Brn-2*$^{flox/flox}$ will yield a 250-bp PCR product.

Transgenic mice

For the generation of Cre recombinase-expressing mice, we used an 18-kb NotI *Dhh* genomic clone encompassing the *Dhh* promoter, exons 1, 2, and 3 (gift from Dr. Andy MacMahon, Harvard). The *Cre* gene was extended at its N terminus with a nuclear localization peptide sequence and cloned in exon 1 on the start codon of *Dhh*. The 19-kb transgene construct was separated from vector sequences and microinjected into fertilized FVB/N oocytes. Founder lines were crossed back to FVB/N mice. The genotype of the mice was determined by PCR analysis of genomic DNA isolated from mouse tails. Cre-specific primers 5′-ACCCTGTTACGTATAGCCGA-3′ and 5′-CTCC GGTATTGAAACTCCAG-3′ were used to amplify a 300-bp fragment from the DhhCre construct.

The HA-tag expression cassette was generated by subcloning a 2.3-kb NotI/HindIII fragment containing the HA-tagged *Oct-6* fusion gene described before (Mandemakers et al. 2000) into pBluescript (pHA-Oct-6). A BglII/SpeI/NcoI synthetic polylinker was inserted as a blunt/NcoI fragment into MscI/NcoI-digested pHA-Oct-6, placing the linker just behind the triple HA tag and removing most of the Oct-6 coding sequences (HA-tag cloning vector). A 2-kb BamHI fragment containing the *Brn-2* coding sequence, isolated from pCMV-Brn-2, was subcloned into the HA-tag cloning vector linearized with BglII (HA-Brn-2). A 0.9-kb BamHI/XbaI fragment containing Brn-5 coding sequences, isolated from pCMV-Brn-5, was cloned into the HA-tag cloning vector digested with BglII/SpeI (HA-Brn-5). The NotI/SwaI fragments from HA-Brn-2 and HA-Brn-5 were then ligated into NotI/SwaI-digested R3HAOct-6-SCE vector, creating constructs SCE-HABrn-2 and SCE-HABrn-5. EcoRI restriction fragments containing the transgene construct were isolated and microinjected into fertilized FVB/N oocytes. Transgenic lines were crossed into an *Oct-6*$^{\Delta SCE/\Delta SCE}$ background.

Electron microscopy

Electron microscopy on sciatic nerves was performed as described (Jaegle et al. 1996). Mice were anesthetized with Nembutal and transcardially perfused with PBS followed by 3% paraformaldehyde (PFA) and 1% glutaraldehyde in 0.1 M sodium cacodylate buffer at pH 7.5. Sciatic nerves were isolated and placed in fresh fixative overnight at 4°C. The sciatic nerves were washed in 0.2 M cacodylate buffer overnight at 4°C before being postfixed in 1% OsO_4 for 3 h, dehydrated, and embedded in Epon. Semithin sections were stained with para-phenylenediamine (ppd; Estable-Puig et al. 1965) and viewed under an Olympus microscope. Ultrathin sections were stained with uranyl acetate and lead citrate, and analyzed with a Philips CM100 electron microscope. For quantification, five random nonoverlapping electron micrographs were produced for every nerve at a final magnification of 2600×. Myelinating and promyelin figures were counted (250–450 fibers per nerve).

Whole-mount X-gal staining

Embryos were isolated and fixed by immersion for 1 h at room temperature in 2% formaldehyde, 0.2% glutaraldehyde, 2 mM $MgCl_2$, 5 mM EGTA at pH 8, and 0.02% NP-40 in PBS. Embryos were washed three times for 10 min in PBS with 0.02% NP-40 and stained overnight at room temperature in PBS containing 1 mg/mL Bluo-gal, 5 mM $K_3Fe(CN)_6$, 5mM $K_4Fe(CN)_6$, 2 mM $MgCl_2$, 0.01% SDS, and 0.02% NP-40. Subsequently, the stained embryos were washed twice in PBS with 0.02% NP40, postfixed overnight in 4% formaldehyde, and embedded into paraffin. Sections (8 µm) were cut, counterstained with eosin, and viewed under the microscope. Images were collected using an Olympus DP50 digital camera.

Antibodies and immunohistochemistry

Rabbit polyclonal antibodies were raised against the N terminus of Brn-2 protein (amino acids 155–271). Animals were immunized with His-tagged fused protein expressed in *Escherichia coli* and purified on Ni^{2+}-NTA-agarose beads (QIAGEN). Specificity of the Brn-2 antiserum was confirmed by EMSA (data not shown). Antibodies raised against the N-terminal portion of the Oct-6 protein have been described (Ilia et al. 2002).

Sciatic nerves were isolated, teased into single fibers, and fixed for 30 min with 4% PFA at room temperature. The tissue was blocked in 1% BSA, 0.05% Tween-20 in Tris-buffered sa-

line (TBS). Rabbit anti-Brn-2 antibodies and mouse anti-Neurofilament (hybridoma 2H3, Developmental Studies Hybridoma Bank) antibodies, both diluted 1:200, were incubated simultaneously in TBS/0.05% Tween-20 overnight at room temperature. Oregon Green-conjugated goat anti-rabbit IgGs (Molecular Probes) and Texas Red-conjugated goat anti-mouse IgGs (Molecular Probes) were subsequently used as secondary antibodies. The tissue was viewed using a Leica fluorescence microscope.

Western blotting

Sciatic nerves were isolated and directly lysed in loading buffer, followed by sonication and heating in a boiling water bath. Western blotting was performed as described (Ghazvini et al. 2002). Primary antibodies include anti-HA (rabbit polyclonal Y-11; Santa Cruz Biotechnology; used at dilution 1:2000), anti-Brn-2 (goat polyclonal C-20; Santa Cruz Biotechnology; used at 1:100), anti-Oct-6 (rabbit polyclonal; 1:1000), anti-P-zero (mouse monoclonal, hybridoma clone P07; 1:1000 (Archelos et al. 1993), and acetylated α-Tubulin (mouse monoclonal Sigma T-6793; 1:10,000). Secondary antibodies were either conjugated with alkaline phosphatase (Dako) or horseradish peroxidase (Dako) for the detection of primary antibodies.

Electrophoretic mobility shift assay

Sciatic nerve and Schwann cell extracts were prepared by placing the tissue or cells in 5–10 tissue volumes of 20 mM Hepes-KOH at pH 7.9, 400 mM KCl, 1 mM EDTA, 10 mM DTT, 10% glycerol supplemented with 1 mM PMSF, and 1× protease inhibitor cocktail (Sigma; Meijer et al. 1992). The tissue was disrupted by four cycles of snap-freezing in liquid nitrogen and thawing on ice. Cellular debris was removed by centrifugation at 14000*g* for 5 min at 4°C. The supernatant was snap-frozen and stored in aliquots at –80°C. Equal amounts of extract were used in a bandshift assay using 10 fmole of a ^{32}P end-labeled double-strand oligonucleotide probe (*GAGAGGA*ATTTG CAT*TTCCACCGACCTTCC*). Probe and protein were incubated on ice, in the absence or presence of antiserum, for 20 min in 20 mM Hepes-KOH at pH 7.9, 1 mM EDTA, 1 mM EGTA, 4% Ficoll in a total volume of 20 µL. Complexed and free probe were separated on a 4% polyacrylamide gel in 0.25× TBE electrophoresis buffer at room temperature. Gels were fixed in 10% methanol/10% acetic acid, dried, and exposed to a PhosphorImager screen (Molecular Dynamics). Relative band intensities were calculated using the ImageQuant 5.2 software.

Acknowledgments

We thank Elaine Dzierzak and Sjaak Philipsen for their comments and encouragement. John Kong a San is thanked for his expert help in microinjection, Manoussos Koutsourakis for blastocyst injection, and Matthijs Uyl and Ludo Broos for help in immunohistochemistry. The genomic *Dhh* clone was a kind gift from Dr. Andy MacMahon (Harvard University, Boston). The 2H3 monoclonal antibody, developed by T.M. Jessell and J. Dodd, was obtained from the Developmental Studies Hybridoma Bank developed under auspices of the NICHD and maintained by The University of Iowa, Department of Biological Sciences. The monoclonal P07 against the extra-cellular domain of P-zero was a kind gift from Dr. Juan Archelos (Graz University, Austria). This work was supported in part by grants from the Dutch Research Council NWO (ALW 805-17.281 and MW 903-42-195).

The publication costs of this article were defrayed in part by payment of page charges. This article must therefore be hereby marked "advertisement" in accordance with 18 USC section 1734 solely to indicate this fact.

References

Ambrosetti, D.C., Basilico, C., and Dailey, L. 1997. Synergistic activation of the fibroblast growth factor 4 enhancer by Sox2 and Oct-3 depends on protein–protein interactions facilitated by a specific spatial arrangement of factor binding sites. *Mol. Cell. Biol.* **17:** 6321–6329.

Andersen, B., Weinberg, W.C., Rennekampff, O., McEvilly, R.J., Bermingham Jr., J.R., Hooshmand, F., Vasilyev, V., Hansbrough, J.F., Pittelkow, M.R., Yuspa, S.H., et al. 1997. Functions of the POU domain genes Skn-1a/i and Tst-1/Oct-6/SCIP in epidermal differentiation. *Genes & Dev.* **11:** 1873–1884.

Archelos, J.J., Roggenbuck, K., Schneider-Schaulies, J., Linington, C., Toyka, K.V., and Hartung, H.P. 1993. Production and characterization of monoclonal antibodies to the extracellular domain of P0. *J. Neurosci. Res.* **35:** 46–53.

Arroyo, E.J. and Scherer, S.S. 2000. On the molecular architecture of myelinated fibers. *Histochem. Cell. Biol.* **113:** 1–18.

Arroyo, E.J., Bermingham Jr., J.R., Rosenfeld, M.G., and Scherer, S.S. 1998. Promyelinating Schwann cells express Tst-1/SCIP/Oct-6. *J. Neurosci.* **18:** 7891–7902.

Bermingham, J.R., Scherer, S.S., O'Connell, S., Arroyo, E., Kalla, K.A., Powell, F.L., and Rosenfeld, M.G. 1996. Tst-1/Oct-6/SCIP regulates a unique step in peripheral myelination and is required for normal respiration. *Genes & Dev.* **10:** 1751–1762.

Bitgood, M.J. and McMahon, A.P. 1995. Hedgehog and Bmp genes are coexpressed at many diverse sites of cell–cell interaction in the mouse embryo. *Dev. Biol.* **172:** 126–138.

Blanchard, A.D., Sinanan, A., Parmantier, E., Zwart, R., Broos, L., Meijer, D., Meier, C., Jessen, K.R., and Mirsky, R. 1996. Oct-6 (SCIP/Tst-1) is expressed in Schwann cell precursors, embryonic Schwann cells, and postnatal myelinating Schwann cells: Comparison with Oct-1, Krox-20, and Pax-3. *J. Neurosci. Res.* **46:** 630–640.

Britsch, S., Goerich, D.E., Riethmacher, D., Peirano, R.I., Rossner, M., Nave, K.A., Birchmeier, C., and Wegner, M. 2001. The transcription factor Sox10 is a key regulator of peripheral glial development. *Genes & Dev.* **15:** 66–78.

Estable-Puig, J.F., Bauer, W.C., and Blumberg, J.M. 1965. Technical note; paraphenylenediamine staining of osmium-fixed plastic embedded tissue for light and phase microscopy. *J. Neuropathol. Exp. Neurol.* **24:** 531–536.

Fields, R.D. and Stevens-Graham, B. 2002. New insights into neuron–glia communication. *Science* **298:** 556–562.

Ghazvini, M., Mandemakers, W., Jaegle, M., Piirsoo, M., Driegen, S., Koutsourakis, M., Smit, X., Grosveld, F., and Meijer, D. 2002. A cell type-specific allele of the POU gene Oct-6 reveals Schwann cell autonomous function in nerve development and regeneration. *EMBO J.* **21:** 4612–4620.

Ghislain, J., Desmarquet-Trin-Dinh, C., Jaegle, M., Meijer, D., Charnay, P., and Frain, M. 2002. Characterization of *cis*-acting sequences reveals a biphasic, axon-dependent regulation of Krox20 during Schwann cell development. *Development* **129:** 155–166.

Hudson, L.D. 2001. Control of gene expression by oligodendrocytes. In *Glial cell development* (eds. K.R. Jessen, W.D. Richardson), pp. 209–222. Oxford University Press, Oxford, UK.

Ilia, M., Beasley, C., Meijer, D., Kerwin, R., Cotter, D., Everall, I., and Price, J. 2002. Expression of Oct-6, a POU III domain transcription factor, in schizophrenia. *Am. J. Psychiatry* **159:** 1174–1182.

Jaegle, M. and Meijer, D. 1998. Role of Oct-6 in Schwann cell differentiation. *Microsc. Res. Tech.* **41:** 372–378.

Jaegle, M., Mandemakers, W., Broos, L., Zwart, R., Karis, A., Visser, P., Grosveld, F., and Meijer, D. 1996. The POU factor Oct-6 and Schwann cell differentiation. *Science* **273:** 507–510.

Kuhlbrodt, K., Herbarth, B., Sock, E., Enderich, J., Hermans-Borgmeyer, I., and Wegner, M. 1998a. Cooperative function of POU proteins and SOX proteins in glial cells. *J. Biol. Chem.* **273:** 16050–16057.

Kuhlbrodt, K., Herbarth, B., Sock, S., Hermans-Borgmeyer, I., and Wegner, M. 1998b. Sox10, a novel transcriptional modulator in glial cells. *J. Neurosci.* **18:** 237–250.

Kuhn, R., Monuki, E.S., and Lemke, G. 1991. The gene encoding the transcription factor SCIP has features of an expressed retroposon. *Mol. Cell. Biol.* **11:** 4642–4650.

Le Douarin, N.M. and Kalcheim, C. 1999. *The neural crest*, pp. 328–335. Cambridge University Press, Cambridge, UK.

Levavasseur, F., Mandemakers, W., Visser, P., Broos, L., Grosveld, F., Zivkovic, D., and Meijer, D. 1998. Comparison of sequence and function of the Oct-6 genes in zebrafish, chicken, and mouse. *Mech. Dev.* **74:** 89–98.

Mandemakers, W., Zwart, R., Jaegle, M., Walbeehm, E., Visser, P., Grosveld, F., and Meijer, D. 2000. A distal Schwann cell-specific enhancer mediates axonal regulation of the Oct-6 transcription factor during peripheral nerve development and regeneration. *EMBO J.* **19:** 2992–3003.

McEvilly, R.J., de Diaz, M.O., Schonemann, M.D., Hooshmand, F., and Rosenfeld, M.G. 2002. Transcriptional regulation of cortical neuron migration by POU domain factors. *Science* **295:** 1528–1532.

Meijer, D., Graus, A., Kraay, R., Langeveld, A., Mulder, M.P., and Grosveld, G. 1990. The octamer binding factor Oct6: cDNA cloning and expression in early embryonic cells. *Nucleic Acids Res.* **18:** 7357–7365.

Meijer, D., Graus, A., and Grosveld, G. 1992. Mapping the transactivation domain of the Oct6 POU transcription factor. *Nucleic Acids Res.* **20:** 2241–2247.

Mirsky, R., Jessen, K.R., Brennan, A., Parkinson, D., Dong, Z., Meier, C., Parmantier, E., and Lawson, D. 2002. Schwann cells as regulators of nerve development. *J. Physiol. Paris* **96:** 17–24.

Nagarajan, R., Svaren, J., Le, N., Araki, T., Watson, M., and Milbrandt, J. 2001. EGR2 mutations in inherited neuropathies dominant-negatively inhibit myelin gene expression. *Neuron* **30:** 355–368.

Nakai, S., Kawano, H., Yudate, T., Nishi, M., Kuno, J., Nagata, A., Jishage, K., Hamada, H., Fujii, H., Kawamura, K., et al. 1995. The POU domain transcription factor Brn-2 is required for the determination of specific neuronal lineages in the hypothalamus of the mouse. *Genes & Dev.* **9:** 3109–3121.

Nickols, J.C., Valentine, W., Kanwal, S., and Carter, B.D. 2003. Activation of the transcription factor NF-κB in Schwann cells is required for peripheral myelin formation. *Nat. Neurosci.* **6:** 161–167.

Richardson, W.D. 2001. Oligodendrocyte development. In *Glial cell development* (eds. K.R. Jessen and W.D. Richardson), pp. 21–54. Oxford University Press, Oxford.

Ryan, A.K. and Rosenfeld, M.G. 1997. POU domain family values: Flexibility, partnerships, and developmental codes. *Genes & Dev.* **11:** 1207–1225.

Scherer, S.S., Wang, D.Y., Kuhn, R., Lemke, G., Wrabetz, L., and Kamholz, J. 1994. Axons regulate Schwann cell expression of the POU transcription factor SCIP. *J. Neurosci.* **14:** 1930–1942.

Schonemann, M.D., Ryan, A.K., McEvilly, R.J., O'Connell, S.M., Arias, C.A., Kalla, K.A., Li, P., Sawchenko, P.E., and Rosenfeld, M.G. 1995. Development and survival of the endocrine hypothalamus and posterior pituitary gland requires the neuronal POU domain factor Brn-2. *Genes & Dev.* **9:** 3122–3135.

Sim, F., Zhao, C., Li, W., Lakatos, A., and Franklin, R. 2002. Expression of the POU-domain transcription factors SCIP/Oct-6 and Brn-2 is associated with Schwann cell but not oligodendrocyte remyelination of the CNS. *Mol. Cell. Neurosci.* **20:** 669.

Soriano, P. 1999. Generalized lacZ expression with the ROSA26 Cre reporter strain. *Nat. Genet.* **21:** 70–71.

Sugitani, Y., Nakai, S., Minowa, O., Nishi, M., Jishage, K., Kawano, H., Mori, K., Ogawa, M., and Noda, T. 2002. Brn-1 and Brn-2 share crucial roles in the production and positioning of mouse neocortical neurons. *Genes & Dev.* **16:** 1760–1765.

Topilko, P. and Meijer, D. 2001. Transcription factors that control Schwann cell development and myelination. In *Glial cell development* (eds. K.R. Jessen and W.D. Richardson), pp. 223–244. Oxford University Press, Oxford.

Topilko, P., Schneider-Maunoury, S., Levi, G., Baron-Van Evercooren, A., Chennoufi, A.B., Seitanidou, T., Babinet, C., and Charnay, P. 1994. Krox-20 controls myelination in the peripheral nervous system. *Nature* **371:** 796–799.

Waragai, M., Lammers, C.H., Takeuchi, S., Imafuku, I., Udagawa, Y., Kanazawa, I., Kawabata, M., Mouradian, M.M., and Okazawa, H. 1999. PQBP-1, a novel polyglutamine tract-binding protein, inhibits transcription activation by Brn-2 and affects cell survival. *Hum. Mol. Genet.* **8:** 977–987.

Webster, H.d. 1993. Development of peripheral nerve fibers. In *Peripheral neuropathy* (eds. P.J. Dyck, P.K. Thomas, J.W. Griffin, P.A. Low, and J.F. Poduslo), pp. 243–266. W.B. Saunders, Philadelphia.

Wu, R., Jurek, M., Sundarababu, S., and Weinstein, D.E. 2001. The POU gene Brn-5 is induced by neuregulin and is restricted to myelinating Schwann cells. *Mol. Cell. Neurosci.* **17:** 683–695.

Chapter 4

A generic tool for biotinylation of tagged proteins in transgenic mice

Siska Driegen, Rita Ferreira, Arend van Zon, John Strouboulis, Martine Jaegle, Frank Grosveld, Sjaak Philipsen and Dies Meijer

Transgenic Research, 2005

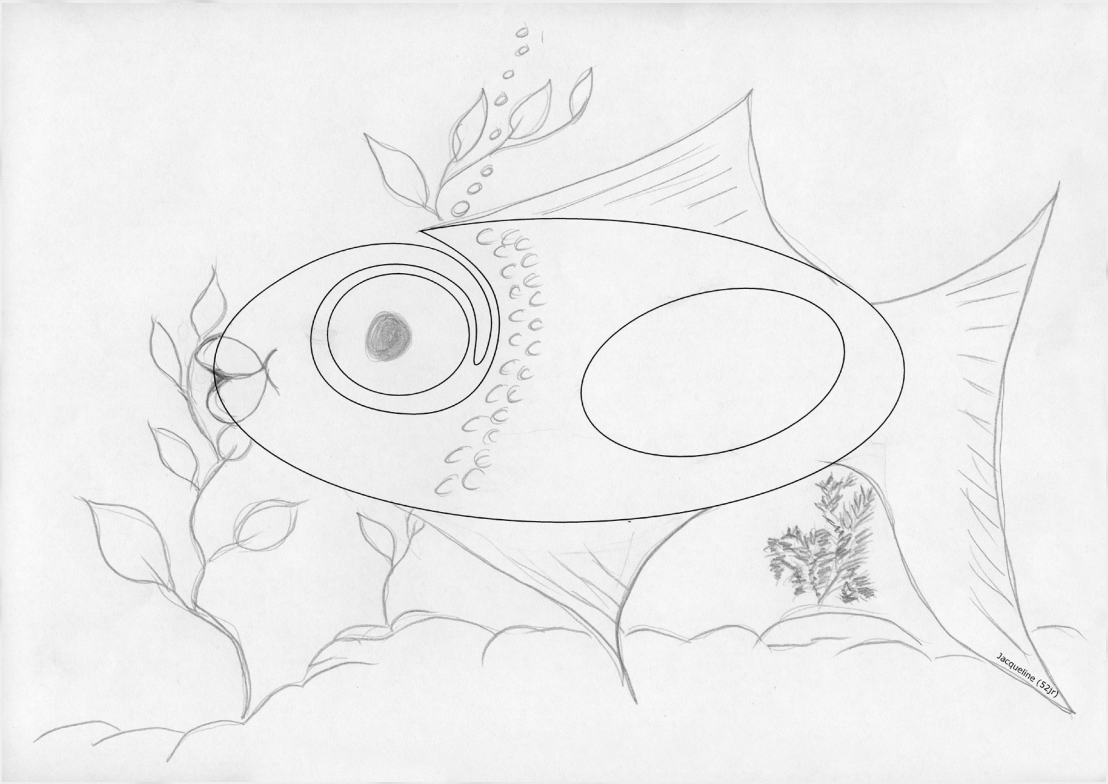

Transgenic Research (2005) 14:477–482
DOI 10.1007/s11248-005-7220-2

Short communication

A generic tool for biotinylation of tagged proteins in transgenic mice

Siska Driegen[1,2], Rita Ferreira[1], Arend van Zon[1], John Strouboulis[1], Martine Jaegle[1], Frank Grosveld[1], Sjaak Philipsen[1] & Dies Meijer[1,*]
[1]*Department of Cell Biology and Genetics, ErasmusMC, Dr Molewaterplein 50, 3015GE, Rotterdam, the Netherlands*
[2]*Department of Neuroscience, ErasmusMC, Dr Molewaterplein 50, 3015GE, Rotterdam, the Netherlands*

Received 28 January 2005; accepted 11 May 2005

Key words: biotinylation, BirA, Gata1, protein tag, ROSA26

Abstract

The remarkable high affinity (Kd $\sim 10^{-15}$ M) of avidin/streptavidin for biotin has been extensively exploited in purification methodologies. Recently a small peptide sequence (Avi-tag) has been defined that can be specifically and efficiently biotinylated by the bacterial BirA biotin ligase. Fusion of this small peptide sequence to a protein of interest and co-expression with the BirA gene in mammalian cells allowed purification of the biotinylated protein together with its associated proteins and other molecules. Ideally, one would like to apply these technologies to purify tagged proteins directly from mouse tissues. To make this approach feasible for a large variety of proteins we developed a mouse strain that expresses the BirA gene ubiquitously by inserting it in the ROSA26 locus. We demonstrate that the BirA protein is indeed expressed in all tissues tested. In order to demonstrate functionality we show that it biotinylates the transgene-encoded Avi-tagged Gata1 and Oct6 transcription factors in erythroid cells of the foetal liver and Schwann cells of the peripheral nerve respectively. Therefore, this mouse can be crossed to any transgenic mouse to obtain efficient biotinylation of an Avi-tagged protein for the purpose of protein (complex) purification.

Introduction

Many different affinity purification techniques have been developed to study protein complexes and identify individual molecules interacting within these complexes. One important experimental strategy is to fuse a protein of interest with a tag for which specific high affinity reagents are readily available. Examples of such tags include the maltose binding protein, the haemagglutinin (HA)-tag, the TAP-tag, the FLAG-tag, the Histidine-tag and the Avi-tag (Rigaut et al., 1999; Terpe, 2003). Of particular interest is the Avi-tag. This short (15aa) peptide sequence contains a central Lysine residue that can be biotinylated at the epsilon nitrogen by the bacterial BirA biotin ligase. Co-expression of a tagged protein and the BirA gene in cells results in a highly specific, quantative biotinylation of the tagged protein (Beckett et al., 1999). Proteins thus biotinylated can be purified from complex sources, such as mammalian cell extracts, in a simple single step procedure that takes advantage of the very high affinity of the biotin moiety for avidin or streptavidin (Cull & Schatz, 2000). The extraordinary power of this approach has been demonstrated in a number of recent publications (Beckett et al., 1999; Chapman-Smith & Cronan, 1999; Cull & Schatz, 2000; de Boer et al., 2003). As future applications of this technology will include the study of complex protein interactions in

*Author for correspondence
E-mail: d.meijer@erasmusmc.nl

developing and adult mouse tissues it is advantageous to develop a mouse strain that will express the bacterial BirA gene in all cell types of the body at all developmental stages. This mouse would then serve as a generic strain that can be crossed with any transgenic mouse expressing an Avi-tagged protein, resulting in biotinylation of that protein.

In the studies presented here, we have generated a transgenic mouse expressing BirA from the ROSA26 locus. We show the ubiquitous expression of BirA and present proof for principle of *in vivo* biotinylation of the Avi-tagged Gata1 and Oct6 transcription factors in compound transgenic foetal liver cells and postnatal Schwann cells, respectively.

Results and discussion

We chose to introduce the BirA gene in the ROSA26 transcription unit, as this gene is active in all cells at all stages of development (Zambrowicz et al., 1997). Furthermore, disruption of the ROSA26 gene does not result in any cellular defect in the heterozygous or homozygous state (Zambrowicz et al., 1997). To reprogram the ROSA26 gene we first introduced the BirA gene in the third exon of the rabbit β-globin gene. We then excised the whole exon, containing the BirA ORF, splice acceptor and transcription termination sequences, and introduced it together with a LoxP flanked puromycin selection cassette, into the first intron of the ROSA26 construct (targeting construct in Figure 1(a)). Homologous recombination into the ROSA26 gene will result in a chimaeric gene in which transcripts are initiated from the ROSA26 promoter and the ROSA26 first exon splices to the β-globin third exon.

Transcription is terminated downstream of the β-globin exon and the primary transcripts are cleaved and polyadenylated resulting in a short chimaeric stable mRNA encoding the BirA protein (data not shown).

The targeting construct was transfected into ES cells and puromycin resistant clones were selected. Homologous recombinants were identified by Southern blot analysis of *Eco*RI digested DNA probed with probe1 and probe2 (Figure 1(b)). Results for two independent clones are presented in Figure 1(B). Approximately 50% of puromycin resistant clones resulted from correct homologous recombination events.

We next checked whether the BirA protein is expressed in these correctly targeted clones. As BirA was extended at the amino-terminal portion with a triple HA-tag, we could detect the protein using a HA antibody. In preliminary experiments we had determined that the presence of the triple HA-tag does not abolish the biotin ligase activity of the BirA protein (data not shown). As shown in Figure 1(c) a protein of correct size (~39 kD) is expressed in the correctly targeted ES cell lines. From these cell lines mouse strains were established. These mice were crossed with a Cre deleter mouse to remove the puromycin selection cassette (see Figure 1(a)) and were examined for expression of the BirA protein. Tissues were dissected from mouse pups at postnatal day 8 and subjected to Western analysis. As shown in Figure 1(d), BirA is expressed in all tissues examined. Although BirA is expressed in all tissues, expression levels vary from tissue to tissue as has been reported for the ROSA26 transcripts (Zambrowicz et al., 1997).

Next we wished to establish whether the expression level of BirA is sufficient to biotinylate a tagged protein in a mouse tissue. We chose two different Avi-tagged transcription factor genes expressed in different tissues to establish the feasibility of our approach. One is an Avi-tagged Gata1 transgene expressed in the erythroid lineage (Elefanty et al., 1996). The second is an Avi-tagged Oct6 allele ($Oct6^{Avi}$) that has been generated by gene targeting and is expressed in the Schwann cells of the developing peripheral nervous system. Breedings were initiated between heterozygous BirA ($ROSA26^{HABirA/+}$) and heterozygous AviGata1 (tg[AviGata1/+]) mice or heterozygous $Oct6^{Avi/+}$ to obtain compound heterozygous mice (Figure 2(a)). Since the Gata1 transgene is highly expressed in proerythrocytes in foetal liver of the mouse (Ohneda & Yamamoto, 2002), we recovered embryos at day 13.5 of gestation and prepared single cell smears from foetal livers. AviGata1 and endogenous Gata1 expression in both AviGata1 and AviGata1:BirA cells was detected using a monoclonal antibody against the Gata1 protein (Figure 2(b), panels a and c). The AviGata1 protein could not be detected in foetal liver cells of single transgenic AviGata1 mice using fluorescein conjugated Avidin indicating that the Avi-tag is not a target for endogenous biotin

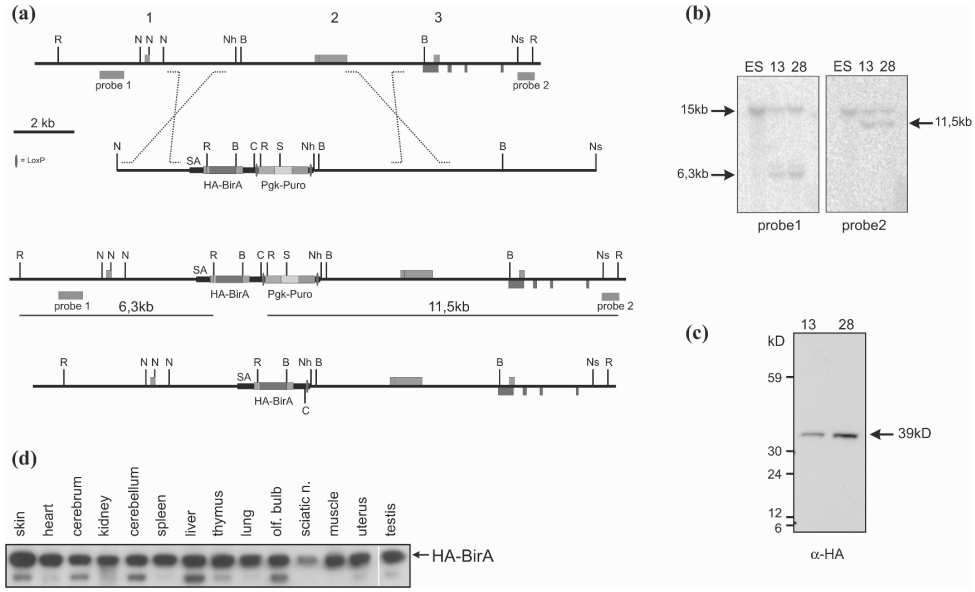

Figure 1. (a) Schematic representation of the targeting strategy. The ROSA26 locus contains the ROSA26 gene that generates two transcripts through alternative splicing of exon 2 and 3 and one anti-sense uncharacterised four-exon gene. The 3xHABirA gene was cloned into the *Eco*RI (R) and *Bg*lII (B) site of the rabbit β-globin third exon including the splice acceptor sequences (450 bp) and termination/polyadenylation sequences. At the 3′ end a LoxP site flanked PGK puromycin selection cassette was introduced. The resulting fragment was cloned into the unique *Nhe*I (Nh) site of the ROSA26 targeting cassette that covers 13 kb of ROSA26 homologous DNA from the *Not*I (N) site to the *Nsi*I (Ns) site. Homologous recombination results in introduction of the HABirA encoding exon and the selection cassette in the first intron of the ROSA26 gene. Subsequent removal of the LoxP flanked puromycin selection cassette results in the situation depicted in Figure 1(a): B, *Bam*HI; C, *Cla*I; S, *Sal*I. (b) Homologous recombinants were selected by Southern blot analysis of *Eco*RI digested DNA using probe1 and probe 2. The length of the expected restriction fragments is indicated in Figure 1(a). The targeting efficiency was around 50%. Two correctly targeted ES cell clones that were injected into mouse blastocyst embryos and implanted into a foster mouse are presented here. (c) Western blot analysis of targeted ES cell clones. In correctly targeted ES cells, transcription from the ROSA26 promoter will result in a chimaeric mRNA encoding the HABirA protein. The HA antibody detects a protein of expected size, 39 kD, in cell extracts of clone 13 and 28 but not in extracts of non-targeted ES cells (ES). (d) Western blot analysis of HABirA expression in tissues of ROSA26$^{HABirA/+}$ mice. Protein extracts (12.5 μg) from tissues dissected from postnatal day 8 mice were size separated on a 10% SDS-polyacrylamide gel and blotted onto nitrocellulose paper. The HA antibody recognises a 39 kD protein in all tissues tested.

ligases (Figure 2(b), panel b). Furthermore, endogenous biotinylated proteins, such as carboxylases, are not detected by the fluorescein-Avidin under the conditions used here. In contrast, biotinylated AviGata1 protein could readily be detected in foetal liver cells of compound AviGata1:BirA mice using fluorescein conjugated Avidin (Figure 2(b), panel d). The fluorescein signal overlaps with the Gata1 signal (Cy5 signal, panel c) indicating that indeed AviGata1 is biotinylated and not another endogenous target protein.

To further demonstrate biotinylation of Gata1 and to examine the extent of this biotinylation, we performed electrophoretic mobility shift assays (EMSA) using foetal liver extracts of transgenic mice and a ^{32}P labelled double stranded oligonucleotide containing a Gata1 binding site (Figure 2(c)). Foetal liver cells of transgenic AviGata1 mice express one specific complex containing Gata1 and AviGata1 that can be shifted to a higher position in the gel using a Gata1 specific antibody (Figure 2(c), lanes 1 and 2). As expected, the Gata1 complex is not shifted in the presence of streptavidin indicating that AviGata1 is not biotinylated (Figure 2(c), lane 3). Furthermore, this result illustrates the fact that the Avi-tag is not a target for endogenous biotin ligases. Next, we similarly examined foetal liver

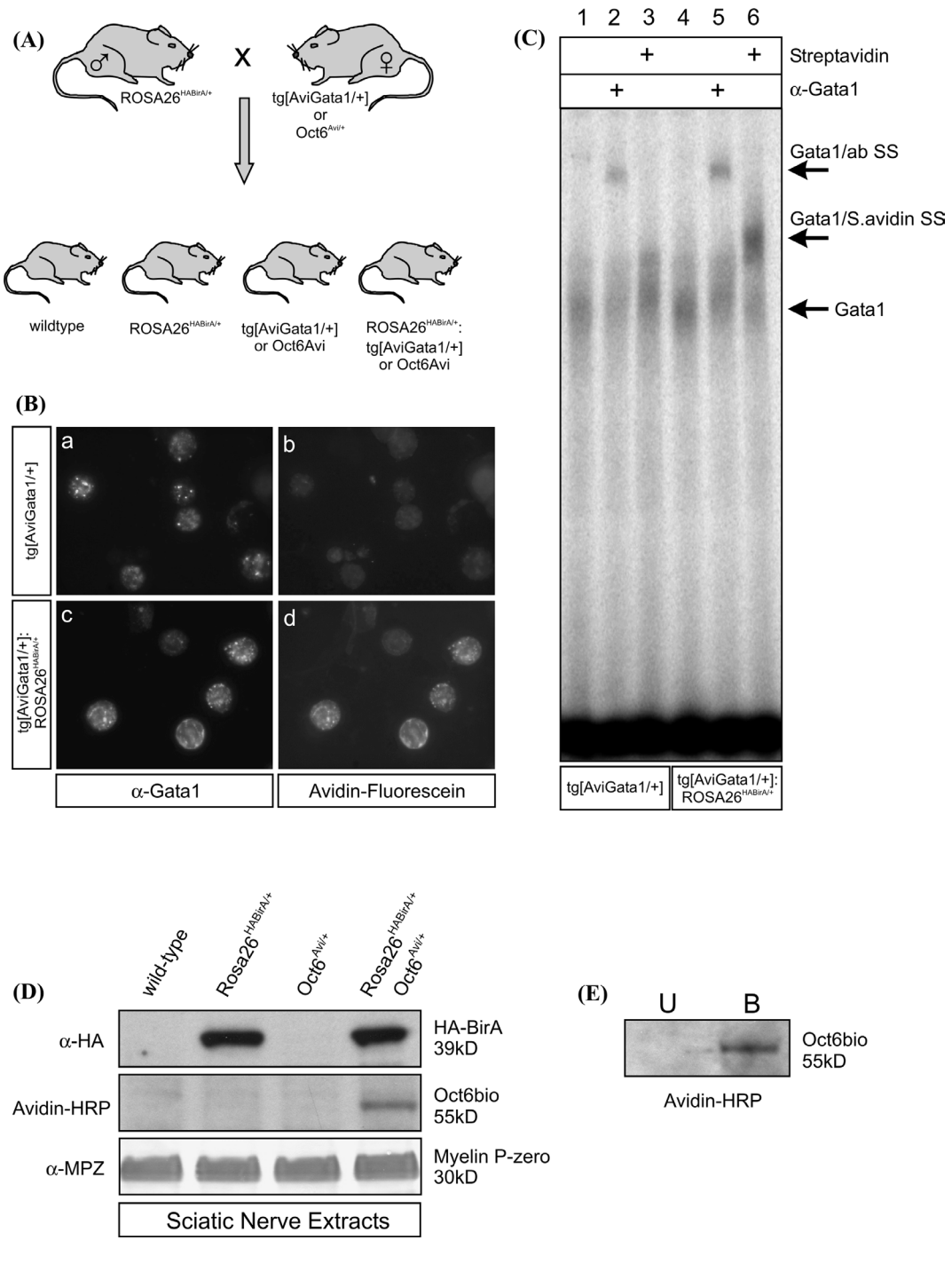
(A)
ROSA26HABirA/+
X
tg[AviGata1/+]
or
Oct6Avi/+
wildtype
ROSA26HABirA/+
tg[AviGata1/+]
or Oct6Avi
ROSA26HABirA/+:
tg[AviGata1/+]
or Oct6Avi
(B)
tg[AviGata1/+]
tg[AviGata1/+]:
ROSA26HABirA/+
a
b
c
d
α-Gata1
Avidin-Fluorescein
(C)
1 2 3 4 5 6
Streptavidin
α-Gata1
Gata1/ab SS
Gata1/S.avidin SS
Gata1
tg[AviGata1/+]
tg[AviGata1/+]:
ROSA26HABirA/+
(D)
wild-type
Rosa26HABirA/+
Oct6Avi/+
Rosa26HABirA/+
Oct6Avi/+
α-HA
HA-BirA
39kD
Avidin-HRP
Oct6bio
55kD
α-MPZ
Myelin P-zero
30kD
Sciatic Nerve Extracts
(E)
U
B
Oct6bio
55kD
Avidin-HRP

Figure 2. (a) Crossing scheme: Male ROSA26HABirA/+ mice were crossed with female tg[AviGata1] or $Oct6^{Avi/+}$ mice to obtain the genotypes depicted. (b) Foetal liver cells were prepared from E13,5 embryos of the genotype indicated and prepared for immunohistochemistry. A monoclonal antibody against Gata1detects the Gata1 protein in the nucleus of erythroid cells (panels a and c). The transgenic AviGata1 protein can be detected with fluorescein conjugated avidin when co-expressed with BirA (d) but not when BirA is not expressed (b). (c) Electrophoretic mobility shift assay. Gata1/DNA complexes were resolved on a 4% native polyacrylamide gel and visualised. Inclusion of a Gata1 specific antibody results in a ternary complex that migrates slower through the gel (Gata1/ab SS in lane 2 and 5). Inclusion of streptavidin results in a ternary complex with reduced mobility (Gata1/S.avidin SS) in foetal liver extracts of compound AviGata1:BirA embryos (lane 6). This complex is not formed in transgenic animals that do not express the HABirA protein (lane 3). The Gata1 complex in lane 6 represents endogenous Gata1 protein that does not contain an Avi-tag. (d) Biotinylation of Avi-tagged Oct6 in Schwann cells of the sciatic nerve at postnatal day 4. Sciatic nerves were dissected from mice with the indicated genotype and directly extracted in loading buffer. Proteins were size separated on a 10% SDS-polyacrylamide gel and transferred to nitrocellulose by electroblotting. Expression of BirA is detected using an HA antibody. Biotinylated Oct6 is detected using Avidin coupled to HRP and myelin P-zero is detected using the mouse monoclonal antibody P07 (Archelos et al., 1993). (e) Sciatic nerves of $ROSA26^{HABirA/+}$:$Oct6^{Avi/+}$ compound heterozygous animals were extracted in a buffer (20 mM Hepes-KOH, pH 7.6, 400 mM KCl, 1 mM DTT, 10% glycerol) by three freeze-thaw cycles. Biotinylated proteins were purified from this extract using magnetic streptavidin beads (Dynal), size separated on a 10% SDS-polyacrylamide gel and transferred to nitrocellulose. Biotinylated Oct6 is detected by Avidin coupled HRP in the bound (B) fraction but not in the unbound (U) fraction.

extracts from AviGata1:BirA compound transgenic embryos. Addition of the Gata1 antibody to the EMSA reaction results in one extra lower mobility complex (Figure 2(c), lanes 4 and 5). It appears that most of the AviGata1 protein present is biotinylated as most of the AviGata1 protein is shifted to a higher mobility by incorporation of streptavidin in the complex (Figure 2(c), lane 6). The remaining Gata1 complex represents endogenous Gata1 protein that does not contain an Avi-tag and therefore does not interact with streptavidin.

In a second set of experiments we analysed the biotinylation of Avi-tagged Oct6 protein expressed from the endogenous Oct6 locus. As Oct6 is expressed in postnatal Schwann cells we isolated sciatic nerves from mouse pups at postnatal day 4 (Scherer et al., 1994) and analysed biotinylation of Avi-Oct6 by Western blotting and purification (Figure 2(d) and (e)). Using Avidin-HRP as a probe we detect a 55 kD band corresponding to biotinylated Oct6 protein (Oct6bio in Figure 2(d)) in nerves of compound heterozygous mice ($Oct6^{Avi/+}$: $ROSA26^{HABirA/+}$ but not in single $Oct6^{Avi/+}$, $ROSA26^{HABirA/+}$ or wildtype mice (Figure 2(d)). Expression of BirA in sciatic nerve is detected using an HA antibody. Expression of the BirA and $Oct6^{Avi}$ transgenes do not affect peripheral nerve development as judged by the normal high level expression of the major peripheral Myelin Protein Zero (MPZ in Figure 2(d)). Furthermore, biotinylated Oct6 could be readily purified from nerve extracts of compound heterozygous animals (Figure 2(e)).

From these experiments we conclude that the BirA mouse strain is an excellent generic strain to obtain biotinylation of an Avi-tagged transgenic protein or endogenous protein that is extended with an Avi-tag through gene targeting. As such, this mouse might prove very useful in a wide range of studies in which complex interactions need to be studied in the developing or adult animal. One potential drawback of this particular mouse strain is that proteins that are translated on the endoplasmic reticulum bound ribosomes and are entering the secretory pathway, will not be efficiently biotinylated by the BirA protein which is located largely in the cytoplasm. Parrot and Barry (2001) have recently shown that proteins in the secretory pathway can be efficiently biotinylated provided that the BirA protein itself is extended with a signal peptide that will direct the protein into the secretory pathway. The generation of such a mouse following the same strategy described here is under way and will allow future studies on proteins or protein domains that function outside the cell or within the secretory pathway itself.

Acknowledgements

This work was supported in part by grants from the Dutch science organisation (ZONMW 903-42-195) and the BSIK program of the Dutch Government (BSIK 03038, Stem Cells in Development and Disease).We thank Elaine Dzierzak for critical reading of the manuscript.

References

Archelos JJ, Roggenbuck K, Schneider-Schaulies J, Linington C, Toyka KV and Hartung HP (1993) Production and characterization of monoclonal antibodies to the extracellular domain of P0. *J Neurosci Res* **35**: 46–53.

Beckett D, Kovaleva E and Schatz PJ (1999) A minimal peptide substrate in biotin holoenzyme synthetase-catalyzed biotinylation. *Protein Sci* **8**: 921–929.

Chapman-Smith A and Cronan JE Jr. (1999) The enzymatic biotinylation of proteins: a post-translational modification of exceptional specificity. *Trends Biochem Sci* **24**: 359–363.

Cull MG and Schatz PJ (2000) Biotinylation of proteins *in vivo* and *in vitro* using small peptide tags. *Methods Enzymol* **326**: 430–440.

de Boer E, Rodriguez P, Bonte E, Krijgsveld J, Katsantoni E, Heck A, Grosveld F and Strouboulis J (2003) Efficient biotinylation and single-step purification of tagged transcription factors in mammalian cells and transgenic mice. *Proc Natl Acad Sci USA* **100**: 7480–7485.

Elefanty AG, Antoniou M, Custodio N, Carmo-Fonseca M and Grosveld FG (1996) GATA transcription factors associate with a novel class of nuclear bodies in erythroblasts and megakaryocytes. *EMBO J* **15**: 319–333.

Ohneda K and Yamamoto M (2002) Roles of hematopoietic transcription factors GATA-1 and GATA-2 in the development of red blood cell lineage. *Acta Haematol* **108**: 237–245.

Parrott MB and Barry MA (2001) Metabolic biotinylation of secreted and cell surface proteins from mammalian cells. *Biochem Biophys Res Commun* **281**: 993–1000.

Rigaut G, Shevchenko A, Rutz B, Wilm M, Mann M and Seraphin B (1999) A generic protein purification method for protein complex characterization and proteome exploration. *Nat Biotechnol* **17**: 1030–1032.

Scherer SS, Wang DY, Kuhn R, Lemke G, Wrabetz L and Kamholz J (1994) Axons regulate Schwann cell expression of the POU transcription factor SCIP. *J Neurosci* **14**: 1930–1942.

Terpe K (2003) Overview of tag protein fusions: from molecular and biochemical fundamentals to commercial systems. *Appl Microbiol Biotechnol* **60**: 523–533.

Zambrowicz BP, Imamoto A, Fiering S, Herzenberg LA, Kerr WG and Soriano P (1997) Disruption of overlapping transcripts in the ROSA beta geo 26 gene trap strain leads to widespread expression of beta-galactosidase in mouse embryos and hematopoietic cells. *Proc Natl Acad Sci USA* **94**: 3789–3794.

Chapter 5

Cell autonomy of the mouse *claw paw* mutation

Aysel Darbas, Martine Jaegle, Erik Walbeehm, Hans van den Burg, Siska Driegen, Ludo Broos, Matthijs Uyl, Pim Visser, Frank Grosveld and Dies Meijer

Developmental Biology, 2004

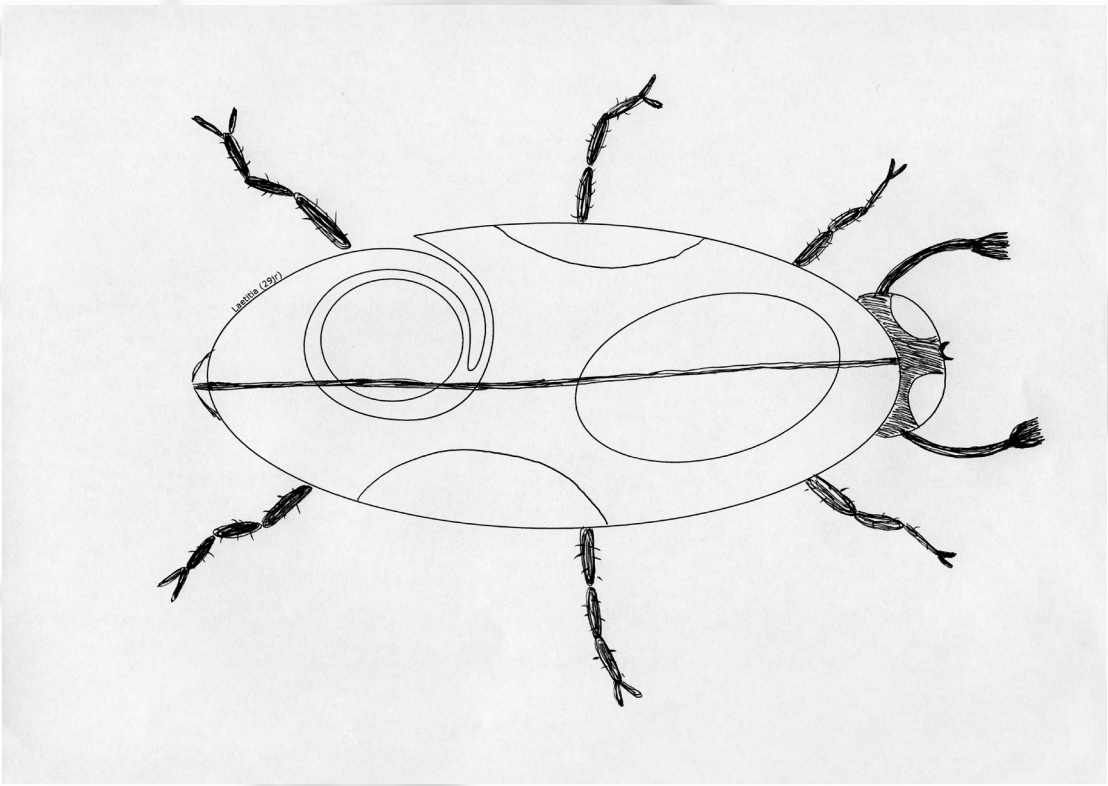

Available online at www.sciencedirect.com
SCIENCE DIRECT
Developmental Biology 272 (2004) 470–482
DEVELOPMENTAL BIOLOGY
www.elsevier.com/locate/ydbio

Cell autonomy of the mouse *claw paw* mutation

Aysel Darbas,[a,1] Martine Jaegle,[a,1] Erik Walbeehm,[b] Hans van den Burg,[c] Siska Driegen,[a,c] Ludo Broos,[a] Matthijs Uyl,[a] Pim Visser,[a] Frank Grosveld,[a] and Dies Meijer[a,*]

[a] *Department of Cell Biology and Genetics, ErasmusMC, Erasmus University Medical Center, 3000DR Rotterdam, Netherlands*
[b] *Department of Reconstructive Surgery, ErasmusMC, Erasmus University Medical Center, 3000DR Rotterdam, Netherlands*
[c] *Department of Neurosciences, ErasmusMC, Erasmus University Medical Center, 3000DR Rotterdam, Netherlands*

Received for publication 4 March 2004, revised 21 May 2004, accepted 21 May 2004

Abstract

Mice homozygous for the autosomal recessive mutation *claw paw* (*clp*) are characterized by limb posture abnormalities and congenital hypomyelination, with delayed onset of myelination of the peripheral nervous system but not the central nervous system. Although this combination of limb and peripheral nerve abnormalities in *clp/clp* mice might suggest a common neurogenic origin of the syndrome, it is not clear whether the *clp* gene acts primarily in the neurone, the Schwann cell or both. In the work described here, we address this question of cell autonomy of the *clp* mutation through reciprocal nerve grafting experiments between wild-type and *clp/clp* animals. Our results demonstrate that the *clp* mutation affects the Schwann cell compartment and possibly also the neuronal compartment. These data suggest that the *clp* gene product is expressed in Schwann cells as well as neurones and is likely to be involved in direct axon–Schwann cell interactions. Within the Schwann cell, *clp* affects a myelin-related signaling pathway that regulates periaxin and Krox-20 expression, but not Oct-6.

Keywords: Myelination; Schwann cell; Arthrogryposis; POU factors; Periaxin

Introduction

Congenital limb posture abnormalities in humans and other vertebrates occur under a variety of circumstances and clinically manifest as a singular abnormality or as part of a syndrome. In clinical practice, such abnormalities are described as arthrogryposis multiplex congenita (AMC; arthron = "joint" and gryposis = "bent"). It is generally accepted that any condition resulting in reduced fetal movement will lead to joint contractures in newborns (Drachman, 1971; Hageman and Willemse, 1983; Hall, 1997). In principle, such conditions could be extrinsic or intrinsic to the developing fetus. An example of the former is provided by experiments in which chick or rat embryos were paralyzed by injection with curare, causing limb posture abnormalities at birth (Del Torto et al., 1983; Drachman and Coulombre, 1962; Moessinger, 1983). Additionally, maternal antibodies that functionally inhibit the fetal acetylcholine receptor cause arthrogryposis in human fetuses (Jacobson et al., 1999; Matthews et al., 2002; Polizzi et al., 2000).

Intrinsic causes of reduced fetal movement can be classified as either myogenic and/or neurogenic in origin. In several clinical cases, AMC was found associated with congenital hypomyelination of the peripheral nerves suggesting a common aetiology (Boylan et al., 1992; Charnas et al., 1988; Seitz et al., 1986). In the peripheral nervous system, myelin formation and maintenance of the peripheral nervous system by Schwann cells is dependent on continuous reciprocal interactions between the axon and Schwann cell (Fields and Stevens-Graham, 2002). Mutations that affect this dialogue by disabling function in the Schwann cell, the axon or in both result in dys- or demyelinating neuropathies as in the human hereditary motor and sensory neuropathies (Suter and Scherer, 2003). Limb posture abnormalities, mostly pes cavus, and distal muscle wasting frequently develop in these patients as consequence of axonal loss.

Congenital limb posture abnormalities are observed in mice homozygous for the murine autosomal recessive mutation *claw paw* (*clp*) (Henry et al., 1991). In affected

* Corresponding author. Department of Cell Biology and Genetics, ErasmusMC, Erasmus University Medical Center, Dr Molewaterplein 50, PO Box 1738, 3000DR Rotterdam, Netherlands. Fax: +31-10-408-9468.
E-mail address: d.meijer@erasmusmc.nl (D. Meijer).
[1] These authors contributed equally to this study.

0012-1606/$ - see front matter © 2004 Elsevier Inc. All rights reserved.
doi:10.1016/j.ydbio.2004.05.017

animals, the forelimbs are flexed at one or more of the joints (shoulder, wrist or digital joints) but extended at the elbow, resulting in the forelimbs pointing in the direction of the hindlimbs. These abnormalities are visible within 2 days of birth. More severely affected animals also show involvement of one or both hindlimbs. Pathological examination of affected animals demonstrates severe congenital hypomyelination with delayed onset of myelination of the peripheral nerves with central nerves unaffected. Persistently blocked myelination is observed in a fraction of the smaller axons (Henry et al., 1991). Additionally, it was found that the mean internodal length is greatly reduced for all axonal size classes in *clp/clp* nerves when compared to heterozygous or wild-type animals (Koszowski et al., 1998). The *clp* gene has not been identified yet, although mapping studies have placed the gene close to the *Gpi* locus on mouse chromosome 7 (Henry et al., 1991). No mutations were found in the *myelin-associated glycoprotein* (*MAG*) gene, close to the *Gpi* locus, excluding this gene as a *clp* candidate (Niemann et al., 1998). The pathology of the *clp/clp* mouse is strikingly similar to the clinically described cases of AMC mentioned above. Hence, *clp/clp* mice provide an opportunity to study the basis of the relationship between arthrogryposis and hypomyelination.

It has been hypothesized that the *clp* gene is part of the neurone–glia signaling system that governs myelination initiation during development. However, it is not known what cellular and molecular components of this signaling system are affected by the *clp* mutation. To further characterize this mutant mouse, we set out to determine whether the gene acts in the neurone, the Schwann cell or both, through reciprocal nerve graft experiments. Additionally, we studied the interaction of the *clp* gene with many known Schwann cell autonomous regulatory genes involved in myelination including the transcription factors *Oct-6* and *Krox-20* (Topilko and Meijer, 2001). Our results indicate that *clp* function is required within the Schwann cell as well as in the neurone. Upregulation of the promyelin transcription factor Oct-6 is not affected by *clp*, while the subsequent Krox-20 activation is delayed. Additionally, embryonic periaxin expression is absent or reduced in *clp/clp* Schwann cells and postnatal expression is delayed. Taken together, these results suggest that *clp* is involved in neurone–glia interactions and furthermore that, within the Schwann cell, *clp* is involved in a pathway that regulates periaxin and Krox-20 expression. This *clp*-dependent pathway is parallel and non-redundant to the myelin-related Oct-6-dependent pathway.

Materials and methods

Animal surgery

Nerve crush experiments were performed on young adult F2 animals from a C57BL6J/Balbc-*clp* heterozygous intercross. Affected and non-affected mice were anesthetized by inhalation of halothane and placed on a heating pad. The left sciatic nerve was exposed and crushed for two times 15 s at mid-femoral level using No.5 Biology forceps. Mice were sacrificed 4 weeks after the operation through trans-cardiac perfusion with a solution of 1% gluteraldehyde/3% paraformaldehyde in 100 mM cacodylate (pH 7.4). The operated and contralateral nerve was isolated for light and electron microscopic analysis.

Transplantation experiment

Reciprocal nerve grafting experiments were performed between wild type and wild type (wt:wt), wild type and *clp/clp* (wt:clp), *clp/clp* and wild type (clp:wt) and between *clp/clp* and *clp/clp* (clp:clp). All animals were of C57BL6J background, obviating the use of immune-suppressants to prevent graft rejection. Operations were performed on two animals at a time, both animals serving as nerve donor and recipient. Two mice of appropriate genotype were anesthetized through inhalation of halothane and placed on a heating pad. The left sciatic nerve was exposed in both animals. Approximately 7.5 –10 mm of nerve was excised and placed in the same orientation in the host animal. Nerve and muscle tissue were kept wet by regular application of a drop of sterile phosphate-buffered saline (PBS). The nerves were sutured at both the proximal and distal anastomosis site with two 10-0 black filament sutures. The retracted muscles were placed back in position and the skin was sutured. All surgical manipulations were done under a microscope. Animals were transferred to a clean cage and allowed to recover under a heating lamp. Animals were carefully monitored for wound healing on a daily basis. Four weeks after transplantation, animals were sacrificed.

Perineurium permeability

A 1% Evans Blue (Sigma) solution in 5% bovine serum albumin (fraction V)/PBS (pH 7.4) was dialyzed overnight in PBS. The sciatic nerves of an adult claw paw animal and a wild-type littermate were dissected out and placed immediately in 4 ml of Evans blue albumin (EBA) solution at room temperature. After a 30- or 60-min incubation period, nerves were briefly washed in PBS and fixed in 4% paraformaldehyde for 2 h. Nerves were cryoprotected in 30% sucrose/PBS, frozen and sectioned at 24 μm. Sections were mounted in Vectashield® (Vector laboratories) and viewed immediately under a fluorescence microscope.

Quantitative RT-PCR

Total RNA was extracted from sciatic nerves using RNA-Bee (Tel Test Inc.). First-strand cDNA was generated using Superscript II (Invitrogen) reverse transcriptase and oligo-dT as primer. The following primers were used to amplify *dhh* and *cyclophilin* transcripts: dhh forward, CATGTGGC-

CCGGAGTACGCC; dhh reverse, CGCTGCATCAGCGGCCAGTA; cyclophilin forward, GGTCAACCCCACCGTGTTCTTCGACAT; cyclophilin reverse, GGACAAGATGCCAGGACCTGTATGCT. Annealing temperature for dhh primers: 60 °C, annealing temperature for cyclophilin primers 68 °C. Aliquots were taken from the reaction with two cycle intervals and amplification products were analyzed on a 1.8% agarose gel.

Light/electron microscopy

Anesthetized animals were sacrificed through transcardial perfusion with PBS (pH 7.4) for 3 min followed by fixative [3% PFA (Sigma); 1% glutaraldehyde (Sigma) in 100 mM cacodylate buffer, pH 7.2] for 10 min. Sciatic nerves were isolated, fixed overnight in the same fixative at 4 °C. The next day, nerves were rinsed with 0.2 M cacodylate buffer, osmicated in 1% osmium tetroxide solution and embedded in Epon. Sections (1 μm) of Epon-embedded sciatic nerves were mounted on glass slides and stained with methylene blue. Ultra-thin cross sections from nerve grafts at mid-graft level were cut and uranyl acetate and lead citrate stained for electron microscopic analysis (Philips CM100).

Nerve conduction velocities

Nerve conduction velocities were measured on the tail nerve of anesthetized animals. Animals were placed on a thermo-comfort heating pad at 38 °C. Recording and stimulation electrodes were made of 300-μm tungsten needles with a 10-μm tip. The stimulus frequency and stimulation period was 1 Hz and 0.1 ms, respectively. Impedance of the recording electrode was 100 and 25 kΩ/kHz for the stimulation electrode.

Immunohistochemistry

Rabbit polyclonal antibodies used in this study are directed against Oct-6 (Jaegle et al., 2003), Periaxin (Scherer et al., 1995) and Krox-20 (1:400). The Krox-20 antibody was raised against the unique amino-terminal portion of the protein (amino acids 1–180). Animals were immunized with 6xHis-tagged Krox-20^{1-180} protein expressed in *E. coli* (M15 strain) and purified on Ni^{2+}-NTA-agarose beads (QIAGEN). Mouse monoclonal antibodies used were against P-zero (1:1000) (Archelos et al., 1993) and neurofilament medium chain (1:200, hybridoma 2H3, Developmental Studies Hybridoma Bank).

Embryos and tissues were isolated, fixed in a mixture of methanol, acetone, acetic acid and water (35:35:5:25) for 1 h at 4 °C, embedded in paraffin and sectioned at 7 μm. After dewaxing, tissue sections were hydrated and blocked in 1% BSA, 0.05% Tween-20 in PBS. Rabbit antibodies and mouse monoclonal antibodies were incubated simultaneously in PBS/0.05% Tween-20 overnight at room temperature. Oregon Green-conjugated goat anti-rabbit IgGs (Molecular Probes) and Texas Red-conjugated goat anti-mouse IgGs (Molecular Probes) were subsequently used as secondary antibodies. The tissue was viewed using a Leica fluorescence microscope.

Results

Morphological examination of clp nerves and comparison with Oct-6 mutant nerves

Our interest in the *clp* mouse mutant was initially raised by the similarities in peripheral nerve phenotypes between claw paw mice and *Oct-6* transcription factor mutant mice (Bermingham et al., 1996; Henry et al., 1991; Jaegle et al., 1996). Both mice are characterized by delayed initiation of myelination of their peripheral nerves. The similarities between these phenotypes suggested several possible interactions between the *Oct-6* and *clp* genes. For example, it is possible that the *clp* gene product is involved in those signaling pathways that activate *Oct-6* or, *clp* could be a major regulatory target of Oct-6. Alternatively, *clp* could act in a non-redundant pathway parallel to Oct-6. To begin to answer these questions, we first compared nerve morphology in both mutant and wild-type mice at several postnatal stages of development. Previously, nerve morphology in *clp/clp* animals has been described only from postnatal day 14 (P14) onwards (Henry et al., 1991). Therefore, we extended this analysis to include earlier stages of nerve development. Fig. 1 shows a comparison of representative transverse sections through the sciatic nerve of animals of different genetic background at different stages of postnatal development.

The sorting of prospectively myelinated axonal fibers by Schwann cells during late fetal development culminates in the promyelin stage of cell differentiation in which a Schwann cell has established a one to one relationship with its axon. These cells will exit the cell cycle, elaborate a basal lamina and initiate myelination. The majority of myelin-competent cells transit through this stage during the first week of postnatal life. This is evident in transverse section of the wild-type sciatic nerve at birth, in which many promyelin cells can be observed with some cells already actively myelinating (Fig. 1A, panel a). By P8, a majority of cells is actively myelinating and at P16 almost all myelin-competent cells are in an advanced stage of myelination (Fig. 1A, panels d and g). In contrast to wild-type, *clp/clp* Schwann cells are still at a very immature sorting stage at birth (Fig. 1, panel b). Most Schwann cells are found at the periphery of naked axon bundles, with cellular extensions pioneering into the bundles. This configuration of Schwann cells and naked axon bundles is typically observed in embryonic nerves around mouse embryonic day 17 (E17) (Feltri et al., 2002). To illustrate this developmental stage of *clp/clp* Schwann cells more graphically, we traced the

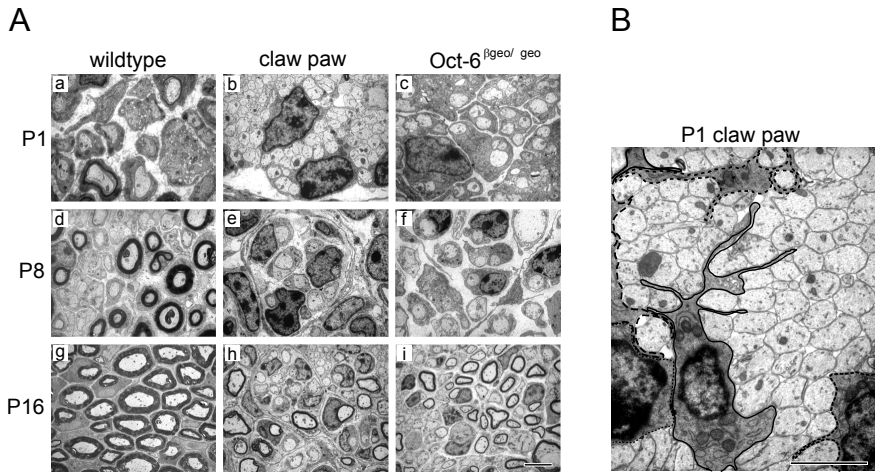

Fig. 1. Abnormal development of peripheral nerves in *clp/clp* and *Oct-6* mutant mice. (A) Shown are representative micrographs of transverse sections of sciatic nerves from wild-type, *clp/clp* (claw paw) and *Oct-6* mutant (Oct-6$^{\beta geo/\beta geo}$) animals at P1 (a, b and c), P8 (d, e and f) and P16 (g, h and i). At P1, axonal sorting is well advanced in wild-type nerves, with many axons in a 1:1 relationship with Schwann cells and few in an early myelinating stage (a). In contrast, axonal sorting in *clp/clp* nerves is in a very early stage with large groups of unsorted axons (b). Sorting in Oct-6 mutant nerves is well advanced with most cells in a late sorting and promyelin stage (c). At P8, the majority of myelin-competent Schwann cells in wild-type nerves are actively engaged in myelination (d), while in *clp/clp* nerves Schwann cells have now adopted a promyelin configuration (e). At this time, most Oct-6 mutant Schwann cells are still at the promyelin stage of differentiation (f). At P16, myelination is well advanced in wild-type nerves (g). In contrast, only a fraction of *clp/clp*, and Oct-6 mutant, Schwann cells have progressed to the myelinating stage of differentiation with many cells still at the promyelin stage (h and i). Scale bar: (a–c) 1.6 μm; (d–f) 2.8 μm; (g–i) 5 μm. (B) Axonal sorting is delayed in nerves of *clp/clp* (claw paw) mice. In this representative micrograph, *clp/clp* Schwann cells are just beginning to send out processes in the axon bundles. The outline of sorting Schwann cells is traced with a colored pencil. Each color represents an individual Schwann cell. Scale bar: 2 μm.

outline of several cells in a P1 nerve highlighting the cytoplasmic extensions of the sorting Schwann cell (Fig. 1B). One week later, these axon bundles are sorted out and a majority of Schwann cells have acquired a promyelin configuration (Fig. 1, panel e). Over the next week, many promyelin cells initiate myelination, such that by P16, a large number of myelin figures are observed. However, a substantial number of Schwann cells are still at the promyelin stage of cell differentiation, suggesting that this transition occurs at a lower rate in *clp/clp* Schwann cells than in wild-type Schwann cells (Fig. 1, panel h). By P32, the majority of *clp/clp* Schwann cells are actively meylinating with only few cells remaining in the promyelin configuration (data not shown and Henry et al., 1991). In contrast to *clp/clp* Schwann cells, *Oct-6* mutant Schwann cells transit through the sorting stage of development normally, but then stall at the promyelin stage for several days before initiating myelination (Fig. 1A, panels c, f and i). Thus, *clp/clp* Schwann cells appear strongly inhibited in the sorting stage of nerve development and to a lesser extent in the promyelinating to myelinating transition.

One other remarkable difference between *clp/clp* nerves and *Oct-6* mutant nerves (and wild-type nerves) is the extensive fasciculation of the former. Division of the endoneurium by flattened, perineurial-like cells is already apparent at P8 in *clp/clp* nerves (Fig. 1A, panel e). As illustrated in Fig. 2A, these cells contain, like perineurial sheath cells, many caveolae and secrete a basal lamina (arrows and arrowheads, respectively, in Fig. 2A, panel a). The number of cell layers that make up the perineurium and the morphology of the perineurial cells appear normal in *clp/clp* nerves at P16 and adult (Fig. 2A, panel b, and data not shown). The hyper-fasciculation phenotype observed in *clp/clp* peripheral nerves is reminiscent of that observed in *dhh* mutant animals (Parmantier et al., 1999). Therefore, it is possible that this particular aspect of the claw paw phenotype results from a failure to express *dhh* in the developing nerve. We therefore examined expression of *dhh* mRNA in *clp/clp* and wild-type nerves at P12 using quantitative PCR normalized to *cyclophilin* expression. We found that *dhh* is expressed in P12 *clp/clp* nerves, albeit at reduced levels (Fig. 2B). It is therefore possible that the extensive subdivision of *clp/clp* nerves by perineurial sheath cells is a consequence of reduced *dhh* expression. It has been hypothesized that the hyperfasciculation of *dhh* mutant nerves results from a functionally defective perineurium (Parmantier et al., 1999). A major function of the perineurium is to prevent the invasion of cells and macromolecules from the surrounding tissue into the endoneurium (Thomas et al., 1993). This nerve–tissue barrier function of the perineurium is compromised in *dhh* mutant animals as evidenced by the penetration of dye loaded serum albumin into the endoneu-

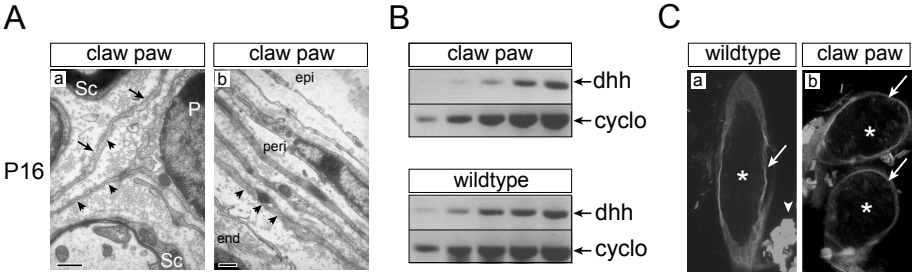

Fig. 2. Morphological and functional characterization of the perineurium of claw paw nerves. (A) Perineurial-like cells subdivide the endoneurium of claw paw nerves (panel a). This electron micrograph shows the typical flattened extensions of perineurial-like cells studded with numerous caveolae (arrows) and the basal lamina produced by these cells (arrowheads). Schwann cells (Sc) and the nucleus of a perineurial cell (P) are indicated. The number of cellular layers and the morphology of the perineurial cells appear normal in the developing perineurium of claw paw nerves (panel b). The epineurium is poorly defined at this stage and later stages. Scale bar: 500 nm. (B) *dhh* mRNA expression is reduced in claw paw nerves. Expression levels of *dhh* were estimated using quantitative RT-PCR during the exponential phase of the reaction and normalized against cyclophilin (cyclo), a housekeeping gene expressed at rather constant levels. Samples were taken with two-cycle intervals. It is estimated that *dhh* mRNA levels are 4- to 16-fold lower in claw paw nerves at P12. (C) The nerve–tissue barrier function of the perineurium is intact in claw paw nerves. Following submersion of dissected sciatic nerve of wild-type (panel a) or claw paw nerve (panel b) for 1 h in EBA solution, EBA is found associated with the epi- and perineurial sheath of the nerve (arrows). EBA did not penetrate the endoneurium of wild-type or claw paw nerves (asterisk). However, strong EBA staining is seen within muscle tissue lying next to the nerve (arrowhead).

rium (Parmantier et al., 1999). We similarly tested the integrity of the tissue–nerve barrier in claw paw nerves. After 1 h exposure to a Evans blue albumin solution ex vivo, nerves were processed for fluorescence microscopy. No dye complex had penetrated the endoneurium of wild-type or claw paw nerves (Fig. 2C, panels a and b, respectively) demonstrating that, in contrast with *dhh* mutant nerves, the nerve–tissue barrier in claw paw mice is intact. Thus, *clp/clp* nerves resemble *dhh* mutant nerves in their extensive subdivision into smaller fascicles by perineurial sheath cells but have, unlike *dhh* mutant nerves, a functionally intact perineurium.

Activation of Oct-6 expression in clp/clp nerves

As previous work has demonstrated that the transcription factors Oct-6 and Krox20 are major cell-autonomous regulators of the Schwann cell myelination program, it is possible that the delayed myelination phenotype in *clp/clp* nerves can in part be explained by a failure to activate Oct-6 and subsequently Krox-20, in *clp/clp* animals (Ghislain et al., 2002). We therefore examined expression of Oct-6, Krox-20 and the myelin proteins P-zero and periaxin in *clp/clp* animals at P8 and P16 by immunohistochemistry and compared it with the expression of these proteins in wild-type and *Oct-6* mutant Schwann cells (Fig. 3). At P8, most *clp/clp* Schwann cells are, like most *Oct-6* mutant cells, at the promyelin stage of cell differentiation (see Fig. 1) and will commence myelination in the course of the next 2 weeks. As shown in Fig. 3A, Oct-6 is expressed in Schwann cells of *clp/clp* animals at P8. This is in agreement with previous mRNA expression data (Bermingham et al., 2002). As reported earlier, Oct-6 is an upstream regulator of Krox-20 and hence, *Oct-6* mutant Schwann cells do not express Krox-20 (Ghazvini et al., 2002; Ghislain et al., 2002). Despite the expression of Oct-6 in *clp/clp* Schwann cells, Krox-20 is not expressed at P8, but eventually is activated in *clp/clp* nerves (and *Oct-6* mutant nerves) when myelination proceeds (Ghazvini et al., 2002 and Fig. 3B, panel a). As expected, P-zero expression is very low in both mutant mouse strains at P8, as the majority of Schwann cells have not yet produced compact myelin (Fig. 3A, panels h and i). However, at P16, *clp/clp* nerves show strong P-zero immunoreactivity in myelin-forming Schwann cells (Fig. 3B, panel b). Interestingly, the myelin protein periaxin appears reduced or misexpressed in *clp/clp* Schwann cells at P8. This is in contrast to promyelin-arrested *Oct-6* mutant Schwann cells in which periaxin is expressed at near normal levels (panels j, k and j). However, once *clp/clp* cells form compact myelin, high levels of periaxin are observed in these cells (Fig. 3B, panel c). Thus, in contrast to *Oct-6* mutant Schwann cells, periaxin protein does not accumulate in promyelin-arrested *clp/clp* Schwann cells suggesting that the *clp* mutation affects activation of periaxin expression or subcellular localization and/or processing.

To distinguish between these possibilities, we further examined periaxin expression at late fetal stages of development in *clp/clp* and wild-type animals. Periaxin is first expressed in the nuclei of embryonic Schwann cells at E14. By E17, periaxin expression shifts to the cell membrane and by E18, periaxin is no longer found in the nucleus (Sherman and Brophy, 2000). We examined periaxin expression in *clp/clp* Schwann cells of embryonic nerves at E17, the stage at which claw paw animals can first be recognized. No periaxin is detected in *clp/clp* nerves at this stage (Fig. 4A, panel d). In contrast, wild-type Schwann cells express periaxin in the nucleus and/or in the cytoplasm (Fig. 4A, panel c). Thus, the *clp* mutation affects onset of periaxin expression at this embryonic stage and subsequently, also the subcellular localization of the periaxin protein.

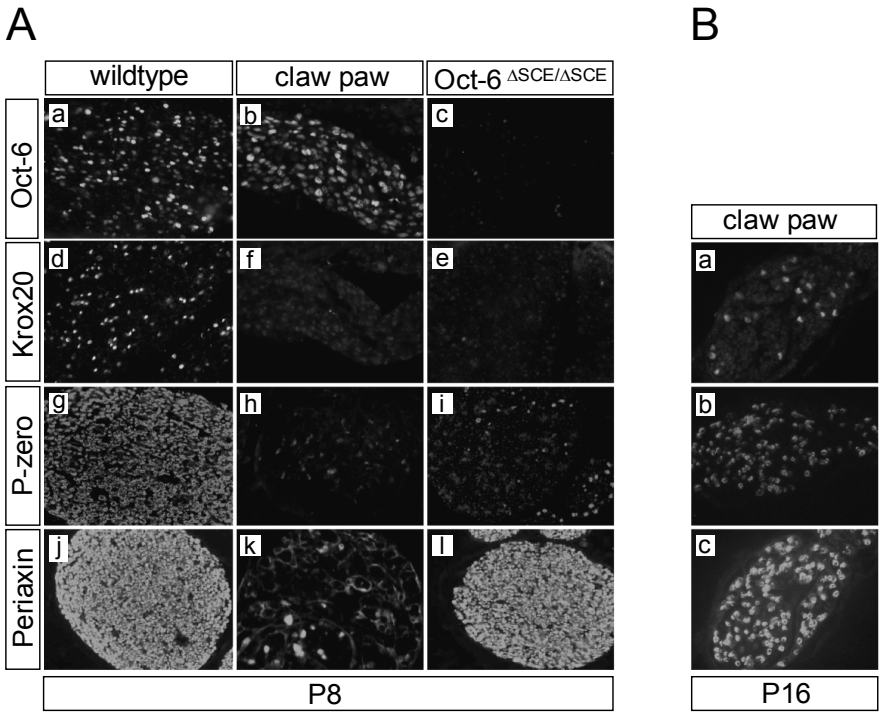

Fig. 3. Developmental expression of Oct-6, Krox-20, P-zero and periaxin in *clp/clp* and *Oct-6* mutant nerves. (A) Transverse sections of sciatic nerves of *clp/clp* (claw paw), *Oct-6* mutant (Oct-6$^{\Delta SCE/\Delta SCE}$) and control (wild-type) mice at P8 were stained for Oct-6 (a–c), Krox-20 (d–e), P-zero (g–i) and periaxin (j–l). In the control nerve, myelinating Schwann cells express Oct-6, Krox-20 and the myelin proteins P-zero and periaxin (a, d, g and j). At P8, most *clp/clp* Schwann cells have adopted a promyelin configuration and express Oct-6 (b) but not the myelination-associated transcription factor Krox-20 (f). Some cells express appreciable levels of P-zero. These cells are probably in an advanced promyelin stage as there is no evidence of compact myelin yet at this stage (h). Very low cytoplasmic periaxin expression is observed in many, but not all, cells (k). Few cells exhibit high level of periaxin expression. No nuclear periaxin staining is observed at this stage. Like *clp/clp* Schwann cells, *Oct-6* mutant Schwann cells do not express Oct-6 or Krox-20 at this stage (c and e). The few cells that have initiated myelin formation are strongly positive for P-zero (i). In strong contrast to *clp/clp* Schwann cells (k), *Oct-6* mutant cells express already high levels of periaxin at this stage (l). Magnification ×40. (B) Myelin formation is evident in *clp/clp* nerves at P16. An appreciable number of Schwann cells have initiated myelination and express Krox-20 (a). High levels of P-zero and periaxin are present in Schwann cells that have formed compact myelin (b and c). Magnification ×40.

We next examined whether Oct-6 is also delayed in its onset of expression. Oct-6 protein normally starts to accumulate in the nuclei of immature Schwann cells of the sciatic nerve at late fetal stages and reaches maximum levels in promyelin cells during the first postnatal week of development. As *clp/clp* Schwann cells at P1 morphologically resemble Schwann cells in E16–E17 wild-type embryonic nerves, we examined Oct-6 expression in P1 *clp/clp* nerves. At this stage, we found that *clp/clp* Schwann cells already express appreciable levels of Oct-6 (Fig. 4B, panel b), demonstrating that the clp gene product does not affect activation of Oct-6 expression. In contrast to wild-type Oct-6-positive Schwann cells, Oct-6-positive *clp/clp* Schwann cells do not express appreciable levels of P-zero protein (Fig. 4B, panels c and d).

Taken together, these data demonstrate that the *clp* mutation affects nerve maturation through a pathway that includes activation of periaxin, but not Oct-6, and thus strongly suggest that during Schwann cell differentiation, periaxin and Oct-6 are regulated through distinct signaling pathways.

Nerve conduction velocities of clp nerves are reduced

The delayed maturation of peripheral nerves in *clp/clp* animals results in reduced internodal lengths for all diameter classes and thus, in the absence of axonal loss, increased Schwann cell numbers. In addition, myelin thickness is reduced in some, but not all, *clp/clp* animals and no decrease in mean axon diameter was reported (Henry et al., 1991;

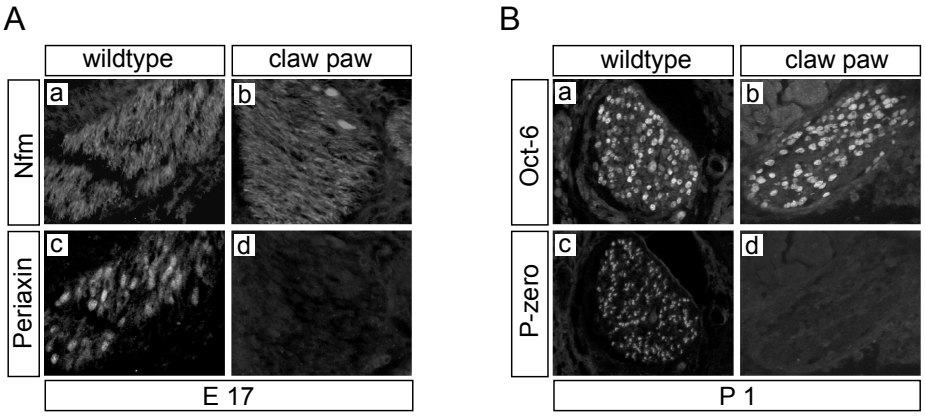

Fig. 4. Expression of periaxin and Oct-6 in *clp/clp* Schwann cells. (A) Embryonic sciatic nerve is visualized by expression of the neurofilament medium chain in the axonal fibers (Nfm; a and b). Embryonic Schwann cells within the nerve express periaxin in their cytoplasm or nucleus (c). In contrast, no periaxin expression is observed in nerves of claw paw embryos at this stage of development (d). (B) Oct-6 is expressed in all Schwann cells in newborn wild-type sciatic nerves (a). Also, Schwann cells in sciatic nerves of *clp/clp* animals express Oct-6 (b). Other than wild-type Schwann cells, *clp/clp* Schwann cells uniformly express high levels of Oct-6. In wild-type nerves, many Schwann cells are at the promyelin configuration and some have initiated myelination and thus express high levels of P-zero (c). In contrast, *clp/clp* Schwann cells appear at an early sorting stage at P1 (see Fig. 1) and do not express detectable levels of P-zero protein (d).

Koszowski et al., 1998). The mean internodal length in every axonal diameter class in *clp/clp* animals is approximately half of that of wild-type animals. Intuitively, and on theoretical considerations, it is to be expected that propagation of action potentials will be slowed when the mean internodal length drops well below its optimum (Brill et al., 1977; Goldman and Albus, 1968; Rushton, 1951). To assess nerve conduction velocity (NCV) in *clp* and wild-type animals, we measured compound action potentials (CAP) of the tail nerve (Fig. 5A). The mean NCV in wild-type and heterozygous mice was 35.3 m/s (SD 1.8). In contrast, the mean NCV in *clp/clp* mice was 23.9 m/s (SD 2.2), a reduction of 35% (Fig. 5B). A similarly reduced conduction velocity was observed for motor nerves within the sciatic nerve of *clp/clp* animals as compared to wild type (data not shown). Reduced NCV in the tail nerve of claw paw mice shows little variance, and this variance does not correlate with age or severity of the behavioral phenotype. Thus, it is possible that the reduction in NCV in *clp/clp* animals can be accounted for, at least in part, by the reduction in mean internodal length.

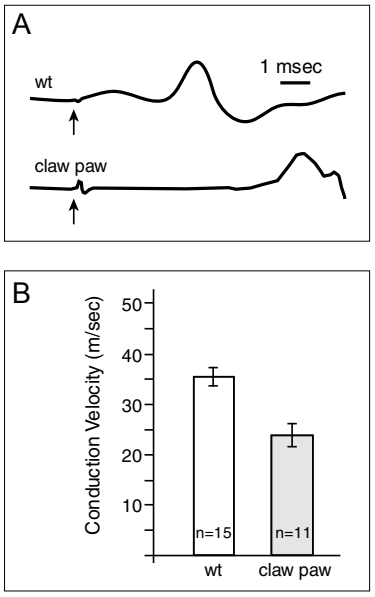

Fig. 5. Nerve conduction velocities are reduced in *clp/clp* nerves. (A) Representative recordings of compound action potentials of the tail nerve of wild-type (wt) and *clp/clp* (claw paw) animals. Arrows indicate the stimulation artefact. (B) Mean conduction velocity for wild-type (wt) and *clp/clp* (claw paw) nerves. The number (*n*) of animals from which recordings were obtained in each group is indicated. The error bar represents standard deviation. The difference in mean NCV between *clp/clp* and wild-type animals is significant ($P < 0.00001$, Student's *t* test).

Response to nerve injury

Although the claw paw phenotype has been described as a developmental abnormality, it is not clear from these observations whether the phenotype results from an intrinsic defect in one or more components of the developing nerve or through defects in other organs of the developing fetus. Studying the damage response of the nerve in the adult animal allows examination of Schwann cell–axon interac-

tions that are largely a reiteration of developmental events (Scherer and Salzer, 1996). Following nerve transection, axons and myelin in the distal nerve segment disintegrate in a process called Wallerian degeneration. Schwann cells revert back to an immature pre-myelinating phenotype, proliferate and participate with macrophages in the removal of myelin and axonal debris. These reactive Schwann cells create an environment that stimulates axonal regeneration of the transected neurones. Upon restoration of axonal contact, Schwann cells differentiate into myelin or non-myelin forming cells (Scherer and Salzer, 1996). Therefore, if the *clp* defect resides within the nerve tissue, it is likely that at least part of the defect will be recapitulated during nerve regeneration following nerve axotomy in an adult animal. On the other hand, if the *clp* defect is strictly developmental and not intrinsic to the nerve tissue, it is expected that regeneration will be relatively normal.

To examine the effect of the *clp* mutation on Schwann cell–axon interaction during regeneration, the sciatic nerve of adult *clp/clp* and wild-type mice were crushed and studied morphologically 4 weeks later (Fig. 6). The nerves were sectioned at two levels distal to the injury, 3 and 6 mm, respectively, representing two successive stages of regeneration. In wild-type animals, regeneration is well advanced, with only few remnants of myelin remaining (arrows in Fig. 6A, panel b) and most axons associated with compact myelin. Regeneration of *clp/clp* nerves differs significantly from wild-type nerves in some aspects. First, most large-caliber axons are ensheathed by a single Schwann cell, but only a few of these are associated with a thin compact myelin sheath (Fig. 6A, panels e and f). Second, supernumerary Schwann cells surround large axon–Schwann cell units and are associated with numerous thin axons (Fig. 6B). These structures are enclosed by the original basal lamina (arrows in Fig. 6B), indicating excessive sprouting of the regenerating axon. Third, excessive fasciculation results in a further subdivision of the *clp* nerve (Fig. 6A, panels e and f). Thus, while *clp* axons do grow back into the distal nerve stump, regeneration is clearly disturbed. Some of these regeneration abnormalities, such as delayed myelination and hyper-fasciculation, are also observed during development suggesting that the *clp* defects are caused by a nerve intrinsic defect in one or more components within the developing or regenerating nerve.

Nerve grafting

To distinguish between a Schwann cell and neuronal defect in the regeneration of *clp/clp* nerves, we performed nerve grafting experiments. Nerve transplantation experiments create a situation in which Schwann cells, genetically distinct from the host, differentiate in association with host-derived neurons (Aguayo et al., 1977; de Waegh and Brady, 1991; Scaravilli and Jacobs, 1981). We performed nerve transplantation operations in which a wild-type host was engrafted with a segment of a wild-type (wt:wt) or *clp/clp* (clp:wt) sciatic nerve segment. Also, the converse set of transplantations was performed in which a *clp/clp* host was engrafted with a wild-type (wt:clp) or *clp/clp* (clp:clp) sciatic nerve segment. The poorly developed epineurium of *clp/clp* nerves as compared to that of wild-type nerves made the grafting of the segments particularly demanding on the technical level. Four weeks after the operation, the transplanted nerves were isolated and examined microscopically. Each nerve was serially sectioned and examined at 250-μm intervals. Representative sections from the middle of the graft and proximal and distal to the anastomosis site are shown in Fig. 7. In the wt:wt transplantation, regenerat-

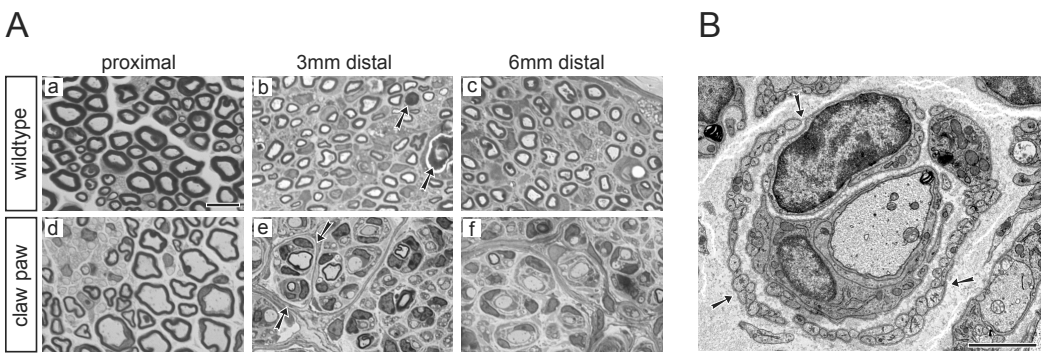

Fig. 6. Abnormal response to nerve injury in *clp/clp* mice. (A) Light micrographs of cross sections of sciatic nerves of young adult wild-type and *clp/clp* (claw paw) animals 4 weeks after nerve crush. The myelin sheath in *clp/clp* nerves is thinner than in wild-type nerves, as described earlier (a and d). In wild-type nerves, regeneration is well advanced, both at 3 and 6 mm distal of the nerve crush (b and c), with only little myelin debris remaining (arrows in panel b). All regenerated axons are myelinated. Regeneration in *clp/clp* nerves is delayed with only few regenerated axons myelinated. This is even more pronounced at 6 mm distal to the lesion, corresponding to a later time point in regeneration (f). Excessive fasciculation is evident in the regenerating nerve. A layer of epineural cells enclosing a group of regenerating fibers is indicated with arrows (e). Scale bar: 10 μm. (B) In this electron micrograph of a regenerating *clp/clp* nerve, supernumerary Schwann cells are associated with regenerating axons. In addition to the large central axon, excessive numbers of axon sprouts (red asterisks) are observed within the regenerating unit that is enclosed by one basal lamina (arrows). The cross section is through three Schwann cells. Scale bar: 2 μm.

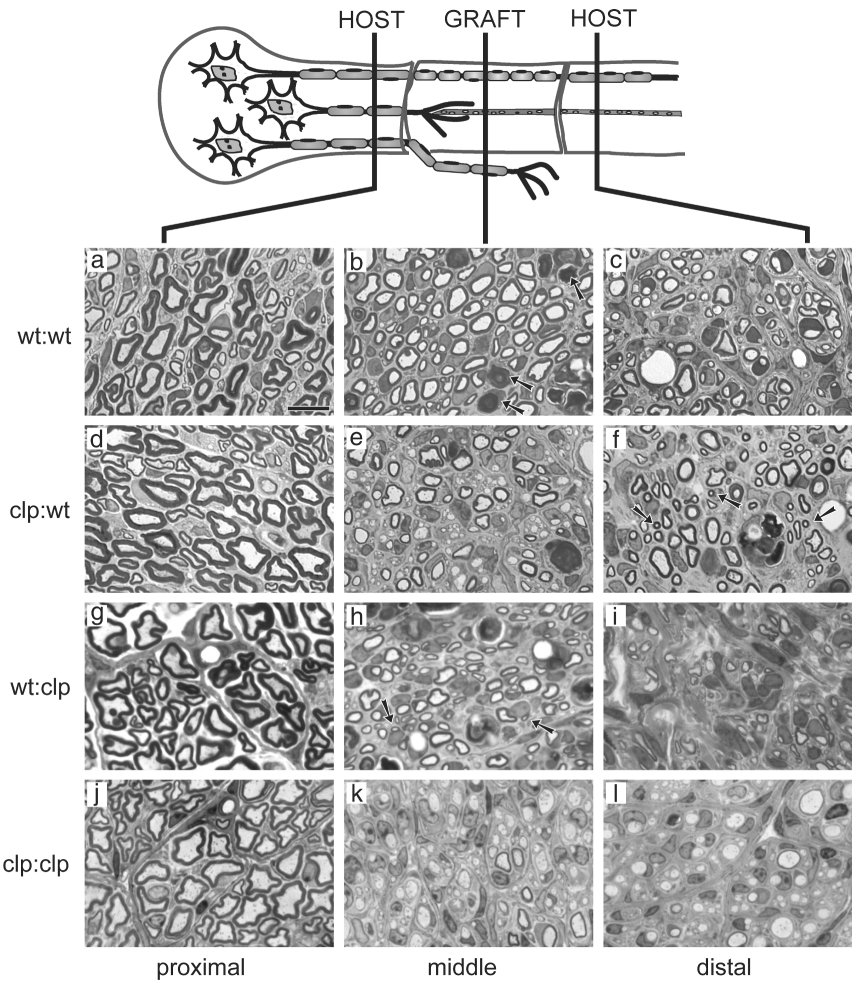

Fig. 7. Nerve grafting experiments reveal Schwann cell and neuronal expression of the *clp* defect. Light micrographs of semi-thin cross sections of sciatic nerve at three different levels of the engrafted nerve 4 weeks after the operation. The position of the sections relative to the engrafted segment is schematically depicted in the diagram above the micrographs. At the level of the engrafted segment and distal to this segment, three different configurations are expected: regenerated axons myelinated by graft-derived Schwann cells (blue in diagram); Schwann cell tubes (blue) that do not get re-innervated by host neurones and host axons that do not enter the nerve graft and are associated with host-derived Schwann cells (gray in diagram) that migrate with the regenerating axons. Donor and recipient genotypes (donor/recipient) are listed to the left. Non-innervated Schwann cell tubes with myelin debris are indicated with arrows in panel b. Thinly myelinated axons that have re-innervated the distal nerve segment of the wild-type host are indicated in panel f with arrows. Arrows in panel h also point to regenerating wild-type axons that are myelinated by *clp/clp* Schwann cells. For further details, see text. Scale bar: 10 μm.

ing axons have grown through the graft and entered the distal nerve stump. Wild-type Schwann cells in the graft and distal nerve stump have formed compact myelin around regenerated axons (Fig. 7, panels b and c). Schwann cell tubes (reactive Schwann cells within their basal lamina: bands of Bunger) that were not re-innervated still contain some myelin debris (arrows in panel b). In the clp:wt transplantation, wild-type axons do regenerate through a *clp/clp* nerve graft into the distal nerve stump (Fig. 7, panels e and f). Moreover, in contrast to wild-type Schwann cells, *clp/clp* Schwann cells have only myelinated the larger axons in the graft and many axons are still in an early ensheathing

or promyelin configuration (panel e). Smaller axons that have navigated through the graft and have entered the distal nerve stump are normally myelinated (arrows in panel f). These observations suggest that at least part of the delayed myelination phenotype in *clp/clp* animals is Schwann cell autonomous.

Transplantations of wild-type nerve segments into *clp/clp* hosts were less successful as ligations to the distal nerve stump did not hold. Nevertheless, *clp/clp* axons did enter the wild-type nerve graft and were myelinated by the wild-type Schwann cells within the graft (Fig. 7, panel h). Also smaller-caliber claw paw axons were myelinated (arrows in panel h). Distal to the second anastomosis site, regrowing axons did not enter the distal nerve stump, but were found associated with a large blood vessel (not shown). Most likely, graft-derived perineural cells and Schwann cells accompany these axons (panel i). Notwithstanding, these data suggest that wild-type Schwann cells receive appropriate signals from *clp/clp* neurones to myelinate them. Finally, the clp:clp transplantations show that *clp/clp* axons do grow through the grafted segment into the distal nerve stump. Consistent with the results in the *clp/clp* nerve crush experiment (Fig. 6), regenerating *clp/clp* axons are associated with supernumerary Schwann cells and only few axons are thinly myelinated (Fig. 7, panels k and l). We also observe a further increase in the extent of fasciculation. This increased fasciculation was less pronounced in the clp:wt and in wt:clp transplantations. Therefore, this specific aspect of the claw paw phenotype arises mainly from interaction of *clp/clp* axons with the *clp/clp* endoneurium. This is also true for the delayed myelination phenotype, as it is much more severe in the clp:clp transplantation than in the clp:wt and wt:clp transplantations. Thus, while the former two grafting experiments (wt:clp and clp:wt) suggest a Schwann cell autonomous effect of the *clp* mutation on myelination, the nerve crush and clp:clp transplantation suggest that there is also an important Schwann cell non-autonomous, most likely neuronal, aspect to the *clp* mutation.

Discussion

We have studied the cellular and molecular basis of the congenital limb abnormality manifested by claw paw mutant mice. Our findings demonstrate that the *clp* mutation affects both the axonal and endoneural/Schwann cell compartment, resulting in axonal sorting and myelination defects. At the molecular level, *clp* affects a signaling pathway that is parallel and non-redundant to the Oct-6-dependent pathway, suggesting that axonal signals that drive Schwann cell differentiation and myelination are transduced through multiple parallel pathways. These findings suggest several possible roles for the *clp* gene and, additionally, define a set of requirements for *clp* candidate genes, to be identified in the ongoing positional cloning effort.

What process in nerve development is affected by the clp mutation?

The development of peripheral nerve tissue can be conveniently thought of as an ordered series of cellular transitions that result from several complex interactions between Schwann cells, axons, mesenchymal cells and extracellular components (Jessen and Mirsky, 1999; Webster, 1993). The first transition occurs when migrating neural crest cells associate with outgrowing axon bundles and acquire Schwann cell precursor characteristics (Jessen and Mirsky, 1991; Jessen et al., 1994). These cells proliferate, migrate with the growing axons and, in a second transition, differentiate into immature Schwann cells that invade the axon bundles and start the process of radial sorting of nerve fibers. This process culminates in larger axons singled out by individual Schwann cells (promyelin stage) which, in a third transition, will go on to myelinate their axon and multiple smaller axons associated with Schwann cells to form the so-called Remak fibers of non-myelinated axons. During this last phase, immature Schwann cells exit the cell cycle and elaborate an extracellular matrix. The peri- and epineural layers that surround and protect the nerve differentiate from the surrounding mesenchyme in a process that requires Schwann cell-derived desert hedgehog signaling (Bunge et al., 1989; Du Plessis et al., 1996; Parmantier et al., 1999).

The major defects in the developing and adult peripheral nerves of claw paw mutant mice were originally described as a general delay of myelination initiation and the persistence of promyelin fibers in adult animals (Henry et al., 1991). On the basis of these morphological observations, Henry et al. hypothesized that the *clp* defect affects the complex signaling between axon, Schwann cell and extracellular components that control the transition of promyelin Schwann cells into myelinating cells. Molecular studies have shown that this transition is mediated by the activity of the transcription factors Oct-6 and Krox-20 acting consecutively in the Schwann cells (Ghislain et al., 2002). Our finding that *clp* does not affect activation of Oct-6 expression but that Krox-20 activation is delayed suggests that *clp* acts either downstream of Oct-6 or in a second non-redundant pathway.

Several observations presented here argue in favor of the second possibility. Morphological examination of nerves of newborn claw paw animals revealed that Schwann cells are still at an early sorting stage of development while wild-type and *Oct-6* mutant Schwann cells are at the end of the sorting stage. This early sorting stage observed in P1 *clp/clp* nerves would be appropriate for embryonic nerves in E16–E18 wild-type embryos. Sorting and ensheathment of axons by Schwann cells critically depends on rearrangements of the Schwann cell cytoskeleton. Deletion of the β1 integrin or the laminin γ1 gene in Schwann cells results in impaired sorting of axon bundles, suggesting that these rearrangements are mediated through interactions between the extracellular matrix laminins and their integrin receptors (Chen

and Strickland, 2003; Feltri et al., 2002; Saito et al., 2003). The similarity in ultrastructural abnormalities observed in newborn *clp/clp*, β1 integrin and laminin γ1 mutant nerves, suggests that clp acts in these pathways. In contrast to laminin γ1 null Schwann cells, *clp/clp* Schwann cells are not permanently blocked at the sorting stage. It is therefore likely that a *clp* redundant function exists or that the *clp* allele is a hypomorph.

In addition, *clp/clp* nerves exhibit hyperfasciculation, a phenotype resembling that observed in *dhh* mutant mice, suggesting the possibility that this specific aspect of the claw paw mutant phenotype results from downregulation of dhh expression. In agreement with this suggestion, we found that *dhh* mRNA is expressed at reduced levels in *clp/clp* nerves (at P12). However, in contrast to *dhh* mutant animals, the nerve–tissue barrier function of the perineurium in claw paw animals is not affected (Fig. 2). As the biological effects of hedgehog proteins are known to be dose-dependent, it is tempting to speculate that the differences in phenotype between *dhh* mutant and *clp/clp* nerves reflect differences in *dhh* expression levels in the developing nerves of these two mutant animals.

Nuclear periaxin expression in embryonic Schwann cells, and the later accumulation of periaxin in promyelin cells at P8, is not observed in claw paw nerves at these stages (Figs. 2 and 3), although periaxin does eventually accumulate in Oct-6 and Krox-20 expressing myelinating *clp/clp* Schwann cells (Fig. 2). It has recently been suggested that a dual mechanism of periaxin regulation exists in which Krox-20 amplifies an earlier Krox-20 independent activation of the periaxin gene (Parkinson et al., 2003). Our results suggest further that the early Krox-20 independent activation of periaxin is regulated through a *clp*-dependent pathway. Alternatively, it is possible that *clp* Schwann cells at E17 represent an earlier differentiation stage at which periaxin is not expressed yet (they will have to be very early Schwann cell precursors, as E14 Schwann cell precursors express periaxin in their nuclei, (Sherman and Brophy, 2000). It is unlikely that the absence of detectable levels of periaxin in *clp* Schwann cells contributes significantly to the peripheral nerve phenotype in claw paw mice, as peripheral nerve development is morphologically normal in *periaxin* null mice (Gillespie et al., 2000).

Thus, in contrast to what has been suggested earlier, the *clp* mutation affects nerve development at a stage well before the promyelin-myelinating transition. The particular defects suggest that *clp* is involved in axon–Schwann cell interactions that drive the invasion and sorting of immature Schwann cells and the subsequent elaboration of a basal lamina and myelination initiation.

On the nature of the claw paw mutation

In the absence of knowledge about the mutation underlying the claw paw phenotype, we do not know what mechanism could account for the peripheral nerve developmental defect and the behavioral defect in claw paw animals. However, on the basis of the observed developmental defects, the recessive nature of the *clp* mutation and in particular the results of regeneration and nerve transplantation experiments, we can speculate on possible scenarios. Although the morphological abnormalities observed in the nerve of claw paw animals suggest that the *clp* mutation affects primarily Schwann cells, the transplantation and nerve regeneration experiments suggest that *clp* function might also be required in the neurone and possibly the endoneurial fibroblasts. It is therefore likely that the *clp* gene product is expressed and functioning in both Schwann cells and neurones and that the *clp* mutation is not a gain of function mutation. These suggestions are compatible with *clp* functioning in, or regulating, homo- or heterophilic interactions between axons and Schwann cells. For example, it is possible that the claw paw protein is involved in bringing adhesion molecules to the cell surface or that claw paw itself is a cell surface protein directly involved in cell–cell interactions. Alternatively, it is possible that the *clp* mutation is a regulatory mutation affecting expression of genes involved in the abovementioned interactions. These impaired axon Schwann cell interactions at an early stage could have repercussions for nerve activity during fetal stages and affect the normal spontaneous movement of the fetus, important for proper posture development.

In summary, we have provided evidence that the mouse *clp* mutation affects the Schwann cell compartment and possibly the neuronal compartment of the regenerating and, by extension, the developing nerve, suggesting that the *clp* gene is expressed in Schwann cells and neurones and is involved in direct axon–Schwann cell interactions. Furthermore, the *clp* mutation affects early activation of periaxin expression and Krox20 expression in Schwann cells, but does not affect the signaling pathway that activates Oct-6 expression, suggesting that axonal signals that initiate myelination are transduced through multiple parallel, non-redundant pathways.

Acknowledgments

We thank Elaine Dzierzak and Sjaak Philipsen for their comments and encouragement. Thanks also to Peter Brophy and Juan Archelos who provided the periaxin antibody and the P-zero antibody, respectively. All animal work was performed according to institutional and European guidelines and approved by the animal experimentation review board (DEC). This work was supported in part by grants from the Dutch Research Council NWO (MW-901-01-205 and 903-42-195).

References

Aguayo, A.J., Attiwell, M., Trecarten, J., Perkins, S., Bray, G.M., 1977. Abnormal myelination in transplanted Trembler mouse Schwann cells. Nature 265, 73–75.

Archelos, J.J., Roggenbuck, K., Schneider-Schaulies, J., Linington, C., Toyka, K.V., Hartung, H.P., 1993. Production and characterization of monoclonal antibodies to the extracellular domain of P0. J. Neurosci. Res. 35, 46–53.

Bermingham, J.R., Scherer, S.S., Oconnell, S., Arroyo, E., Kalla, K.A., Powell, F.L., Rosenfeld, M.G., 1996. Tst-1/Oct-6/SCIP regulates a unique step in peripheral myelination and is required for normal respiration. Genes Dev. 10, 1751–1762.

Bermingham Jr., J.R., Shumas, S., Whisenhunt, T., Sirkowski, E.E., O'Connell, S., Scherer, S.S., Rosenfeld, M.G., 2002. Identification of genes that are downregulated in the absence of the POU domain transcription factor pou3f1 (Oct-6, Tst-1, SCIP) in sciatic nerve. J. Neurosci. 22, 10217–10231.

Boylan, K.B., Ferriero, D.M., Greco, C.M., Sheldon, R.A., Dew, M., 1992. Congenital hypomyelination neuropathy with arthrogryposis multiplex congenita. Ann. Neurol. 31, 337–340.

Brill, M.H., Waxman, S.G., Moore, J.W., Joyner, R.W., 1977. Conduction velocity and spike configuration in myelinated fibres: computed dependence on internode distance. J. Neurol., Neurosurg. Psychiatry 40, 769–774.

Bunge, M.B., Wood, P.M., Tynan, L.B., Bates, M.L., Sanes, J.R., 1989. Perineurium originates from fibroblasts: demonstration in vitro with a retroviral marker. Science 243, 229–231.

Charnas, L., Trapp, B., Griffin, J., 1988. Congenital absence of peripheral myelin: abnormal Schwann cell development causes lethal arthrogryposis multiplex congenita. Neurology 38, 966–974.

Chen, Z.L., Strickland, S., 2003. Laminin gamma1 is critical for Schwann cell differentiation, axon myelination, and regeneration in the peripheral nerve. J. Cell Biol. 163, 889–899.

de Waegh, S.M., Brady, S.T., 1991. Local control of axonal properties by Schwann cells: neurofilaments and axonal transport in homologous and heterologous nerve grafts. J. Neurosci. Res. 30, 201–212.

Del Torto, U., Bianchi, O., Pone, G., Sante, G., 1983. Experimental study on the etiology of congenital multiple arthrogryposis. Ital. J. Orthop. Traumatol. 9, 91–99.

Drachman, D.B., 1971. The syndrome of arthrogryposis multiplex congenita. Birth Defects, Orig. Artic. Ser. 7, 90–97.

Drachman, D.B., Coulombre, A.J., 1962. Experimental clubfoot and arthrogryposis multiplex congenita. Lancet 15, 523–526.

Du Plessis, D.G., Mouton, Y.M., Muller, C.J., Geiger, D.H., 1996. An ultrastructural study of the development of the chicken perineurial sheath. J. Anat. 189, 631–641.

Feltri, M.L., Graus Porta, D., Previtali, S.C., Nodari, A., Migliavacca, B., Cassetti, A., Littlewood-Evans, A., Reichardt, L.F., Messing, A., Quattrini, A., Mueller, U., Wrabetz, L., 2002. Conditional disruption of beta 1 integrin in Schwann cells impedes interactions with axons. J. Cell Biol. 156, 199–209.

Fields, R.D., Stevens-Graham, B., 2002. New insights into neuron–glia communication. Science 298, 556–562.

Ghazvini, M., Mandemakers, W., Jaegle, M., Piirsoo, M., Driegen, S., Koutsourakis, M., Smit, X., Grosveld, F., Meijer, D., 2002. A cell type-specific allele of the POU gene Oct-6 reveals Schwann cell autonomous function in nerve development and regeneration. EMBO J. 21, 4612–4620.

Ghislain, J., Desmarquet-Trin-Dinh, C., Jaegle, M., Meijer, D., Charnay, P., Frain, M., 2002. Characterisation of cis-acting sequences reveals a biphasic, axon-dependent regulation of Krox20 during Schwann cell development. Development 129, 155–166.

Gillespie, C.S., Sherman, D.L., Fleetwood-Walker, S.M., Cottrell, D.F., Tait, S., Garry, E.M., Wallace, V.C., Ure, J., Griffiths, I.R., Smith, A., Brophy, P.J., 2000. Peripheral demyelination and neuropathic pain behavior in periaxin-deficient mice. Neuron 26, 523–531.

Goldman, L., Albus, J.S., 1968. Computation of impulse conduction in myelinated fibers; theoretical basis of the velocity–diameter relation. Biophys. J. 8, 596–607.

Hageman, G., Willemse, J., 1983. Arthrogryposis multiplex congenita. Neuropediatrics 14, 6–11.

Hall, J.G., 1997. Arthrogryposis multiplex congenita: etiology, genetics, classification, diagnostic approach, and general aspects. J. Pediatr. Orthop., B 6, 159–166.

Henry, E.W., Eicher, E.M., Sidman, R.L., 1991. The mouse mutation claw paw: forelimb deformity and delayed myelination throughout the peripheral nervous system. J. Heredity 82, 287–294.

Jacobson, L., Polizzi, A., Morriss-Kay, G., Vincent, A., 1999. Plasma from human mothers of fetuses with severe arthrogryposis multiplex congenita causes deformities in mice. J. Clin. Invest. 103, 1031–1038.

Jaegle, M., Mandemakers, W., Broos, L., Zwart, R., Karis, A., Visser, P., Grosveld, F., Meijer, D., 1996. The POU factor Oct-6 and Schwann cell differentiation. Science 273, 507–510.

Jaegle, M., Ghazvini, M., Mandemakers, W., Piirsoo, M., Driegen, S., Levavasseur, F., Raghoenath, S., Grosveld, F., Meijer, D., 2003. The POU proteins Brn-2 and Oct-6 share important functions in Schwann cell development. Genes Dev. 17, 1380–1391.

Jessen, K.R., Mirsky, R., 1991. Schwann cell precursors and their development. Glia 4, 185–194.

Jessen, K.R., Mirsky, R., 1999. Schwann cells and their precursors emerge as major regulators of nerve development. Trends Neurosci. 22, 402–410.

Jessen, K.R., Brennan, A., Morgan, L., Mirsky, R., Kent, A., Hashimoto, Y., Gavrilovic, J., 1994. The Schwann cell precursor and its fate: a study of cell death and differentiation during gliogenesis in rat embryonic nerves. Neuron 12, 509–527.

Koszowski, A.G., Owens, G.C., Levinson, S.R., 1998. The effect of the mouse mutation claw paw on myelination and nodal frequency in sciatic nerves. J. Neurosci. 18, 5859–5868.

Matthews, I., Sims, G., Ledwidge, S., Stott, D., Beeson, D., Willcox, N., Vincent, A., 2002. Antibodies to acetylcholine receptor in parous women with myasthenia: evidence for immunization by fetal antigen. Lab. Invest. 82, 1407–1417.

Moessinger, A.C., 1983. Fetal akinesia deformation sequence: an animal model. Pediatrics 72, 857–863.

Niemann, S., Sidman, R.L., Nave, K.A., 1998. Evidence against altered forms of MAG in the dysmyelinated mouse mutant claw paw. Mamm. Genome. 9, 903–904.

Parkinson, D.B., Dickinson, S., Bhaskaran, A., Kinsella, M.T., Brophy, P.J., Sherman, D.L., Sharghi-Namini, S., Duran Alonso, M.B., Mirsky, R., Jessen, K.R., 2003. Regulation of the myelin gene periaxin provides evidence for Krox-20-independent myelin-related signalling in Schwann cells. Mol. Cell. Neurosci. 23, 13–27.

Parmantier, E., Lynn, B., Lawson, D., Turmaine, M., Namini, S.S., Chakrabarti, L., McMahon, A.P., Jessen, K.R., Mirsky, R., 1999. Schwann cell-derived Desert hedgehog controls the development of peripheral nerve sheaths [see comments]. Neuron 23, 713–724.

Polizzi, A., Huson, S.M., Vincent, A., 2000. Teratogen update: maternal myasthenia gravis as a cause of congenital arthrogryposis. Teratology 62, 332–341.

Rushton, W.A., 1951. A theory of the effects of fibre size in medullated nerve. J. Physiol. 115, 101–122.

Saito, F., Moore, S.A., Barresi, R., Henry, M.D., Messing, A., Ross-Barta, S.E., Cohn, R.D., Williamson, R.A., Sluka, K.A., Sherman, D.L., Brophy, P.J., Schmelzer, J.D., Low, P.A., Wrabetz, L., Feltri, M.L., Campbell, K.P., 2003. Unique role of dystroglycan in peripheral nerve myelination, nodal structure, and sodium channel stabilization. Neuron 38, 747–758.

Scaravilli, F., Jacobs, J.M., 1981. Peripheral nerve grafts in hereditary leukodystrophic mutant mice (twitcher). Nature 290, 56–58.

Scherer, S.S., Salzer, J.L., 1996. Axon–Schwann cell interactions during peripheral nerve degeneration and regeneration. In: Jessen, K.R., Richardson, W.D. (Eds.), Glial Cell Development. Bios Scientific Publishers Ltd., Oxford, pp. 165–196.

Scherer, S.S., Xu, Y.T., Bannerman, P.G., Sherman, D.L., Brophy, P.J., 1995. Periaxin expression in myelinating Schwann cells: modulation by axon-glial interactions and polarized localization during development. Development 121, 4265–4273.

Seitz, R.J., Wechsler, W., Mosny, D.S., Lenard, H.G., 1986. Hypomyeli-

nation neuropathy in a female newborn presenting as arthrogryposis multiplex congenita. Neuropediatrics 17, 132–136.

Sherman, D.L., Brophy, P.J., 2000. A tripartite nuclear localization signal in the PDZ-domain protein L-periaxin. J. Biol. Chem. 275, 4537–4540.

Suter, U., Scherer, S.S., 2003. Disease mechanisms in inherited neuropathies. Nat. Rev., Neurosci. 4, 714–726.

Thomas, P.K., Berthold, C.-H., Ochoa, J., 1993. Microscopic anatomy of the peripheral nervous system. In: Dyck, P.J., Thomas, P.K. (Eds.), Peripher. Neuropathy, vol. 1. W.B. Saunders Company, Philadelphia, PA, pp. 28–73.

Topilko, P., Meijer, D., 2001. Transcription factors that control Schwann cell development and myelination. In: Jessen, K.R., Richardson, W.D. (Eds.), Glial Cell Development. Oxford Univ. Press, Oxford, pp. 223–244.

Webster, H.d., 1993. Development of peripheral nerve fibers. In: Dyck, P.J., Thomas, P.K., Griffin, J.W., Low, P.A., Poduslo, J.F. (Eds.), Peripheral Neuropathy. W.B. Saunders Company, Philadelphia, pp. 243–266.

Chapter 6

The *claw paw* mutation reveals a role for *Lgi4* in peripheral nerve development

John R Bermingham Jr, Harold Shearin, Jamie Pennington, Jill O'Moore, Martine Jaegle, Siska Driegen, Arend van Zon, Aysel Darbas, Ekim Özkaynak, Elizabeth J Ryu, Jeffrey Milbrandt and Dies Meijer

Nature Neuroscience, 2006

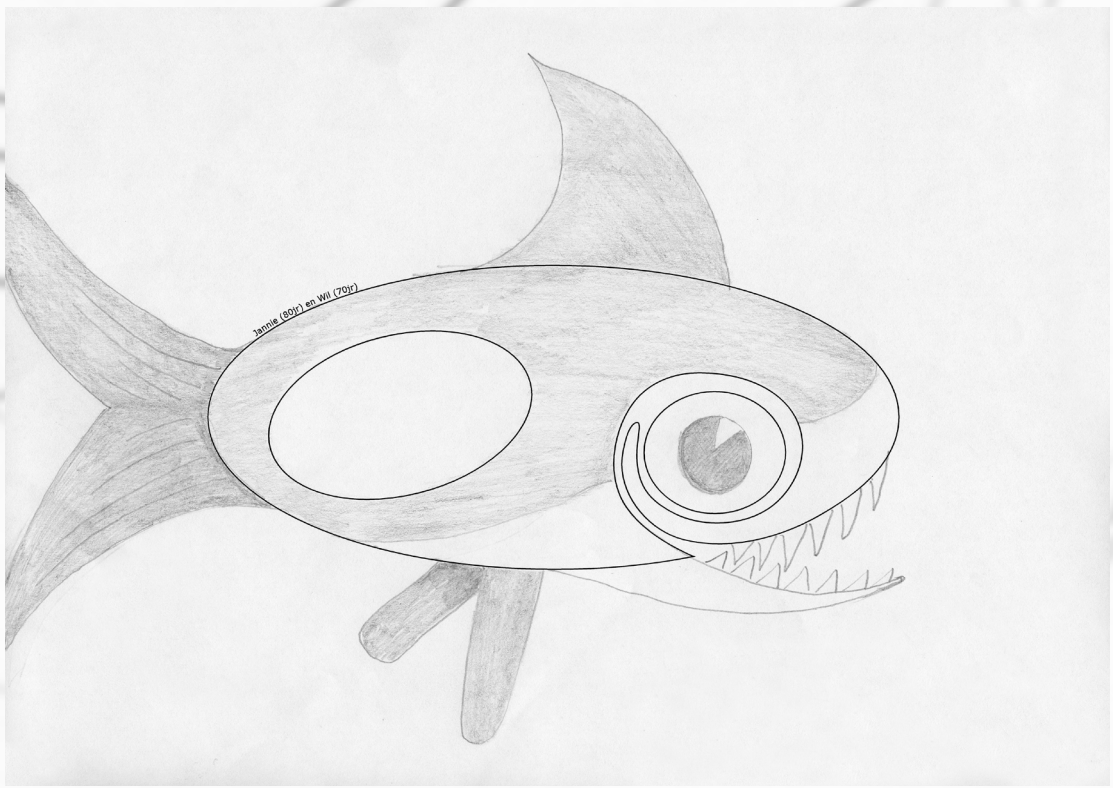

nature neuroscience

The *claw paw* mutation reveals a role for *Lgi4* in peripheral nerve development

John R Bermingham Jr[1], Harold Shearin[1], Jamie Pennington[1], Jill O'Moore[1], Martine Jaegle[2], Siska Driegen[2], Arend van Zon[2], Aysel Darbas[2], Ekim Özkaynak[2], Elizabeth J Ryu[3,4], Jeffrey Milbrandt[3] & Dies Meijer[2]

Peripheral nerve development results from multiple cellular interactions between axons, Schwann cells and the surrounding mesenchymal tissue. The delayed axonal sorting and hypomyelination throughout the peripheral nervous system of *claw paw* (*clp*) mutant mice suggest that the *clp* gene product is critical for these interactions. Here we identify the *clp* mutation as a 225-bp insertion in the *Lgi4* gene. *Lgi4* encodes a secreted and glycosylated leucine-rich repeat protein and is expressed in Schwann cells. The *clp* mutation affects *Lgi4* mRNA splicing, resulting in a mutant protein that is retained in the cell. Additionally, siRNA-mediated downregulation of Lgi4 in wild-type neuron–Schwann cell cocultures inhibits myelination, whereas exogenous Lgi4 restores myelination in *clp/clp* cultures. Thus, the abnormalities observed in *clp* mice are attributable to the loss of Lgi4 function, and they identify Lgi4 as a new component of Schwann cell signaling pathway(s) that controls axon segregation and myelin formation.

In the peripheral nervous system (PNS), Schwann cells synthesize myelin sheaths, which permit the rapid, saltatory conduction of nerve impulses. The debilitating effects of diseases that disrupt myelin emphasize the importance of understanding the mechanisms that control its synthesis. The development of peripheral nerve tissue results from a series of coordinated interactions between neurons and Schwann cells (reviewed in refs. 1 and 2). Schwann cell precursors originate from the neural crest and migrate along embryonic nerve trunks, proliferating in response to axonal cues and subdividing the nerve into smaller groups of fibers; ultimately, they differentiate into myelinating or non-myelinating Schwann cells. Several signaling proteins that regulate Schwann cell development and myelin formation are known. Axonal membrane–bound neuregulin-1 (NRG1) isoform III, signaling through the ErbB2-ErbB3 receptor on Schwann cells, is required for Schwann cell survival, proliferation and myelination[3–6]. The competing effects of neurotrophin-3 (NT3) and brain-derived neurotrophic factor (BDNF) modulate Schwann cell myelination[7], and nerve growth factor (NGF) seems to stimulate Schwann cell myelination indirectly through binding to the TrkA receptor on dorsal root ganglion (DRG) axons[8]. In parallel, neuronal activity triggers axonal release of ATP that inhibits Schwann cell proliferation and myelination (reviewed in ref. 9). Nevertheless, many important aspects of axon–Schwann cell signaling are not yet understood. In addition to axonal contact, the sorting of nerve fibers and Schwann cell myelination also require the synthesis of a basal lamina (reviewed in ref. 1).

Axon–Schwann cell and Schwann cell–basal lamina interactions activate multiple signaling pathways that converge onto the nucleus to regulate the transcriptional programs for myelinating or non-myelinating fates[1,10,11]. Critical roles in Schwann cell proliferation, differentiation and myelination have been established for the transcription factors Sox10, Sox2, Jun, NFκB, Oct6 (the product of the *Pou3f1* gene) and Krox-20 (the product of the *Egr2* gene) (reviewed in refs. 12 and 13). In particular, the cessation of Schwann cell proliferation and the initiation of myelin formation require the downregulation of Sox2 and the upregulation of *Pou3f1*/Oct6 to induce *Egr2*/Krox-20, which in turn—together with Sox10—activates the myelination program[14–17]. Sox10 is also required in Schwann cell precursors for their survival, where its actions are mediated at least in part through the regulation of the neuregulin receptor ErbB3 gene[18].

The *clp* mouse is a particularly interesting model for the study of Schwann cell development *in vivo*. These mice are characterized by limb posture abnormalities and peripheral hypomyelination, with no sign of dysmyelination in the CNS[19–21]. The *clp* mutation, which arose spontaneously in C57BL/6-*ob* mice at the Jackson Laboratory, is recessive and has been mapped to proximal mouse chromosome 7 (ref. 19). The similarities in delayed myelination observed in *Pou3f1*/Oct6 mutant mice and in *clp* mice suggest an interaction between the two genes. We have shown previously that perinatal *Pou3f1*/Oct6 upregulation is not affected by the *clp* mutation, but that downstream effectors, such as *Egr2*/Krox-20, are activated with delayed kinetics[21,22]. Additionally, the radial sorting of nerve fibers is delayed in *clp* animals, and nerve-grafting experiments demonstrate that *clp* gene function is required in Schwann cells and possibly in neurons[21]. Taken together, these data demonstrate that *clp* function

[1]McLaughlin Research Institute, 1520 23rd Street South, Great Falls, Montana 59405, USA. [2]Department of Cell Biology & Genetics, Erasmus MC University Medical Center, PO Box 1738, 3000 DR Rotterdam, The Netherlands. [3]Department of Pathology and Immunology and [4]Department of Psychiatry, Washington University, Box 8118, 660 South Euclid Avenue, St. Louis, Missouri 63110, USA. Correspondence should be addressed to J.R.B. Jr. (jrbjr@po.mri.montana.edu) or D.M. (d.meijer@erasmusmc.nl).

Received 21 September; accepted 18 October; published online 11 December 2005; doi:10.1038/nn1598

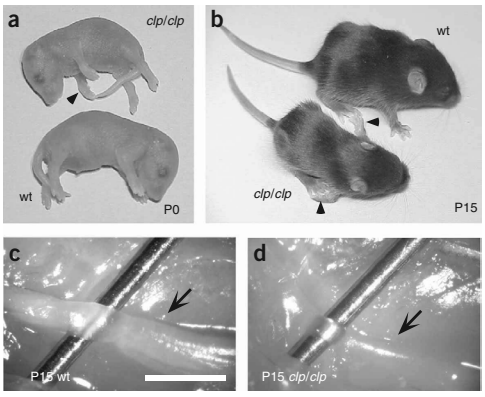

Figure 1 The claw paw phenotype. (**a**,**b**) P0 (**a**) and P15 (**b**) wild-type and *clp/clp* mutant mice on a C57BL/6 genetic background. Arrowheads highlight the forelimb defect in these mice. (**c**,**d**) Sciatic nerves from the mice shown in **b**. For clarity, a 30-gauge needle has been inserted behind the nerves. Note hypotrophy of the *clp/clp* sciatic nerve (arrows).

is required for peripheral nerve development and that, in Schwann cells, *clp* functions in a myelination pathway that is distinct from *Pou3f1*/Oct6 activation.

To understand the molecular basis of the claw paw phenotype, we identified the genetic defect by positional cloning. Here we show that the *clp* mutation is caused by a repetitive element insertion that precludes splicing of exon 4 of *Lgi4*, one of four members of the leucine-rich glioma-inactivated (*Lgi*) family of genes that encode putative secreted proteins[23]. Lgi4 is dynamically expressed in Schwann cells and restricted populations of neurons. The *clp* mutation results in the production of Lgi4 protein with an interstitial deletion that fuses two of its leucine-rich repeats (LRRs). We demonstrate that, although Lgi4 is glycosylated and secreted, $Lgi4^{clp}$ is retained within the cell. Moreover, we show that siRNA-mediated downregulation of Lgi4 in sensory neuron–Schwann cell cocultures inhibits myelination, whereas the addition of Lgi4 to *clp/clp* neuron–Schwann cell cocultures significantly restores myelination. Thus, our data indicate that the claw paw phenotype results from a loss of Lgi4 and identify Lgi4 as an important signaling molecule that controls axon sorting and gene expression in peripheral nerve myelination.

RESULTS

The *clp* mutation produces an arthrogryposis-like phenotype that affects the forelimbs (**Fig. 1a**,**b**) and, in severe cases, also the hind limbs. The growth of *clp/clp* pups is often delayed, and many of the most severely affected individuals die before weaning. Notwithstanding the variability of the limb posture abnormality, all peripheral nerves in *clp* mice are hypotrophic (**Fig. 1c**,**d**; refs. 19 and 21).

Positional cloning of the *clp* gene

The initial backcross involving the *clp* locus revealed that it resides on proximal chromosome 7 (ref. 19). As a first step toward the identification of the *clp* gene, we localized it more precisely using *clp*/+ C57BL/6J × BALB/c intercrosses and *clp*/+ C57BL/6J × CAST backcrosses. These genetic mapping studies (**Supplementary Figs. 1** and **2** online) resulted in the definition of a *clp* candidate region that spanned approximately 150 kilobase (kb) from microsatellite marker D7MRI6 to D7MIT155 and contained at least eight genes (**Fig. 2**).

To identify the *clp* mutation, we analyzed the *clp* candidate region for exons and putative regulatory sequences. Each of these sequences was amplified using the polymerase chain reaction (PCR) from *clp*/+ and *clp/clp* DNA, and sequenced. PCR products from primers that flanked exon 4 of the *Lgi4* gene consistently produced a larger than expected product from *clp/clp* mice. The sequencing of this product revealed that 4 base pairs (bp), CTCT, located six nucleotides 5′ to exon 4 were replaced with a 225-bp repetitive sequence. This repetitive sequence was 100% homologous to a repeat element located 797 bp upstream, but in the reverse orientation (**Fig. 3a**,**b**). To confirm the presence of the insertion in *clp/clp* mice, we performed exon 4 PCR on *clp/clp* mice that were congenic with BALB/c mice (data not shown) and, using Southern hybridization, we examined DNA from *clp/clp* mice and wild-type mice for the *clp* restriction fragment length polymorphism (RFLP, **Fig. 3c**). In each case, a larger fragment segregated with the claw paw phenotype, and therefore it is likely that this insertion allele is the *clp* mutation. Formally, *clp* is an allele of *Lgi4* ($Lgi4^{clp}$), but for simplicity we will continue to call it *clp*.

The identification of an insertion associated with the *clp* mutation facilitated genetic complementation studies with wild-type DNA from the *clp* candidate region. We generated a transgenic mouse line with a bacterial artificial chromosome (BAC), 75-D7, containing wild-type mouse genomic DNA that spanned the *clp* candidate region (**Fig. 2b**). To confirm that the *clp* locus resides within the candidate region, we crossed mice that were heterozygous for *clp* to mice that were heterozygous for *clp* and carried the BAC 75-D7 transgene (**Supplementary Fig. 3** online summarizes the genotyping of these mice and **Table 1** details the offspring from such a complementation cross). We observed no *clp/clp* transgene-positive mice with the claw paw phenotype, whereas all *clp/clp* homozygous mice without the transgene were phenotypically claw pawed. To confirm the rescue of the claw paw phenotype, we performed direct microscopic examination of the sciatic nerves from *clp*/+ and *clp/clp* offspring carrying the 75-D7 BAC transgene (**Fig. 3c** and **3d**, respectively). These sciatic nerves appeared healthy and myelinated, and in marked contrast to nerves from *clp/clp* mice (**Fig. 1c**), were indistinguishable from the nerves of wild-type mice (**Fig. 1d**). Thus, we concluded that the 75-D7 BAC transgene complements the *clp* mutation. Because the *Lgi4* insertion was the only polymorphism identified in this region that segregated with the *clp* mutation, the *Lgi4* insertion is the most probable cause of the claw paw phenotype.

Expression of the *Lgi4* gene in the PNS

Previously we showed that *clp* gene function is required by Schwann cells and possibly by neurons[21]. Therefore, we examined the expression

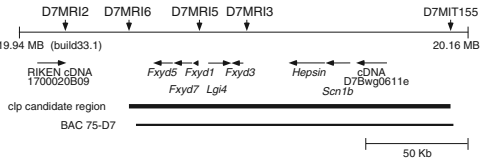

Figure 2 The *clp* candidate region (NCBI build 33.1) consists of eight genes: *Fxyd5*, *Fxyd7*, *Fxyd1*, *Lgi4*, *Fxyd3*, *Hepsin*, *Scn1b* and D7Bwg0611e. The *clp* candidate region as defined by 27R and 187R backcross mice (**Supplementary Fig. 2**) is shown as a thick bar; below it, CAST BAC 75-D7 is shown as a thinner bar.

ARTICLES

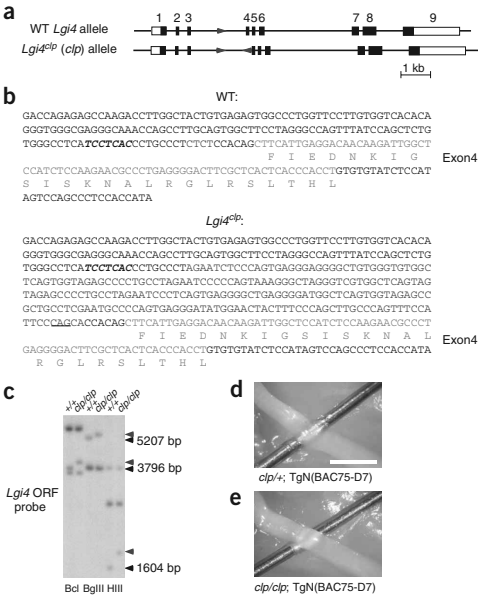

Figure 3 The *clp* mutation is an insertion in *Lgi4*. (**a**) The structure of the wild-type *Lgi4* gene is shown, with a repetitive element in intron 3 shown in red. This repetitive element has been duplicated and inserted in the opposite orientation adjacent to exon 4 in the *clp* allele of the *Lgi4* gene ($Lgi4^{clp}$). (**b**) Partial sequence of wild-type *Lgi4* and $Lgi4^{clp}$. Exon 4 is shown in blue, the four bases that are replaced by the *clp* insertion are shown in red and a sequence with strong homology to the branchpoint consensus[49] is shown in bold italics. The CAG sequence for a potential 3′ splice site in the *clp/clp* sequence is underlined. (**c**) Southern blot of genomic DNA from wild-type and $Lgi4^{clp}$ mice depicting the RFLP that results from the *clp* insertion. (**d**,**e**) BAC transgene complementation of the *clp* mutation. Two F2 FVB-Tg75-D7 × C57BL/6J-*clp* mice, (**d**) no. 145 and (**e**) no. 148 (**e**), showing that presence of the 75-D7 transgene permits development of normal sciatic nerves in *clp/clp* mice (compare with **Fig. 1d**). Genotyping of these mice is depicted in **Supplementary Figure 3**.

pattern of *Lgi4* in the embryonic and early postnatal PNS of wild-type mice and compared it to the expression of the closely related *Lgi1*, *Lgi2* and *Lgi3* genes. On embryonic day 14 (E14), *Lgi4* was expressed in developing peripheral nerves. Lgi4 was strongly expressed in the trigeminal nerve and ganglion, and was particularly abundant in the boundary cap cells (**Fig. 4a**,**b**)—a transient population of cells that contributes to the Schwann cell population of the dorsal root nerve[24]. The pattern of *Lgi4* expression at E14 was distinct from those of *Lgi1*, *Lgi2* and *Lgi3* (data not shown). Moderate *Lgi4* expression was observed in the DRG (**Fig. 4c**), and in the intestine in a pattern consistent with its expression in the developing enteric nervous system (**Fig. 4d**). Together, these observations demonstrate that *Lgi4* is expressed in the entire PNS at E14. Although it was clear that *Lgi4* is expressed in the Schwann cells of the embryonic nerve, it was not clear, from *in situ* hybridization to embryonic DRG, whether *Lgi4* expression is in sensory neurons, satellite glia or both.

To determine whether *Lgi4* is also expressed in postnatal Schwann cells and whether its expression is altered by the absence of Oct6, we performed *in situ* hybridization on sciatic nerves from wild-type and $Pou3f1^{-/-}$ (Oct6-null) mice. Previous data suggest that in postnatal nerve development, Lgi4 acts downstream of Oct6 or in parallel with it[21,22]. We found that *Lgi4* was expressed independently of Oct6 (**Fig. 4e**). Thus, Lgi4 and Oct6 function in independent pathways in myelinating Schwann cells.

To further define the effects of the *clp* mutation, we examined the expression of Lgi4 and additional genes in *clp/clp* mice (**Fig. 4f**). In *clp/clp* sciatic nerves on postnatal day 4 (P4), *Lgi4* expression was upregulated, most probably reflecting the temporal delay in Schwann cell differentiation. *Egr2*/Krox-20 mRNA expression was strongly downregulated in *clp/clp* mice, demonstrating that the reduction of Krox-20 protein in these mice[21] occurs as a result of reduced *Egr2*/Krox-20 transcription. To determine whether the reduction in wild-type *Lgi4* activity was compensated for by the upregulation of other members of the Lgi family, we examined the expression of *Lgi1*, *Lgi2* and *Lgi3* in sciatic nerves from P4 wild-type and *clp/clp* mice. In nerves from wild-type mice, we observed modest expression of *Lgi1* (**Fig. 4f**) and no expression of *Lgi2* or *Lgi3* (data not shown). In nerves from P4 *clp/clp* mice, we observed no expression of *Lgi1* (**Fig. 4f**), *Lgi2* or *Lgi3* (data not shown). These observations revealed a potential role for *Lgi1* in mature Schwann cells and indicated that compensation for the $Lgi4^{clp}$ mutation by Lgi1, Lgi2 and Lgi3 was unlikely.

To determine if *Lgi4* and the other *Lgi* genes were expressed in sensory neurons during postnatal development, we examined their expression in P4 DRGs by *in situ* hybridization. *Lgi1* was expressed at very low levels throughout the DRG (**Fig. 4g**), presumably reflecting its low expression in Schwann cells (**Fig. 4g**). *Lgi2* and *Lgi3* were expressed abundantly in a pattern that corresponded to the position of sensory neurons in the DRG. In contrast, *Lgi4* was expressed at moderate levels uniformly throughout the DRG, probably by intraganglionic Schwann cells. A comparison of these patterns of expression with the embryonic data suggests that, during development, early *Lgi4* expression in DRG is supplanted postnatally by *Lgi2* and *Lgi3* in sensory neurons. To determine whether *Lgi4* is expressed by peripheral motor neurons, we hybridized adjacent transverse sections of P4 spinal cord with probes for *Lgi4* and, as a control, the proteolipid protein gene (*Plp1*; **Fig. 4h**). *Plp1* expression was observed in white matter tracts, as

Table 1 Rescue of the claw paw phenotype by BAC 75-D7

Lgi4 alleles	BAC 75-D7 transgene	Number of mice	Phenotype
FVB/FVB	no	4	normal
clp/FVB	no	14	normal
clp/clp	no	7	claw paw
FVB/FVB	yes	10	normal
clp/FVB	yes	18	normal
clp/clp	yes	17	normal

To determine whether homozygous *clp/clp* mice that carry the BAC 75-D7 transgene are phenotypically claw paw, *clp/+* C57BL/6J × FVB TgN(BAC75-D7) mice were mated to generate F1 *clp/+* TgN(BAC75-D7) and *clp/+* mice. These F1 mice possess a wild-type *Lgi4* allele on an FVB chromosome and a *clp* allele on a C57BL/6 chromosome. This makes it possible to unambiguously genotype alleles at the endogenous *Lgi4* locus in the presence of the wild-type *Lgi4* locus on the BAC75-D7 transgene, by using C57BL/6 and FVB-specific markers that are linked to *Lgi4* but are not present on BAC 75-D7. Genotype analysis of the F1 mice *clp/+* no. 108 and *clp/+* TgN(BAC75-D7) no. 93 are shown in **Supplementary Figure 3**. These mice were mated to obtain the F2 progeny that are listed in the table. No *clp/clp* transgene–positive mice that were phenotypically claw paw were observed, eliminating the hypothesis that the transgene has no effect on the claw paw phenotype. This result indicates that the sequences within BAC 75-D7 complement the *clp* mutation. A statistically significant excess of transgene carrying mice was observed, likely as a result of segregation of two independent insertion sites of the transgene in mouse no. 93. Southern blot and quantitative RT-PCR analysis (data not shown) indicate that transgene-positive mice possess two or three copies of BAC 75-D7.

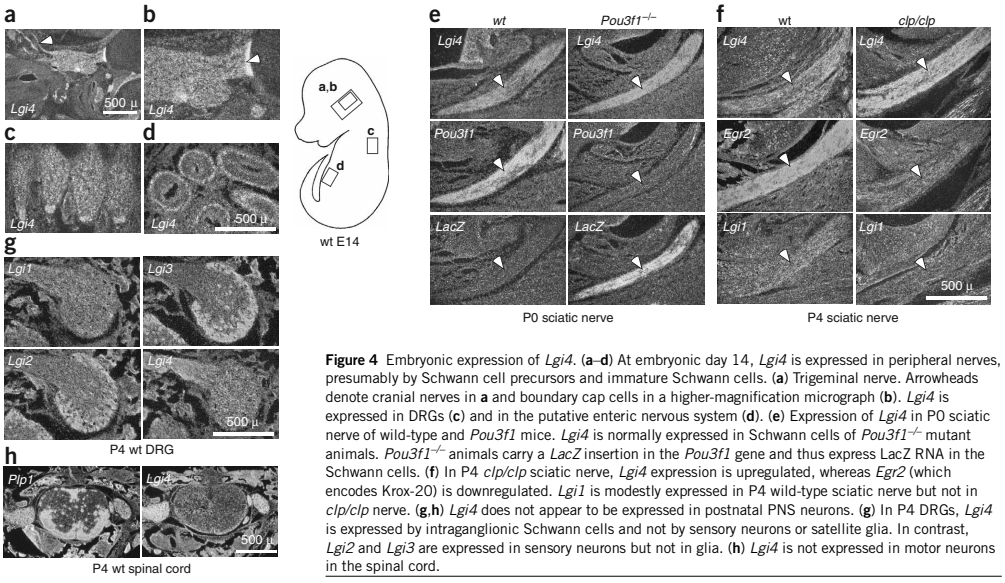

Figure 4 Embryonic expression of *Lgi4*. (**a**–**d**) At embryonic day 14, *Lgi4* is expressed in peripheral nerves, presumably by Schwann cell precursors and immature Schwann cells. (**a**) Trigeminal nerve. Arrowheads denote cranial nerves in **a** and boundary cap cells in a higher-magnification micrograph (**b**). *Lgi4* is expressed in DRGs (**c**) and in the putative enteric nervous system (**d**). (**e**) Expression of *Lgi4* in P0 sciatic nerve of wild-type and *Pou3f1* mice. *Lgi4* is normally expressed in Schwann cells of *Pou3f1*$^{-/-}$ mutant animals. *Pou3f1*$^{-/-}$ animals carry a *LacZ* insertion in the *Pou3f1* gene and thus express LacZ RNA in the Schwann cells. (**f**) In P4 *clp/clp* sciatic nerve, *Lgi4* expression is upregulated, whereas *Egr2* (which encodes Krox-20) is downregulated. *Lgi1* is modestly expressed in P4 wild-type sciatic nerve but not in *clp/clp* nerve. (**g**,**h**) *Lgi4* does not appear to be expressed in postnatal PNS neurons. (**g**) In P4 DRGs, *Lgi4* is expressed by intraganglionic Schwann cells and not by sensory neurons or satellite glia. In contrast, *Lgi2* and *Lgi3* are expressed in sensory neurons but not in glia. (**h**) *Lgi4* is not expressed in motor neurons in the spinal cord.

expected. Although *Lgi4* expression was observed in dorsal and ventral roots, it was not observed in motor columns. Thus, *Lgi4* does not seem to be expressed in postnatal motor neurons. Together, these data demonstrate that in the PNS, it is primarily Schwann cells that express Lgi4.

The *clp* mutation alters splicing of *Lgi4**

The proximity of the *clp* insertion to *Lgi4* exon 4 suggested that it could alter *Lgi4* splicing in three possible ways: (i) the insert could disrupt exon 4 splicing by interrupting the polypyrimidine tract of the adjacent 3′ splice site and shifting a putative branchpoint 221 bp away; (ii) it could introduce a new 3′ splice site that would enlarge exon 4 and prematurely terminate Lgi4 translation; or (iii) the *clp* insertion and the oppositely oriented repeat (located 797 bp away in intron 3; **Fig. 5a**) could form a pre-mRNA stem-loop structure that occludes the third intron 3′ splice site. To distinguish between these possibilities, we performed reverse transcriptase PCR (RT-PCR) on RNA from the brain and sciatic nerves of *clp*/+ and *clp/clp* animals, using primers mapping to exons 2 and 5. A shorter DNA fragment was amplified from *clp/clp* brain and nerve samples than from *clp*/+ cDNA samples (**Fig. 5b**). We cloned and sequenced these DNA fragments and found that the *clp*-derived cDNAs lacked exon 4. To assess whether stem-loop formation blocked the use of the 3′ splice site on exon 4 in *Lgi4*^{clp} pre-mRNAs, we generated minigenes that spanned exons 2 through 6 and contained the *clp* insertion, but with the nearby oppositely oriented repeat sequence either removed or inverted (**Supplementary Fig. 4** online). The expression of these minigenes in COS1 cells and the sequencing of the resulting cDNAs demonstrated that *Lgi4* exon 3 was spliced to exon 5, regardless of the presence or orientation of the additional cognate repeat. Thus, we concluded that the insertion of the repeat element in the *clp* allele disrupted the third intron 3′ splice site, which resulted in the skipping of exon 4. As exon 4 is 72 nucleotides long, we predict that the Lgi4 protein encoded by the *clp* allele has a 24–amino acid interstitial deletion.

Cellular processing of Lgi4 and Lgi4^{clp}

Lgi4 shares common protein structural domains with the other three members of the Lgi family: an N-terminal signal sequence, LRRs and a C-terminal epilepsy-associated repeat (EAR) or epitempin domain[25,26]. The predicted domain organization of Lgi4 and Lgi4^{clp} (**Fig. 5c**), based on the wild-type amino acid sequence (**Fig. 5d**), revealed a putative signal sequence; the presence of this sequence suggested that Lgi4 enters the secretory pathway and may be secreted. In support of this, the LRR repeats of Lgi4 and the Lgi1, Lgi2 and Lgi3 proteins were flanked by cysteine-rich sequences (LRRNT and LRRCT in **Fig. 5d**) that typified extracellular LRR proteins[27,28]. In addition, one potential glycosylation site (Asn177) was present in the LRRCT of Lgi4.

To determine whether Lgi4 and Lgi4^{clp} are indeed secreted proteins, we stably expressed a Myc-epitope- and 6×Histidine-tagged Lgi4 or Lgi4^{clp} in CHO cells. Using an antibody to Myc, we observed Lgi4 protein expression in a reticular pattern that largely overlapped with the ER of the cell, suggesting that it enters the secretory pathway (**Fig. 6a**). To check whether Lgi4 and Lgi4^{clp} were secreted into the medium, we purified the recombinant proteins from cell extracts and medium on NiNTA-agarose beads. In this analysis, we included CHO cells expressing V5- and 6×Histidine-tagged Lgi1 as a positive control and Oct6-expressing cells as a negative control. Lgi4 and Lgi1 could be purified from the culture medium, whereas Lgi4^{clp} and Oct6 could not (**Fig. 6b**). Thus, in contrast to the readily secreted wild-type Lgi4 and Lgi1 proteins, Lgi4^{clp} was retained within the cell.

We next checked whether Lgi4 and Lgi4^{clp} proteins are glycosylated by treating them with endoglycosidase H (EndoH) or peptide

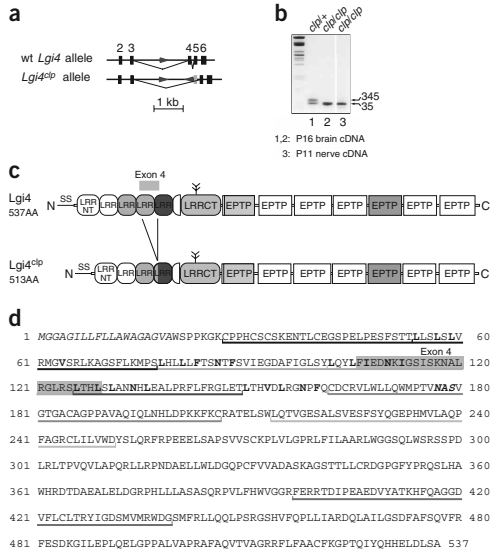

Figure 5 Skipping of *Lgi4*^{clp} exon 4 generates a protein with an internal deletion. (**a**) Diagram of *Lgi4* splicing patterns in wild-type and *clp/clp* mice, showing skipping of exon 4 in *Lgi4*^{clp} transcripts. (**b**) PCR of cDNA from *clp/+* brain and nerve and *clp/clp* nerve, showing absence of exon 4 in *clp/clp* transcripts. (**c**) Structure of mouse wild-type Lgi4 and Lgi4^{clp} proteins. SS, signal sequence that is predicted to be cleaved between amino acids 19 and 20 (SignalP3.0; ref. 46); LRRNT, leucine-rich N-terminal domain; LRR, leucine-rich repeat; LRRCT, leucine-rich C-terminal repeat; EPTP, epitempin repeat. Colored or shaded domains are recognized by the SMART database. The red LRR has a lower *E* value (probability with which the sequence would appear at random) than the orange LRR domains, and the dark gray epitempin domain has a lower *E* value than the light gray domain. White domains are not recognized by the SMART or CDART databases. A branched structure depicts a putative glycosylation site within the LRRCT (blue). The part of the protein that is encoded by exon 4 is overshadowed in green. 513AA Lgi4^{clp} is shown below wild-type Lgi4, with the third and fourth putative leucine-rich repeats fused. (**d**) Mouse Lgi4 protein sequence. Signal sequence is depicted in italics. A putative N-linked glycosylation site (Asn177 or NXS/T)[50] in the LRRCT domain is shown in bold italics, and conserved amino acids in leucine-rich repeats are shown in bold. Amino acids encoded by exon 4 are highlighted in green. Leucine-rich domains and conserved epitempin domains depicted in **a** are underlined. The sequence is derived from mouse *Lgi4* cDNA NM_144556.1.

N-glycosidase F (PNGaseF). EndoH cleaves the high-mannose structures that are found in ER resident proteins, whereas PNGaseF cleaves both the high-mannose structures and the complex oligosaccharides present on mature glycosylated proteins. We observed that secreted Lgi4 was not cleaved by EndoH but was cleaved by PNGaseF—as was apparent from the downward shift in molecular weight (**Fig. 6c**). Thus, secreted Lgi4 carries complex oligosaccharides. Lgi4 purified from cell extracts was largely EndoH sensitive, indicating that the proteins were rapidly secreted after maturation in the Golgi compartment. Lgi4^{clp} also was largely EndoH sensitive, demonstrating that the interstitial deletion in Lgi4^{clp} did not inhibit glycosylation *per se*. The observation that little mature glycosylated Lgi4^{clp} accumulated in the cell suggested that the protein was retained within the ER. These data suggested that Lgi4 functions extracellularly and that the claw paw phenotype results from loss of Lgi4 function. An alternative possibility, that Lgi4^{clp} retention exerts a dominant-negative effect on Schwann cells, is unlikely because the claw paw phenotype is largely recessive and is complemented by wild-type *Lgi4* genes.

Lgi4 controls myelination in neuron–Schwann cell cocultures

If the loss of Lgi4 function caused the claw paw phenotype, then the downregulation of Lgi4 by means of siRNA should phenocopy the *clp* defect. We established myelinating neuron–Schwann cell cocultures from dissociated DRGs derived from *clp/+* and *clp/clp* E13 mouse embryos. *clp/clp* cultures did not myelinate, whereas *clp/+* cultures exhibited robust myelination (**Fig. 7a**). A lentivirus that expressed Lgi4-specific siRNA was constructed and shown to suppress *Lgi4* mRNA expression in cultured rat Schwann cells by approximately 80% (**Fig. 7b**). The transduction of neuron–Schwann cell cocultures with the Lgi4 siRNA lentivirus resulted in reduced numbers of myelin internodes as compared to cultures transduced with a control lentivirus (**Fig. 7a**,**c**). Quantification of these results showed that the expression of Lgi4 siRNA resulted in a decrease of myelin internodes by approximately 70% (**Fig. 7c**). These experiments strongly suggested that the myelination defect in *clp* mice and in *clp* DRG explant cultures results from a loss of Lgi4 function.

The data presented above suggested that Lgi4 acts extracellularly. Therefore, we anticipated that the addition of Lgi4 to *clp/clp* neuron–Schwann cell cocultures would restore their myelination defect (**Fig. 7a**). We treated *clp/clp* DRG cultures with medium conditioned by either CHO cells expressing Lgi4 or, as a control, non-recombinant CHO cells. We analyzed the progression of Schwann cell differentiation

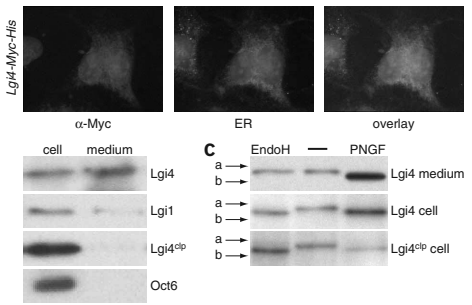

Figure 6 The *clp* mutation affects processing and sorting of Lgi4. (**a**) Myc-tagged Lgi4 protein expressed in CHO cells is detected with an antibody to Myc (α-Myc) in a pattern that largely overlaps (overlay) with that of the GRP-94 antigen, present on the ER resident protein GRP-94. (**b**) Lgi4 and Lgi1 protein can both be purified from cell lysates (cell) and culture medium (medium) of stably transfected CHO cells. Lgi4^{clp} is present in cell extracts but not in medium. The nuclear protein Oct6 can be purified only from the cell extract, demonstrating that there is very little contamination of the medium fraction with the cellular fraction. Lgi4 is detected with a Myc antibody, Lgi1 with a V5 antibody and Oct6 with an Oct6 antibody. (**c**) Lgi4 purified from medium is resistant to cleavage by EndoH but sensitive to PNGaseF as judged by the shift in electrophoretic mobility (indicated with arrows labeled 'a' and 'b'). Lgi4 protein isolated from cell lysates (cell) is largely EndoH sensitive (below).

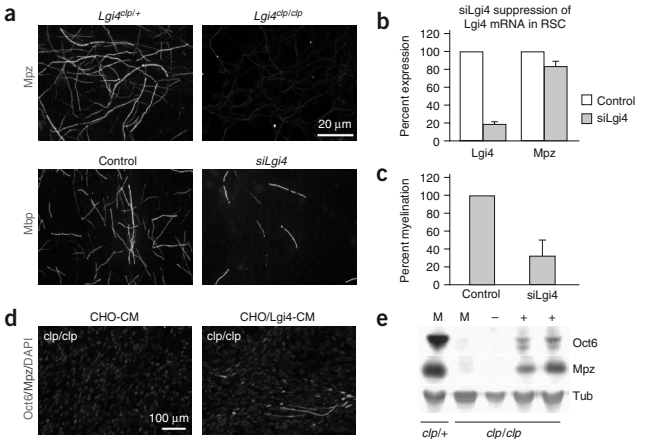

Figure 7 Inhibition of Lgi4 results in reduced myelination in DRG cultures and exogenous Lgi4 restores myelination in *clp/clp* DRG cultures. (**a**) Anti-Mpz immunostaining of dissociated *clp/+* or *clp/clp* DRG cultures 12 d after addition of ascorbic acid to induce myelination (top panels). Immunostaining by antibodies to Mbp of sensory neuron–Schwann cell cocultures infected with lentivirus expressing Lgi4 siRNA (siLgi4) or non-recombinant lentivirus (control) after ascorbic acid treatment. (**b**) Quantitative RT-PCR of Lgi4 and Mpz RNA expression levels in Schwann cells infected with siLgi4 or control lentivirus. (**c**) Quantification of myelin profiles in control and siLgi4 panels. Percent myelination value is calculated from three independent experiments. Error bars represent s.e.m. (**d**) Mpz (red) and Oct6 (green) immunostaining of dissociated *clp/clp* DRG cultures 12 d after addition of ascorbic acid to induce myelination. Nuclei are blue (DAPI). Cultures were grown in the presence of 50% non-recombinant CHO cell–conditioned medium (CHO-CM) or Lgi4-expressing CHO cell–conditioned medium (CHO/Lgi4-CM). Myelin internodes are recognized by their strong Mpz staining. (**e**) Expression of Oct6 and Mpz in dissociated DRG cultures 12 d after addition of ascorbic acid was assessed on immunoblots. Acetylated α-tubulin (Tub), which is highly enriched in neurites, was used as a protein loading control. DRG cultures derived from heterozygous (*clp/+*) or *clp*-homozygous (*clp/clp*) embryos were grown in standard medium (M) or standard medium supplemented (1:1) with CHO-CM (–) or CHO/Lgi4-CM (+).

and myelination in these cultures by immunocytochemistry and western blotting (**Fig. 7d**,**e**). No myelin internodes were observed in *clp/clp* Schwann cell cocultures grown in the presence of medium conditioned by non-recombinant CHO cells (CHO-CM; **Fig. 7d**), and very little of the myelin-associated protein Mpz was expressed in these *clp/clp* cultures (**Fig. 7e**). In contrast, *clp/clp* DRG cultures grown in the presence of medium conditioned by Lgi4-expressing CHO cells (CHO/Lgi4-CM) showed myelination, as demonstrated by the strong Mpz staining of several internodes (**Fig. 7d**) and elevated Mpz protein expression (**Fig. 7e**). High Oct6 expression marks immature and premyelinating Schwann cells. We observed many Oct6-positive Schwann cells in the CHO-Lgi4-CM cultures, but not in the CHO-CM cultures (**Fig. 7d**). This was corroborated by increased Oct6 protein expression in the CHO/Lgi4-CM *clp/clp* cultures as compared to CHO-CM *clp/clp* cultures (**Fig. 7e**).

Taken together, these experiments demonstrated that exogenous Lgi4 can restore the myelination defect in *clp/clp* neuron–Schwann cell cocultures, suggesting that Lgi4 can indeed function extracellularly.

DISCUSSION

Through genetic and cell biological studies of *clp* mutant mice, we have identified the secreted protein Lgi4 as an essential molecule in PNS development. The *clp* mutation results in intracellular retention of mutant Lgi4. Downregulation of *Lgi4* in wild-type neuron–Schwann cell cocultures inhibits myelination, whereas exogenous Lgi4 restores myelination in *clp/clp* cocultures. Thus, Lgi4 is involved in Schwann cell signaling pathways that control axonal ensheathment and myelination.

Lgi4 protein

The Lgi4 protein belongs to a small family of proteins that are characterized by the presence of a signal peptide and two putative protein interaction domains: an LRR domain and an epitempin or EAR domain. The function of these proteins is unknown, although their structural characteristics suggest that they function extracellularly and are involved in multiple molecular interactions.

LRR domains provide a versatile protein interaction interface that is found in many proteins from phylogenetically diverse organisms[27,28]. The LRR domain of Lgi4 has highest homology to the *Drosophila* Slit D3 LRR. Slit proteins are extracellular guidance molecules for both neurons and some non-neuronal cells, and function by binding to the transmembrane Roundabout (Robo) receptors (reviewed in ref. 29)—an interaction that is mediated through the LRR domain of Slit[30]. Also, the C-terminal half of the Lgi proteins is potentially involved in direct molecular interactions. This domain is predicted to adopt a β-sheath structure and may represent a version of the seven-bladed β-propeller fold, a structural element involved in protein-protein interactions. For example, this structural motif is also found in the semaphorins, a family of proteins involved in axon guidance (reviewed in ref. 31), and in the integrins, a major family of basal lamina receptors. The epitempin domain is shared by the four members of the Lgi family, by C21orf29 (TSPEAR) and by the extracellular domain of the G protein–coupled receptor MASS1 (also known as VLGR). Two of these proteins are altered in epilepsy: *LGI1* mutations have been found in patients with autosomal-dominant partial epilepsy with auditory features (ADPEAF), whereas the *MASS1* (or *VLGR)* gene is mutated in Frings audiogenic seizure mice[32] and in humans with audiogenic seizures[33]. In humans with ADPEAF, point mutations in LGI1 have been found in both the LRR and epitempin domains[34–37]. The human *LGI4* gene resides in 19q13, a region linked to benign familial infantile convulsions (BFIC; OMIM 601764), and *LGI4* polymorphisms are associated with childhood absence epilepsy[38]. Thus far, however, no mutations in *LGI4* have been detected in patients with either type of epilepsy.

The interstitial deletion of 24 amino acids within the LRR domain of Lgi4 results in intracellular retention of the mutant protein, most probably within the ER. The unique peptide junction in $Lgi4^{clp}$ does not resemble any known ER retention signal and thus refutes a simple gain-of-function mechanism. A stringent quality control regime within the ER eliminates improperly folded or assembled proteins[39]. In the peripheral nerve, the association of contactin-associated protein (Caspr) and contactin within the ER is required for maturation and

ARTICLES

surface expression of the Caspr-contactin complex[40]. Perhaps the altered protein-interaction characteristics of the mutant LRR domain of Lgi4 inhibit its incorporation into a complex destined for transport to the cell surface. Alternatively, possibly Lgi4^{clp} is recognized as a misfolded protein, retained within the ER and eliminated through proteasome-mediated decay. Notably, a variety of ADPEAF-associated mutations in Lgi1 all result in intracellular retention of the protein when overexpressed in 293T cells, whereas the wild-type Lgi1 protein is normally secreted by these cells[41].

Possible roles for Lgi4 in peripheral nerve development

The transplantation of wild-type sciatic nerve segments from wild-type mice into nerves of *clp/clp* mice and vice versa suggested both Schwann cell–autonomous and Schwann cell–non-autonomous functions for the *clp* gene product[21]. We found that Lgi4 is expressed primarily by Schwann cells in the PNS, implicating it in Schwann cell–axon interactions. The embryonic and postnatal secretion of Lgi4 by Schwann cells suggests several potential roles for this protein in nerve development. First, it is possible that Schwann cells signal axons through Lgi4 to stimulate axon growth, reduce axon-axon adhesiveness or trigger axonal signaling back to Schwann cells. Lgi4 could bind directly to an axonal receptor or it could bind to an extracellular ligand. Second, Lgi4 could modulate an axonal signal to Schwann cells. Third, the axonal sorting defect in *clp* nerves resembles the defects observed in several different mice that possess laminin or integrin mutations[21]. Similarly, in neuron–Schwann cell cocultures treated with a low concentration of cyochalasin D that only subtly affects the actin cytoskeleton, Schwann cells project processes into fascicles of axons but fail to segregate them completely[42]. These similarities raise the possibility that Lgi4 modulates basal lamina signaling through integrins, thereby triggering the cytoskeletal rearrangements that are required for elaboration of Schwann cell processes and subsequent axon segregation.

clp/clp mice have a forelimb phenotype (**Fig. 1**) that is uncommon among peripheral dysmyelinating mutants. Abnormal forelimb posture at birth is also observed in Sox10 and cysteine-rich domain–NRG1 knockout mice; however, in these mice, it is associated with paralysis resulting from significant motor and sensory neuron cell death as a consequence of the loss of Schwann cells[18,43]. *clp* mice are not paralyzed and do not show excessive Schwann cell death or loss of sensory and motor neurons[19,21]. In fact, it is possible that this particular aspect of the phenotype is not associated with loss of Lgi4 expression in Schwann cells. Lgi4 is expressed in restricted regions of the CNS (refs. 41,44 and data not shown), and therefore the limb defect could be related to the CNS. Purkinje cells in the adult cerebellum express Lgi4, but the appearance of the limb defect precedes Purkinje cell maturation[45], suggesting that their involvement is unlikely. Identification of the etiology of the limb defect in *clp* mutant mice will be facilitated by the generation of tissue-specific deletions of *Lgi4*.

In summary, the identification and characterization of the *clp* mutation presented here demonstrates that the loss of Lgi4 expression underlies the claw paw phenotype and implicates the Lgi4 protein in Schwann cell differentiation and peripheral nerve development. Identification of Lgi4-interacting proteins will be instrumental in uncovering the signaling pathways in which Lgi4 participates and, additionally, may elucidate the functions of other Lgi proteins in oncogenesis and epileptogenesis. As a secreted protein that is required for Schwann cell development, Lgi4 is a promising target for therapies to stimulate myelination.

METHODS

Mice. We obtained C57BL/6J *clp/+* mice from the Jackson Laboratory, and FVB and CAST mice from the McLaughlin Research Institute breeding colony. Animal experiments were performed according to protocols that had been approved by the Institutional Animal Care and Use Committee at the McLaughlin Research Institute and the Institutional Animal Experimentation Committee at Erasmus University. Procedures for mapping of the *clp* mutation are presented in **Supplementary Methods** online.

Genotyping of *Lgi4^{clp}* mutant mice. Mice were genotyped by PCR using two primers that flank the *clp* insertion (5′-CTTGACAATGACCAGAGAGC CAAGAC-3′ and 5′-TGGCACCCTCGGATGACAGC-3′) and a third primer that covers the 3′ junction of the repeat insert (5′-CCATTCCCAGCAC CACAGCTTCA-3′).

cDNA amplification. We isolated RNA from adult C57BL/6 *Lgi4$^{+/+}$* and *clp/+* mouse sciatic nerves using Trizol (Invitrogen) and then carried out cDNA synthesis using Superscript II (Invitrogen) and a Clontech Advantage kit (BD Biosciences and Clontech). The Lgi4 open reading frame was amplified from this cDNA using the primers 5′-AAACTCGAGGAGCAACATGGGAGG GGCGGGCATCTTG-3′ and 5′-GGGTCTTTCCCGGTACCCGGCACTGAG ATCCAATTCATGGTG-3′ to improve the Kozak consensus around the ATG start site and to remove the stop codon. We cloned the 1,645-bp PCR product into pCRII+ (Invitrogen), sequenced it and subsequently cloned it into pcDNA3.1/Myc-His(–)C (Invitrogen) as an *Eco*RI-*Kpn*I fragment.

***In situ* hybridization.** We anesthetized and perfused mice with formalin. Hindquarters were dissected to expose the sciatic nerve and stored at 4 °C in formalin. Tissues were frozen in a 1:1 mixture of OCT and Aquamount, and sectioned at 20 μm. We performed *in situ* hybridization as described[22] and prepared single-stranded ^{35}S-labeled antisense transcripts from the clones described above. Emulsion-dipped sections were exposed for 7–21 d, counterstained in 0.001% bisbenzimide (Sigma) and photographed using dark-field optics and Kodak Ektachrome 160T film.

Transgenic complementation of the *clp* mutation. BACs were identified from the CAST/Ei BAC library at the Children's Hospital of Oakland Research Institute, by hybridizing filters with radiolabeled *Fxyd3* cDNA according to the manufacturer's protocol. BAC transgenic mice were made by pronuclear injection of 75-D7 BAC DNA that was purified using the Qiagen large construct kit (Qiagen), purified by density centrifugation in a CsCl gradient and dialyzed against 10 mM Tris (pH 8.0), 0.1 mM EDTA using Slide-A Lyzer 10K dialysis cassettes (Pierce). We identified BAC transgenic mice by PCR amplification of a 350-bp sequence from the pTARBAC 2.1 plasmid backbone using the primers 5′-CGCAGGTAAATGTGTCAAAATCTG-3′ and 5′-GCCGTTCGCTAACTCAG CATC-3′. We analyzed FVB and C57BL/6 chromosome-7 sequences using MIT microsatellite markers that differ in size between FVB and C57BL/6. These microsatellites were identified using the Center for Inherited Disease Research website (http://www.cidr.jhmi.edu/mouse/mouse_dif.html). M13-tagged primers for the D7MIT267 microsatellite marker were used for PCR amplification and analysis by electrophoresis on LI-COR apparatus (LI-COR Biosciences) as described above.

Bioinformatics. We analyzed sequences using the Celera Discovery System and the public mouse and human genome databases. We performed signal sequence prediction using Signal P3.0 (ref. 46) and TMHMM (version 2.0). Intron splice sites prediction using NetGene2. We identified conserved sequences between mouse and human using VISTA[47].

Cell transfection, immunohistochemistry and western blotting. CHO1 cells were grown in DMEM/F10 (Whitaker) medium supplemented with 5% fetal calf serum, penicillin and streptomycin. We obtained polyclonal cell lines stably expressing Lgi4, Lgi4^{clp} or Lgi1 after transfection of CHO1 cells with pcDNA3.1 Myc-His– or pcDNA3.1 V5-His–based expression cassettes and selection in G418 (1 mg ml^{-1}). For immunohistochemistry, the cells were grown in two-well microchamber slides, washed with phosphate-buffered saline (PBS) and fixed for 5 min in 4% paraformaldehyde (PFA) followed by 5 min in ice-cold methanol. Cells were preincubated with blocking solution (0.5% normal goat serum (DAKO), 0.5% bovine serum albumin (BSA), 0.01% Triton X-100, 0.2 mM glycine in PBS) for 5 min. First antibodies were diluted in blocking solution (1:200 for the anti-Myc 9E1 (Roche) mouse monoclonal antibody and

1:100 for the GRP-94 (DAKO) ER marker rabbit serum), applied to the cells and incubated for 2 h. Cells were washed extensively with PBS–0.001% Triton X-100 before addition of dilutions of secondary antibodies in blocking buffer (1:100 of Alexa 594–conjugated goat anti–mouse antibody and 1:100 Alexa 488–conjugated goat anti–rabbit antibody (Molecular Probes)). After 1 h, cells were extensively washed with PBS–0.01% Triton X-100, PBS and demineralized water; and mounted. We examined the cells using a Leica Aristoplan epifluorescence microscope and collected images using a Sony video camera.

We purified proteins from cell extracts and medium using Ni^{2+}-NTA beads (Qiagen) and separated them on a 12% SDS-PAGE gel. Proteins were transferred to a polyvinylidene fluoride (PVDF) membrane (Millipore) and detected with primary antibodies to Myc (Lgi4), V5 (Lgi1) or Oct6. We visualized proteins using an ECL western blot detection kit (Pierce).

Neuron–Schwann cell cocultures and lentiviral infection. Dissociated mouse DRG cultures: DRGs were dissected from E13 *clp/clp*, *clp/+* and wild-type embryos, and collected in Leibovitz's L-15 medium (Invitrogen). DRGs from individual embryos were dispersed using trypsin and plated in a small drop of MEM (Invitrogen) supplemented with 10% FBS (HyClone) and 100 ng ml^{-1} 7S NGF (Promega) on collagen-coated coverslips. We cultured and induced myelination by the addition of 50 μg ml^{-1} ascorbic acid (Sigma) as described in ref. 8. We visualized myelin figures by staining PFA-fixed cultures with antibodies to the major myelin proteins Mpz (ref. 48) or Mbp. Lgi4-Myc-His–expressing CHO cells (polyclonal) or non-recombinant CHO cells were grown in MEM supplemented with 10% FBS for 5 d. The conditioned medium was harvested, filtered and used to supplement medium for dissociated *clp/clp* DRG cultures. The conditioned medium was added the day after plating and was present during the whole time period of the experiment. For rat DRG–Schwann cell cultures, primary DRG neuron cultures were established using DRGs harvested from E16 rat pups. DRGs were disassociated, and approximately two DRG were plated per well in four-well Nunc plates coated with Matrigel (BD Biosciences). Neurons were grown in supplemented neural basal medium (Invitrogen) (B27 supplement, Invitrogen; 4 g l^{-1} D-glucose, 2 mM glutamine and 50 ng ml^{-1} NGF, Harlan) with or without a mixture of 10 μM 5-fluoro-2′-deoxyuridine and uridine (Sigma) for two or three 48-h cycles to eliminate fibroblast growth. Primary rat Schwann cells were harvested from sciatic nerves of P1 and P2 rat pups according to Brockes' method and cultured as described[17]. For myelination, 100,000 lentiviral-infected Schwann cells were seeded onto DRG cultures in DMEM/F12 medium (Invitrogen) supplemented with 15% FBS (Sigma), 2 mM glutamine and 50 ng ml^{-1} NGF. After 48–96 h, the medium was switched to myelin-promoting medium consisting of DMEM/F12, 15% FBS, 2 mM glutamine, 50 ng ml^{-1} NGF and 50 μg ml^{-1} ascorbic acid (Sigma). Myelination medium was changed three times every week, and the cultures were allowed to myelinate for up to 2 weeks.

The *Lgi4* siRNA vector was produced by cloning annealed oligos, which encoded a hairpin loop and the targeting sequence 5′-CTGTCACT CTCTCTCGTCA-3′ into a lentiviral vector containing the U6 promoter and a puromycin resistance cassette. Non-recombinant lentivirus without a hairpin oligo insertion was used as the control. Lentivirus production and infection was performed as described[16]. Infected Schwann cells were selected for by treating with 1 μg/ml puromycin for 48 h.

Immunohistochemistry of rat DRG–Schwann cell cocultures. Cultures were fixed for 10 min in 4% paraformaldehyde and then permeabilized for 20 min in cold methanol at –20° C. Incubation with primary antibody was performed overnight at 4° C with monoclonal antibodies to Mbp (1:200; Sternberger Monoclonals) in blocking buffer (5% BSA (Sigma), 1% goat serum (Zymed), 0.2% Triton in PBS). Goat anti–mouse IgG–Cy3 (Jackson Immunoresearch) was used at 1:200 dilution for 1 h at room temperature. Percent myelination was calculated by counting the total number of Mbp-positive internodes in five random fields per culture viewed at 10× magnification and setting the control to 100%. Each condition was performed in triplicate or quadruplicate, and the data presented is the average ± s.e.m. of three independent experiments.

Quantitative RT-PCR. For cDNA synthesis, 1 μg of total RNA isolated from lentiviral-infected cultured Schwann cells (Trizol reagent, Invitrogen) was used. Gene expression was quantified as previously described[17] and normalized to glyceraldehyde-3-phosphate dehydrogenase (GAPDH) levels. Each sample was quantified in triplicate, and the results shown are the averages ± s.e.m. of a representative experiment.

Note: Supplementary information is available on the Nature Neuroscience website.

ACKNOWLEDGMENTS

We thank D. Krajacich for technical assistance, as well as the undergraduate summer students who worked on this project at the McLaughlin Research Institute: C. Schedl, M. Chen, S. Brauer, J. Anspach-Hanson and B. Cook. We also thank C. Ebeling for assistance with LI-COR analysis; S.S. Scherer for providing the PLP plasmid; N. Jenkins, N. Copeland, J. Chan and T. Watkins for protocols and advice; and E. Dzierzak for critical reading of the manuscript. This work was funded by the National Institute of Neurological Diseases and Stroke (NINDS) grant NS40751 and Muscular Dystrophy Association grant 3476 to J.R.B. Jr.; NINDS grants NS049087 and NS40745 to J.M.; and by grants from the Nederlandse Organisatie van Wetenschappelijk Onderzoek (NWO; ZonMW 903-42-195 and 901-01-205) to D.M.

COMPETING INTERESTS STATEMENT

The authors declare that they have no competing financial interests.

Published online at http://www.nature.com/natureneuroscience/
Reprints and permissions information is available online at http://npg.nature.com/reprintsandpermissions/

1. Jessen, K.R. & Mirsky, R. Schwann Cell Development. in *Myelin Biology and Disorders* Vol. 1 (ed. Lazzarini, R.A.) 329–370 (Elsevier Academic, San Diego, 2004).
2. Lobsiger, C.S., Taylor, V. & Suter, U. The early life of a Schwann cell. *Biol. Chem.* **383**, 245–253 (2002).
3. Britsch, S. *et al.* The ErbB2 and ErbB3 receptors and their ligand, neuregulin-1, are essential for development of the sympathetic nervous system. *Genes Dev.* **12**, 1825–1836 (1998).
4. Garratt, A.N., Britsch, S. & Birchmeier, C. Neuregulin, a factor with many functions in the life of a Schwann cell. *Bioessays* **22**, 987–996 (2000).
5. Michailov, G.V. *et al.* Axonal neuregulin-1 regulates myelin sheath thickness. *Science* **304**, 700–703 (2004).
6. Taveggia, C. *et al.* Neuregulin-1 type III determines the ensheathment fate of axons. *Neuron* **47**, 681–694 (2005).
7. Cosgaya, J.M., Chan, J.R. & Shooter, E.M. The neurotrophin receptor p75NTR as a positive modulator of myelination. *Science* **298**, 1245–1248 (2002).
8. Chan, J.R. *et al.* NGF controls axonal receptivity to myelination by Schwann cells or oligodendrocytes. *Neuron* **43**, 183–191 (2004).
9. Fields, R.D. & Stevens-Graham, B. New insights into neuron-glia communication. *Science* **298**, 556–562 (2002).
10. Atanasoski, S. *et al.* The protooncogene Ski controls Schwann cell proliferation and myelination. *Neuron* **43**, 499–511 (2004).
11. Ogata, T. *et al.* Opposing extracellular signal-regulated kinase and Akt pathways control Schwann cell myelination. *J. Neurosci.* **24**, 6724–6732 (2004).
12. Wegner, M. Transcriptional control in myelinating glia: the basic recipe. *Glia* **29**, 118–123 (2000).
13. Topilko, P. & Meijer, D. Transcription factors that control Schwann cell development and myelination. in *Glial Cell Development* (eds. Jessen, K.R. & Richardson, W.D.) 223–244 (Oxford Univ. Press, Oxford, 2001).
14. Ghislain, J. *et al.* Characterisation of cis-acting sequences reveals a biphasic, axon-dependent regulation of Krox20 during Schwann cell development. *Development* **129**, 155–166 (2002).
15. Jaegle, M. *et al.* The POU proteins Brn-2 and Oct-6 share important functions in Schwann cell development. *Genes Dev.* **17**, 1380–1391 (2003).
16. Le, N. *et al.* Analysis of congenital hypomyelinating Egr2Lo/Lo nerves identifies Sox2 as an inhibitor of Schwann cell differentiation and myelination. *Proc. Natl. Acad. Sci. USA* **102**, 2596–2601 (2005).
17. Nagarajan, R. *et al.* EGR2 mutations in inherited neuropathies dominant-negatively inhibit myelin gene expression. *Neuron* **30**, 355–368 (2001).
18. Britsch, S. *et al.* The transcription factor Sox10 is a key regulator of peripheral glial development. *Genes Dev.* **15**, 66–78 (2001).
19. Henry, E.W., Eicher, E.M. & Sidman, R.L. The mouse mutation claw paw: forelimb deformity and delayed myelination throughout the peripheral nervous system. *J. Hered.* **82**, 287–294 (1991).
20. Koszowski, A.G., Owens, G.C. & Levinson, S.R. The effect of the mouse mutation claw paw on myelination and nodal frequency in sciatic nerves. *J. Neurosci.* **18**, 5859–5868 (1998).
21. Darbas, A. *et al.* Cell autonomy of the mouse claw paw mutation. *Dev. Biol.* **272**, 470–482 (2004).
22. Bermingham, J.R., Jr. *et al.* Identification of genes that are downregulated in the absence of the POU domain transcription factor pou3f1 (Oct-6, Tst-1, SCIP) in sciatic nerve. *J. Neurosci.* **22**, 10217–10231 (2002).
23. Gu, W. *et al.* The LGI1 gene involved in lateral temporal lobe epilepsy belongs to a new subfamily of leucine-rich repeat proteins. *FEBS Lett.* **519**, 71–76 (2002).

ARTICLES

24. Maro, G.S. *et al.* Neural crest boundary cap cells constitute a source of neuronal and glial cells of the PNS. *Nat. Neurosci.* **7**, 930–938 (2004).
25. Staub, E. *et al.* The novel EPTP repeat defines a superfamily of proteins implicated in epileptic disorders. *Trends Biochem. Sci.* **27**, 441–444 (2002).
26. Scheel, H., Tomiuk, S. & Hofmann, K. A common protein interaction domain links two recently identified epilepsy genes. *Hum. Mol. Genet.* **11**, 1757–1762 (2002).
27. Buchanan, S.G. & Gay, N.J. Structural and functional diversity in the leucine-rich repeat family of proteins. *Prog. Biophys. Mol. Biol.* **65**, 1–44 (1996).
28. Kajava, A.V. Structural diversity of leucine-rich repeat proteins. *J. Mol. Biol.* **277**, 519–527 (1998).
29. Wong, K., Park, H.T., Wu, J.Y. & Rao, Y. Slit proteins: molecular guidance cues for cells ranging from neurons to leukocytes. *Curr. Opin. Genet. Dev.* **12**, 583–591 (2002).
30. Howitt, J.A., Clout, N.J. & Hohenester, E. Binding site for Robo receptors revealed by dissection of the leucine-rich repeat region of Slit. *EMBO J.* **23**, 4406–4412 (2004).
31. Gherardi, E., Love, C.A., Esnouf, R.M. & Jones, E.Y. The sema domain. *Curr. Opin. Struct. Biol.* **14**, 669–678 (2004).
32. Skradski, S.L. *et al.* A novel gene causing a mendelian audiogenic mouse epilepsy. *Neuron* **31**, 537–544 (2001).
33. Nakayama, J. *et al.* A nonsense mutation of the MASS1 gene in a family with febrile and afebrile seizures. *Ann. Neurol.* **52**, 654–657 (2002).
34. Kalachikov, S. *et al.* Mutations in LGI1 cause autosomal-dominant partial epilepsy with auditory features. *Nat. Genet.* **30**, 335–341 (2002).
35. Berkovic, S.F. *et al.* LGI1 mutations in temporal lobe epilepsies. *Neurology* **62**, 1115–1119 (2004).
36. Ottman, R. *et al.* LGI1 mutations in autosomal dominant partial epilepsy with auditory features. *Neurology* **62**, 1120–1126 (2004).
37. Pisano, T. *et al.* Abnormal phonologic processing in familial lateral temporal lobe epilepsy due to a new LGI1 mutation. *Epilepsia* **46**, 118–123 (2005).
38. Gu, W., Sander, T., Becker, T. & Steinlein, O.K. Genotypic association of exonic LGI4 polymorphisms and childhood absence epilepsy. *Neurogenetics* **5**, 41–44 (2004).
39. Ellgaard, L. & Helenius, A. Quality control in the endoplasmic reticulum. *Nat. Rev. Mol. Cell Biol.* **4**, 181–191 (2003).
40. Bonnon, C., Goutebroze, L., Denisenko-Nehrbass, N., Girault, J.A. & Faivre-Sarrailh, C. The paranodal complex of F3/contactin and caspr/paranodin traffics to the cell surface via a non-conventional pathway. *J. Biol. Chem.* **278**, 48339–48347 (2003).
41. Senechal, K.R., Thaller, C. & Noebels, J.L. ADPEAF mutations reduce levels of secreted LGI1, a putative tumor suppressor protein linked to epilepsy. *Hum. Mol. Genet.* **14**, 1613–1620 (2005).
42. Fernandez-Valle, C., Gorman, D., Gomez, A.M. & Bunge, M.B. Actin plays a role in both changes in cell shape and gene-expression associated with Schwann cell myelination. *J. Neurosci.* **17**, 241–250 (1997).
43. Wolpowitz, D. *et al.* Cysteine-rich domain isoforms of the neuregulin-1 gene are required for maintenance of peripheral synapses. *Neuron* **25**, 79–91 (2000).
44. Runkel, F., Michels, M. & Franz, T. Fxyd3 and Lgi4 expression in the adult mouse: a case of endogenous antisense expression. *Mamm. Genome* **14**, 665–672 (2003).
45. McKay, B.E. & Turner, R.W. Physiological and morphological development of the rat cerebellar Purkinje cell. *J. Physiol. (Lond.)* **567**, 829–850 (2005).
46. Bendtsen, J.D., Nielsen, H., von Heijne, G. & Brunak, S. Improved prediction of signal peptides: signalP 3.0. *J. Mol. Biol.* **340**, 783–795 (2004).
47. Mayor, C. *et al.* VISTA: visualizing global DNA sequence alignments of arbitrary length. *Bioinformatics* **16**, 1046–1047 (2000).
48. Archelos, J.J. *et al.* Production and characterization of monoclonal antibodies to the extracellular domain of P0. *J. Neurosci. Res.* **35**, 46–53 (1993).
49. Zhuang, Y.A., Goldstein, A.M. & Weiner, A.M. UACUAAC is the preferred branch site for mammalian mRNA splicing. *Proc. Natl. Acad. Sci. USA* **86**, 2752–2756 (1989).
50. Hart, G.W., Brew, K., Grant, G.A., Bradshaw, R.A. & Lennarz, W.J. Primary structural requirements for the enzymatic formation of the N-glycosidic bond in glycoproteins. Studies with natural and synthetic peptides. *J. Biol. Chem.* **254**, 9747–9753 (1979).

Chapter 7

Conclusions and summary

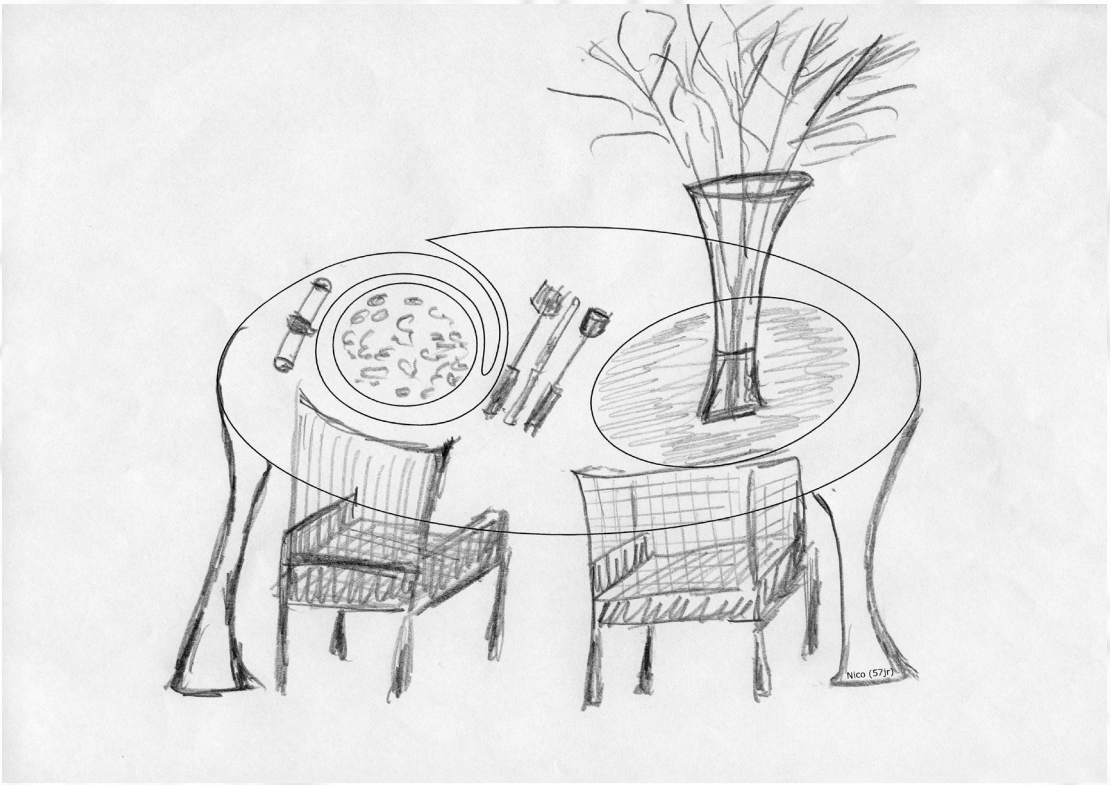

Conclusions and summary

Schwann cells are derived from the neural crest. It is thought that migrating crest cells associate with the outgrowing axonal fibers and adopt a Schwann cell precursor identity. Schwann cell precursors proliferate and invade the axonal bundles with cytoplasmic extensions, sorting the fibers into smaller groups. This process of radial sorting continues until the larger calibre axons are singled out by Schwann cells that will go on to produce the myelin sheath. Smaller (diameter < 1 μm) axons will not be myelinated but will instead be ensheathed by a Schwann cell that will accommodate several of the small calibre axons in cytoplasmic cuffs forming so-called Remak bundles (see introduction). Classic experiments have indicated that the binary choice to become a myelin forming or non-myelin forming Schwann cell is determined by the axon[1]. The nature of the axonal signal that dictates Schwann cell identity and that triggers the intracellular cascade of cell differentiation has long remained elusive. Several molecules have been proposed to play a key role in the acquisition of a myelinating fate and in the initiation of myelination. In particular, the neuregulins (NRG) and the neurotrophins and their respective receptors have gained prominence in recent years[2-4].

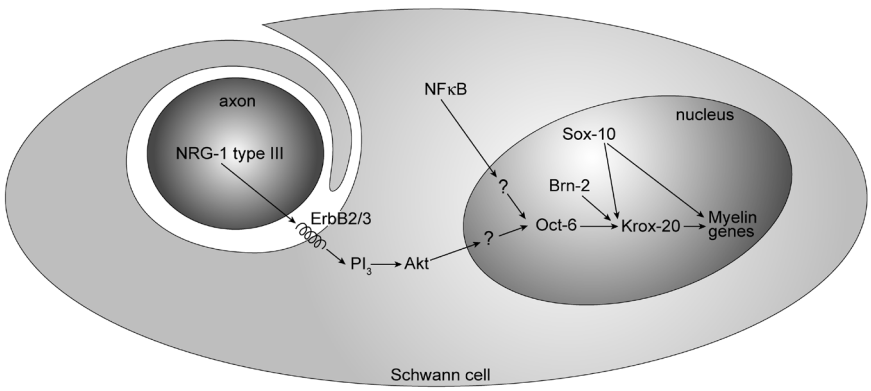

Figure 1. Model of the different molecules interacting with each other in the developing myelinating Schwann cell.

The NRGs are a group of related membrane-bound or secreted peptides that are generated from the NRG-1 gene through differential promoter usage and alternative splicing[5,6]. These proteins can be grouped in three major types (I-III) that differ in their amino-terminal sequence[7]. All forms of NRG bind to the ErbB tyrosine-kinase receptors. Schwann cells express ErbB2 and ErbB3, which form a functional heterodimeric receptor. *In vitro* experiments have demonstrated that soluble NRGs are required for the differentiation of Schwann cell precursors from neural crest stem cells and their subsequent survival[8,9]. In addition, genetic experiments indicate that myelin sheath thickness is graded to the strength of the NRG signal[10]. More recently it was demonstrated that the membrane bound type III NRG is required for the Schwann cell axon interaction, axonal sorting and initiation of myelin formation[11]. However, type III NRG does not induce myelin gene expression in Schwann

cells when expressed on the cell surface of CHO cells, indicating that additional axonal membrane associated molecules contribute to NRG function[11]. Activation of the ErbB2/ErbB3 receptor on the Schwann cell membrane by axonal type III NRG-1 results in activation of the PI3K pathway and activation of Akt/PKB. Pharmacological inhibition of PI3K activity in Schwann cell-sensory neuron co-cultures inhibits Schwann cell sorting and myelination, phenocopying the type III NRG mutation[12]. Thus, the effects of type III NRG-1 appears to be mediated through the PI3K-PKB pathway. One major target of PKB are the O-class forkhead transcription factors; Foxo1, Foxo3, Foxo4 and Foxo6[13]. It is not known whether Foxo proteins are expressed in Schwann cells. Whatever the exact nature of these signals, they will converge on the Oct-6 Schwann cell enhancer (SCE)[14] to initiate myelination. Interestingly, potential forkhead binding sites are present in those parts of the Oct-6 SCE found to be essential for enhancer function (unpublished results from our lab). Future experiments should address the role of Foxo proteins in SCE activity.

Another signal that has been thought to be involved in initiation of myelination is nuclear factor kappa B (NF-κB). Schwann cells express the p65 and p50 NF-κB proteins that can homo- or heterodimerize to form active complexes. At early stages of myelination p65 is the major form of NF-κB while at later stages p50 is more prominently expressed[15]. Both forms of NF-κB are bound by IκBα and retained in the cytoplasm. Upon phosphorylation of IκBα, NF-κB is translocated to the nucleus where it will activate a set of target genes. It was demonstrated that p65 null DRG explant cultures do not myelinate, while wild type cultures were myelinated. The transcription of *Oct-6* was not activated in $p65^{-/-}$ Schwann cells and Nickols *et al*. concluded that the translocation of NF-κB was an important signal for the activation of transcription of *Oct-6*[15]. However, we have found no evidence for a direct role of NF-κB in activation of Oct-6 as no NF-κB binding sites are present in the Oct-6 SCE nor does p65 activate the SCE in a co-transfection assay (M. Ghazvini, unpublished observations).

As mentioned earlier, Schwann cell specific transcription of the *Oct-6* gene is controlled by a remote enhancer element called the SCE (Schwann cell enhancer). This notion is based on two lines of evidence. First, linking the Oct-6 SCE element to a minimal unrelated promoter confers temporally correct expression of a reporter gene in Schwann cells of transgenic mice[16]. Second, deletion of the SCE from the *Oct-6* locus in mice results in the selective loss of *Oct-6* gene expression in Schwann cells[14]. Consequently, mice homozygous for the ΔSCE allele, $Oct\text{-}6^{\Delta SCE/\Delta SCE}$, exhibit delayed myelination of their peripheral nerves similar to what is observed in *Oct-6* knock out mice[14,17]. In contrast to full *Oct-6* knock out mice ($Oct\text{-}6^{\beta geo/\beta geo}$), $Oct\text{-}6^{\Delta SCE/\Delta SCE}$ mice are viable and allowed us to study later stages of nerve development.
The relatively mild peripheral nerve developmental defect in $Oct\text{-}6^{\Delta SCE/\Delta SCE}$ and $Oct\text{-}6^{\beta geo/\beta geo}$ mice suggested the existence of a molecule that could partly substitute for Oct-6. It was found that Schwann cells express at least two additional POU proteins; Oct-1

and Brn-2[18-20]. Oct-1 is a ubiquitously expressed protein belonging to the class II subfamily. Brn-2 is closely related to Oct-6, and is expressed in a similar pattern as Oct-6. Furthermore, Brn-2 expression is not dependent on Oct-6. In chapter 3 we demonstrate that Brn-2 is indeed functionally redundant to Oct-6 in that deletion of Brn-2 in the Oct-6 mutant background results in a severe developmental delay of Schwann cell development while moderate transgenic overexpression of Brn-2 in Oct-6$^{\Delta SCE/\Delta SCE}$ Schwann cells results in amelioration of the phenotype. These findings raise the question why we see a peripheral nerve phenotype in *Oct-6* mutant mice to begin with, despite high levels of Brn-2 in the nuclei of these Schwann cells? Possibly Brn-2 and Oct-6 DNA binding affinities differ, requiring higher Brn-2 concentrations to achieve appropriate binding site occupancy. Alternatively, Oct-6 and Brn-2 differ in their affinity for other proteins involved in regulation of the target gene repertoire of these POU proteins. Although the DNA binding affinities of Oct-6 and Brn-2 have not been determined, the near identity of their respective DNA binding domains (the POU domain) suggests that they are not significantly different. Furthermore, replacement through gene knock in of Oct-6 by Brn-1, another member of the class III POU domain subfamily, did not result in any obvious alterations in the development of the peripheral nerve[21]. These results strongly suggest that the level of class III POU domain protein expression is more important for timely Schwann cell differentiation than the identity of the class III POU protein expressed. As the class III POU domain proteins are almost identical in their primary amino acid sequence of the POU domain it is likely that all the important interactions are mediated through the POU domain. Indeed, the solvent exposed surface of the helical coils that make up the POU specific and POU homeodomains of Oct-1 and Oct-2 have been demonstrated to interact with co-factors such as HCF/VP16 (in case of Oct-1) and OCAB/Bob1 (in case of Oct-2) and that these interactions are functionally important[22].

Two aspects of the primary amino acid sequence of Oct-6 and Brn-2 suggest that they contribute to differential interactions with other proteins. First, one distinctive feature of the Oct-6 POU domain is the presence of a Histidine residue at position 115 in the POU homeodomain and a Threonine at position 68 in the POU-specific domain (residues are highlighted in figure 2A). All other class III proteins have a Glutamine and an Alanine in these respective positions. When the primary amino acid sequence of Oct-6 and Brn-2 POU domain is modelled on the structure of the Oct-1 POU domain it is clear that the two amino acid side chains are solvent exposed and thus open for protein interactions (see figure 2B). The specific amino acids in these positions have been maintained in Oct-6 proteins from vertebrate species that are separated from their common ancestor by hundreds of millions of years of evolution. Thus, these amino acids may be involved in functional interactions with other molecules, most likely proteins. At present it is unknown what these proteins are and we have taken a proteomic approach to identify Oct-6 interacting proteins[23]. The fact that Brn-1 can functionally substitute for Oct-6 in Schwann cells suggests that Oct-6 Thr/His interactions play a more important role in other Oct-6 expressing cells such as brainstem or hippocampal neurons.

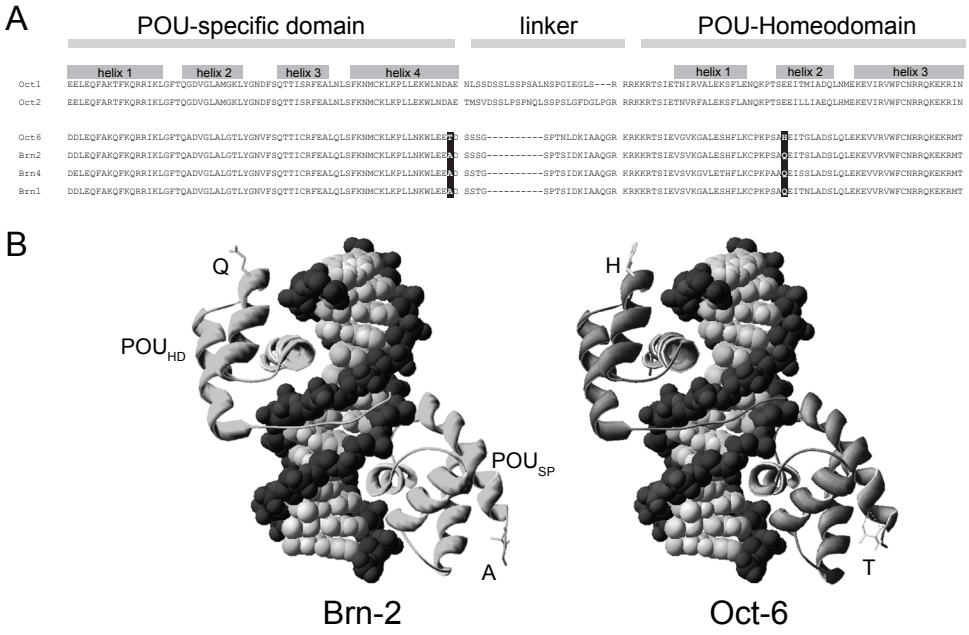

Figure 2. (A) Protein alignment of the POU-specific domain and the POU-homeodomain of several POU proteins. The residues that differ between the Oct-6 and the Brn proteins are indicated in white on black. (B) The protein crystal structures of Brn-2 and Oct-6 are shown and the residues that differ in the protein alignment are shown on the structures.

A second interesting difference between Brn-2 and Oct-6 (and Brn-1), is the presence of a long (23 aa) stretch of glutamine residues in the amino-terminal half of Brn-2. It has been demonstrated that a protein called poly-glutamine binding protein or PQBP-1 can bind such glutamine stretches. Binding of PQBP-1 to the polyglutamine stretch of ataxin1 was demonstrated to affect RNA polymerase activity resulting in motorneuron death[24]. Furthermore, mutations in PQBP-1 are associated with Renpenning syndrome, a form of X-linked mental retardation. PQBP-1 was originally identified in a yeast-two-hybrid screen using the Brn-2 transcription factor as bait. It was subsequently shown that PQBP-1 could repress Brn-2 mediated activation of a reporter gene in transfection experiments[25]. It is therefore tempting to speculate that Brn-2/PQBP-1 interactions could attenuate/repress Brn-2 function in Schwann cells. Indeed, we found that PQBP-1 is expressed in Schwann cells. However, co-immune precipitation experiments have so far failed to confirm a direct interaction between PQBP-1 and Brn-2. Future experiments should further clarify the possible interaction between the two proteins.

Several lines of evidence suggest that the zinc-finger transcription factor *Krox-20* is a major target of Oct-6/Brn-2 regulation in Schwann cells. First, Krox-20 expression is strongly reduced in Schwann cells of newborn *Oct-6* mutant animals[26]. Second, the Krox-20 enhancer that directs Krox-20 expression in Schwann cells contains a number of high affinity

binding sites for Oct-6 and Brn-2. Mutation of the binding sites results in loss of Schwann cell specific expression of a linked beta-Galactosidase reporter gene in transgenic mice[27]. Sox10 enhances activation of the myelinating Schwann cell element (MSE) by Oct-6 or Brn-2 in a co-transfection assay. Multiple potential binding sites for Sox10 exist within this enhancer making it likely that Sox10 binds to the MSE. Therefore, Krox-20 activation at the onset of myelination results from the activity of at least Oct-6/Brn-2 and Sox10[26].

It is generally accepted that Krox-20 activation in promyelinating Schwann cells is sufficient to initiate the myelin gene expression program. These genes include the classical myelin genes such as P_0 and *PMP22* but also genes that encode enzymes in lipid metabolism and cell adhesion molecules such as Neurofascin and Gliomedin. The evidence that Krox-20 directly regulates these genes is however rather sparse. The best-studied myelin gene regulatory sequences are those of the *MBP* gene. A 400bp enhancer fragment 9kb upstream of the MBP promoter confers Schwann cell specificity on the promoter. Although this fragment contains potential Krox-20 binding sites these sites do not contribute to the Schwann cell specificity of the enhancer but do affect the level of expression[28]. However, recent work from Dr. John Svaren's group has identified a conserved module in the first intron of the P_0 gene[29]. They demonstrate that this element functions as a Krox-20 dependent enhancer in co-transfection experiments. It is likely that this element represents a major P_0 enhancer element that contributes to the strong myelination associated expression of the gene.

Another factor that appears to be of great importance for Schwann cell specific expression is Sox10. Sox10 binding sites are found in promoters and enhancers of myelin genes such as P_0 and *PMP22* and these promoters are activated by Sox10 in co-transfection experiments[29-32].

Thus, the onset and execution of the myelination gene program is primary controlled by a genetic hierarchy in which Oct-6/Brn-2 serves as an integrator of extra and intracellular signals and in turn activate *Krox-20* and myelination. Sox10 appears to play major roles in activating and maintaining expression of myelin genes in cooperation with Krox-20. Maintenance of the myelination program does not require Oct-6.

The experiments discussed above demonstrated that Krox-20 activation largely depends on Oct-6. But is Oct-6 also sufficient to activate Krox-20 or are there other factors involved? We found that Oct-6 is highly expressed in immature sorting and promyelinating Schwann cells of *clp* mice, that do not express Krox-20 until myelination commences[33]. This observation suggested that the *clp* gene is directly involved in Oct-6 mediated regulation of Krox-20 or that clp is involved in a parallel non-redundant pathway. Interestingly, forced transgenic expression of Krox-20 under control of the Oct-6 SCE in *clp* animals failed, whereas expression of another non-related protein under the same enhancer was expressed in *clp* Schwann cells at this stage of development (M. Jaegle; unpublished observations). This suggests that Krox-20 expression is under negative feedback control, most likely at the co- or posttranslational level. If such a posttranslational mechanism of Krox-20 regula-

tion indeed exists, it is predicted that a *LacZ* reporter gene under control of the Krox-20 MSE is normally active. It will be of interest to investigate Oct-6 and Krox-20 expression in other mouse mutants that exhibit promyelin arrest, such as the P_0 overexpressing mice generated in the Wrabetz and Feltri lab[34].

Our initial interest in the *clp* mouse was raised because of the similarities in the peripheral nerve defect observed in *clp* and *Oct-6* mutant mice. These similarities suggested that Oct-6 and clp might be involved in similar pathways. We found that the clp phenotype results from homozygosity of a mutation in the *Leucine rich glioma inactivated (Lgi)-4* gene[35]. *Lgi4* is a member of the family of Lgi genes, which also includes *Lgi1*, *Lgi2* and *Lgi3* that encodes a class of related secreted proteins. *Lgi1* was the first member of this family to be described as a gene inactivated in a glioma cell line. More recently, it was found that *Lgi1* is frequently mutated in specific forms of epilepsy. Most mutations affect the proper processing of the protein resulting in decreased levels. Interestingly, these forms of epilepsy are inherited in a dominant fashion, consistent with haploinsufficiency or dominant negative action of the mutant protein. In contrast, the *Lgi4 clp* allele is a recessive allele, with no detectable phenotype in heterozygotes.
Lgi4 affects Schwann cell development largely in a cell-autonomous fashion. Lgi4 is expressed by and secreted from the Schwann cell[33]. How Lgi4 affects Schwann cell differentiation is not clear yet but several mechanisms can be envisaged (figure 3). First it is possible that Lgi4 binds to a receptor on the axonal membrane resulting in an axon-derived signal that directs proper sorting and myelination. It is of interest to note that the NRG-1 type III expressed on the axonal membrane is also required for sorting and myelination. Perhaps Lgi4 interacts with type III NRG-1 and modulates its interaction with the Schwann cell expressed ErbB2/3 receptor. Second it is possible that Lgi4 interacts with a factor secreted by the axon or with a receptor for that molecule. For example, it has been demonstrated that neuronal activity results in the release of adenosine from the axo-lemma and release of intracellular calcium in Schwann cells that express purinergic receptors[36]. This activity is important in regulating several aspects of Schwann cell proliferation and differentiation in Schwann cell-neuronal co-cultures. A third possibility is that Lgi4 acts in an autocrine fashion, directly binding to a Schwann cell receptor or extracellular matrix component. Such autocrine interactions operate in basal lamina interactions such as between the extracellular laminins and their integrin receptors. These interactions are important for axonal sorting. Engineered mutations in laminin or the integrin or dystroglycan receptor result in severe axonal sorting defects. It is possible that Lgi4 modulates these interactions. To determine through which mechanism Lgi4 works, it is of prime importance to identify the interacting partners of Lgi4 in nerve development. Using human Fc-Lgi4 fusion molecules or otherwise tagged Lgi4 molecules it should be possible to determine whether Lgi4 binds to axons or Schwann cells and its basal lamina or both. Preliminary experiments in our laboratory have provided some evidence for the existence of a Lgi4 binding activity on the axonal surface, while no such binding could be detected on cultured Schwann cells. Sev-

eral approaches can be taken to identify the putative Lgi4 receptor or interacting partner. One approach is expression cloning. However, this will only work when the Lgi4 receptor is a monomeric or homo-multimeric protein. We have therefore chosen a more direct approach, using the biotinylation strategy described in chapter 6. To this end we have generated a transgene that carries an avi-tagged *Lgi4* gene. This transgene will be crossed into the clp background to test whether it will rescue the clp phenotype. If so, we will establish DRG explants of these mice and directly purify cross-linked Lgi4 interacting molecules using the avi tag and identify these partners by mass spectrometry.

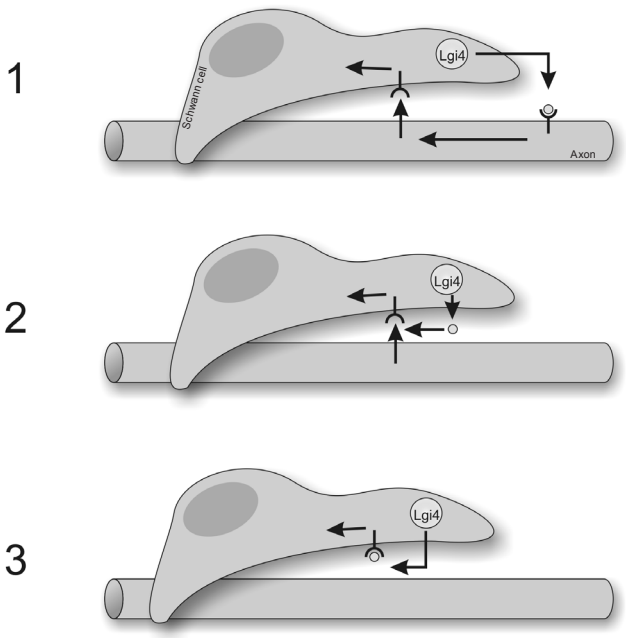

Figure 3. Three models of possible mechanism of Lgi4 functioning, as explained above.

One recent development suggests that Lgi4 could interact with potassium (K^+) channels. This suggestion is based on the work of Schulte and co-workers who sought to identify molecules associated with rapidly inactivating potassium channels in the hippocampus. Gene knock out studies had already demonstrated that loss of potassium channel α-subunit Kv1.1 results in severe epileptic seizures[37,38]. Using a proteomic approach Schulte *et al.* demonstrated a tight interaction between Lgi1 and potassium channels in membrane preparations of hippocampal neurons. They further demonstrate through expression in Xenopus oocytes that Lgi1 modulates the kinetics of K^+ channel inactivation. K^+ channels consist of 4 α-subunits and a variable number of β-subunits. These Kv1 channels are rapidly inactivating: following membrane depolarisation the potassium current declines rapidly (low τ

values). This rapid inactivation is caused by a cytoplasmic domain of the channel (Kv1.4) or by a β-subunit (Kv1.1). It was demonstrated that Lgi1 specifically increases the length of the inactivation time constant (t) of K^+ channels that consist of Kv1.1/Kvβ1 subunits[39]. It is believed that these properties of the potassium channels are important in regenerating the action potential and dampening excitability of a synapse. It is therefore no surprise that mutations in Lgi1 can cause epilepsy. In analogy with Lgi1 it is conceivable that Lgi4 interacts with axonal potassium channels. The major potassium channels at the juxtaparanodes are the Kv1.1 and Kv1.2 α-subunits and Kvβ1 and Kvβ2 subunits. We found that these channels are already expressed, together with Lgi4, in embryonic nerves at E13. It is possible that Lgi4 K^+ channel interaction represents a paracrine or cell adhesion interaction that affects axonal sorting at these early stages of nerve development. One intriguing, but highly speculative, possibility is that Lgi4 K^+ channel interactions affect the spontaneous excitability of late gestation neurons providing a tentative explanation for the limb posture abnormality observed in claw paw neonates.

References

1. Aguayo AJ, Epps J, Charron L, Bray GM. Multipotentiality of Schwann cells in cross-anastomosed and grafted myelinated and unmyelinated nerves: quantitative microscopy and radioautography. Brain Res 1976;104(1):1-20.
2. Garratt AN, Britsch S, Birchmeier C. Neuregulin, a factor with many functions in the life of a schwann cell. Bioessays 2000;22(11):987-96.
3. Notterpek L. Neurotrophins in myelination: a new role for a puzzling receptor. Trends Neurosci 2003;26(5):232-4.
4. Corfas G, Velardez MO, Ko CP, Ratner N, Peles E. Mechanisms and roles of axon-Schwann cell interactions. J Neurosci 2004;24(42):9250-60.
5. Lemke G. Neuregulins in development. Mol Cell Neurosci 1996;7(4):247-62.
6. Burden S, Yarden Y. Neuregulins and their receptors: a versatile signaling module in organogenesis and oncogenesis. Neuron 1997;18(6):847-55.
7. Buonanno A, Fischbach GD. Neuregulin and ErbB receptor signaling pathways in the nervous system. Curr Opin Neurobiol 2001;11(3):287-96.
8. Shah NM, Anderson DJ. Integration of multiple instructive cues by neural crest stem cells reveals cell-intrinsic biases in relative growth factor responsiveness. Proc Natl Acad Sci U S A 1997;94(21):11369-74.
9. Shah NM, Marchionni MA, Isaacs I, Stroobant P, Anderson DJ. Glial growth factor restricts mammalian neural crest stem cells to a glial fate. Cell 1994;77(3):349-60.
10. Michailov GV, Sereda MW, Brinkmann BG, Fischer TM, Haug B, Birchmeier C, Role L, Lai C, Schwab MH, Nave KA. Axonal neuregulin-1 regulates myelin sheath thickness. Science 2004;304(5671):700-3.
11. Taveggia C, Zanazzi G, Petrylak A, Yano H, Rosenbluth J, Einheber S, Xu X, Esper RM, Loeb JA, Shrager P and others. Neuregulin-1 type III determines the ensheathment fate of axons. Neuron 2005;47(5):681-94.

12. Maurel P, Salzer JL. Axonal regulation of Schwann cell proliferation and survival and the initial events of myelination requires PI 3-kinase activity. J Neurosci 2000;20(12):4635-45.
13. Birkenkamp KU, Coffer PJ. Regulation of cell survival and proliferation by the FOXO (Forkhead box, class O) subfamily of Forkhead transcription factors. Biochem Soc Trans 2003;31(Pt 1):292-7.
14. Ghazvini M, Mandemakers W, Jaegle M, Piirsoo M, Driegen S, Koutsourakis M, Smit X, Grosveld F, Meijer D. A cell type-specific allele of the POU gene Oct-6 reveals Schwann cell autonomous function in nerve development and regeneration. Embo J 2002;21(17):4612-20.
15. Nickols JC, Valentine W, Kanwal S, Carter BD. Activation of the transcription factor NF-kappaB in Schwann cells is required for peripheral myelin formation. Nat Neurosci 2003;6(2):161-7.
16. Mandemakers W, Zwart R, Jaegle M, Walbeehm E, Visser P, Grosveld F, Meijer D. A distal Schwann cell-specific enhancer mediates axonal regulation of the Oct-6 transcription factor during peripheral nerve development and regeneration. Embo J 2000;19(12):2992-3003.
17. Jaegle M, Mandemakers W, Broos L, Zwart R, Karis A, Visser P, Grosveld F, Meijer D. The POU factor Oct-6 and Schwann cell differentiation. Science 1996;273(5274):507-10.
18. Jaegle M, Ghazvini M, Mandemakers W, Piirsoo M, Driegen S, Levavasseur F, Raghoenath S, Grosveld F, Meijer D. The POU proteins Brn-2 and Oct-6 share important functions in Schwann cell development. Genes Dev 2003;17(11):1380-91.
19. Sim FJ, Zhao C, Li WW, Lakatos A, Franklin RJ. Expression of the POU-domain transcription factors SCIP/Oct-6 and Brn-2 is associated with Schwann cell but not oligodendrocyte remyelination of the CNS. Mol Cell Neurosci 2002;20(4):669-82.
20. Levavasseur F, Mandemakers W, Visser P, Broos L, Grosveld F, Zivkovic D, Meijer D. Comparison of sequence and function of the Oct-6 genes in zebrafish, chicken and mouse. Mech Dev 1998;74(1-2):89-98.
21. Friedrich RP, Schlierf B, Tamm ER, Bosl MR, Wegner M. The class III POU domain protein Brn-1 can fully replace the related Oct-6 during schwann cell development and myelination. Mol Cell Biol 2005;25(5):1821-9.
22. Wysocka J, Herr W. The herpes simplex virus VP16-induced complex: the makings of a regulatory switch. Trends Biochem Sci 2003;28(6):294-304.
23. Driegen S, Ferreira R, van Zon A, Strouboulis J, Jaegle M, Grosveld F, Philipsen S, Meijer D. A generic tool for biotinylation of tagged proteins in transgenic mice. Transgenic Res 2005;14(4):477-82.
24. Okuda T, Hattori H, Takeuchi S, Shimizu J, Ueda H, Palvimo JJ, Kanazawa I, Kawano H, Nakagawa M, Okazawa H. PQBP-1 transgenic mice show a late-onset motor neuron disease-like phenotype. Hum Mol Genet 2003;12(7):711-25.
25. Waragai M, Lammers CH, Takeuchi S, Imafuku I, Udagawa Y, Kanazawa I, Kawabata M, Mouradian MM, Okazawa H. PQBP-1, a novel polyglutamine tract-binding protein, inhibits transcription activation by Brn-2 and affects cell survival. Hum Mol Genet 1999;8(6):977-87.
26. Ghislain J, Desmarquet-Trin-Dinh C, Jaegle M, Meijer D, Charnay P, Frain M. Characterisation of cis-acting sequences reveals a biphasic, axon-dependent regulation of Krox-20 during Schwann cell development. Development 2002;129(1):155-66.
27. Ghislain J, Charnay P. Control of myelination in Schwann cells: a Krox-20 cis-regulatory element integrates Oct-6, Brn-2 and Sox10 activities. EMBO Rep 2006;7(1):52-8.
28. Denarier E, Forghani R, Farhadi HF, Dib S, Dionne N, Friedman HC, Lepage P, Hudson TJ, Drouin R, Peterson A. Functional organization of a Schwann cell enhancer. J Neurosci 2005;25(48):11210-7.

29. LeBlanc SE, Jang SW, Ward RM, Wrabetz L, Svaren J. Direct regulation of myelin protein zero expression by the Egr2 transactivator. J Biol Chem 2006;281(9):5453-60.
30. Hai M, Bidichandani SI, Patel PI. Identification of a positive regulatory element in the myelin-specific promoter of the PMP22 gene. J Neurosci Res 2001;65(6):508-19.
31. Maier M, Berger P, Nave KA, Suter U. Identification of the regulatory region of the peripheral myelin protein 22 (PMP22) gene that directs temporal and spatial expression in development and regeneration of peripheral nerves. Mol Cell Neurosci 2002;20(1):93-109.
32. Maier M, Castagner F, Berger P, Suter U. Distinct elements of the peripheral myelin protein 22 (PMP22) promoter regulate expression in Schwann cells and sensory neurons. Mol Cell Neurosci 2003;24(3):803-17.
33. Darbas A, Jaegle M, Walbeehm E, van den Burg H, Driegen S, Broos L, Uyl M, Visser P, Grosveld F, Meijer D. Cell autonomy of the mouse claw paw mutation. Dev Biol 2004;272(2):470-82.
34. Wrabetz L, Feltri ML, Quattrini A, Imperiale D, Previtali S, D'Antonio M, Martini R, Yin X, Trapp BD, Zhou L and others. P(0) glycoprotein overexpression causes congenital hypomyelination of peripheral nerves. J Cell Biol 2000;148(5):1021-34.
35. Bermingham JR, Jr., Shearin H, Pennington J, O'Moore J, Jaegle M, Driegen S, van Zon A, Darbas A, Ozkaynak E, Ryu EJ and others. The claw paw mutation reveals a role for Lgi4 in peripheral nerve development. Nat Neurosci 2006;9(1):76-84.
36. Fields RD, Stevens B. ATP: an extracellular signaling molecule between neurons and glia. Trends Neurosci 2000;23(12):625-33.
37. Smart SL, Lopantsev V, Zhang CL, Robbins CA, Wang H, Chiu SY, Schwartzkroin PA, Messing A, Tempel BL. Deletion of the K(V)1.1 potassium channel causes epilepsy in mice. Neuron 1998;20(4):809-19.
38. Rho JM, Szot P, Tempel BL, Schwartzkroin PA. Developmental seizure susceptibility of kv1.1 potassium channel knockout mice. Dev Neurosci 1999;21(3-5):320-7.
39. Schulte U, Thumfart JO, Klocker N, Sailer CA, Bildl W, Biniossek M, Dehn D, Deller T, Eble S, Abbass K and others. The epilepsy-linked Lgi1 protein assembles into presynaptic Kv1 channels and inhibits inactivation by Kvbeta1. Neuron 2006;49(5):697-706.

Chapter 8

Samenvatting

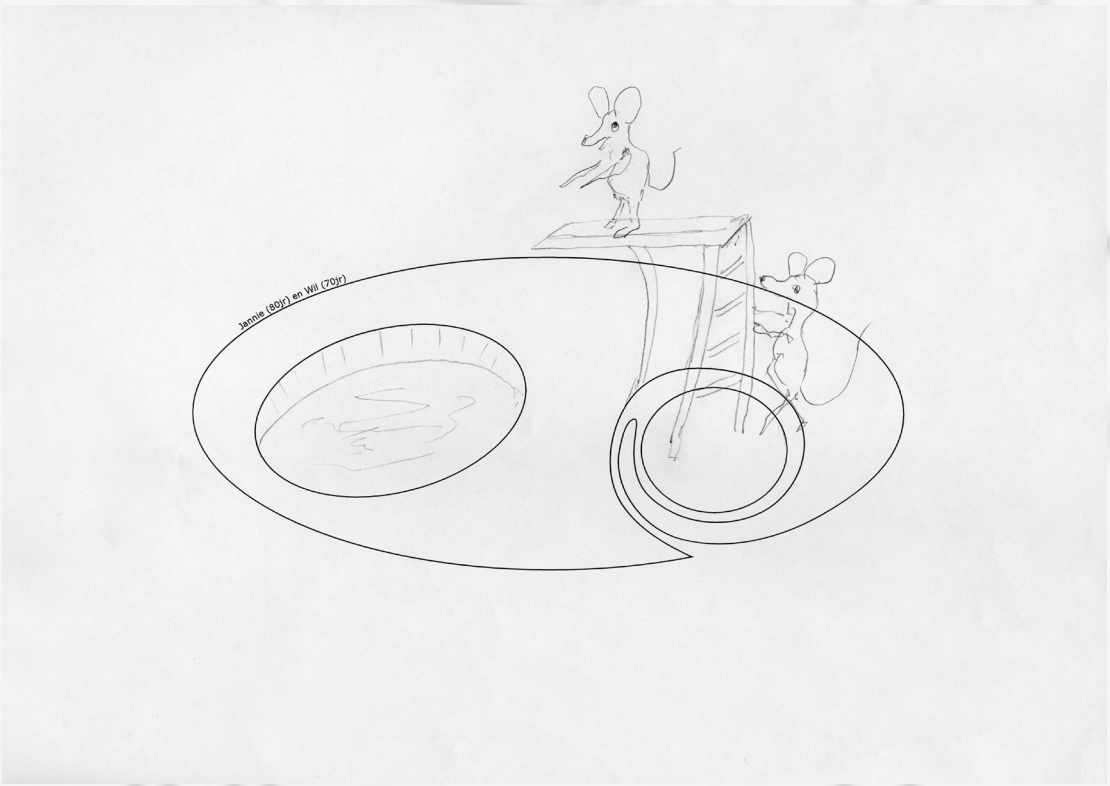

Samenvatting

De Schwann cellen die de perifere zenuwen bevolken ontstaan, evenals de rest van het perifere zenuwstelsel, uit de neurale lijst. De neurale lijst is een tijdelijke embryologische structuur die zich aan de dorsale randen van de zich sluitende neuraalbuis vormt. Schwann cel voorloper cellen vermenigvuldigen zich en migreren langs de axonen van de embryonale zenuwen. Uiteindelijk zullen deze cellen differentiëren in de twee typen Schwann cellen die kunnen worden onderscheiden; Schwann cellen die een myelineschede vormen rondom de dikkere axonen en de niet-myeline vormende Schwann cellen die meerdere dunne axonen omgeven.

De myelineschede wordt gevormd door de spiraalsgewijze omwikkeling van het axon door het celmembraan van de Schwann cel. Het myeline membraan is verrijkt in bepaalde lipiden zoals cholesterol en eiwitten zoals 'myelin protein zero' en 'myelin basic protein'. De myelineschede verdeelt het axonale membraan in domeinen waarbij de natrium en kalium kanalen geclusterd worden in respectievelijk het nodale (knoop van Ranvier) en juxtaparanodale domein. Deze specifieke organisatie resulteert in een zeer grote geleidingssnelheid van de actiepotentiaal. Afbraak van de myelineschede leidt tot neurologische problemen welke levensbedreigend kunnen zijn zoals bijvoorbeeld in multiple sclerose. Het doel van het in dit proefschrift beschreven onderzoek is inzicht te verkrijgen in de basale mechanismen van Schwann cel differentiatie en myelinisatie en met name de transcriptionele netwerken die deze processen beheersen.

De ontwikkeling van de perifere zenuw komt tot stand door directe cellulaire interacties tussen de Schwann cel en het axon. Een belangrijke component in deze interacties wordt gevormd door het neureguline1 signaal molecuul, welke gegenereerd wordt op het axon, en de ErbB2/3 receptoren op de Schwann cel. Deze interactie speelt een essentiële rol gedurende alle stadia van ontwikkeling inclusief de aanzet en uitvoering van het myelinisatie proces. De initiatie van het myelinisatie proces leidt tot de activiteit van een specifieke set genen welke beheerst wordt door een netwerk van transcriptie factoren. Genetische studies van onder andere ons laboratorium hebben laten zien dat de transcriptie factoren Oct-6 en Krox-20 een essentiële rol spelen in de initiatie en uitvoering van het myelinisatie programma. Oct-6 en Krox-20 functioneren in een simpele hiërarchie waarbij Oct-6 functie vereist is voor de juiste temporele activering van Krox-20 en myeline vorming. Dus in *Oct*-6 muismutanten is de activering van Krox-20 en myelinisatie vertraagd. Oct-6 genexpressie neemt sterk toe in Schwann cellen die zich opmaken om myeline te vormen, hetgeen suggereert dat Oct-6 expressie direct aangestuurd wordt door signaal routes die beheerst worden door neureguline-1. Hoewel de identiteit van de signaal routes nog niet geheel opgehelderd is, is duidelijk dat ze uiteindelijk aangrijpen op de *Oct-6* enhancer. Deze enhancer bevindt zich in een gebied van zo'n 4kb dat ongeveer 10kb achter het *Oct-6* gen ligt. Onze genetische proeven hebben laten zien dat dit DNA element voldoende is voor de juiste temporele expressie van het *Oct-6* gen in Schwann cellen. Verder laten we in dit proefschrift zien (hoofdstuk 2) dat de Oct-6 Schwann cell enhancer (SCE) ook essentieel is voor Schwann cel specifieke expressie van Oct-6. Deletie van de SCE resulteert in een

selectief verlies van Oct-6 expressie in Schwann cellen terwijl de expressie van Oct-6 in bijvoorbeeld CA1 neuronen van de hippocampus niet is veranderd. Het is dus waarschijnlijk dat het complete expressie patroon van Oct-6 tot stand komt door de activiteit van verschillende enhancer modules waarvan wij er dus nu een hebben geïdentificeerd.
Hoewel onze genetische studies hebben uitgewezen dat Krox-20 activatie afhankelijk is van Oct-6 activiteit is de ontwikkeling van de perifere zenuwen ernstiger verstoord in *Krox-20* muismutanten dan in *Oct-6* mutanten. Dus, terwijl in afwezigheid van Oct-6 myeline vorming vertraagd is, blijkt het proces geheel te stagneren in afwezigheid van Krox-20. Inderdaad, in afwezigheid van Oct-6 wordt Krox-20 vertraagd geactiveerd. Deze observaties suggereerden dat een eiwit met een aan Oct-6 verwante functie tot expressie komt in Schwann cellen dat in staat is Krox-20 te activeren. In hoofdstuk 3 van dit proefschrift laten we zien dat Brn-2, nauw verwant aan Oct-6, tot expressie komt en dat Schwann cel specifieke deletie van dit gen en Oct-6 een zeer ernstige vertraging van myeline vorming veroorzaakt. Deletie van alleen *Brn-2* in Schwann cellen, dus Oct-6 komt normaal tot expressie, heeft geen merkbaar effect op de ontwikkeling en myelinisatie van de perifere zenuwen. Dus, Oct-6 is de belangrijkste factor voor Krox-20 regulatie maar in afwezigheid van Oct-6 kan Brn-2 die taak gedeeltelijk overnemen. Het feit dat Brn-2 niet volledig compenseert voor verlies van Oct-6 hangt hoogstwaarschijnlijk samen met het niveau van Brn-2 expressie. Overexpressie van Brn-2 in een Oct-6 mutant, door middel van een transgen, leidt tot een gedeeltelijk herstel van het verloop van myelinisatie.
Het is echter onwaarschijnlijk dat Oct-6 en Brn-2 geheel functioneel equivalent zijn. Een aantal structurele verschillen tussen Oct-6 en Brn-2 (en de andere verwante eiwitten Brn-1 en Brn-4) suggereren dat deze eiwitten met verschillende eiwitten interacties aangaan. Om dergelijke eiwitten te identificeren hebben we een muizen lijn gegenereerd die Oct-6 met een zeer sterke affiniteit voor avidine expresseert. Dit maakt het mogelijk om Oct-6 complexen uit weefsel extracten te isoleren en de eiwitten die met Oct-6 mee zuiveren te identificeren door middel van massaspectroscopie. Deze methode is ontwikkeld in het laboratorium van prof. Frank Grosveld en is succesvol aangewend om eiwitten die een complex met Gata-1 in rode bloedcellen vormen te identificeren. De ontwikkeling van deze muizen lijn is beschreven in hoofdstuk 4.
Natuurlijke muismutanten zijn van onschatbare waarde voor ons onderzoek naar de ontwikkeling en functioneren van het zenuwstelsel. Een natuurlijke muismutant, genaamd *claw paw* (*clp*), had onze aandacht getrokken omdat de aandoening, vertraagde ontwikkeling en hypomyelinatie van de perifere zenuwen, erg leek op wat we waarnamen in *Oct-6* mutanten. Dit suggereerde dat het *clp* gen of door Oct-6 gereguleerd wordt, of dat clp *Oct-6* reguleert, of dat clp functioneert in een route parallel met Oct-6. Een bijzonder interessante mogelijkheid was dat clp een directe regulator van *Oct-6* is die of in het neuron of in de Schwann cel actief is. Om nu in eerste instantie het defect in deze mutanten beter te karakteriseren en te bepalen in welk celtype clp tot expressie komt, hebben we een serie experimenten uitgevoerd welke beschreven staan in hoofdstuk 5. Deze experimenten suggereerden dat clp in Schwann cellen tot expressie komt. Verder lieten onze experimenten

zien dat Schwann cel differentiatie in *clp* muizen al verstoord is in een stadium voor dat *Oct-6* geactiveerd wordt.
Het genetische defect dat ten grondslag ligt aan het clp fenotype hebben we in samenwerking met de onderzoeksgroep van dr. John Bermingham bepaald door middel van 'positional cloning'. De *clp* mutatie bleek een allel te zijn van het *Lgi4* gen. *Lgi4* behoort tot een kleine familie van vier genen (*Lgi1-4*) welke voornamelijk in het zenuwstelsel tot expressie komen maar waarvan verder nog zeer weinig bekend is. Het *clp* allel van *Lgi4* bevat een kleine insertie in intron 3 van het gen wat leidt tot exclusie van exon 4 gedurende splicing van het Lgi4 mRNA. We toonden aan dat Lgi4 normaliter in Schwann cellen geëxpresseerd wordt en dat het eiwit wordt uitgescheiden door de cel. Exon 4 is 72 nucleotiden lang en exclusie van dit exon in processing van het *clp* gen resulteert in een in-frame deletie van 24 aminozuren in het LRR domein van Lgi4. In tegenstelling tot Lgi4 wordt Lgi4clp helemaal niet door de cel uitgescheiden. Verder hebben we laten zien dat toevoeging van Lgi4 bevattend medium aan Schwann cel/neuron co-cultures die afgeleid waren van claw paw embryo's het myelinatie proces in deze cultures herstelt. Op grond van deze gegevens is het dus zeer waarschijnlijk dat Lgi4 een cruciale rol speelt in de communicatie tussen het axon en de Schwann cel. Wat deze rol precies is en met welke andere moleculen Lgi4 een interactie aangaat zal toekomstig onderzoek moeten uitwijzen.

List of abbreviations

ATP	Adenosine Tri Phosphate
BDNF	Brain Derived Neurotrophic Factor
Caspr	Contactin-associated protein
CH	Congenital Hypomyelination
clp	claw paw
CMT	Charcot Marie Tooth
CNS	Central Nervous System
Cx32	Connexin32
Dhh	Desert Hedgehog
DNA	Deoxy Ribonucleic Acid
DRG	Dorsal Root Ganglion
DSS	Dejerine-Sottas Syndrome
eGFP	enhanced Green Fluorescent Protein
ER	Endoplasmatic Reticulum
GDNF	Glial Derived Neurotrophic Factor
HMSN	Hereditary Motor and Sensory Neuropathies
HNPP	Hereditary Neuropathy with liability to Pressure Palsies
Lgi	Leucine-rich, glioma activated
MSE	Myelinating Schwann cell Element
MTMR-2	Myotubularin-related protein 2
NGF	Nerve Growth Factor
NRG-1	Neuregulin 1
NT-3	Neurotrophin 3
PNS	Peripheral Nervous System
P_0	Myelin Protein Zero
PMP22	Peripheral Myelin Protein-22
PQBP-1	Poly-glutamine tract Binding Protein
POU	Pit-1, Oct1/2, Unc-86
SCE	Schwann cell specific enhancer
Sp	Splotch
Sp^d	Splotch delayed
Tr	Trembler
TrJ	Trembler J
Trk	Tyrosine receptor kinase

Curriculum Vitae

Naam:	Margretha Johanna Franciska
Geboren:	26 maart 1977, Enkhuizen
1989 - 1996:	VWO, atheneum aan het Ichtus College te Kampen
1996 - 2001:	Universiteit Maastricht Gezondheidswetenschappen, afstudeerrichting Biologische Gezondheidskunde Afstudeerstage vanuit de afdeling Psychologie & Neuro-psychologie, faculteit geneeskunde aan de University of Michigan, Mental Health Research Institute 'Nitric oxide and serotonin' (prof.dr. H. Steinbusch & dr. C. Norton)
2001 - 2005:	Promotieonderzoek, Erasmus MC, Neurowetenschappen & Celbiologie 'Genetic Control of Schwann Cell Differentiation' (prof.dr. F.G. Grosveld & dr.ir. D.N.Meijer)
2005 - heden:	Research assistant & labmanager

List of Publications:

- Bermingham, J. R., Jr., Shearin, H., Pennington, J., O'Moore, J., Jaegle, M., Driegen, S., van Zon, A., Darbas, A., Ozkaynak, E., Ryu, E. J., *et al*. (2006). The *claw paw* mutation reveals a role for *Lgi4* in peripheral nerve development. Nat Neurosci *9*, 76-84.

- Darbas, A., Jaegle, M., Walbeehm, E., van den Burg, H., Driegen, S., Broos, L., Uyl, M., Visser, P., Grosveld, F., and Meijer, D. (2004). Cell autonomy of the mouse *claw paw* mutation. Dev Biol *272*, 470-482.

- Driegen, S., Ferreira, R., van Zon, A., Strouboulis, J., Jaegle, M., Grosveld, F., Philipsen, S., and Meijer, D. (2005). A generic tool for biotinylation of tagged proteins in transgenic mice. Transgenic Res *14*, 477-482.

- Drissen, R., von Lindern, M., Kolbus, A., Driegen, S., Steinlein, P., Beug, H., Grosveld, F., and Philipsen, S. (2005). The erythroid phenotype of EKLF-null mice: defects in hemoglobin metabolism and membrane stability. Mol Cell Biol *25*, 5205-5214.

- Ghazvini, M., Mandemakers, W., Jaegle, M., Piirsoo, M., Driegen, S., Koutsourakis, M., Smit, X., Grosveld, F., and Meijer, D. (2002). A cell type-specific allele of the POU gene *Oct-6* reveals Schwann cell autonomous function in nerve development and regeneration. Embo J *21*, 4612-4620.

- Jaegle, M., Ghazvini, M., Mandemakers, W., Piirsoo, M., Driegen, S., Levavasseur, F., Raghoenath, S., Grosveld, F., and Meijer, D. (2003). The POU proteins Brn-2 and Oct-6 share important functions in Schwann cell development. Genes Dev *17*, 1380-1391.

Dankwoord

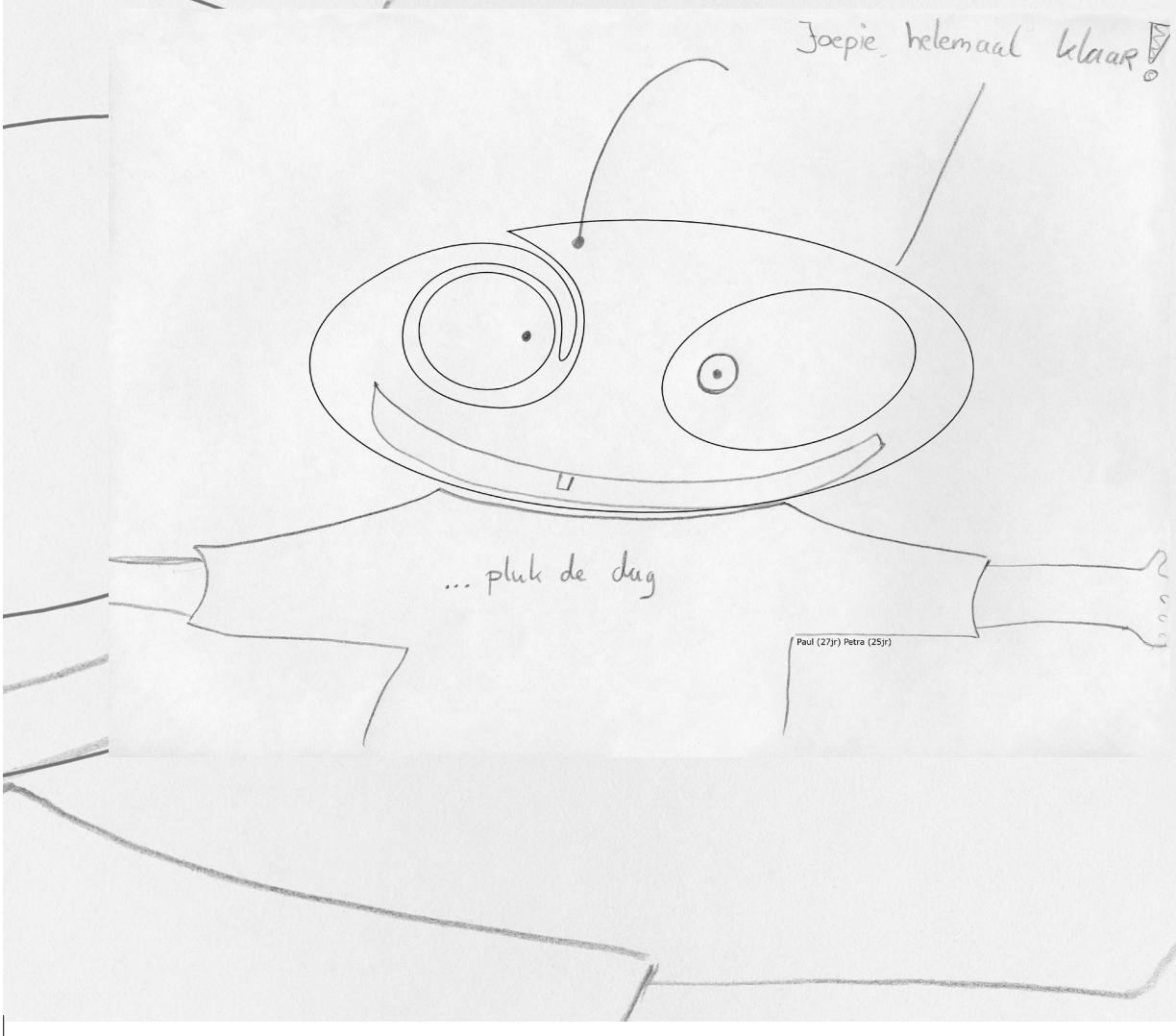

Dankwoord

Na veel tijd in het schrijven te hebben gestoken van dit boekje, ben ik nu bij het laatste (en belangrijkste) hoofdstuk aangekomen. Dit gedeelte geeft mij de kans om mijn dank uit te laten gaan naar de mensen die naar mijn inzicht een (grote) bijdrage hebben geleverd aan het tot stand komen van dit boekje.

Allereerst wil ik Dies bedanken voor alles wat hij heeft gedaan om het mogelijk te maken dat ik zo ver ben gekomen. Mijn AIO-schap is niet zo standaard verlopen als bij anderen (wel de normale ups en downs van het onderzoek) maar mede doordat jij mij bent blijven stimuleren om het toch af te maken sta ik vandaag hier. Ik heb tot nu toe heel veel geleerd: Hoe een goed experiment uit te voeren, maar ook hoe in de keuken van een recept iets eetsbaars te maken. Ook probeer je ons al jaren te overtuigen dat Bob Dylan hele goede muziek heeft en de laatste cd lijkt inderdaad ook binnen je lab aan te slaan. Daarnaast heb ik ook heel veel plezier gehad in je lab, maar ook daarbuiten: lunchen op *Oct-6* dag of het uitzwaaien van een stagiaire. En het Bob-Rossen van het huisje zal ik zeker niet vergeten.

Frank jij hebt als promotor wat meer een bijdrage geleverd op de achtergrond en dan met name in de eerste paar jaar. De werkbesprekingen bij jou zal ik niet vergeten, maar wat ik niet mis zijn de vragen die je stelde, op de een of andere manier kreeg jij me altijd wel stil en kon ik niet zo goed een antwoord bedenken.

Joan jij was met name op de achtergrond aanwezig; ik wil je bedanken voor wat ik heb mogen leren van je in de afgelopen jaren.

Natuurlijk zou ik nergens zijn gekomen zonder de hulp van mijn labgenoten. Martine, tu m'as appris beaucoup de choses, techniques bien sûr, mais tu aussi appris à me taire quand il le faut...bien que ce dernier point soit encore 'a work-in-progress'. Arend, dankjewel bij alle hulp nu aan het einde van het boekje. Die laatste loodjes blijken toch inderdaad wel wat te wegen. Matthijs je werkt niet meer op dit lab, maar ik ben absoluut niet al je hulp vergeten en soms is het bepaald lastig dat ik niet even je hulp kan vragen als ik een paar handen meer nodig hebt. Dorota you came into our lab with your own research because labspace was needed. I enjoyed your company and hope you will be able to finish quickly too. Ekim you showed me that there are more movies except the ones that come in the cinemas. I definitely watched some movies I would otherwise never have checked out. Noorie you were the last one to come in and you have a few more years to convince me that certain Indian food is not spicy and that I should try it.

Naast de mensen van mijn eigen lab zijn er natuurlijk ook andere mensen op de afdeling te bedanken die belangrijk zijn geweest voor hulp bij experimenten of gewoon dat beetje steun dat zo belangrijk is als je bezig bent met je AIO-schap. Allereerst Sjaak en de mensen van zijn lab Nynke, Roy, Rita, Harald, Thamar (we missen jullie eigenlijk nog steeds stiekem wel een beetje). Ook Elaine en de mensen van haar lab Esther, Marianne, German-Katrin, French-Catherine, Sandra, Claudia, Karin, Karine, Chris and Fredrik (het was heel gezellig met zijn allen op één lab).

De dames van de keuken (Jopie, Fatima, Chenelva, Prema en Joke) dank jullie wel voor jullie hulp. Jullie hebben er een aantal malen voor gezorgd dat geplande experimenten toch

door konden gaan door op het laatste moment nog even iets voor ons te autoclaveren of anderszins schoon te maken. Jullie zijn gezellige buren, jullie maken altijd geluid.
Melle, Petra en Mieke en Koos jullie staan altijd klaar om te helpen bij bestellingen die we snel nodig hebben of die veel te lang op zich laten wachten. Wat natuurlijk erg sjiek is dat we onze eigen afdelingsbezorgdienst hebben.
De jongens van de computers Sjozef, Ton, Pim, Leo en Mario, dankjewel voor de hulp en waarom die computers toch altijd kapot gaan op het moment dat je vlak voor een deadline zit is mij nog steeds een raadsel.
Elize, Mandy en Erika, ik denk dat als ze een decibel test zouden doen als jullie alledrie op het lab aanwezig zijn, dat iedereen wordt verplicht met gehoorbescherming te lopen, maar het is wel gezellig hoor. Hartelijk bedankt voor jullie praktische hulp of af en toe gewoon een praatje.
Nynke (leuk hè? jullie krijgen je eigen stukje) en Ton jullie wil ik hartelijk bedanken voor de gezellige avondjes en Nynke ik weet niet of het zo verstandig is om hier neer te zetten dat als ze mij zoeken op het lab ze misschien eens even bij jou op het lab navraag moeten doen. Dank jullie wel voor alle steun die jullie me vaak boden met nuchter commentaar om deze stresskip tot rust te brengen.
Marike en Jasperina, ik weet niet of jullie mij ooit nog mee willen nemen naar een kerstnachtdienst, want ik kan mij niet stil houden. Ik vind de avondjes met jullie heel gezellig en hoop dat we dat nog een poosje vol houden.
De mooie lay-out van dit boekje is tot stand gekomen met de inzet van Tom. Dankjewel voor je hulp, want zonder die hulp was het maar een gewoon boekje geweest. Met deze vormgeving is het ook leuk om naar het boekje te kijken als het niet hoeft te worden ingekeken voor de tekstuele inhoud.
Basketbal is een hele leuke sport om te doen en een nog veel leukere sport om aan kinderen te leren. Kees dankjewel dat ik de kans heb gekregen om van jou te leren hoe een goede en ook leuke (want dat is nog veel belangrijker) training te geven. Wedstrijden zijn nog veel gaver, want dat is proberen de kinderen de goede kant op te sturen en ook ze leren dat verliezen niet erg is zo lang je maar volle inzet toont en je best doet ook als het een keertje niet zo goed lukt. En als je dan wel een keer wint is het ook dubbel feest.
Ik wil mijn beide paranimfen heel hartelijk bedanken voor alle hulp en steun die ze mij geven.
Merhnaz jij bent al door de promotie heen geweest en weet dus wat er moet gebeuren, dat is erg handig. Ook toen je nog bij ons op het lab zat heb ik van je geleerd en plezier met je gehad. Je pizza's zijn goed, maar je hamburgers kunnen er ook wat van. Ik wens je nu alle tijd toe om te genieten met Saeed en Arian.
Laetitia, met jou heb ik samen een fantastische stage gelopen in Ann Arbor, Michigan, waar we samen bij Jeanette in huis hebben gewoond. We hebben gave dingen gedaan daar en veel geleerd, positieve en negatieve dingen. Rollercoasters zijn gaaf, maar je wordt er ook onwijs misselijk van als je vervolgens een chocolade-ijsje eet. Vorig jaar terug geweest naar Amerika op vakantie naar Cape Cod om Jeanette te zien en ik heb het erg leuk gevon-

den dat je spontaan zei dat je meeging. Jij bent ook bijna zover en ik wens je succes met jouw afronding. Het komt allemaal goed! Jullie beide dankjewel dat jullie naast me staan op het moment suprème.
Jeanette you gave me and Laetitia an incredible cheap place to stay (only mowing the lawn now and then) during our intern. Thank you for all your help and love. You gave us a place to feel at home away from home.
Pap en mam zonder jullie steun had ik nooit deze vier jaar kunnen volbrengen. Lekker thuis uitrusten of gezellig op vakantie. Vaak hebben jullie geslikt dat ik wat vroeger weg moest van huis omdat ik nog ‘s avonds even wat moest doen als voorbereiding voor de volgende dag of simpel weg mijn cellen verzorgen. Georg, Lara, Marit en Meike, bij jullie was het af en toe even heerlijk ontspannen en even lekker nergens aan denken. Dat is goed anders ben je alleen maar met wetenschap bezig maar af en toe zijn er ook andere dingen. Paul en Petra jullie zaten in eerste instantie wat verder weg in Frankrijk, maar het was leuk om daar een keer langs te gaan en nu jullie weer terug zijn is het leuk dat jullie lekker dichtbij zitten. Dan kun je af en toe een gezellig avondje doen of ik kan jullie ‘s morgens om 5 uur van de bus halen.
Ome Niek en tante Jacqueline, gezellig kletsen aan de telefoon of een weekendje of dagje bij jullie langs. Het is altijd gezellig en veel te snel weer voorbij.
Paul nog bedankt voor de foto van je golf, ik hoop dat je vindt dat hij er mooi op staat. Ik wil jullie allemaal (ook oma en tante Willy) bedanken voor jullie inzet om een mooie tekening te maken van de figuur die ik jullie heb gegeven. Mede daardoor is dit denk ik een heel speciaal boekje geworden dat een leerzame periode van mijn leven afsluit om door te gaan met de volgende.

Sirka